DEVELOPMENT OF A DETAILED SIMULATION MODEL TO SUPPORT EVALUATION OF WATER LOAD SHIFTING ACROSS A RANGE OF USE PATTERNS

Nicolas Kelly (Senior Lecturer), Aizaz Samuel (Senior Researcher), Paul Tuohy (Lecturer)
Energy Systems Research Unit, University of Strathclyde, Glasgow, UK

ABSTRACT

As electrical power networks become increasingly dominated by intermittent renewable generation both at the grid level and decentralised, their operation presents new challenges. One mechanism that has been proposed as a potential solution is demand shifting of loads. This potential for load shifting is difficult to assess given variations and uncertainties in user behaviour and weather particularly for modern hybrid systems, which often include weather dependent solar and heat pump systems and complex controls.

This paper provides details of an integrated building simulation modelling approach intended to support load shifting studies, with a specific focus on the load shifting potential of hybrid domestic hot water storage systems. The example domestic hot water system investigated here comprises an air source heat pump coupled with solar thermal collectors and a storage tank featuring supplementary immersion heating for control of Legionella and top up heating. The hybrid hot water system and its controls are explicitly modelled at a level of detail sufficient to closely replicate the actual system behaviour.

User behaviour in this case affecting the quantity and timing of hot water draws has the potential to strongly influence water heating requirements, the solar hot water system effectiveness, and the potential for load shifting. The development of a set of stochastic water draw profiles to represent an appropriate range of behaviours for the UK context is described.

These different domestic hot water use patterns are then made available to facilitate the evaluation, in a detailed building and hybrid energy system model, of load shifting potential and effectiveness across a representative range of weather and behaviour.

While the case study presented here is for a specific situation, it is proposed that the methodology is more generally applicable.

INTRODUCTION

Concerns regarding volatility of fossil fuel prices, security of supply and climate change have increased for the use of renewable energy sources in the built environment. Considerable renewable penetration is expected over the next few decades with projections in Europe set to exceed 20% gross electrical generation by the year 2020 (EEA 2014). Exploitation of solar energy, wind and other renewables is a formidable challenge because of unpredictability of supply and mismatch in timing of energy demands and supplies. For example, solar energy is usually available when there is no need for heating and high winds at night will not contribute to offsetting daytime peak electrical demand. The need therefore is to provide a mechanism to match supply and demand. Whereas not much can be done to shift renewable supplies it is possible to shift demand and reasonably maintain operating performance acceptable to the user.

THE ORIGIN SYSTEM

We report initial results from the EU FP7 project ORIGIN (Orchestration of Renewable Integrated Generation in Neighbourhoods) (URL 1). Within the project, a system to facilitate demand shifting of thermal and electrical loads is to be commissioned to enhance overall energy performance in terms of reducing dependence on conventional energy resources and increasing dependence on renewable resources. The sites for energy management are three eco-villages in Scotland, Italy and Portugal. Representative domestic buildings are being monitored extensively to inform about energy use patterns and potential demand shifting potential. Climatic boundary conditions are also monitored using local weather stations. The ORIGIN system overview is shown in figure 1.

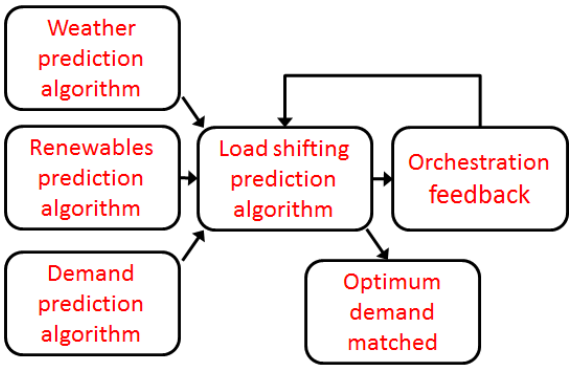

Figure 1 ORIGIN algorithm

The algorithm for the ORIGIN system relies on automatic acquisition of local weather data from which a weather prediction algorithm will generate weather for the near future (24 hours). This includes dry bulb temperature, direct and diffuse solar radiation and wind speed. Near future weather and demand predictions allow an assessment of supply / demand matching to be made, the available opportunities for load shifting are quantified (and adjusted based on feedbacks) and a decision made on

how best to orchestrate these opportunities to close the gap.

The simulation modelling described here is to underpin various elements of the ORIGIN project:

- The first is to give insights and assist in the quantification of orchestration opportunities,
- The second is to assist in the evaluation and quantification of effectiveness of proposed orchestration algorithms,
- The third is to support investigations into improvements in existing systems or design of new systems which better support load shifting in future.

AIM

This paper reports on the development of detailed dynamic simulation modelling at sufficient detail to provide a test bed for load shifting analysis. The specific case presented is of hot water heating in a solar / heat pump / storage hybrid system. The importance of variations and uncertainties in behaviours is identified and a set of representative water draw patterns proposed. The case study is used to demonstrate how patterns of water use are related to potentials for load shifting and have an impact on solar utilization and heat pump energy input. Several examples of model outputs are used to illustrate the operation of the detailed model and the type of system performance insights made available for use in load shifting analysis.

SITE DETAIL AND MONITORING

Domestic buildings built to modern standards lend themselves well to the ORIGIN scheme because they are well insulated and have lower air leakage rates than older buildings. These factors make load orchestration more feasible. Heating and cooling are not necessarily the predominant energy loads in such buildings, rather the provision of hot water and electricity can form the major proportion of demand and these offer prime opportunities for orchestration.

The simulation model chosen as case study represents a building and hybrid thermal energy system of a type common in the ORIGIN communities and of a type becoming more common in general because of increasing building performance requirements across Europe. The model is built utilising fabric and systems specifications taken from design documents and was initially calibrated by comparing against available monitored data from which control settings and occupancy profiles have been tuned. This monitored data is obviously limited to the specifics of climate and occupant behaviour during the monitoring period. Therefore, further comparisons have been made against similar data gathered in other monitoring exercises to confirm that simulation results provide reasonable results out with the winter monitored period.

Figure 2 shows Findhorn; the Scottish eco-village where monitoring studies are being carried out. Figure 3 shows the example apartment building that is the focus in the work presented here. The apartment block is built to modern Scottish Building Regulations (SBS 2012). Extensive monitoring has been deployed across the ORIGIN communities including system and environmental measurements.

Figure 2 Findhorn eco-village (monitoring

Figure 3 Apartment block (monitoring site)

BUILDING AND SYSTEM MODELLING

A top floor apartment was selected from the building of figure 3 for detailed thermal modelling. The apartment was zoned into living area, sleeping area, sunspace and roof space. Figure 4 shows a wireframe rendering of the thermal simulation model used for predicting performance. ESP-r (Hand 2011, ESRU 2001) was used as the modelling tool because of its integrated simulation capabilities across thermodynamic “domains” (i.e. constituent parts of a model) as described by Clarke and Tang (2004). In order to fully assess the thermal performance of the building and the interaction between its fabric, occupants control and systems, the following domains are included within this model: building fabric, HVAC plant, solar insolation and shading, mass flow networks for both air flow and water flow in the hydronic circuit and electrical power flow network domains.

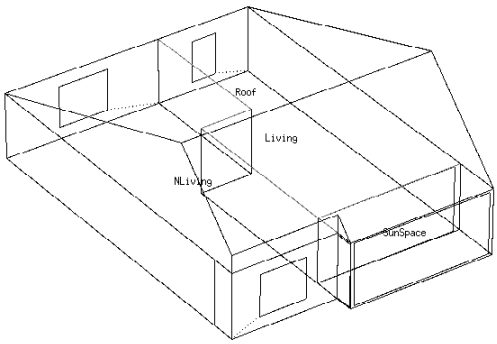

Figure 4 ESP-r dynamic thermal model

Within the model each of these domains is explicity defined. Well defined optimised solvers exist for these domains that solve for governing thermodynamic parameters at short intervals of time (time steps). The critical feature of integrated simulation is the time step level information exchange between these solvers due to which domains are solved based on fresh information becoming available each time step. For example the air flow solver gets inputs from thermal simulation regarding air temperature in each space and can dynamically accommodate density variations of the air in its solution. As a further example the electrical network knows about the state of the heat pump which is controlled from knowlede of space and buffer tank temperature which in turn are calculated during building and plant solution respectively. From this knowledge adjustments are made to the electrical network.

This form of the model described above allows interactions between the different energy subsystems in the building to be accounted for. For example, a sun space is present in the real building and this necessitates explicit shading and insolation analysis be carried out in conjunction with thermal simulation. This is coupled with an explicit model of the hydronic plant shown in figure 5. In the plant model, flows are predicted using a hydronic mass flow network in order to explicitly account for pressure and flow relationships. Finally, the building

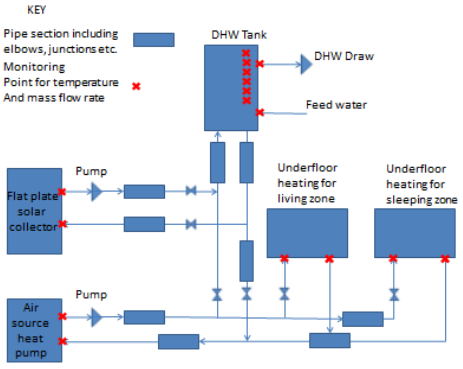

Figure 5 Explicit plant model schematic

model includes an electrical network that allows the electrical demand (lighting, HVAC, appliances) and production (PV) to be explicitly tracked. Various air flows in an around the building are modelled by a zonal / network air flow model.

The dwelling has highly insulated and airtight construction and mechanical ventilation with heat recovery. The conditioning system servicing the dwelling (figure 5) is a wet central heating system consisting of a low temperature air source heat pump that supplies both space and water heating. Space heating is by means of underfloor heaters within the whole of the dwelling except the sun space. The heat pump also supplies water to a hot water storage tank and can service both space and water heating simultaneously. A solar thermal system provides renewable heating to the water tank that can be heated either from the heat pump or from the solar collector. A boost immersion heater is also present in the hot water tank for topping up hot water and fulfilling hygiene obligations. It is important to note that hot water tank charging is done either by the heat pump or by the solar collector but not by both simultaneously. The boost immersion heater is independent of both.

Due to the various flow configurations in parallel branches and associated control interactions it was desirable to model flow by resolving it using network flow analysis (Lorenzetti 2002). Hence, a flow network modified for hydronic systems was developed and coupled with the plant network. The flow network simultaneously solves for flow rates as functions of pressure difference in each of the connections while maintaining mass balance. A pump curve modified from Grundfos (2005) was used to model water pump performance and a water stratification algorithm (Wang *et al* 2007) was used to predict the hot water storage tank performance. The solar collector performance prediction relied on an algorithm described by Thevenard *et al* (2004).

CONTROLS MODELLING

Recommended control for heating of the water tank is provided in the installation and operation manual (Daikin 2010). It includes set points for operation of solar collector, heat pump and immersion heater. Figure 6 shows the decision flow diagrams for solar heating and top up immersion heater. The figure is annotated by sensor information represented by S1 to S7, which are the sensors that are needed for recommended control. In brief, the solar collector was set to operate any time its temperature was more than 10^{o}C above the inlet point in the tank. The heat pump was time controlled; with manufacturer recommended control imposed that allowed water heating between 0700-0900 in the morning and 1600-2300 in the evening. This timing was changed to study load shifting as described later. The immersion heater provided top up heating and

was scheduled to be operated once a week for one hour ostensibly for legionella treatment.

The system control logic was decomposed to digital (ON/OFF) logic and implemented as such within the simulation environment as shown in table 2. Within the table the first 7 controllers are sensed conditions as described in Figure 9 (S1 to S7). The next 4 controllers (8 to 11) are the logical inverse (logical NOT) of controllers 1 to 4, these ease in further control logic implementation. Controllers 12 to 16 are the result of logical operations described in figure 9 with controller 17 switching the immersion heater. Controllers 18 and 19 sense operative temperature in controlled zones and actuate respective heating valves for the underfloor system. Similarly controllers 20, 21 and 26 to 28 perform logical operations described in figure 9 for operation of the heat pump and solar collector respectively. Controllers 22 to 25 and 29 to 32 control the operation of the heat pump, solar collector and associated valves.

MODEL CALLIBRATION

The simulation model was subject to calibration against monitored results over a period of several days, tank temperature at various heights and space operative temperature were compared. The calibration process was quantified using statistical goodness of fit metrics described by Williamson (1995). Figure 7 shows these temperatures at heights of one third and two thirds along the water tank and the living space operative temperature at the end of the calibration process. Monitored data is currently only available for winter time and the representative day shown in figure 6 was chosen by visual inspection of water heating patterns over the heating season to ascertain a typical heating and use scenario. Weather data for this day was imposed on the simulation model as were set point temperatures and space and water heating profiles. Table 1 shows statistical goodness of fit results, these were obtained with greater than 95% confidence. Pearson's coefficient is calculated on value (magnitude) and Spearman's coefficient is calculated on rank i.e. how well do the shapes of the two data set match.

Table 1: goodness of fit parameters for predicted tank temperatures at one and two thirds height and space temperature

(a) Mean and standard deviation

		Mean (°C)	Std Dev (°C)
2/3	Monitored	54.8	8.3
	Simulated	50.0	9.2
1/3	Monitored	34.0	8.6
	Simulated	38.8	7.0
Space	Monitored	18.7	0.5
	Simulated	18.5	0.8

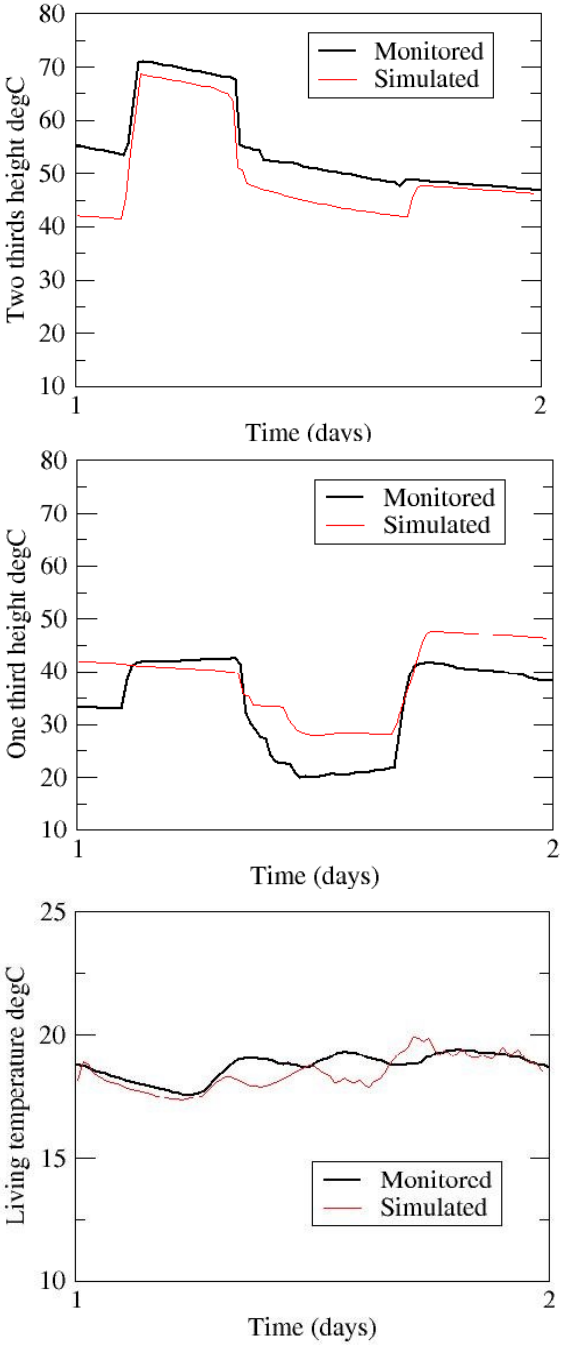

Figure 7 Simulated and monitored temperatures at two and one third height along water tank and operative temperature in the living room

Table 1(b) Correlation coefficients

	RMS error	Normalized RMS error	Pearson's correlation coefficient	Spearman's rank correlation coefficient	Inequality coefficient
2/3	0.63	0.01	0.91	0.42	0.06
1/3	0.65	0.02	0.88	0.58	0.09
Space	0.07	0.00	0.61	0.55	0.02

It was found that whereas calibration of tank heat loss and gain characteristics was relatively straightforward, it was not easy to emulate exact water draw offs. The reason for this is that exact timing and volumes of small water draws are difficult to monitor given the measuring precision of the heat meters employed. This is evident from the divergence between measured and modelled data for the bottom most sections of the tank where impact of fresh makeup water is maximum. Another important observation made during the calibration phase was that the decay rate of the top most section is lowest even though this is the warmest section. This is due to buoyancy driven water movement from lower sections to the upper sections replenishing the top section. Downward buoyance driven flow of cooled water from the tank appear as temperature losses in lower tank sections. Consequently the bottom section of the tank cools more rapidly.

WATER USE PROFILES

Hot water heating load is the biggest thermal load within the dwelling and therefore has the greatest potential benefit regarding shifting. Water heating demand can vary significantly with hot water use. Therefore, a number of hot water usage profiles were considered taking an approach similar to that described for the US context by Hendron *et al* (2010) but adjusted for the UK context. This was imposed as stochastic draw patterns using logic embedded within the modelling software as described by Jordan and Vajen (2005). Daily use profiles were divided into high, medium and low hot water volume used. Further distinction is made between users who stay home the major part of the day and users who stay away during the day time. Still further distinction is made between morning and evening biased users. The complete set of draw profiles for the low usage case is given in figure 8; similar patterns exist for the medium and high volume usage case.

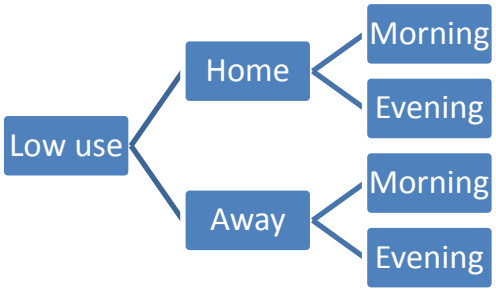

Figure 8 Water use variants: low use case

The levels of actual water usage are taken from EST (2008) where the low, medium and high levels have been equated to the lower quartile, median and upper quartile of UK hot water usage. Figure 9a shows a weekly averaged water draw profile comparing high, medium and low usage morning draw options that shows normalised high draws in the morning and evening with low draws during office hours. Figure 9b compares similar water draw profiles with occupants at home and away; there are lower draws during early morning and evening and higher draws during office hours for 'at home'. Figure 9c compares a morning biased draw pattern with evening biased draw. These week averaged profiles show how the water draws are profiled; the specifics for a given day can be seen in figure 12.

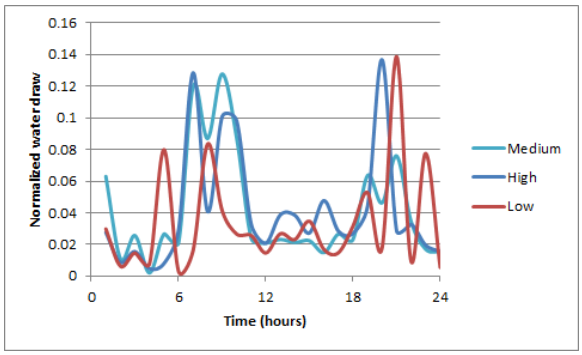

Figure 9a Comparing high, medium and low water draws for occupants away during office hours

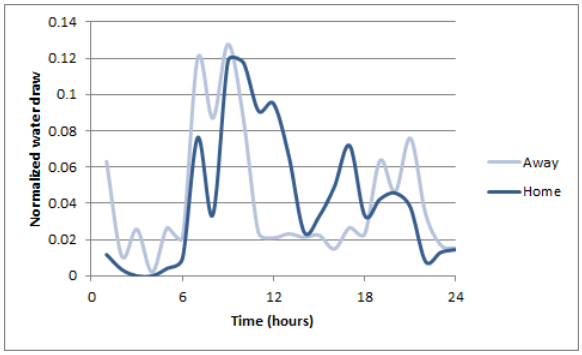

Figure 9b Comparing water draws when occupants are away or at home during office hours

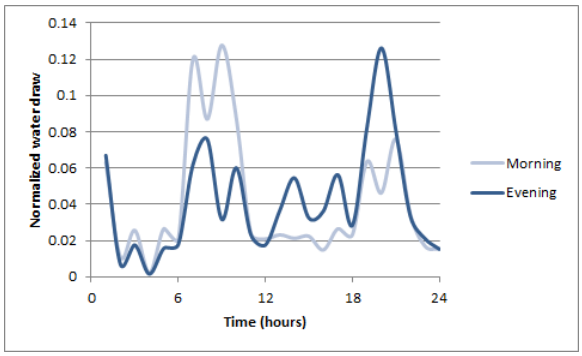

Figure 9c Comparing morning and evening biased water draw profiles

RESULTS

To demonstrate the functionality available through the model, integrated simulations were carried out for three representative weeks during winter, spring and summer. Provision of hot water from the heat pump was constrained to be available

only within certain times (in this case between 16:00 and 18:00) to allow its effect on tank temperatures and solar utilization to be clearly shown. The water use profile adopted as a base case is the medium use profile with morning biased draws and occupants away during office hours. While many aspects of system operation can be evaluated, a selection is given here which illustrate the potential useful model outputs.

Figure 10 shows results for the spring simulation. It shows the tank supply temperature (labelled tank top), temperature at the tank bottom and water supply from the heat pump to the tank heat exchanger (labelled ASHP to DHW) and also from the solar collector to the same heat exchanger. It can be seen that for this period there are significant inputs from the solar collector but the heat pump comes on only once i.e. when the tank temperature drops below the set point. Furthermore solar input heats the whole tank because the inlet is placed at the bottom. The sharp rise in tank top temperature on day 5 is because of immersion heater coming on as it follows its weekly schedule. As the immersion heater is at a mid-height in the tank it primarily heats the upper portion of the tank (which makes its effectiveness for tank sterilisation questionable).

This can be compared to the same draw profile when simulated for winter as shown in Figure 11. As expected there is less solar input and heat pump comes on more often. For the summer case (not shown), there are no instances of heat pump charging and all the hot water is serviced by the solar collector for all draw profiles.

These model outputs illustrate the seasonal variation in load shifting possibilities. The heat pump and boost heater can both in theory be used to absorb excess renewable generation when this is available but the amount that can be absorbed will depend on the specifics of the system state. This in turn depends on the solar inputs and the water draw patterns of the occupants. In periods when the potential for solar thermal energy inputs is likely, pre-charging of the water tank will be at the expense of solar inputs, and may eliminate potential gains. The appropriate use of the water tanks as renewable energy buffers is clearly situation specific, dynamic and complex.

Figure 12 shows a more detailed view of tank temperatures and water draw profile for a spring day for the medium use case with morning bias. There is a large draw in the morning and the temperature of all the sections drops but starting at around 0900hours the tank receives solar inputs and comes back up to temperature in time for the evening draws. Figure 13 shows similar data for a winter day. It can be seen that whereas tank temperatures drop for the lower sections as fresh water is drawn to make up for hot water draws the tank top is replenished by warm water from the lower sections and its temperature does not drop significantly with the tank coming up

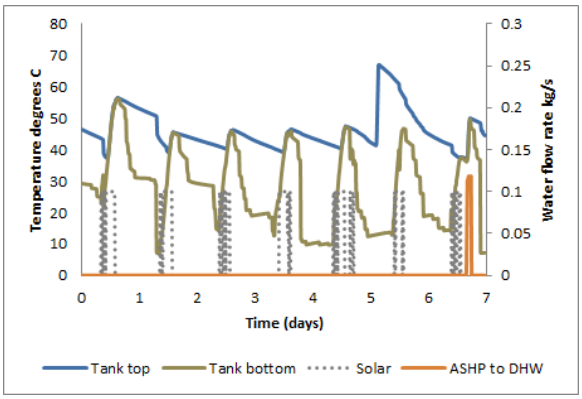

Figure 10 Tank temperature and heat supply to hot water tank, spring case

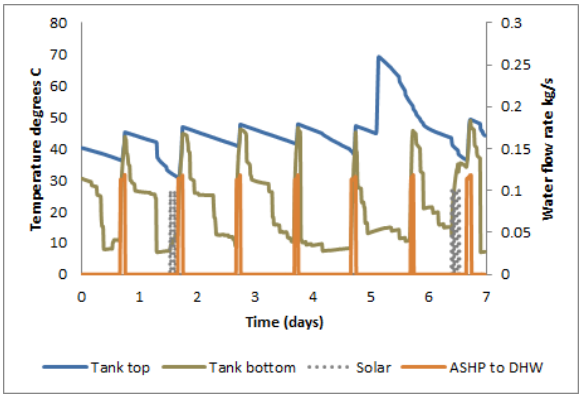

Figure 11 Tank temperature and heat supply to hot water tank, winter case

to temperature again after heat pump switches on at 1600hours.

Figures 12 and 13 show that for the specific water draw patterns on those days, heat from the heat pump is not required for the spring case where solar contributions are made early in the day but is required for the winter day where there is minimal solar energy input.

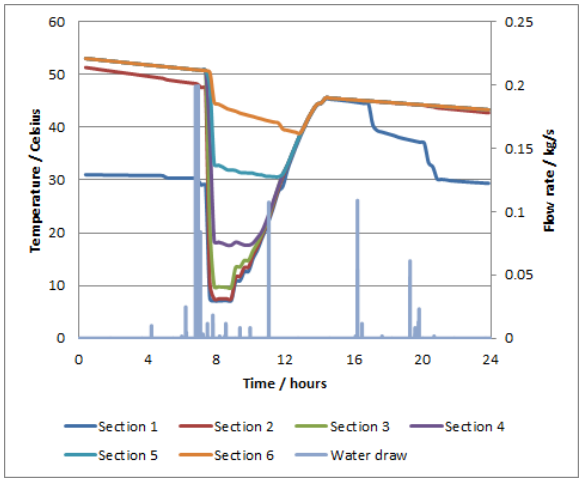

Figure 12 Tank temperatures at various heights and water draw, spring case (6 is top)

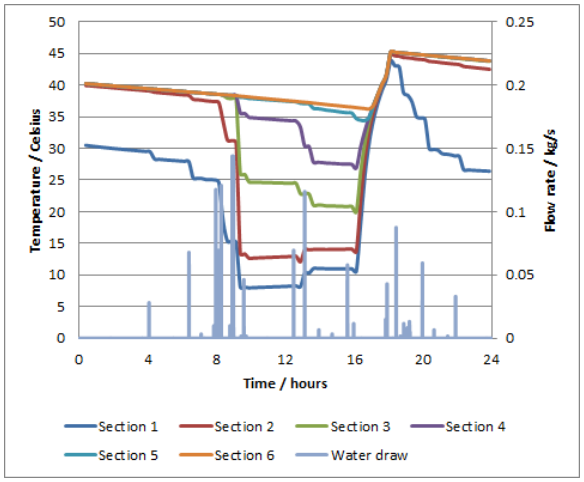

Figure 13 Tank temperatures at various heights and water draw, winter case (6 is top)

Figures 14a and 14b show the same data for the spring simulation as figure 12, but for the high water use case. It is assumed that this is the worst case for solar utilization because most of the draws are made early in the day when there might be no solar availability. Two consecutive days are shown and whereas the system delivers satisfactory heating on the first day, the supply temperature (section 6) is shown to be too low for comfort (< 38^0C) on the second day (heat pump held off). This illustrates violation of one of the constraints to be satisfied by any load shifting schema involving domestic hot water systems i.e. the delivery of hot water to meet occupant demands.

Load shifting studies were conducted for the various draw profiles. Winter season was focused on because this affords the most load shifting potential for the heat pump that is the major contributor to water heating during this time. For the base case simulation heat pump operation time is 1600-1800hours for hot water. Figure 11 shows that water heating takes place every day at this time. The water heating schedule was changed to be active at 0000-0200hours, 0600-0800hours and 1000-1200hours and the effect on tank temperatures and energy evaluated.

Figure 15 shows tank temperatures for the four times of operation. It can be seen that the 1000-1200hours case gives lowest temperatures. This situation can be mitigated by enabling the boost heater to become operative whenever the supply temperature drops below 38^0C and for brevity is not shown here.

The total energy used for these load shifting studies is given in table 3 that shows that more energy is used when water heating is done earlier rather than later. Such a heating pattern is obtained due to a number of, sometimes conflicting, reasons. These include water draw profile used, state of charging of the hot water tank and heat losses from the tank.

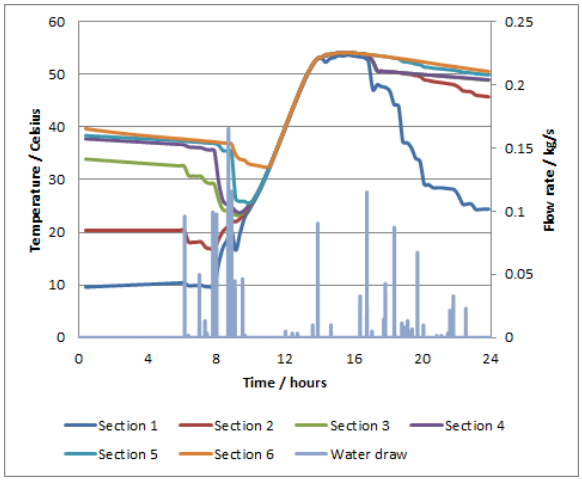

Figure14a Tank temperatures and water draw for spring day for high use, morning bias case. Solar energy easily meets demand.

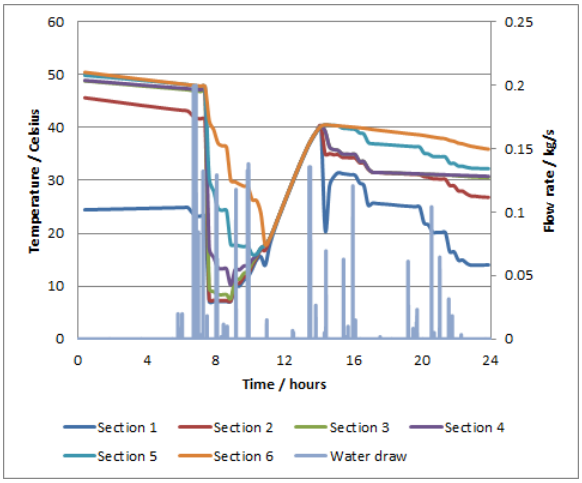

Figure 14b Same as figure 14a but for next day. Solar energy is not sufficient to meet demand and tank temperature falls because heat pump is off.

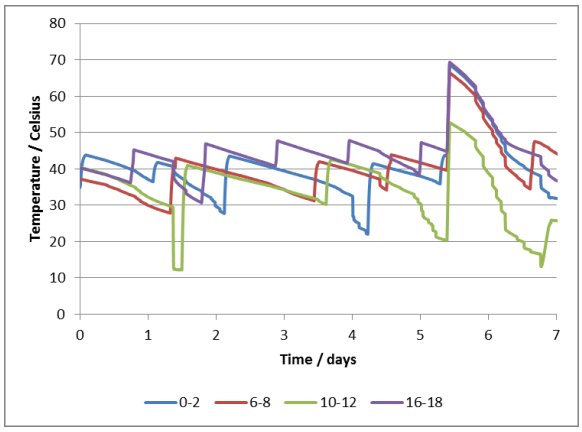

Figure 15 Tank top section (hot water supply) temperatures for different water charging scenarios.

Table 3 Tank heating energy for load shifting cases.

Heating allowed during this time	Heating energy delivered (kWh)
0000-0200	19.7
0600-0800	18.5
1000-1200	13.6
1600-1800	18.0

The requirement then is of a comprehensive parametric analysis to quantify feasible charging schedules, in the context of varying user demands and weather conditions, that:

1. Can be varied daily or in extreme cases more frequently.
2. Consider state of charge of the tank and possible energy and cost implications of remedial measures i.e. boost top up heating that may be required at peak demand hours when there is no renewable energy.
3. Take account of tank heat loss characteristics.
4. Optimize renewable energy utilization.

DISCUSSION

As stated in the introduction the purpose of the simulation modelling approach described here is to underpin various elements of the ORIGIN project i.e.

- Give insights and assist in the quantification of orchestration opportunities,
- Assist in the evaluation of proposed orchestration algorithms,
- Support investigations into improvements in system design to better support load shifting.

The modelling presented here to address these requirements is of necessity detailed and dynamic. This level of modelling is required in order to capture both the system specifics and the variations in weather and user behaviours. These systems and contexts are often presented in literature as simple storage nodes but in reality have complex behaviour that must be considered in detail where a practical implementation is being considered.

The future challenges being addressed in the ORIGIN project are:

1. To develop weather, renewable generation and user demand prediction algorithms that will give a 24hour look ahead.
2. To capture current system state and orchestration opportunities.
3. To determine the appropriate load shifting opportunities to be selected in order to best meet the optimisation objectives (enhanced use of local renewable generation).

These activities are ongoing and the work presented in this paper will provide a test bed to support these activities.

While the work presented here is primarily designed to support the ORIGIN objectives, several elements of the work are in themselves steps forward in the application of integrated modelling of detailed system performance and user behaviours in terms of representative sets of stochastic water draw profiles.

The focus of this paper has been on the hot water storage aspects of load shifting, similar consideration of space heating loads can also be supported by the same general modelling approach.

CONCLUSIONS

A detailed simulation model is developed and presented which has a sufficient level of detail to support load shifting analysis for practical domestic water heating systems of a type which is becoming increasingly common. The model consists of an air source heat pump supplying heat to an underfloor heating system and domestic hot water tank. Also included are a solar thermal collection system and top up / boost immersion heating system. All major thermodynamic domains are explicitly represented in an integrated fashion.

Research is focussed on water heating as this is a major shiftable load. For this purpose a number of water draw profiles are modelled and the effects on draw temperature and solar utilization are studied.

The use of this modelling approach in support of load shifting analysis is proposed and applications discussed.

ACKNOWLEDGEMENT

Grateful acknowledgement is made to the European Union Seventh Framework Programme (EU FP7) for funding made available to conduct this research within their project titled “Orchestration of Renewable Integrated Generation in Neighbourhoods” (URL 1).

REFERENCES

Clarke J and Tang D (2004). A co-operating solver approach to building simulation. Proc. ESim '04, Vancouver, Canada.

Daikin (2010). Solar kit for air to water heat pump system. Installation and Operation Manual. Altherma by Daikin. EKSOLHWAV1. Daikin London, UK.

EEA (2014). Huge renewable energy growth this decade if EU countries meet projections. European Environment Agency. http://www.eea.europa.eu/highlights/massive-renewable-energy-growth-this (accessed 31/03/2014)

ESRU (2001). ESP-r building simulation program. Energy Systems Research Unit. www.strath.ac.uk/esru (accessed 15/01/2014).

EST (2008). Measurement of domestic hot water consumption in dwellings. Energy Savings Trust

final report for Department for Environment, Food and Rural Affairs (DEFRA), UK. Crown Copyright 2008.

Grundfos 2005. Technical Data Sheet. Grundfos. uk.grundfos.com/content/dam/UK/Brochure/UPS2%20datasheet%20revised%201812%20.pdf (accessed 26/04/2014)

Hand J (2011). The ESP-r Cookbook. Strategies for Deploying Virtual Representations of the Built Environment. Energy Systems Research Unit, University of Strathclyde, UK.

Hendron B, Burch J and Barker G (2010). Tool for generating realistic residential hot water event schedules. Proc. SimBuild 2010, New York, USA.

Jordan U and Vajen K (2005). DHWcalc: Program to generate domestic hot water profiles with statistical means for user defined conditions. Proc. ISES Solar World Congress 2005, Orlando, USA.

Lorenzetti, D. M. 2002. Computational Aspects of Nodal Multizone Airflow Systems. Building and Environment 37 (2002).

SBS (2012). Scottish Building Standards. www.scotland.gov.uk/Topics/Built-Environment/Building/Building-standards (accessed 26/04/2014).

Thevenard D, Haddad K and Purdy J (2004). Development of a new solar collector model in ESP-r. Canadian Solar Buildings Conference, Montreal, Canada.

URL 1 (2014). http://www.origin-energy.eu/ (accessed 07/04/2014)

Wang W, Beausoleil-Morrison I, Thomas M, Ferguson A (2007). Validation of a fully mixed model for simulating gas fired water storage tanks. Proc. Building Simulation 2007, Beijing, China.

Williamson T (1995). A confirmation technique for thermal performance simulation models. *Building Simulation 1995*, Wisconsin, USA.

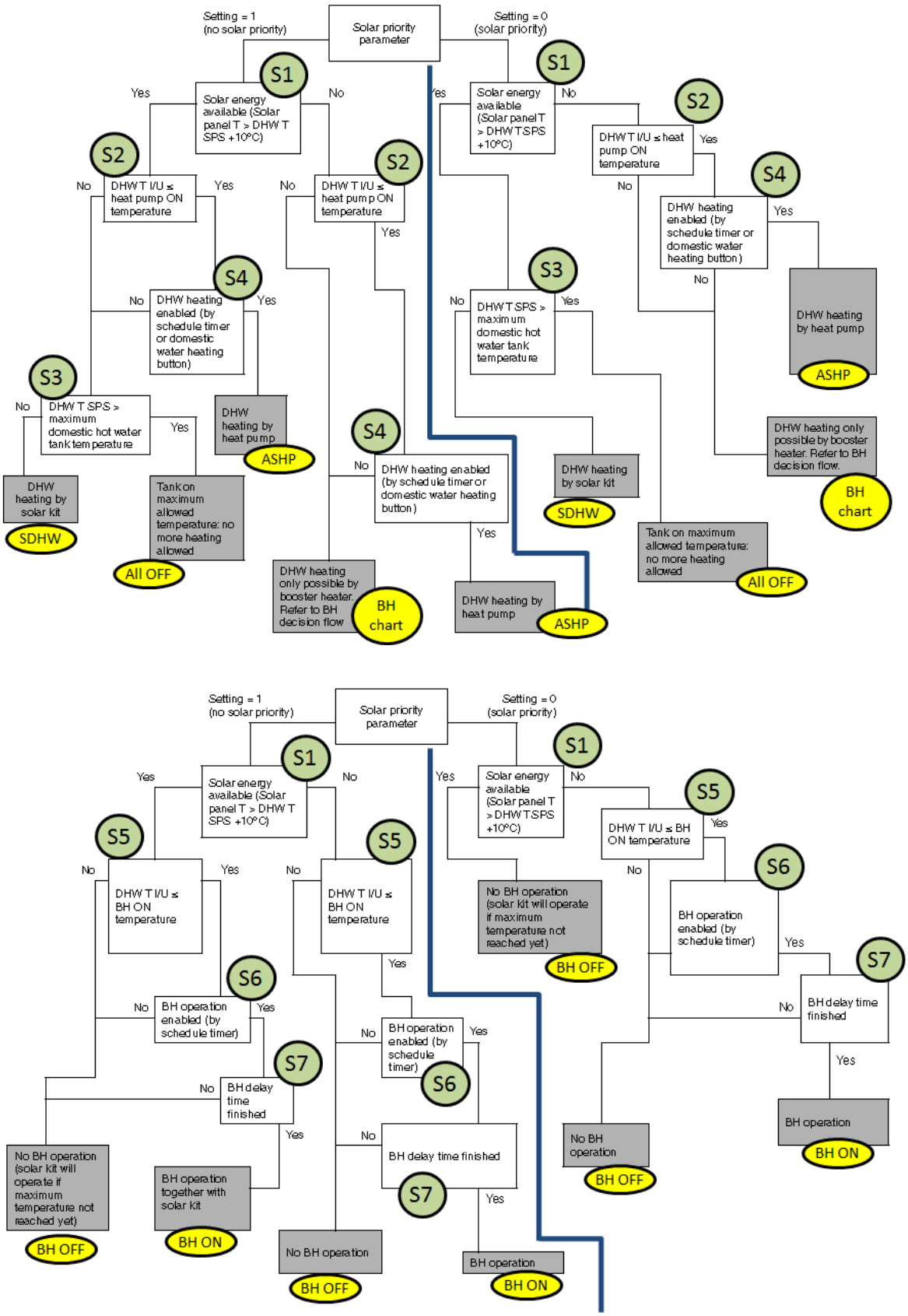

Figure 6 Manufacturer supplied control charts; solar collector control chart at top and boost (immersion) heater (BH) at bottom. These are annotated with required sensors (S1 to S7) and state of final operation (ON/OFF). Abbreviations used are ASHP for heat pump, SDHW for solar domestic hot water and BH for boost (immersion) heater.

Table 2 Control decomposition for heating system, showing contol type, description and control laws used for controlling immersion heater, solar collector and air source heat pump

#	**Control Type**	**Control description**	**Control law**	
1	Sensor	ON if T_SDHW > T_SPS + 10	ON-OFF	**Sensors**
2	Sensor	ON if T_IU <= T_ASHP Flow [ON temperature]	ON-OFF	
3	Sensor	ON if T_SPS > Maximum allowed temperature	ON-OFF	
4	Timer	ON if ASHP timer is ON i.e. 7-9 & 16-23	ON-OFF	
5	Sensor	ON if T_IU <= T_BHON	ON-OFF	
6	Timer	ON if BH timer is ON i.e. 0-6 & 16-24	ON-OFF	
7	Sensor	ON if BH delay time is finished	ON-OFF	
8	Logical operation	!S1		
9	Logical operation	!S2		
10	Logical operation	!S3		
11	Logical operation	!S4		
12	Logical operation	ON if !S1(S8) & !S2(S9)		Boost heater
13	Logical operation	ON if !S1(S8) & S2 & !S4(S11)		
14	Logical operation	ON if S12 | S13		
15*	Logical operation	ON if S5 & S6 & S7 *{no solar priority}* ON if !S1(S8) & S5 & S6 & S7 *{solar priority}*		
16	Logical operation	ON if S14 & S15		
17	Actuator	Sense: S16 Actuate: BH	ON-OFF	
18	Actuator	Sense: Operative Temperature Living Zone Actuate: Zone valve	Proportional	ASHP
19	Actuator	Sense: Operative Temperature Sleeping Zone Actuate: Zone valve	Proportional	
20*	Logical operation	ON if S2 & S4 *{no solar priority}* ON if !S1(S8) & S2 & S4 *{solar priority}*		
21	Logical operation	ON if S18 | S19 | S20		
22	Actuator	Sense: S21 Actuate: ASHP	ON-OFF	
23	Actuator	Sense: S21 Actuate: ASHP Pump	ON-OFF	
24	Actuator	Sense: S20 Actuate: ASHP-DHW valves	ON-OFF	
25	Actuator	Sense: S20 Actuate: ASHP-DHW valves	ON-OFF	
26*	Logical operation	ON if S1 & !S3(S10) & !S2(S9) *{no solar priority}* ON if S1 & !S3(S10) *{solar priority}*		SDHW
27*	Logical operation	ON if S1 & !S3(S10) & S2 & !S4(S11) *{no solar priority}* Always ON *{solar priority}*		
28	Logical operation	ON if S26 | S27		
29	Actuator	Sense: S28 Actuate: SDHW	ON-OFF	
30	Actuator	Sense: S28 Actuate: SDHW Pump	ON-OFF	
31	Actuator	Sense: S28 Actuate: SDHW valves	ON-OFF	
32	Actuator	Sense: S28 Actuate: SDHW valves	ON-OFF	

Abbreviations and Notes:

* These loops change from solar priority case to no solar priority case

Numbers preceded by S represent controller numbers in the table e.g., S12 represent controller 12 in the table

DHW = domestic hot water

SDHW = solar domestic hot water

T_ = temperature of

IU = tank internal unit (at two thirds tank height)

SPS = solar pump station

ASHP = air source heat pump

BH = boost (immersion) heater

BHON = boost (immersion) heater ON set point

& = logical AND function

| = logical OR function

! = logical NOT function

Research and Application of RCF Technology in Public Buildings

Radiant Ceiling plus Fresh Air

燕通科技（香港）有限公司
AirStar Air Conditioning Technology Group (HK) Ltd
思達環境科技有限公司
AirStar Environment Technology Group Ltd
燕通珠海環境科技開發有限公司
YanTong ZhuHai Environmental Science & Technology Ltd
www.yantong.cn

Research and Application of RCF Technology in Public Buildings

Author's Background

Mr. Jiguang Yan

* BS
* Senior HVACR Engineer
* RCF Patent Holder
* Director of CAR
* Vice Chairman of RACEC

Ms. Danna Xuedan Pan

* BS., MS.
* State Charted Engineer
* ASHRAE Member

Research and Application of RCF Technology in Public Buildings

Research and Application of RCF Technology in Public Buildings

1. BACKGROUND

1.1 Application Fact

- RCF, with radiant panel installed & fresh air supplied
- 40% energy saving verified
- 90% maintenance cost reduction proven

- Solved European product problem of condensation & low radiant intensity

Based on over 14-year research & 8-year empirical applications

Assessed on the thermal test for various envelope structures, seasons and different space functions

Patent achieved in China Mainland, Hong Kong, Singapore, Australia, Japan

Patent in progress for Europe, the USA

1.2 Author's Viewpoint

- The radiant heat transfer, **Stephen-Boltzmann's Law**, the foundation of the RCF
- Existing computing method for the convective air conditioning no longer appropriate to the RCF
- RCF's thermal figures should be obtained through experimentation
- Thermal radiation replaces thermal convection for more comfortable space cooling , achievable with less cost

Research and Application of RCF Technology in Public Buildings

2. THE MICRO-MECHANISM OF HEAT TRANSFER

2.1 Thermal Conduction, Convection & Fourier's Theorem

$$Q = -\lambda \, \mathrm{grad}\, t \quad W/m^2$$

- Foundation for the **AIR** conditioning

(Ref: Zhang Ximin and Ren Ze, 1993)

Research and Application of RCF Technology in Public Buildings

2. THE MICRO-MECHANISM OF HEAT TRANSFER

2.2 Thermal Radiation& Stephen-Boltzmann's Law

$$Q_{12} = C_{12}\,\Phi_{12}F_1\left[\left(\frac{T_1}{100}\right)^4 - \left(\frac{T_2}{100}\right)^4\right] \quad W/m^2$$

- Stephen-Boltzmann's Law

- Features of thermal radiation
  - Happens between any objects (T> 0 ˚K)
  - Has strong direction (b/t object – object)
  - Transfers by electromagnetic waves
  - Accompanied with twice energy exchange
    - Heat power firstly converts to electromagnetic waves which reach the object
    - The waves are then absorbed by the object through the changed style of heat energy

    (Ultimately demonstrate by the variation of the object's T)
  - The waves can travel in a vacuum (**AIR** unnecessary as a medium)
  - Transfer rapidly (as the light speed)

- **RCF, based on Stephen-Boltzmann's Law**

Research and Application of RCF Technology in Public Buildings

3. THERMAL ANALYSIS OF THE RCF TECHNOLOGY

3.1 RCF Application Background

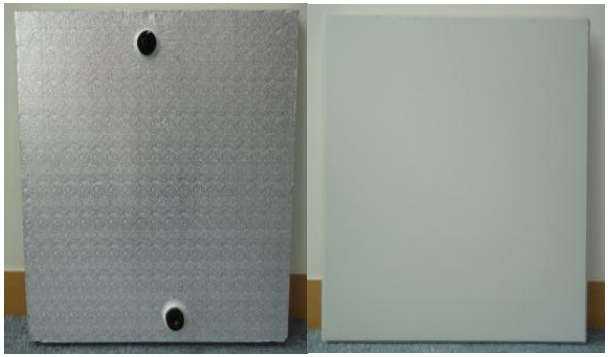	
RCF Patent Panel (standard)	RCF Patent PAU

Research and Application of RCF Technology in Public Buildings

3. THERMAL ANALYSIS OF THE RCF TECHNOLOGY

3.1 RCF Application Background

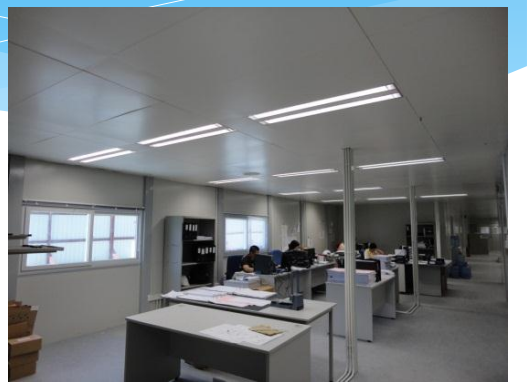

- The client, Cathy Pacific Services Limited
- AEM, Active Energy Management, British, to evaluate this RCF system
- Three consecutive days testing/recording, in July, 2010

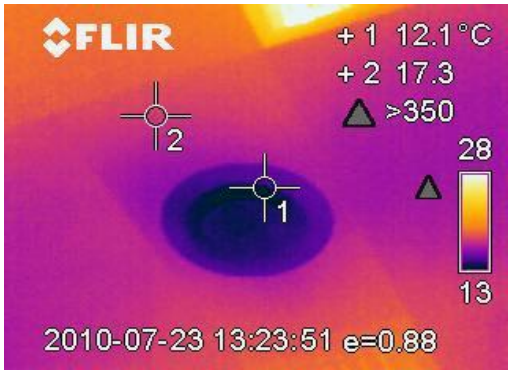

RCF Operative Photo, July 23, 2010, Image Courtesy of AEM

(Ref: Phil Healey, et, 2010)

Research and Application of RCF Technology in Public Buildings

3. THERMAL ANALYSIS OF THE RCF TECHNOLOGY

3.2 RCF Testing Data

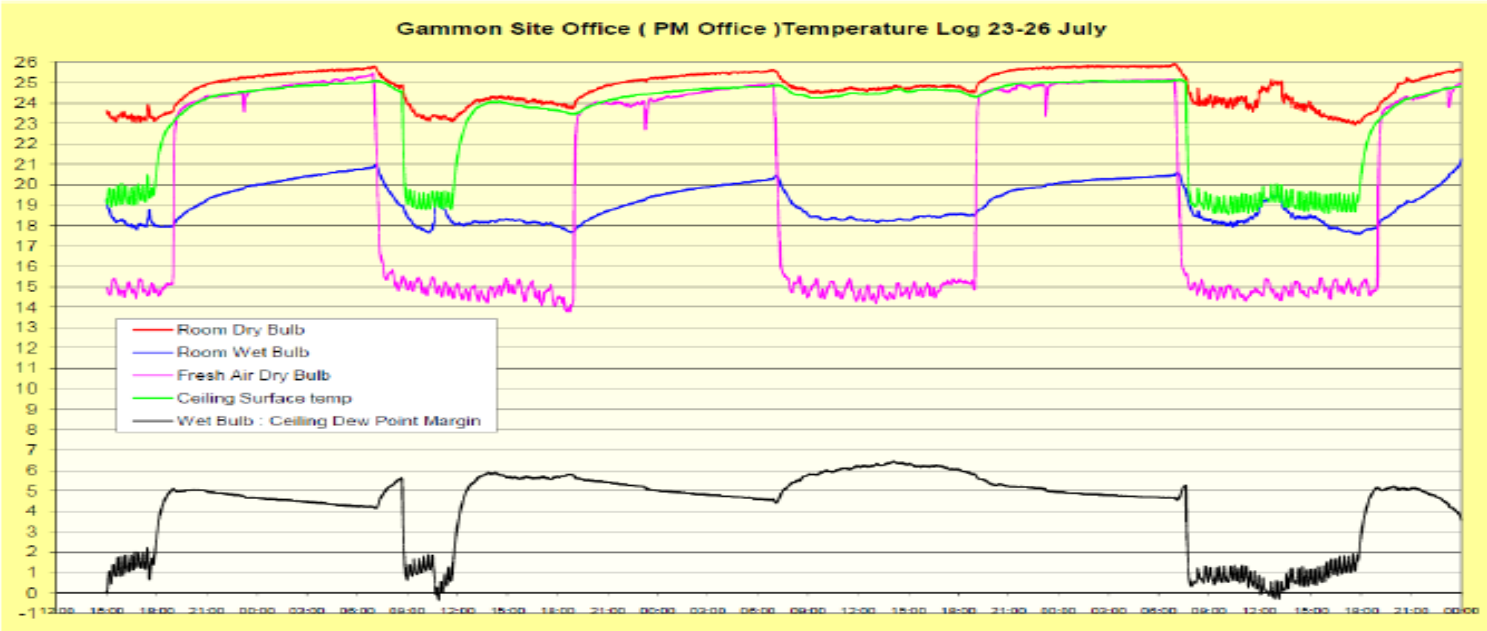

- Excellent IAQ
- Even T distribution
- Only ± 0.5 ˚C T fluctuation

(Ref: Phil Healey, et, 2010)

Research and Application of RCF Technology in Public Buildings

3. THERMAL ANALYSIS OF THE RCF

3.3 RCF Testing Report by AEM

- **Indoor data**: T_{DB}=23˚C, RH = 60%, **T_P = 17.1˚C** and **T_{WI} = 21˚C**

NO condensation, in Hong Kong, a humid region, in the hottest and wettest season

- **Key Finding**: T_{WI} = 21˚C < T_{AI} = 23~24˚C, i.e. **T_{WI} distribution with RCF** system, **unlike** the T_{WI} in the space used **traditional air conditioning**

- **Higher indoor comfort level,** compared to the traditional air conditioning

Research and Application of RCF Technology in Public Buildings

3. THERMAL ANALYSIS OF THE RCF APPLICATION

3.4 Thermal Calculation Based on Thermal Convention Theory

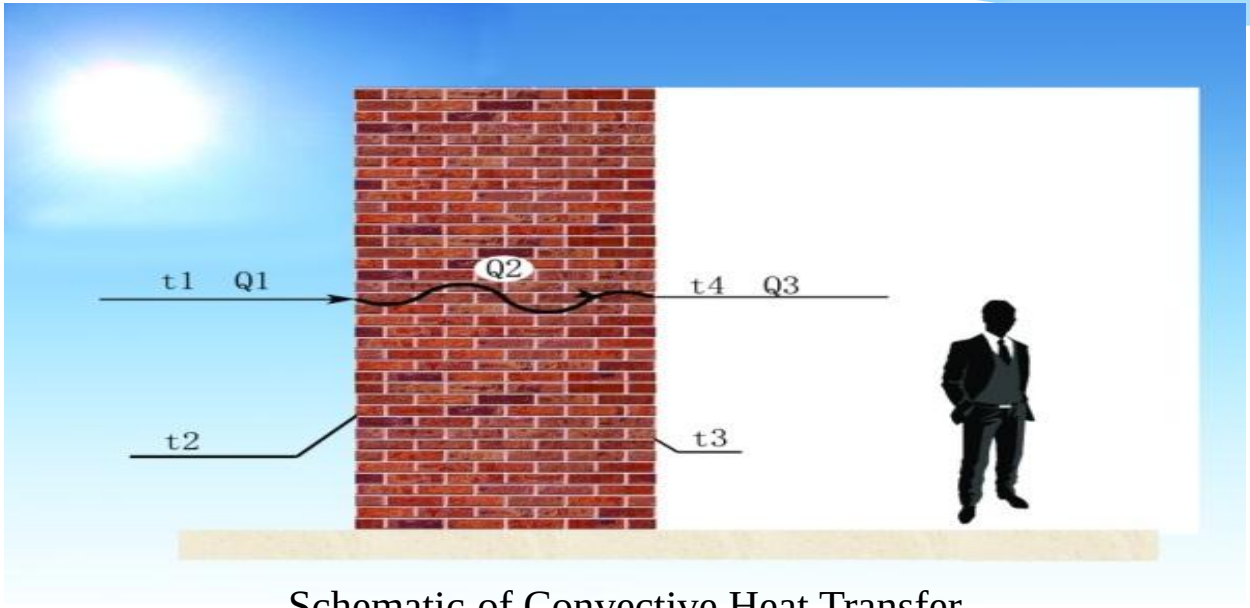

Schematic of Convective Heat Transfer

- In line with the traditional air-conditioning thermal model
- Based on the continuity characteristics of mathematical equation
  - Should have $Q_1 = Q_2 = Q_3$, as known by the Fourier's Law
  - The prerequisite of $t_1 > t_2 > t_3 > t_4$ has to be satisfied
  - But it hasn't, see section 3.5

Research and Application of RCF Technology in Public Buildings

3 THERMAL ANALYSIS OF THE RCF APPLICATION

3.5 Thermal Calculation According to Thermal Radiation Model

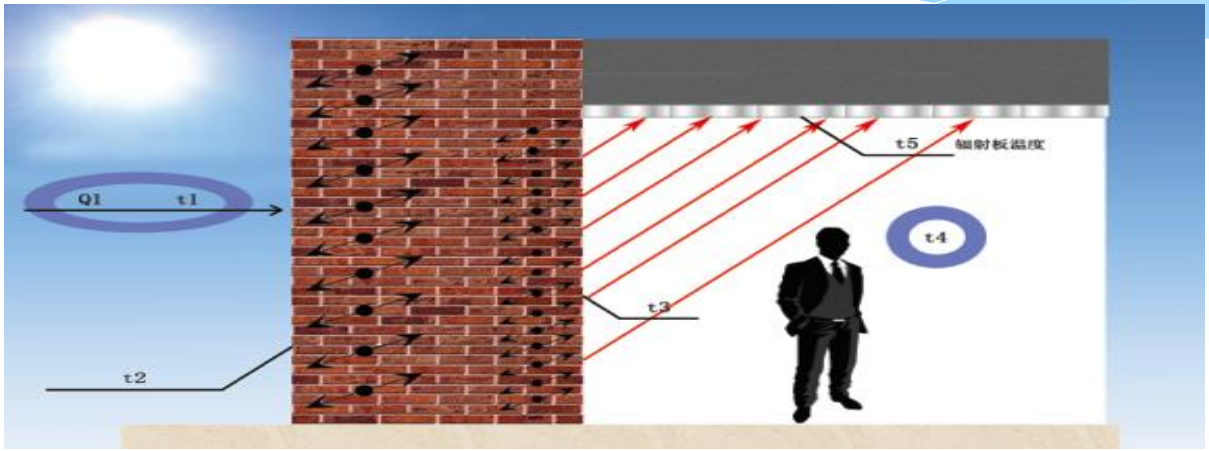

Diagram of Radiant Heat Transfer (Derived from the fore-mentioned infrared photo)

- **Space scenario with the RCF System applied**
  - Temperature pattern: $t_1 > t_2 > t_3 <$ **t_4**
- **Why?** The **direct radiation** between surfaces exists:
  - $t_3 < t_4$, **when** $Q_{WI\text{-}P} > Q_2$
- $t_3 < t_4$, also a result of the **AIR** is "transparent" in the thermal radiation process, **in line with the Stephen-Boltzman's law**

Research and Application of RCF Technology in Public Buildings

3. THERMAL ANALYSIS OF THE RCF APPLICATION

3.6 Heat Transfer Investigation through Walls in Thermal Radiation Model

- Based on the traditional air-conditioning theory
  - $Q_{RCF} > Q_{AC}$ because the t_3 of the RCF < t_3' of the traditional air-conditioning
  - **QUESTIONING** how the RCF system can save more energy

- Based on the micro heat transfer & thermal radiation
  - The molecule in the wall structure vibrating, T_W raised up, the molecule kinetic energy rise
  - This kinetic energy transmits to the inside wall with macro-performance of the elevated interior wall surface temperature T_{WI}
  - Simultaneously the molecule near the interior surface of the wall get the cold radiation from the chilled panel with constant momentum lose
  - Consequently $t_3 < t_4$, when $Q_{WI-P} > Q_2$
  - Due to $t_3 < t_4$ exists, Q_{WI-P} could be more and more close to 0, Consequently Q_1 & Q_2 would be zero too

Research and Application of RCF Technology in Public Buildings

3. THERMAL ANALYSIS OF THE RCF APPLICATION
3.7 The Author's Inference

- $t_3 = t_4$ or $t_3 < t_4$ working conditions exist in the RCF system
- Dissimilar thermal scenarios between RCF & traditional air conditioning
- The thermal calculation model for the traditional air-conditioning, no longer suitable to the RCF system

- The efficiency of panels' heat exchange
  - Depends on radiant panels' structure & configuration
  - Vary for different products from different manufacturers
  - Data should be gained through application model

- The specified testing parameter achieved for one pattern of panel can only be proper to this type of panel itself

Research and Application of RCF Technology in Public Buildings

4. HUMAN COMFORT LEVEL AND RCF SYSTEM LOAD STUDY

4.1 Thermal Comfort Analysis in a RCF Room

- Human Thermal Comfort
  - Head T, 32˚C
  - Clothing surface T, 28˚C
  - All surfaces T ≤ person's body T
  - ΔT of human head and radiation ceiling,14.5˚C
  - 10.5˚C T distinction for the human clothing and ceilings

- The occupant, in **an environment with strong radiative heat transition** & **powerful cold feeling**

(Ref: Phil Healey et, 2010)
(Ref: Sam. C. M. Hui et, 2012)

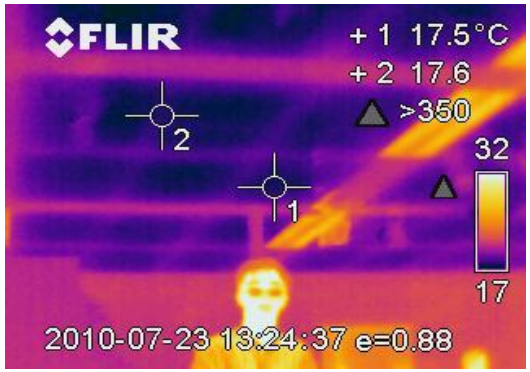

Infrared Image of Human and Enclosures with RCF System
Image Courtesy of AEM

Research and Application of RCF Technology in Public Buildings

4. HUMAN COMFORT LEVEL AND RCF SYSTEM LOAD STUDY

4.1 Thermal Comfort Analysis in a RCF Room

- Enclosures
  - All inner surface with about ΔT of 5˚C with the cool ceilings (22.5˚C, 17.5˚C)

- RCF Performance Characteristics
  - Tracing the heat source of human which only has a few load to the RCF panel
  - T of **all interior surfac**e to the radiant panel, relatively very low compared to AIR conditioning (ΔT b/t indoor air and supplied air is larger than 5˚C)
  - Much lower energy consumption against AIR Conditioning for the same comfort level

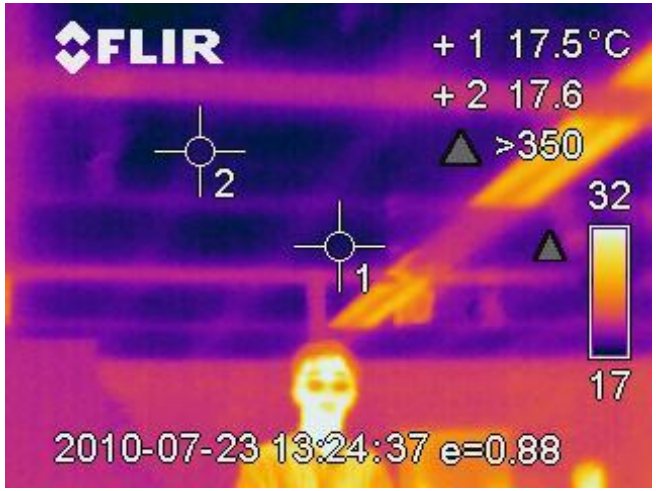

(Ref: Phil Healey et, 2010)
(Ref: Sam. C. M. Hui et, 2012)

Research and Application of RCF Technology in Public Buildings

4. HUMAN COMFORT LEVEL AND RCF SYSTEM LOAD STUDY

4.2 RCF Start-up and Running Load

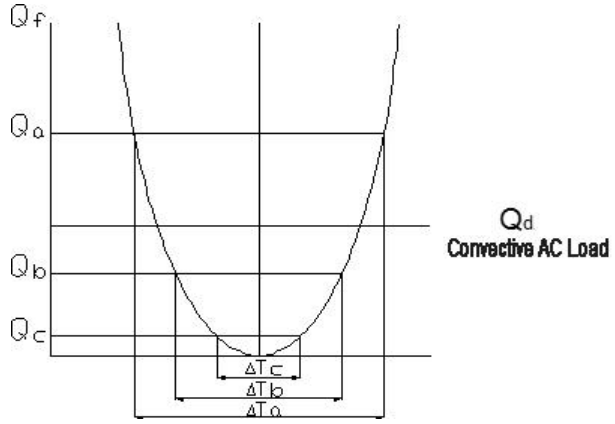

RCF System Start-up and Running Load Curve

- "a" startup stage with the maximum load
- "c" status, typical operative phase with extremely low load
- T_P of ceiling surface can be stabilized at a certain level
- The enclosure surface T should progressively approach to the T_P, consequently less and less running capacity would need for the RCF system

- The site assessment on the PMV and PPD comply with ASHRAE Standard

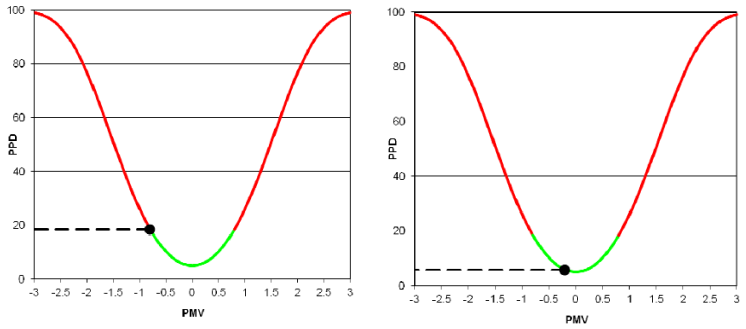

(Ref: Sam. C. M. Hui et, 2012, Phil Healey, et, 2010)

Research and Application of RCF Technology in Public Buildings

5. RCF APPLICATION IN JINWAN AVIATION EXHIBITION CENTER

5.1 Architectural Background

- Emblem building in Zhuhai
- Exhibit the City's planning & design on high-tech project and green low-carbon scheme
- Construction area of 6,000 M^2 including 1,600 M^2 office area
- Post-modernism architecture design

	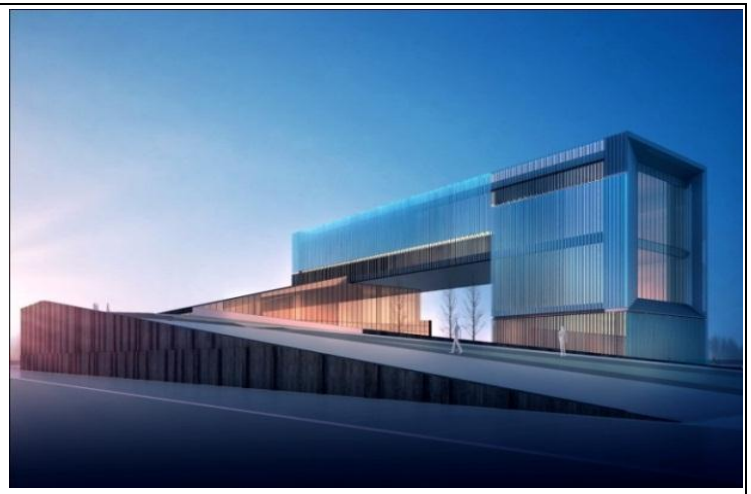
Front View	Back View

Research and Application of RCF Technology in Public Buildings

5. RCF Application in Jinwan Aviation Exhibition Center

5.2 RCF Design Factor

RCF System Installed	VAV System Required
75 w/m2	165 w/m2

5.3 RCF Chillers Installed

Equipment	Specification, KW	Motor Power, KW	Unit	Qty.
Air-cooled Heat Pump	193.5	52.8	Pcs	2
Air-cooled Heat Pump	64.5	17.6	Pcs	1

◆ **RCF decreases 55% chiller installation capacity compared to original design**

Research and Application of RCF Technology in Public Buildings

5. RCF Application in Jinwan Aviation Urban Planning Exhibition Center
5.4 RCF Indoor Operative Data and Photo

- Indoor operative data satisfies the standard of ASHRAE55-2010.

Panel Surface T	Wall Surface T	RH	CO_2 Content
17.5 ℃	22 ℃	58~65%	500~750 PPM

Research and Application of RCF Technology in Public Buildings

5. RCF Application in Jinwan Aviation Exhibition Center

5.4 RCF Indoor Operative Data and Photo

Reception

Large Space Exhibition Hall

Multimedia Centre

Conference Room

Research and Application of RCF Technology in Public Buildings

5. RCF Application in Jinwan Aviation Exhibition Center
5.5 RCF Application Contribution

- Principally difficult for it to achieve the goal of low-carbon green building
- RCF technology application makes this goal fulfilled
- Applying China Green Building Label

Research and Application of RCF Technology in Public Buildings

6. CONCLUSION OF RCF APPLICATION

6.1 RCF Study Outcome

- Better regulate human comfort level through the thermal radiation
- Advance indoor air quality by deeply dehumidified fresh air and discharge of CO_2 without sacrifice human comfort
- Solved European problem on this kind of product application
- Inspire more and more scholars/engineers to take part in thermal radiation research and development, such as HKU, AEM, HKIE, CIBSE and so on

Research and Application of RCF Technology in Public Buildings

6. CONCLUSION OF RCF APPLICATION
6.3 Author's Viewpoints

- Energy expense hugely vary for different heat transfer methods
- Cooling equipment start-up capacity and regulating ability for partial load are particularly vital
- Ceiling thermal radiation cannot be analyzed based on convective heat transfer
- Suitable for office building, shopping mall, restaurant, airport, pharmaceutical factory, exhibition center and many other sites

(Ref: 2011~2012 Report, HEACO, Swire, HK)

Research and Application of RCF Technology in Public Buildings

6. CONCLUSION OF RCF APPLICATION

6.4 RCF Conclusion

- RCF with Distinct Features of :-
  - Uniform panel surface temperature
  - Higher radiative intensity
  - Effective air treatment by PAU with super dehumidification capacity
  - Unique & Intelligent control logic
  - Entirely solve the condensation problem in cold operation mode
  - Remote monitoring and operating
- RCF Main Benefits to the Clients/Society:-
  - Excellent IAQ
  - At least 40% energy saving
  - At least 50% maintenance cost reduction
  - NO air draught feeling
  - NO noise
  - Save ceiling void at least 0.3M compared to VAV
  - No need for setting chiller plant rooms on the upper level of the high-rise building
  - Prevent cross-infection due to no air re-circulation
  - Successfully used in many projects in Mainland, Hong Kong

Research and Application of RCF Technology in Public Buildings

AIRSTAR MISSION

Saving energy while improving quality of life
Building a better environment for future generations

Research and Application of RCF Technology in Public Buildings

Thanks

燕通科技（香港）有限公司
AirStar Air Conditioning Technology Group (HK) Ltd
思達環境科技有限公司
AirStar Environment Technology Group Ltd
燕通珠海環境科技開發有限公司
YanTong ZhuHai Environmental Science & Technology Ltd
www.yantong.cn
master@yantong.cn dannapan@yantong.cn

Research and Application of RCF Technology in Public Buildings

7. REFERENCES

ASHRAE, 2013, *"2013 Handbook-Fundamental, Thermal Comfort"*, American Society of Heating, refrigeration and Air-Conditioning Engineers, Inc. Atlanta, American

HEACO, *"Sustainable Development Report 2011&2012"*, HK Airport, Swire, www.heaco.com

Phil Healey, et, 2010, *"Chilled Ceiling Trial Interim Data/Preliminary Report"*, AEM, Active Energy Management, HK Airport

Sam C.M. Hui, Janita Y. C. Leung, 2012, "T*hermal Comfort and Energy Performance of Chilled Ceiling System"*, HK-Fuzhou ASHRAE Chapter, University of Hong Kong

Stanley A. Mumma, *"Overview of Integrated Dedicated DOAS With Parallel Terminal Systems"*, 2001a, ASHRAE Transaction107

Stanley A. Mumma, 2002, *"Chilled Ceiling in Parallel with DOAS"*, ASHRAE Transaction

Wu Qiang and Guo Gunagcan, 1996, *"Optics"*, University of Science and Technology of China Press

Zhang Ximin and Ren Ze, 1993, *"Heat Transfer"*, High Education Press

Development of a Portable Wireless Sensor Network to Enhance Post-Occupancy Commissioning

Sarah Noye[1] PhD candidate
Dr. Robin North Lecturer
Prof. David Fisk Professor
Laing O'Rourke Centre for System Engineering and Innovation
Imperial College London
London, UK

ABSTRACT

In many modern buildings, a performance gap between as-designed and as-operated energy consumption is observed. Through the building life cycle, different commissioning strategies can contribute to reducing this gap. However, before considering the implementation of in-use commissioning measures, it is important to ensure the initial realisation of the design performance. With growing energy challenges, commissioning needs to include energy performance, but the commissioning program usually gets compressed as its principal activities occur toward the end of projects. We propose to extend commissioning to a post-occupancy commissioning (PO-Cx) process. The feasibility of PO-Cx relies on the availability of a low-cost set of appropriate data. This paper presents the initial development phase of a pop-up monitoring™ toolkit using a wireless sensor network system to perform commissioning during the initial year of occupation of a building. Initial results for a simple air conditioning case are presented showing the potential of the method.

INTRODUCTION

From initial design to building operation, various discrepancies can make realised energy consumption disappointing (Bordass et al. 2001; Menezes et al. 2012). Through the building life cycle, different commissioning strategies can contribute to remedying those discrepancies and to reducing the gap between as-designed and as-operated energy efficiency. Annex 40 (Visier 2004) of the International Energy Agency's Energy in Buildings and Communities Programme classifies commissioning processes into initial commissioning (I-Cx) for new buildings, retro commissioning (Retro-Cx) and re commissioning (Re-Cx) for existing buildings, and ongoing commissioning (O-Cx) for commissioning measures running continuously in contrast to the previous types that are all one-off processes.

O-Cx is increasingly recognised as an efficient energy saving measure (Djuric & Novakovic 2009; Keuhn & Mardikar 2013). However, before considering the implementation of O-Cx or other in-use commissioning measures, it is important to ensure the good realisation of the initial design performance. Some significant inefficiency could otherwise go unnoticed as most monitoring methods use 'normal operation' data as a baseline to detect performance degradation (Katipamula & Barambley 2005; Teyssedou et al. 2013). This design realisation check should happen during I-Cx in addition to compliance and 'health and safety' checks.

In the context of growing energy challenges, I-Cx needs to be extended to include energy performance. As the principal I-Cx activities occur toward the end of projects, where time is running out and money is running low, the commissioning program tends to get compressed (York 1988). The building is often delivered when 'practical completion' is reached, which means that, while the building is ready for occupation, there is rarely the opportunity to optimise its energy performance, and to account for variation between the as-designed occupancy pattern and as-operated.

To overcome these barriers the initial construction process needs to extend beyond handover into the early occupation of the building. In 1999, the Probe (post-occupancy review of buildings and their engineering) project looked at 16 newly built non-domestic buildings to identify ingredients for success and common operating issues to provide practical feedback for the building services industry (Cohen et al. 2001). This lead to the introduction of the Soft Landing framework (Way & Bordass 2007). Soft landing is based on

[1] Corresponding author: s.noye11@imperial.ac.uk

the Probe methodology and aims to keep members of the design and construction team involved in the first three years of the building's operation to facilitate a smoother transition between stakeholders and provide feedback to improve the building industry delivery of future projects. Probe and soft landing post-occupancy evaluations mainly use information from questionnaires to occupants and ready available data such as utility bills.

On the system operation side, Isakson et al. (2004) proposed to implement systematic reporting using the available building management system (BMS) data to perform seasonal commissioning. They developed a visualisation tool that enabled the identification of a significant number of problems, such as outdoor temperature sensor malfunction, or the ventilation system operating longer than expected at night. This method relies on the BMS system being fully functional. However since BMS requires all the other systems' commissioning to be completed, and is usually commissioned last, it is likely to have some deficiencies. Painter et al. (2012) used a sensor overlay with standalone data loggers to understand the behaviour of a naturally ventilated building and perform seasonal commissioning of its BMS system. The availability of this additional data provided insight on the building operation, but took an extensive time to collect and one of the authors' recommendation was to use wireless sensors to collect the data.

Indeed, the feasibility of post-occupancy performance evaluation relies on the availability of a low-cost set of appropriate data. The rapid evolution of wireless sensor network (WSN) technology is recognized to provide an opportunity for the building industry (Vähä et al. 2013), in particular for energy consumption reduction and system operation (Heller & Orthmann 2014). Among the identified benefits of WSN for building monitoring and control are fast installation, reduced disruption of building activity (Healy 2005; Jeong et al. 2008) and lower cost compared to wired systems (Kinter-Mayer 2005).

In this paper we propose to extend the I-Cx phase by introducing systematic post-occupancy commissioning (PO-Cx) of new and refurbished buildings. We describe a Portable Wireless Sensor Network (PWSN) system developed to perform pop-up monitoring™ to support extended commissioning during the initial year of occupation of a building. The PWSN collects real-time data in addition to the existing BMS to support building fine-tuning and performance evaluation, taking advantage of the flexibility of wireless communication to reconfigure the monitoring system depending on PO-Cx needs. The system links together four categories of data often considered separately: occupant comfort, energy consumption, system operation and operation conditions

The following section describes PO-Cx and the requirements for a data gathering system to perform it on a common ventilation system. Pilot tests for the PWSN and their results are then described, before discussing the potential of PWSN for PO-Cx.

SYSTEM REQUIREMENTS

Post-occupancy commissioning framework

The first year of operation of a building has a strong bearing on its future operation as this is when Facility Management (FM) takes ownership of the building and learns how to operate its systems. If setting and control problems remain from I-Cx, there are risks that the system will be controlled manually to supress occupant complaints. This may result in conditioning loads running at maximum and even potentially working against each other. There is a missed opportunity during the liability period to move from a merely compliant building to a successful building. The main contractor is usually required to come back to repair defects and solve complaints if the client requires it. The resources allocated for that purpose could be turned into a building performance verification process, namely PO-Cx, which would result in reduced operation cost for the client and better referencing for the contractor.

The proposed scope of PO-Cx includes:

- Systematic performance checking
- Seasonal commissioning
- Solving occupant complaints
- In-use building evaluation

Performance checking consists of evaluating the energy efficiency of the building system to

deliver indoor comfort. This can be done in several ways depending on the means available. It can range from benchmarking of simple performance metrics combined with data trend analysis to feeding back live data to design models to spot divergences.

Seasonal commissioning would normally be part of standard commissioning contract. It consists in fine-tuning heating and cooling loads to ensure settings are adapted to external climate. In practice, this is often done by choosing a cold winter day and a warm summer day to test extreme loads. This might not be representative to the average day of building operation and BSRIA recommend making provision for part-load commissioning as well (Sands 2013). Longer term monitoring could enable fine-tuning of the different intermediate loads of the building.

Solving occupant complaints would already be included in the liability contract, but the availability of easily deployable sensors to collect relevant data could reduce engineering time to solve the problem while providing a more efficient solution.

Since building purposes often change between the original brief and handover, the PO-Cx period could also be used to evaluating the building-occupant interaction and evaluate which parts of the performance gap come from design and construction problem and which ones come from the building usage. This would include comparison of the actual occupancy schedule with design assumptions and evaluate how well the occupants use the building.

Building data

To realise the tasks above mentioned requires extensive data. The different elements of data required to understand building operation performance are summed up in Figure 1. Part of this data would generally be available in new non-commercial buildings, but in a fragmented way.

System data is generally monitored by BMS. Its purpose is to manage operation and maintenance on a daily basis. It can be used to change the system's operation or to detect fault through alert messages. The available data is not used for long-term analysis and it might not be possible to do as the data is often not stored for more than a few weeks.

Energy data is available through utility meters, but while this general overview can give an interesting indication about the overall building operations, it cannot identify where inefficiencies come from. Sub-metering can then provide better temporal and spatial granularity and is required by the British building regulation for some facilities. The quality of the data obtained would typically depend on the design of the building services distribution network (especially gas and electricity).

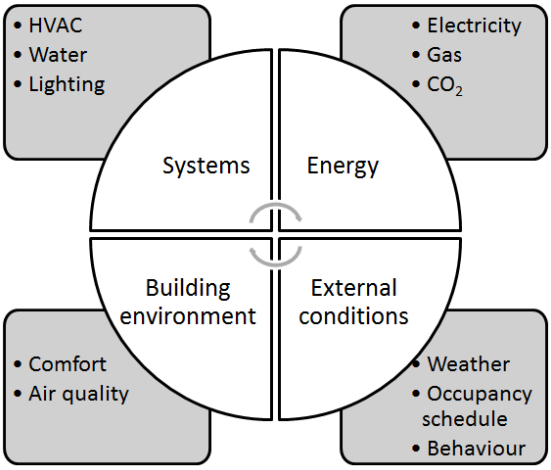

Figure 1. Relevant building data

It is technologically possible to integrate energy and BMS data but the hardware will usually have been obtained from different manufacturer which implies compatibility and integrity issues.

Comfort data would most likely be limited to one BMS temperature reading per heating/cooling zone and external condition to standard normalisation assumptions like yearly degree days for the weather.

Ventilation case

The intention is to apply PO-Cx to building systems in general including HVAC, water distribution and lighting. In the first instance, since HVAC is the biggest share of building energy consumption and air systems are the most challenging to measure, we will focus on ventilation systems. The following section presents the data requirements for PO-Cx of a common ventilation system.

Figure 2 represents the trial system considered in this study. It includes a room and an Air Handling Unit (AHU) with heat recovery. Table 1 summarise the data requirement for PO-Cx of the ventilation system from Figure 2. The typical values are considered in the UK context. Plant measurements are not considered here as we focus on the ventilation part of the system. Additionally BMS data would be more intensive for this part of the system, thus requiring less additional data. The weather data can be monitored on site or they can be imported from a suitable local weather source.

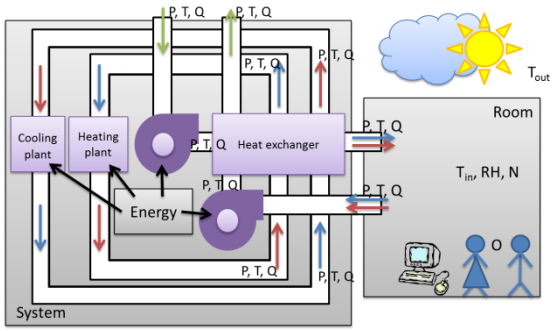

Figure 2. Single ventilation system with AHU

Table 1. Monitored parameters

	Parameters	**Typical values**
System	Temperature Pressure Flow rate Pipe temp.	-40 – 200°C 0 – 2500 Pa 0 – 50 m^3/s 0 – 80°C
Energy	Electrical power	NA
Building environment	Temperature Humidity Radiant temp. Air changes CO_2 level	10 – 30°C 40 – 70 % 0 – 40°C 0 – 60 /h 0 – 2000 ppm
External conditions	External temp. Occupancy	-12 – 32°C NA

Portable Wireless Sensor Network

A sensor network to perform PO-Cx needs to be low cost to limit the capital cost of the process. As the building will be in use and only a minimum of disruption is acceptable, the network would need to be easily deployable. Since the different PO-Cx tasks require more or less data for a more or less extended period of time, the system need to be scalable and flexible. Wireless sensor networks are a good way to achieve all of these objectives.

The authors have previously introduced the concept of a portable wireless sensor network that can be deployed during the first year of operation of a building to perform PO-Cx (Noye et al. 2013). As shown on Figure 3, this system is composed of a meshed network of wireless sensors that sends measurements to a gateway. The data can then be retrieve on site via a mobile device or off-site via a web server.

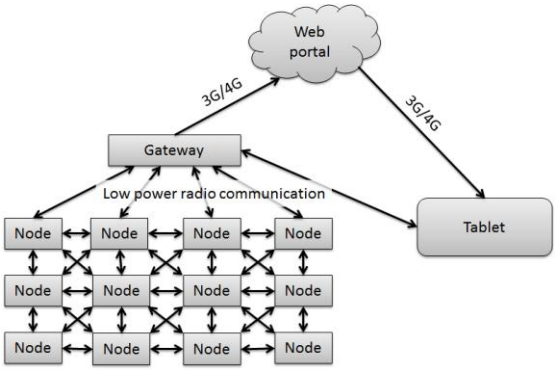

Figure 3. PWSN architecture (Noye et al. 2013)

The different sensing nodes considered to monitor the ventilation system from Figure 2 are summarised in Table 2.

Table 2. Node types description

	Sensors	**Parameters**	**Location**
1	Temperature	Temperature	Room
2	CO_2 Temperature Humidity	CO_2 level Temperature Humidity	Room
3	Radiant temp.	Radiant temp.	Room
4	Passive infra-red	Occupancy	Room
5	Temperature	Pipe temp.	System
6	Temperature CO_2 Humidity Air flow	Air temp. In/out CO_2 Air humidity Flow at vent	System
7	Current Voltage	Electric power	System

Nodes 1 to 5 are commercially available wireless solutions from a BMS manufacturer based on the Zigbee protocol. Node 6 and 7 are self-developed using the architecture showing in Figure 4.

The main development constraint is to find sensors that consume little energy as the nodes need to be deployable for several months with little intervention. In the following section some sensor are tested to assess their suitability for the PWSN.

EXPERIMENRAL METHODOLOGY

Sensor evaluation

To select a sensor for a specific application, it is necessary to consider the following factors: range, accuracy, precision, tolerance, linearity, sensitivity resolution sensitivity (Morris & Langari 2012). Experiments have been carried out with two types of air temperature sensors: 1) type-T thermocouples, and 2) capacitive temperature and humidity sensors integrated with a CO_2 sensor. Both sensor systems are low power, which make them suitable for WSN applications. The stated thermocouple theoretical accuracy is 0.5°C and the capacitive sensor's one is between 0.3 and 0.8°C over the temperature range considered.

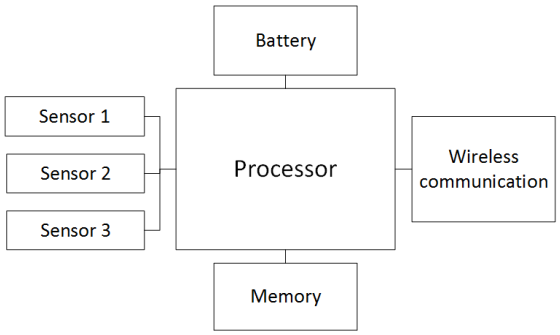

Figure 4. Schematic of self-developed nodes

The sensors have been placed in a SANYO MIR 253 incubator to provide a controlled test environment. The incubator accuracy is stated as +/- 0.2°C with an homogeneity of temperature repartition of +/- 0.5°C. The temperature is varied between 13 and 30°C in steps of 2°C between 19 and 27°C and in steps of 3°C for the rest. The temperature is left to stabilise between each step and then 5 min of data at that temperature is recorded.

Pilot case study

The same sensors are used to monitor temperature, humidity and CO_2 levels in a single office room of 14 m^2 floor area and 34.5 m^3 volume. The office comprises a desk on the window side and a meeting table on the door side (Figure 5). To regulate its thermal comfort, the occupant can open the window, turn on an electric heater or turn on a fan.

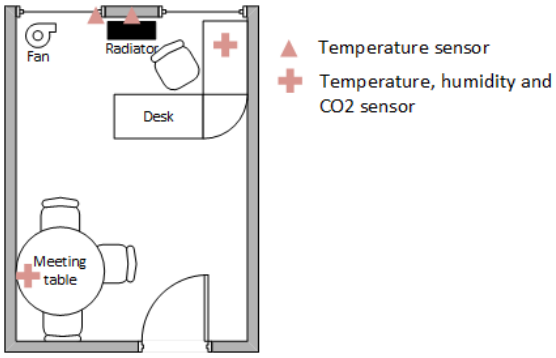

Figure 5. Case study floor plan and sensors location

A CO_2, humidity and temperature sensor has been placed on each table. Thermocouples have been placed on the window frame, on the wall behind the electric heater, and on the desk co-located with the CO_2 and capacitive sensor.

As a first test case, the different thermal control actions are performed in series of 10 minutes with 10 minutes break between each, starting with the window, then the heater, and finally the fan.

This controlled study was then supplemented by measurements taken for two days; one week day and one week-end day. The number of occupants and the thermal control actions have been recorded via a paper log.

RESULTS

Sensor evaluation

Figure 6 shows the median temperatures and the 95% confidence interval where all the measurements for each type of sensor are grouped against the 8 set points of the incubator. The red line represents the y=x equation and the brown line is the linear best fit considering all data points. The coefficient of linearity is close to one with a coefficient of determination R^2=0.99, showing the suitability of the selected sensors over the range of interest.

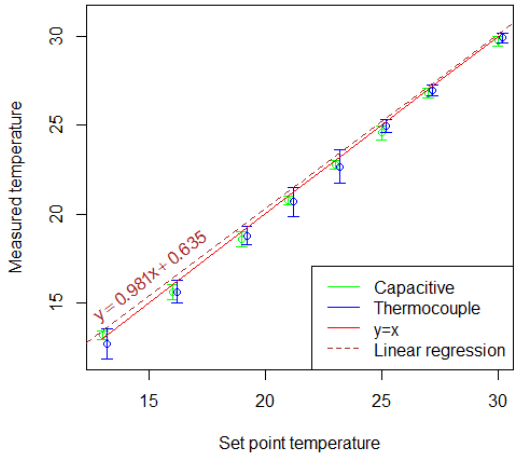

Figure 6. Median and two standard deviations error bars for the two types of sensors

Figure 7 shows the variability of all the tested sensors at 25°C. This particular set point has been chosen as there is less variability in the incubator temperature, probably due to the fact that the temperature elevated above the ambient temperature of the laboratory.

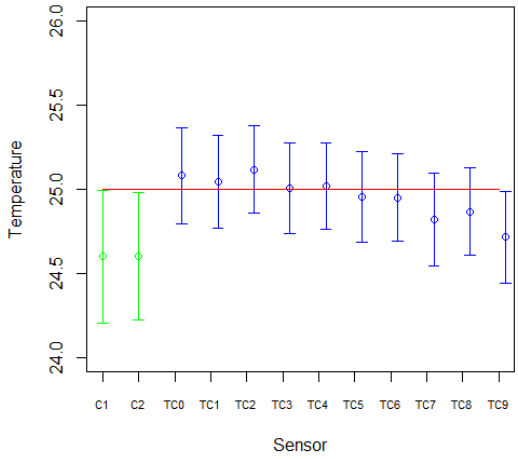

Figure 7. Median and two standard deviations error bars at 25°C

The capacitive sensors (C1 and C2) measure lower temperatures than the thermocouples (TC). This is expected as the temperature and humidity sensor is placed in a plastic enclosure which makes the diffusion of the air to the sensors slower than for the thermocouples which are directly exposed. The 5 min measurements were not long enough for the integrated sensor to assimilate a 2/3°C temperature gradient. Nevertheless, for the longer term monitoring, a good agreement between the capacitive and thermocouple readings was observed, as the temperature variations were slower. The capacitive sensor therefore appears to provide more stable measurements than the thermocouple, but cannot be used to detect fast changes in temperatures.

Pilot case study

Figure 8 shows parts of the data recorded during the activity test. As expected, the window opening provokes a drop of CO_2 and humidity as well as a drop of temperature on the sensor situated on the window frame, but not on the ones further from the window.

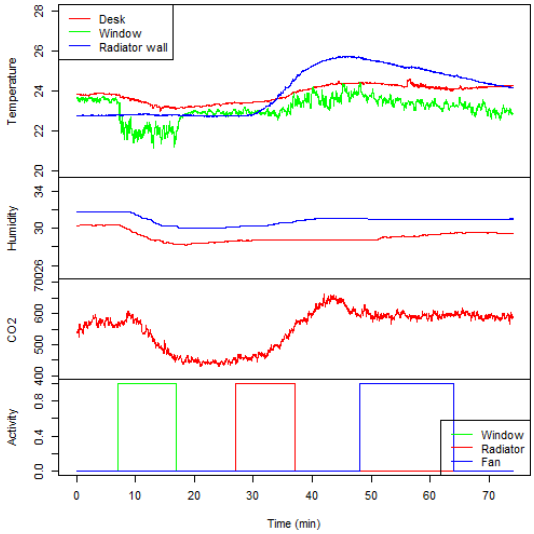

Figure 8. Temperature, humidity and CO_2 variation during ventilation, heating and cooling

The heating period can be detected from the temperature sensor placed on the wall. The delay between the start of the heating period and the increase of temperature detected comes from the warm up period of the electric heater.

The fan causes a slight decrease of CO_2 by mixing the CO_2 produced by the occupant at the desk with the rest of the room.

Figure 9 shows two days of monitoring of a single office. The first 24 hours represents a week day and the following a week-end day. None of the thermal control action has been used for the duration of this test. Only the CO_2 readings from the meeting table have been represented as this sensor gives very similar readings to those measured at the desk.

The CO_2 variations coincide with occupancy and the CO_2 concentration is stable when nobody is in the room. The window was not opened for the

duration of this experiment and the temperature profile coincides with the rest of the room.

The temperature on the meeting table side of the room is between 0.5°C and 3.5°C above the desk side temperature with an average of 2.3°C. This difference can be explained by air leakage from the windows.

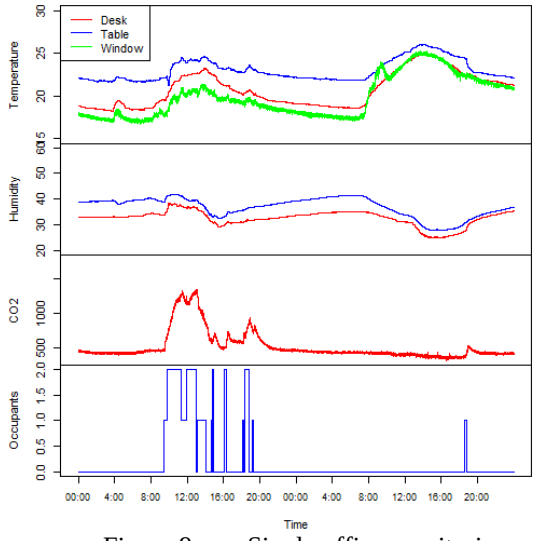

Figure 9. Single office monitoring

DISCUSSION

Experimental results

The thermocouples and CO_2, temperature and humidity sensors proved adequate for use in PWSN to perform PO-Cx. They require low power making them compatible with a long battery life for wireless nodes. They provide measurements close to the reference value over the desired range for building thermal application and are able to detect behavioural and physical events related to thermal comfort.

Also it can be observed that temperature profiles are significantly different around the room. The location of the temperature control sensor can therefore have a great influence on achieved thermal comfort and the ability of the sensor system to accurately capture to occupant experience. Using multiple temperature measurements to commission the BMS location can potentially contribute to improved occupant comfort.

Potential of PWSN for PO-Cx

Energy performance realisation is a growing challenge for the building industry. For financial reasons, clients want to get their buildings occupied as soon as possible, resulting in no time being allocated for overall building performance test during the construction period. It thus needs to be conducted after handover, when the building is already occupied. This presents additional challenges as minimum disruption of building normal operation would be required.

Performance evaluation and other PO-Cx tasks require additional data compared to normal building operation. WSN technologies offer the opportunity to collect data at a relatively low cost and with limited interference to the building activities. Current WSN technology can be found at around $150 per node[2] and the prices are expected to drop in the future. Additionally the capital cost of the pop-up monitoring™ system would be spread by the intention to reuse it on several projects. The main cost after hire costs, would then be installation and removal which would be kept to a minimum by the absence of wiring. The contractor would then only need to go on site if a problem needed special attention as the data would be available off-site.

The use of PWSN for PO-Cx also presents the advantage of keeping part of the design and construction team involved with the building. This can limit the loss of knowledge that normally happens at handover by allowing a transition period. In that perspective, PO-Cx can be considered as a complement to soft landing.

Performing PO-Cx at the beginning of the building life cycle is intended to improve the building energy efficiency at an early life cycle stage, but it also has the potential to improve results from other energy saving measures later on. Fault detection and diagnostic (FDD) and O-Cx would benefit from PO-Cx by getting a better starting point from which to detect performance degradation.

Finally, a PWSN toolkit could have other applications beyond PO-Cx. It could be used for other one-off commissioning process such as Re-Cx and Retro-Cx. In particular, in the case of a

[2] Around £90

refurbishment, the PWSN could enable understanding of the existing systems when documentation has been lost.

Practical challenges for PO-Cx implementation

This section discusses the practical challenges that need to be addressed for PO-Cx to be adopted by the building industry. The first challenge concerns how to incentivise PO-Cx. In the current product-based building services industry, the additional initial investment cost associated with PO-Cx is likely to be a barrier on the client side, even though it would result on long term saving through reduced energy bills. To facilitate PO-Cx adoption and energy saving measures in general, the building services industry would need to move from a product-based model to a service based industry. This change is likely to be driven by energy price increases. The emergence of this kind of delivery model can be seen in British public–private partnership (PPP) and private finance initiative (PFI) projects (Action 2002). PPP and PFI contracts incorporate substantial financial penalties if energy targets are not met, leading to the necessity of new tool such as a pop-up monitoring^{TM}.

Additionally recent evolution of building regulation, energy policy and certification schemes should lead to increasing demand for energy saving measures, but in practice their application is based on design intent. There is also a lack of means to control operating compliance of new buildings (Pan & Garmston 2012). Regulations and policies need to evolve to give a bigger weight operation in there scope.

Another challenge lies in the contractual arrangement around PO-Cx. First PWSN can provide a relatively low cost monitoring system as it can be redeployed from one building to the other. However the current practice is to bill measurement equipment on projects, and part of this equipment is generally lost when the projects ends. Secondly, once problems have been detected, means need to be allocated to solve them and provision need to be made to for this in advance or the contractor might choose to ignore problems that seem costly to fix.

Finally there is a challenge associated with data analysis. This process represents a significant cost of any monitoring measure. The need to build detailed models increases significantly the cost of PO-Cx. Thus it is important to develop analysis methods that can be relatively independent from the building and re-configurable to the demands of different projects. Another solution is to reuse models created at design stage.

CONCLUSION

The operation of new buildings is disappointing when compared to their brief and design. The liability period following handover could be used to improve the life cycle performance of buildings. Better initial performance could be set by performing post-occupancy commissioning (PO-Cx).

Technological advances have made access to more data for a lower cost possible using wireless sensor networks (WSN) and this should be used to have a better understanding of where inefficiencies come from regarding energy consumption to deliver comfort.

We have presented the requirements for a pop-up monitoring^{TM} toolkit to enable the realisation of PO-Cx. Initial sensor tests have been carried out showing the potential of the method. In the future, additional sensing parameters will be added to the study and challenges associated with wireless communication evaluated. The integration of such data with system and process models is also required.

ACKNOWLEDGMENTS

This research is supported through a Laing O'Rouke Studentship and the activities of the Laing O'Rourke Centre for Systems Engineering and Innovation at Imperial College London. The authors gratefully acknowledge the support of Laing O'Rourke and Crown House Technologies. The authors would also like to thank Dr Geoffrey Fowler for providing access to his laboratory facilities.

REFERENCES

Action, E., 2002. Energy efficiency in PPP/PFI contracts for further and higher education.

Bordass, B. et al., 2001. Assessing building performance in use 3: energy performance of the Probe buildings. *Building Research & Information*.

Cohen, R. et al., 2001. Assessing building performance in use 1: the Probe process. *Building Research & Information*, 29, pp.85–102.

Djuric, N. & Novakovic, V., 2009. Review of possibilities and necessities for building lifetime commissioning. *Renewable and Sustainable Energy Reviews*, 13(2), pp.486–492.

Healy, W.M., 2005. Lessons learned in wireless monitoring. *ASHRAE Journal*, 47, pp.54–60.

Heller, A. & Orthmann, C., 2014. Wireless technologies for the construction sector—Requirements, energy and cost efficiencies. *Energy and Buildings*, 73, pp.212–216.

Isakson, P., Wetterström, P. & Carling, P., 2004. BEMS-assisted seasonal functional performance testing in the initial commissioning of Kista Entré and Katsan. In *Proceedings of the Fourth International Conference for Enhanced Building Operations*.

Jeong, J.-W. et al., 2008. Feasibility of wireless measurements for semi-empirical multizone air flow model tuning. *Building and Environment*, 43, pp.1507–1520.

Katipamula, S. & Barambley, M.R., 2005. Methods for Fault Detection, Diagnostics, and Prognostics for Building Systems - A Review, Part I. *HVAC&R Research*, 11, pp.1–25.

Keuhn, P.L. & Mardikar, Y.M., 2013. Energy Conservation through Ongoing Commissioning. *Energy Engineering*, 110, pp.20–41.

Kinter-Mayer, M., 2005. Opportunities of Wireless Sensors and Controls for Building Operation. *Energy Engineering*, 102(5), pp.27–48.

Menezes, A.C. et al., 2012. Predicted vs. actual energy performance of non-domestic buildings: Using post-occupancy evaluation data to reduce the performance gap. *Applied Energy*, 97, pp.355–364.

Morris, A.S. & Langari, R., 2012. *Measurement and Instrumentation - Theory and Application* A. press, ed., Elviser.

Noye, S., Fisk, D. & North, R., 2013. Smart systems commissioning for energy efficient buildings. In *CIBSE Technical Symposium*.

Painter, B., Brown, N. & Cook, M.J., 2012. Practical application of a sensor overlay system for building monitoring and commissioning. *Energy and Buildings*, 48, pp.29–39.

Pan, W. & Garmston, H., 2012. Compliance with building energy regulations for new-build dwellings. *Energy*, 48, pp.11–22.

Sands, J., 2013. *BSRIA Guide: Seasonal commissioning* BSRIA, ed., The Lavenham Press.

Teyssedou, G., Zmeureanu, R. & Giguere, D., 2013. Benchmarking model for the ongoing commissioning of the refrigeration system of an indoor ice rink. *Automation in Construction*, 35, pp.229–237.

Vähä, P. et al., 2013. Extending automation of building construction — Survey on potential sensor technologies and robotic applications. *Automation in Construction*, 36, pp.168–178.

Visier, J.C., 2004. *Annex 40: Commissioning tools for improved energy performance*, International Energy Agency.

Way, M. & Bordass, B., 2007. Making feedback and post-occupancy evaluation routine 2: Soft laning - involving design and building teams in improving performance. *Building Research & Information*, 33, pp.353–360.

York, D., 1988. *Building Commissioning: Survey of Attitudes and Practices in Wisconsin*, Energy Centre of Wisconsin.

Calculation of Integrated NOx Emissions Reductions from Energy Efficiency and Renewable Energy (EE/RE) Programs across State Agencies in Texas

Juan-Carlos Baltazar, Ph.D., P.E.,Jeff S. Haberl, Ph.D., P.E., and Bahman Yazdani, P.E.

Energy Systems Laboratory, Texas A&M Engineering Experiment Station
The Texas A&M University System, College Station, TX.

ABSTRACT

This paper presents an update of the integrated NOx emissions reductions calculations developed by the Energy Systems Laboratory (ESL) for the State of Texas to satisfy the reporting requirements for Senate Bill 5 of the Texas State Legislature. These procedures are used to report annual and Ozone Season Day (OSD) NOx emissions reductions to the Texas Commission on Environmental Quality (TCEQ) from the state-wide energy efficiency and renewable energy programs. These programs include: the impact of code-complaint construction, the Texas Public Utility Commission (PUC), the energy efficiency programs managed by the Texas State Energy Conservation Office (SECO), electricity generated from wind power in the state, and several additional statewide measures, including SEER 13 air conditioners.

Methodologies for Estimating Building Energy Savings Uncertainty: Review and Comparison

Juan Carlos Baltazar, Ph.D., P.E., Yifu Sun, EIT, and David E. Claridge, Ph.D., P.E.
Energy Systems Laboratory, Texas A&M Engineering Experiment Station
Texas A&M University, College Station, TX, 77843

ABSTRACT

The reliability, and accuracy, of the building energy use savings is the factor that customers are interested for evaluation of a project performance. In general, the savings uncertainty is affected by many factors, some related to the quality of the statistics of the baseline model use to estimate savings and others related to the energy use patterns after the energy efficiency measures are applied. This paper includes a review of the commonly used methodologies and other recent approaches for the energy savings uncertainty. The review included the original description of most of the known uncertainty models: Reddy and Claridge, which has different expressions for different interval time of monitored data and different categories of goodness-of-fit baseline models; the improved simplified equation from the matrix algebra equation (Sun and Baltazar; Subbarao, Lei and Reddy propose on determining "local" uncertainty using Nearest Neighborhood method and Shonder and Im on the use of Bayesian inference for a retrofit projects. In this study, besides the review and comparison of these methodologies applied to several actual building cases, a guideline on what should be used for the right case is given.

Case study of Chilled Water Loop Low ΔT Fault Diagnosis

Lei Wang[1], Ph.D., P.E. Ken Meline[2], P.E. James Watt[1], P.E. Bahman Yazdani[1] P.E.,
David E. Claridge[1], Ph.D., P.E
[1]*Energy Systems Laboratory, Texas A&M Engineering Experiment Station, College Station, Texas*
[2] *Command Commissioning, LLC*

ABSTRACT

Low chilled water ΔT, which is the temperature difference between chilled water supply and return temperatures, wastes energy by requiring additional chillers to operate, reduces chiller efficiency, and requires additional pumping power to meet the cooling load. In addition to the energy waste, the low ΔT "strands" capacity in the chillers – which is critical at a time when building expansion is underway.

This paper is to summarize a path for identifying and mitigating the ΔT issue, and increase and maintain the ΔT of the chilled water system for all possible load conditions. The primary causes of the low ΔT issue and specific action items were identified to improve the CHW ΔT by approximately 5.5 – 6.5°F (3.1-3.6°C) during the winter and by about 4°F (2°C) during the summer.

Key Words: chilled water loop ΔT, central distribution system, variable-flow Chilled Water System, energy efficiency, performance verification, degraded performance

DEALING WITH "BIG CIRCULATION FLOW RATE, SMALL TEMPERATURE DIFFERENCE" BASED ON VERIFIED DYNAMIC MODEL SIMULATIONS OF A HOT WATER DISTRICT HEATING SYSTEM

Li Lian Zhong, Senior Sales Consultant, Danfoss Automatic Controls Management (Shanghai) Co.,Ltd, Anshan, China

ABSTRACT

Dynamic models of an indirect hot water district heating system were developed based on the first principle of thermodynamics. The ideal model was verified by using measured operational data. The ideal and verified models were applied to obtain and analyze the system characteristics such as the tendency of the issue relating to "big circulation flow rate, small temperature difference". From the simulated and analyzed results, it is realized that the electrical pumping cost could be significantly reduced due to the over circulation water mass flow rate. It is also shown that by applying proper supply water temperature set point in the control system, the zone air temperature can be automatically adjusted with enough accuracy. The major reasons and solutions for the water mass flow rate and the temperature difference problem have been given in the last section.

KEYWORDS

District heating system; dynamic models; simulations; pumping cost; reasons and suggestions;

NOMENCLATURE

c	specific heat, J/Kg℃ or a factor related to heat transfer coefficient test of heaters
C	controller or thermal capacity, J/℃
e	error
E	electricity consumption, W
f	factor
F	area, m^2
G	mass flow rate, Kg/s
HV	heating value, J/Kg
k_p	proportional gain
k_i	integral gain
KF	heat transfer coefficient, W/℃
q	heat per unit area, W/m^2
Q	heat, W
t	time, s
T	temperature, ℃
TD	temperature difference, ℃
u	control signal
$\alpha_0 - \alpha_3$	factors

Subscripts

1, 2	primary, secondary system
act	actual
arg	average
b	boiler
d	design
en	enclosure
ex	exchanger
f	fuel
h	heater
int	internal
n	number of HES
o	outside
r	return
s	supply
sp	set point
sols	solar radiation from south side
v	verify
w, w2i	water, water in secondary system for each HES
z	zone

1 INTRODUCTION

Due to the most share of energy consumption for district heating (DH) in construction field, the energy efficiency, energy savings and environmental protection play very important rules these days. Therefore, focusing on the current situations combining with future solutions has been attracting researchers to develop applications. For example in the existing issues in DH systems, the operation mode: "big circulation flow rate, small temperature difference" could be found in many DH systems, this phenomenon is mainly resulted from both design and operation phases. In design stage, designers wish to ensure more safety due to the responsibility; they usually try to increase safety factors from the heating load calculation, terminal selection, pipe dimension, pump selection and the equipment for the heat source as well. This in fact will cause over sizing of the overall system configuration. On the other hand, in the system operation stage, some operators and managers also have the same thinking by increasing the operational parameters to overcome the problems resulted from uncomfortable zone air temperature and hopeless system control and adjustment. Some researchers and experts have found the scenarios in system operation, and described the reasons caused it with words. In order to study the situations including the reasons, the results and the deep solutions, a dynamic model of a typical and real indirect district heating (IDH) system was chosen for this research to assist the analyses and advices for reducing the pumping cost from with quantificationally and qualitatively.

Based on this motivation, an actual IDH system with heated floor area 0.44Mm^2 was selected as an objective. The system has been renovated in 2013 by using Danfoss high-technologies and products and operated in 2013-2014 heating period.

In the IDH system, there are 4 high-temperature hot water boilers installed in the heat source, and 5 heat exchange stations (HES) in the overall system with 9 heat exchange units in total. The terminals were installed by radiator. The served buildings were built in 1992-1994 as economic buildings. The simplified system diagram is plotted in Figure 1 with aggregated boilers, heat exchange stations, heaters as three parts with control strategy configuration.

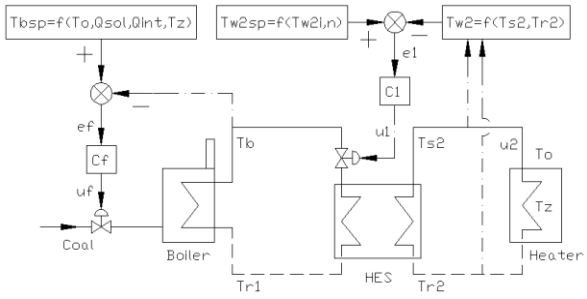

Figure 1. Simplified Diagram With Control Configuration

2 DYNAMIC MODEL DEVELOPMENT

2.1 Ideal Dynamic Model

The design parameters of indoor and outdoor air temperatures, supply and return water temperatures in the primary and secondary systems, water mass flow rates in the primary and secondary systems, and heating load index are given as 18℃, -26℃, 110℃, 70℃, 80℃, 60℃, 475T/h, 951T/h, 50W/m^2 respectively. These parameters are used for the development of the mathematical model.

As known that IDH systems are very complicated systems when considering dynamic processes. To avoid the complexity, certain conditions are assumed: the heat losses and the makeup water losses from the pipe network are ignored without affecting the system responses too much due to limited amounts actually. In addition, several physical parameters are aggregated such as thermal capacity, overall heat transfer rate of HES, radiator and building enclosure. By applying for the first principle of thermodynamics, 5 state variables are taken into account for the simplified ideal dynamic model, and the dynamic equations are expressed as follows.

Boiler model:

$$C_b \frac{d(T_b)}{dt} = u_f G_{fd} HV[\alpha_0 + \alpha_1(\frac{T_b}{T_{bd}}) + \alpha_2(\frac{T_b}{T_{bd}})^2 + \alpha_3(\frac{T_b}{T_{bd}})] - c_w u_1 G_{1d}(T_b - T_{r1}) \quad (1)$$

In Equation (1), the net heat stored in the boiler body is equal to the difference of fuel combustion and the heat transported from the primary network in the heat source. Note that the boiler efficiency is stated as nonlinear property based on experience.

Heat exchanger model:

$$C_{ex1}\frac{d(T_{r1})}{dt}=c_w u_1 G_{1d}(T_b-T_{r1})-f_{ex}KF_{ex}\{[(T_b-T_{s2})-(T_{r1}-T_{r2})][\ln(\frac{T_b-T_{s2}}{T_{r1}-T_{r2}})]^{-1}\} \quad (2)$$

$$C_{ex2}\frac{d(T_{s2})}{dt}=c_w u_1 G_{1d}(T_b-T_{r1})-c_w u_2 G_{2d}(T_{s2}-T_{r2}) \quad (3)$$

In Equations (2) and (3), the net heat stored to the heat exchangers in both sides are considered as the heat transferred from the primary system, the heat exchanger itself and the secondary system. The heat exchangers are selected as plate type, and the temperature difference between the primary and secondary sides is computed by using logarithmic mean temperature difference method.

Radiator model:

$$C_h\frac{d(T_{r2})}{dt}=c_w u_2 G_{2d}(T_{s2}-T_{r2})-f_h KF_h(\frac{T_{s2}+T_{r2}}{2}-T_z)^{(1+c)} \quad (4)$$

Due to the non-linear characteristic of radiators, the heat transfer from the terminals is calculated by using exponential model. In Equation (4), the net heat stored in the heaters is the difference between the heat input from the secondary system and the heat output from the terminals.

Room model:

$$C_z\frac{d(T_z)}{dt}=c_w u_2 G_{2d}(T_{s2}-T_{r2})+q_{sols}F_{sols}+q_{\text{int}}F-f_{en}KF_{en}(T_z-T_o) \quad (5)$$

In Equations (5), the net heat stored in the zone air can be expressed by the differences between the heat obtained from heat inputs (the secondary system, solar radiation and the internal heat gains) and the heat outputs from the building enclosure. For simplicity, the solar radiation is considered by south side of the buildings only, and the internal gains are assumed by 3.6W/m^2 as maximum value.

In summary, the simplified ideal IDH system dynamic model consists of 5 dynamic equations.

2.2 Properties Analysis From The Ideal Model Simulations

Design values of the network are set to the ideal dynamic model for simulations. With the designed fuel consumption and outside air temperature as inputs, the dynamic responses are displayed in Figure (2). From this figure it can be seen that the outputs present identical as the design values, meaning correct relationships among the inputs and the outputs.

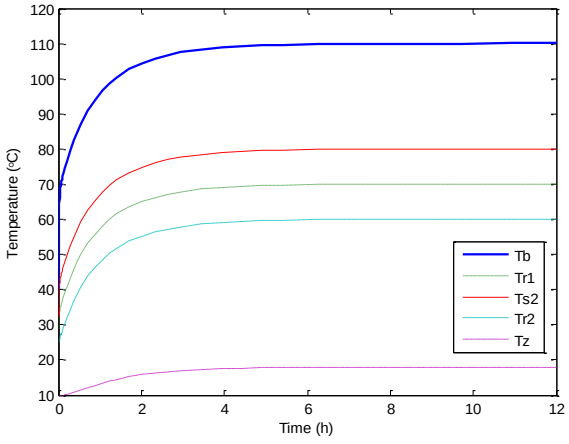

Figure 2. Dynamic Responses In Ideal Conditions

The system properties could be obtained by simulating with the ideal dynamic model, which the method is entitled as open loop tests. When the solar radiation and the internal heat gains are set to ~~be~~ zero, and the zone air temperature maintains 18℃, the

simulation results are addressed in Figure 3 associated with the changes of water mass flow rates in the primary and secondary systems and different outside air temperature. Only one parameter changes while the other was considered as ideal condition in the simulation. As shown in Figure 3(a), it can be observed that, when the water mass flow rate in the primary system varies from lower to over design value, the temperature difference (TD) in the primary side will change from higher to lower values, and the TDs in the secondary system are almost identical; by observing the situation in the secondary side plotted in Figure 3(b), it has the same tendency compared with the Figure 3(a). In addition, the varying rate in the lower outside air temperature is faster than that in the higher outside air temperature.

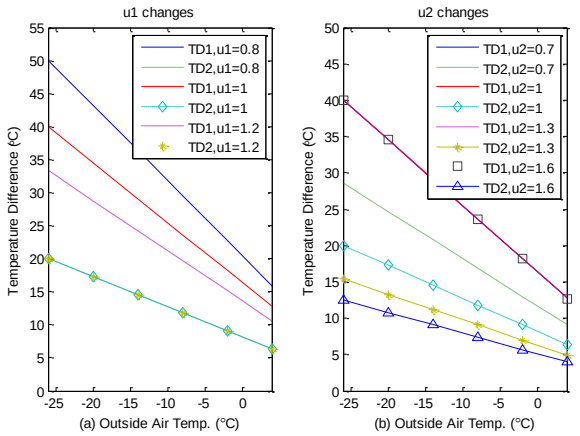

Figure 3. System Properties With The Changes Of Different Parameters (TD and u refer to the temperature difference and water mass flow rate control signal respectively)

2.3 Verified Dynamic Model

Because the developed dynamic model is suitable for ideal conditions only, it should be verified to reach enough accuracy for simulations with actual conditions. A "trial and error" method is applied for obtaining the factors based on actual data from the IDH operation in 2013-2014 and represented by $[f_{ex}, f_h, f_{en}, u_1, u_2] = [1.1, 1.25, 1, 1.35, 1.4]$. The responses of the water temperatures and the fuel consumption with different outside air temperature from the verified model are shown in Figure 4. Comparing the results (lines) from the verified model with the measured data (dots), this verified model could be utilized for system simulations and predictions. Due to the heating value changes of the fuel and manually control of the fuel feed to the boiler(s), the actual fuel consumption is revealed a bit de-centrality. Note that the heat transfer areas of the HESs and the radiators are oversized and the water flow rates in the primary and secondary systems are running with excess of design values in the real system operation.

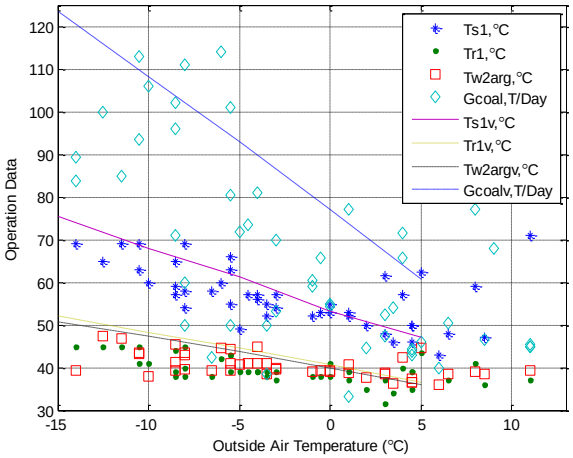

Figure 4. Verified Model Responses With Operational Data

2.4 Properties Analysis From The Verified Model Simulations

Based on the verified model, the factors $[f_{ex}, f_h, f_{en}] = [1.1, 1.25, 1]$ of the IDH system are fixed when the system was implemented. Due to the fact of over circulation flow in system operation, the water mass flow rate control signals of the primary and secondary systems are set between 1 and 1.4, and the simulated data is stated in Figure 5.

From Figure 5(a), the TD changes depending on the outside air temperature and the ratio of the water mass flow rate control signal in the primary system. Increasing water mass flow rate in the primary system by 10%, the TD will be decreased by 2.5~3.5℃ for the design outside air temperature, and it reduces faster in lower outside air temperature than that in higher outside temperature. On the other hand, in order to maintain the design zone air temperature, the water mass flow rates in the secondary (Figure 5(a)) and primary (Figure 5(b)) systems should be the same according to the simulation results depending on which side of water mass flow rate changes.

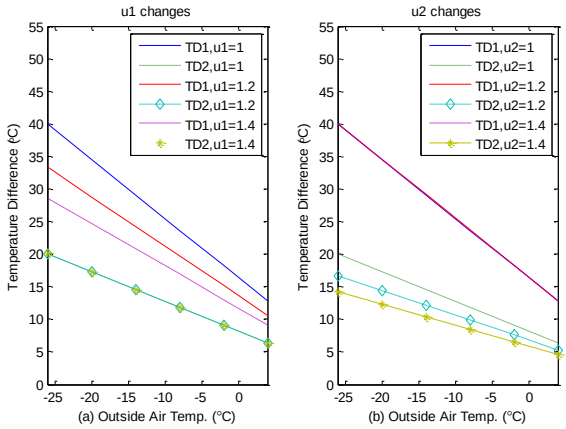

Figure 5. Water Temperature Difference With The Changes Of Outside Air Temperature And Circulation Flow Rate

To this end, no matter which side of water mass flow rate changes, the TD will be reduced when the water mass flow rate is increased, and the other TD in the IDH system does not change too much for keeping the same indoor air temperature.

3 PUMPING COST BASED ON THE CHANGE OF WATER MASS FLOW RATE

The pump affinity law has described the relationship between the water mass flow rate and the electrical power consumption of the circulation pump for the overall pipe network in DH systems. To compare with the pumping cost in the design case, the relationship can be expressed in Equation (6) as below:

$$E_{act} = E_d \left(\frac{u_{act}}{u_d}\right)^3 \tag{6}$$

According to this equation, the power consumed will vary rapidly. In another word, for instance, if the circulation water mass flow rate is decreased by 10%, the electrical pumping cost will be decreased by 27% approximately.

4 TWO DAYS OPERATION WITH DIFFERENT WATER MASS FLOW RATE SETTINGS

According to the verified massage from the verified dynamic model, the control signals of the water mass flow rate in the primary and secondary systems are u_1=1.35 and u_2=1.4 respectively. With these situations, a control system configuration (Figure 1) is suggested to maintain the zone air temperature by setting point temperature as 20℃.

In the selected IDH system operation, the supply water temperature from the heat source has been monitored manually (fuel controller Cf) relating to the outside and inside air temperatures, solar radiation and wind speed; the heat balance has been regulated based on the average water temperature in the secondary system by adjusting the water mass flow rate (u1) of each HES in the primary system; and the water mass flow rate into the buildings has been controlled by using self-active flow control valves with certain settings (u2). However, in this paper for simplicity, the control signals of u1 and u2 are set to be 1.35 and 1.4 respectively, meaning over mass flow rates of circulation water comparing with the design values (u1=1, u2=1), and only Cf is taken into account for this simulation.

A typical PI controller C_f is used to regulate the supply water temperature from the heat source, and the fuel control signal u_f is formulated and computed in the following algorithm:

$$u_f = k_p(T_{bsp} - T_b) + k_i \int_0^t (T_{bsp} - T_b)dt \tag{7}$$

The set point of the supply water temperature from the boiler is given as a function of outside and inside air temperatures, solar radiation and internal heat gains, and expressed in Equation (8) below:

$$T_{bsp} = f(T_o, T_z, Q_{sol}, Q_{\text{int}}) \tag{8}$$

In order to obtain the system dynamic responses, the outside air temperature, the solar radiation, the internal heat gains used in the

simulations are presented in Figures 6 (c) and (d). A design system (u_1=1 and u_2=1) and an actual system (u_1=1.35 and u_2=1.4) are simulated for comparison. As shown in Figures 6(a) and 6(b), the supply water temperatures from the heat source and the HES are almost identical because of the same supply water temperature set points from the heat source. The return water temperatures from the HES and the terminals in actual case are higher than those in the design case. The reason behind is that the over mass flow rate are operated by the primary and secondary systems; and also by doing it, the TDs in the primary and secondary systems are lower by 6-8℃ and 3-4℃ respectively than those in the design case, which means that more electrical power is required to overcome the circulating water resistance. As seen in Figure 6(c), by regulating the supply water temperature from the boiler with the suggested control strategy, the zone air temperature ranges within 20±0.1℃ in the actual case compared with that from 18.9℃ to 19.3℃ in the design system. The difference between the zone air temperatures is resulted from its set point of the supply water temperature from the heat source, and it should be set and monitored according to actual operation strategy. The accuracy achieved is obtained from the compensation of the additional heat gains and the feedback of the measured zone air temperature used to the control system.

In addition, by comparing actual system with the design system, the pumping cost in actual system has consumed about 40% more electricity in operation.

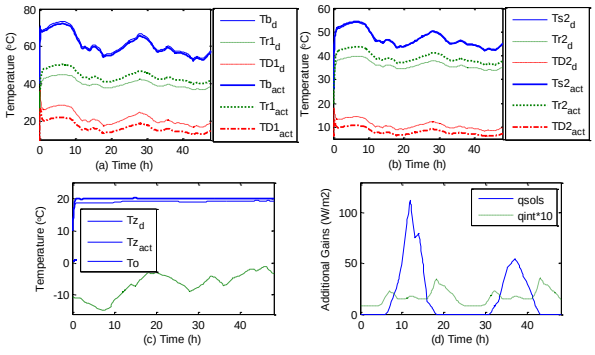

Figure 6. Two Days Operation With C_f Controller

5 SUGGESTIONS OF SOLVING THE ISSUE OF "BIG CIRCULATION FLOW RATE, SMALL TEMPERATURE DIFFERENCE"

The major reasons caused by the issue of "big circulation flow rate, small temperature difference" could be summarized as:

(1) The plan: final planning has been implemented in one step;

(2) The design: the safety factor is needed to be taken into account, but it does not mean that each heat transfer process and equipment selection is required to multiply a factor more than 1;

(3) The operation: the settings of the water mass flow rate in both pipe network sides should be calculated scientifically instead of experience only for each heat season; on the other hand, in order to improve thermal comfort level and cover up the issue of adjustment and control, the water mass flow rate is increased artificially;

(4) Suitable set points: wrong setting points of DH systems not only results in heat and hydraulic unbalance, but also leads to increasing the water mass flow rate easily to conceal the contradictory.

Due to the reasons described above, the solutions to solve this issue could be taken into account accordingly:

(1) The implementation of DH systems should track and follow the overall plan and the actual development in certain time span;

(2) To be careful of considering safety factors in design process; otherwise, it will increase the investment and the operational expense of DH systems greatly;

(3) From the simulation results, it is not necessary to increase the water mass flow rates to reach the design values of zone air temperature set points; on the opposite, it is bigger potential way for operational energy saving by reducing the flow rates;

(4) To reduce the pumping cost in operation, the water mass flow rate in both primary and secondary systems should be decreased according to the operation strategy adjusted for each heating season, and combined with suitable set points of the control system and equipment;

(5) To fulfill the heat and hydraulic balances, the set points of the overall DH systems including the heat amount and the supply water temperature from the heat source and the water mass flow rates in both hydraulic networks need to be calculated based on prediction of heating load requirement and symmetrically optimal process for each heat period.

6 CONCLUSIONS

By applying for the first principle of thermodynamics, ideal and verified dynamic models have been developed for an actual IDH system, and used for obtaining system characteristics and control strategy investigation. From the simulation results, it can be seen that the TD has been decreased associated with the increase of water mass flow rate. In the actual case, the pumping cost is consumed more than 40% comparing with that in the design condition. Also, the simulation has shown that the zone air temperature could be regulated more accuracy with suitable set point of the control system. The issue of the circulation flow rate and temperature difference has been discussed, analyzed and the solutions are suggested considering how to deal with it.

REFERENCES

[1] Lianzhong, L., and Zaheeruddin, M. 2004. A Control strategy for energy optimal operation of a district heating system. *International Journal of Energy Research,Vol.2: 579-612*.

[2] Lianzhong, L., and Zaheeruddin, M. 2008. Dynamic modelling and fuzzy augmented PI control of a high-rise building hot water heating system. *Energy for sustainable development, the journal of the international energy initiative. Vol. XII(2): 49-55*.

[3] Felgner, F., Cladera, R., Merz, R., and Litz, L. 203. Modeling thermal building dynamics with modelica. *Proceedings of the 4th MATHMOD Conference; Vienna*.

[4] 李连众, 丁传国. 2007. 间接连接区域供热系统动态模型及控制策略仿真. *区域供热. 第5 期.*

[5] Zhilong, Z. 2001. Temperature control strategies for radiant floor heating systems. *Concordia University. 16-84*.

[6] Tingyao Chen. A methodology for thermal analysis and predictive control of buiding envelope heating system. Concordia University; 1997, p.47-105.

Biography Form - Please return to icebo@esl.tamu.edu

Name of Paper: Dealing with “big circulation flow rate, small temperature difference” based on verified dynamic model simulations of a hot water district heating system

Author’s Name(s): Li Lian Zhong
Name of Presenter: Li Lian Zhong
Presenter’s Organization: Danfoss Automatic Controls Management (Shanghai) Co.,Ltd
Presenter’s Location: Liao Ning, An Shan
Presenters Address: Qianshan District, Huimin Street, 1#
Presenter’s Telephone: 0412-8410462 Fax: 0412-8229207
Presenter’s email: lilianzhong@danfoss.com

Biography to be used to introduce presenter at conference session

Diagnosis of Effectiveness of HVAC System and Energy Performance of Osaka-Gas Building through Retro-Commissioning
Part 2 Handling the Data Produced by BEMS and Some Results of Analyses

Motoi Yamaha
Professor
Chubu University
Kasugai, Aichi, Japan

Toshihisa Hatanaka
Osaka Gas Co., Ltd.
Osaka, Japan

Ko-ichiro Aoki
Manager
Osaka Gas Co., Ltd.
Osaka, Japan

Norio Matsuda
Building Services Commissioning Asscociation
Nagoya, Japan

Hideki Tanaka
Designated Professor
Nagoya University
Nagoya, Japan

Nobuo Nakahara
Nakahara Laboratory, Enviromental Syst.-Tech
Nagoya, Japan

ABSTRACT

In case of retro-commissioning, utilization of operational data would be very important. We obtained BEMS data of 2003 and from 2009 to 2012. Operation patterns of heat source plants vary from 2003 to 2012 according to change in plant's operational strategy. 90 percent of primary energy was consumed by generators and chillers. Since the plant is run by combined heat and power system, waste heat from the generators is recovered and used for chillers. The efficiency of the generators had been kept around 0.35 which was almost same as specification of the machines. The efficiency of the entire system, however, was decreased, especially in intermediate seasons, or spring and autumn. During these seasons, waste heat from generators which were operated constantly through a year could not be utilized by chillers.

INTRODUCTIONS

On energy performance evaluation of the office building equipped with a gas co-generation system through commissioning, the outline of building, commissioning plan and concepts of evaluation indices were presented in Part 1. In this report, performance evaluation of energy system including co-generation was conducted.

Prior to the evaluation, since a co-generation system produce both electricity and heat, which are not same quality in the second law of thermodynamics view point, some indices were considered. The operating data produced by a building energy management system (BEMS) is usually in inconvenient form for commissioning evaluation. The annual operational data are divided into daily individual files. For annual analysis, each file has to be integrated into one file and treated by scripts for R language.

DESCRIPTION OF THE SYSTEM

The energy system consisted of two generators and absorption chillers. The generators had been operated by electrical output control with maximum electric generated during operation. Two chillers were heat recovery type absorption and other two were gas combustion type. The heat recovery type had operational priority to gas combustion ones. The specification of the system is shown in Table 1 and a schematic diagram is shown in Figure 1. The scope of the system was identified in Figure 2.

PERFORMANCE INDICES FOR CO-GENERATION

Since co-generation produce heat and power, evaluation of performance becomes complicated. Shomoda (Shimoda, 1998) discussed performance in very wide range, such as envriomental, economical, social, safty, and flexisiblity points of view. Some evaluation and quality indices taking account of availability of heat and power were proposed (Enomoto, 2007). The way to evaluate heat efficiency was discussed (Kawashima, 2007) assuming that it was equivalent to power out put. We have defined indicies show below to evaluate the plant efficiency.

Primary Energy Based Efficiency

The index, which is calculated by dividing the heat recovered and power generated by input in primary value is shown in Equation (1).

$$\frac{Q_{DC} + Q_{DH} + E_{CGS} \cdot k_0}{(E_S + E_P) \cdot k_1 + C_P + C_{CGS}} \quad (1)$$

Equivalent Electricity Efficiency

Since electricity is not equivalent to heat considering availability, the amount of heat and power cannot be used for evaluation. The index shown below is calculated heat by multiplying electricity conversion coefficient. This is known as a PURPA Minimum Qualifying Facility (QF) if the coefficient is 0.5.

Table 1. List of main equipment

G-1 G-2	Generators for co-generagtion	Power Output 280kW Gas Consumption 60.6Nm^3/h Nominal Efficiency 40% Heat Recovery / Efficiency 241kW / 34.3%、Overall Efficiency 74.4%
R1 R2	Waste heat recovery type absorption chillers	Cooling Capacity 1,400 kW (12°C～7°C) Heating capacity 1177 kW (45.8°C～50°C) Condensation Water 32°C～37.7°C Heat recovery pumps 5.5kW× 2
CT-1,2	Cooling towers	Fan Capacity 11k×2
CDP-1,2	Condensation water pumps	200φ×6667 L/min×300kPa×55kW×3φ×440V
CHP-1,2	Primary pumps	200φ×4032 L/min×150kPa×18.5kW×3φ×440V
R3 R4	Gas combustion Absorption Chillers	Cooling Capacity 1758kW (12°C～7°C) Heating Capacity 1163kW (51.7°C～55.0°C) Condensation water 32°C～37.0°C
CT-3, 4	Cooling Towers	Fan Capacity 11kW×3φ×440V×2
CDP-3,4	Condensation water pumps	200φ×8333 L/min×300kPa×75kw×3φ×440V

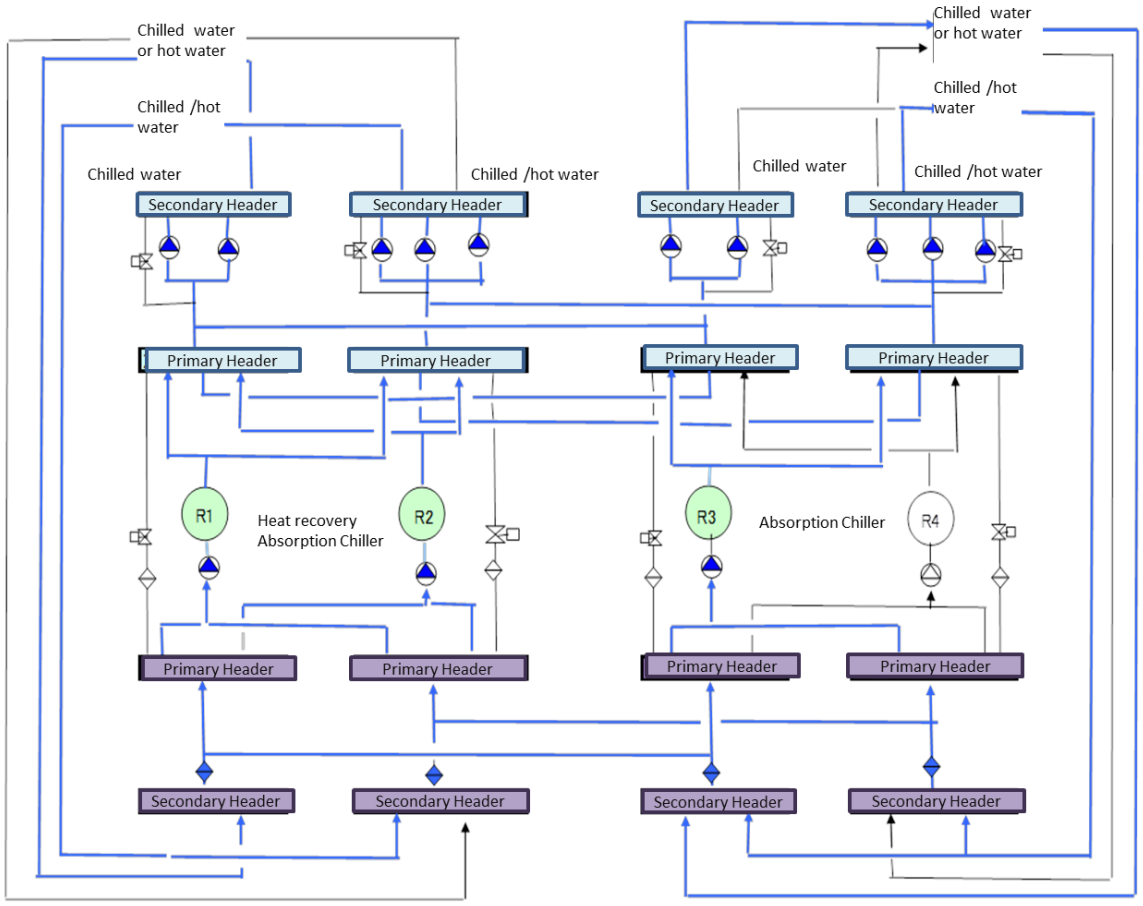

Figure 1. Schimatic diagram of the system

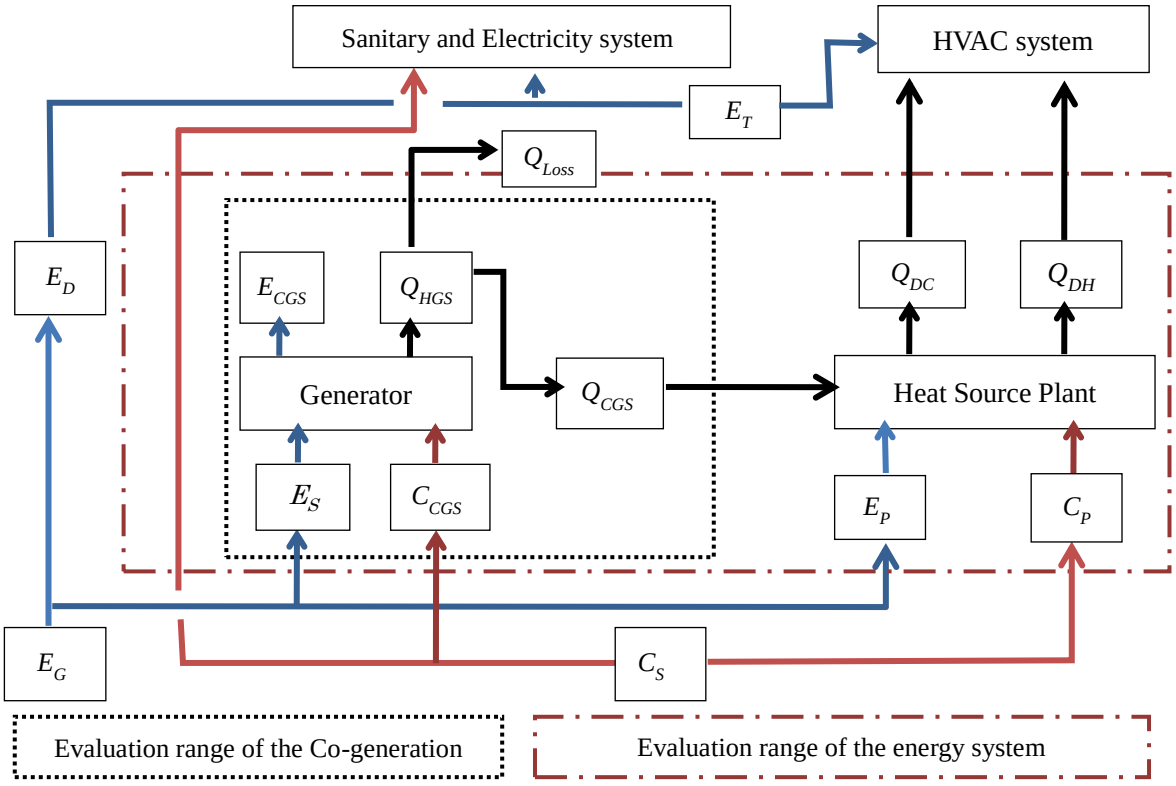

Figure 2. Energy flow for analysis

$$\frac{E_{CGS} + Q_{CGS} \times X}{E_s + C_{CGS}} \quad (2)$$

Equivalent Input Efficiency

The index shown above assumed the conversion coefficient for heat. Assuming equivalent energy of boiler if the recovered heat was produced by boilers, an index, in which the assumed energy was subtracted from input energy, can be defined.

$$\frac{E_{CGS}}{E_s + C_{CGS} - Q_{HGS}/\eta_B} \quad (3)$$

Equivalent Heat Efficiency

An index can be defined if the restored heat was obtained by heat pump chillers.

$$\frac{E_{CGS} + Q_{CGS} \times Y}{E_s + C_{CGS}} \quad (4)$$

Boiler Equivalent Efficiency

Other index can be calculated focusing on the heat. Assuming the electricity generated by co-generation was replaced by utilities, the energy for the electricity was calculated by the efficiency of generation for the utilities.

$$\frac{Q_{CGS}}{C_{CGS} + E_S - E_{CSG}/\eta_E} \quad (5)$$

DATA PROPERTIES FROM BEMS

Table 2 shows the properties of data obtained from BEMS. The objective of data acquisition for the BEMS at the design phase was monitoring of subsystem or equipments. Not all properties needed for performance evaluation was presented. Some values, such as flow rate of chilled, hot and heat recovery were estimated from operational hours.

Table 2. Data properties obtained form BEMS

Equipments	Temperature	Flow rate	Energy	Others
Chiller	Inlet and outlet	n/a	Gas	Operation Hours
Cooling tower	Inlet and outlet	n/a	n/a	n/a
Primary Pumps	n/a	n/a	n/a	n/a
Secondary Pumps	n/a	n/a	n/a	Inverter output
Heat load	n/a	L/min	kWh	
CGS	n/a	n/a	Gas	kWh

At ordinary BEMS system in Japan, measured data is presented in forms of daily reports which are designed for printed in papers. Since the data is delivered in daily individual files, integration of each files into one annual file is needed. For this purpose, a script of R language was written, and integrated files were used for analysis.

For energy evaluation, the higher heat value of gas, or 45MJ/m^3 was used for evaluation of absorption chillers. The lower heat value of gas, or 40.6MJ/m^3 was used evaluation of generators.

RESULTS

Efficiency Of Chillers Over Years

It had been 9 years since the facility was renovated. Deterioration of machines, especially of chillers was expected. since only one flow rate was measured, attempt to estimate coefficient of performance (COP) was conducted for the period when single chiller was in operation. Estimations were conducted for gas combustion absorption chillers.

Figure 3 shows histograms of estimated COP over years. COP in 2003, or completion year distributed in higher value comparing the value in 2009 and 2010. Since the operations for estimated period were in small partial load, it was impossible to conclude the deterioration.

Primary Energy Consumptions

The amount of primary energy consumption is shown figure 4. The consumptions of chillers and generators were calculated from measured gas consumption from BEMS data. The primary energy of pumps were estimated by multiplying nominal electricity consumption and operational hours. The dominant part of primary energy was generators and absorption chillers. The difference of generator consumption due to the change in operational strategy in between 2003 and 2009.

Primary Energy Efficiency

Primary energy efficiency defined by equation (1) is shown in Figure 5. Although the efficiency of the whole year is 0.7, it fluctuated annually. The efficiency increased in summer and winter and decreased in spring and fall, or intermediate season. The waste heat from the generators utilized by absorption chillers. In intermediate season, amount of waste heat surpassed heat demand because the generators operated by electrical output control. Unused heat was released to ambient through cooling towers.

Boiler Equivalent Efficiency

Figure 6 shows the boiler equivalent efficiency based on Equation (5). For the system, Equation (5) was modified to Equation (6)

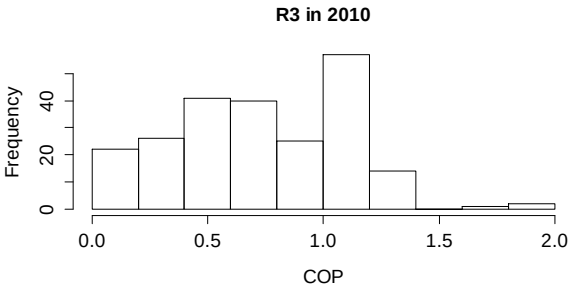

Figure 3-a. Estimated COP of R3 in 2010

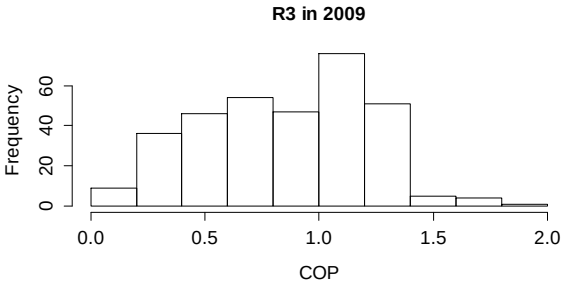

Figure 3-b. Estimated COP of R3 in 2009

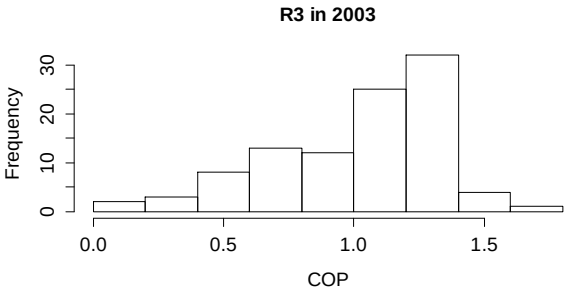

Figure 3-c. Estmated COP of R3 in 2003

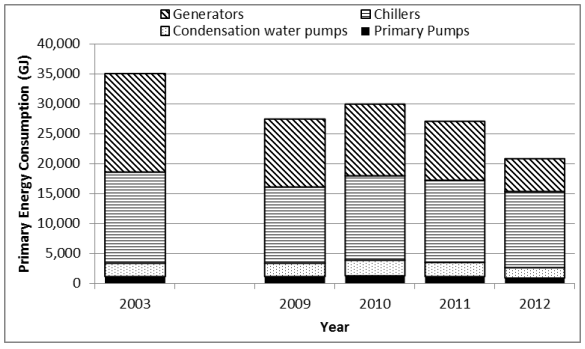

Figure 4. Yeary primary energy consumption

$$\frac{Q_{DC}+Q_{DH}}{C_s+E_P+E_S-E_{CGS}/\eta_E} \quad (6)$$

As electricity part is subtracted from input energy,

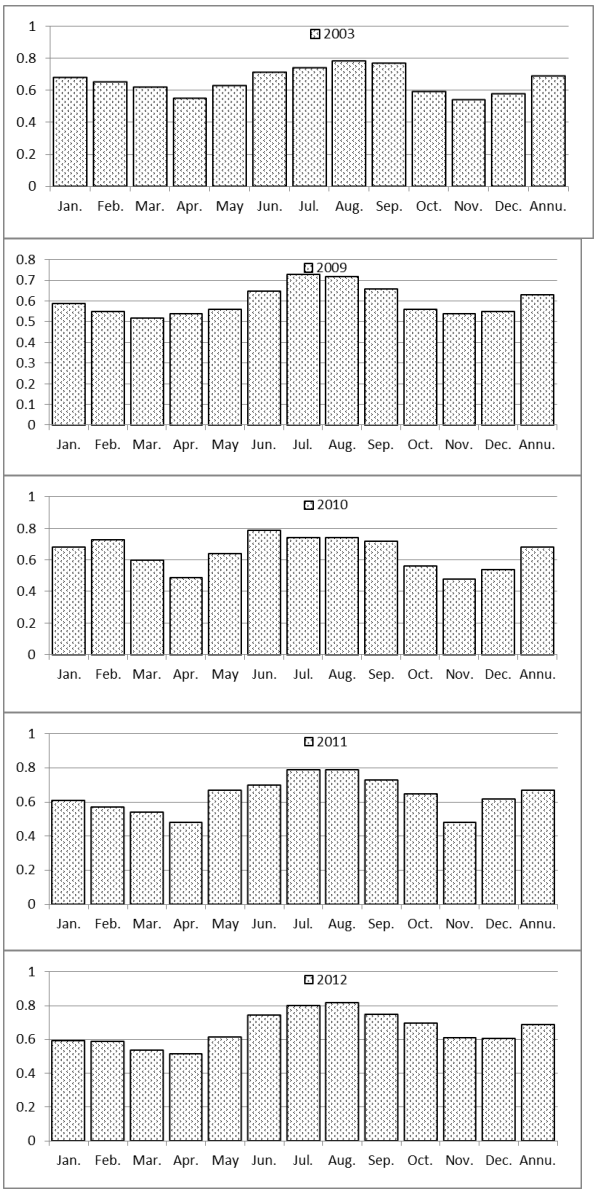

Figure 5. Primary Energy Efficiency

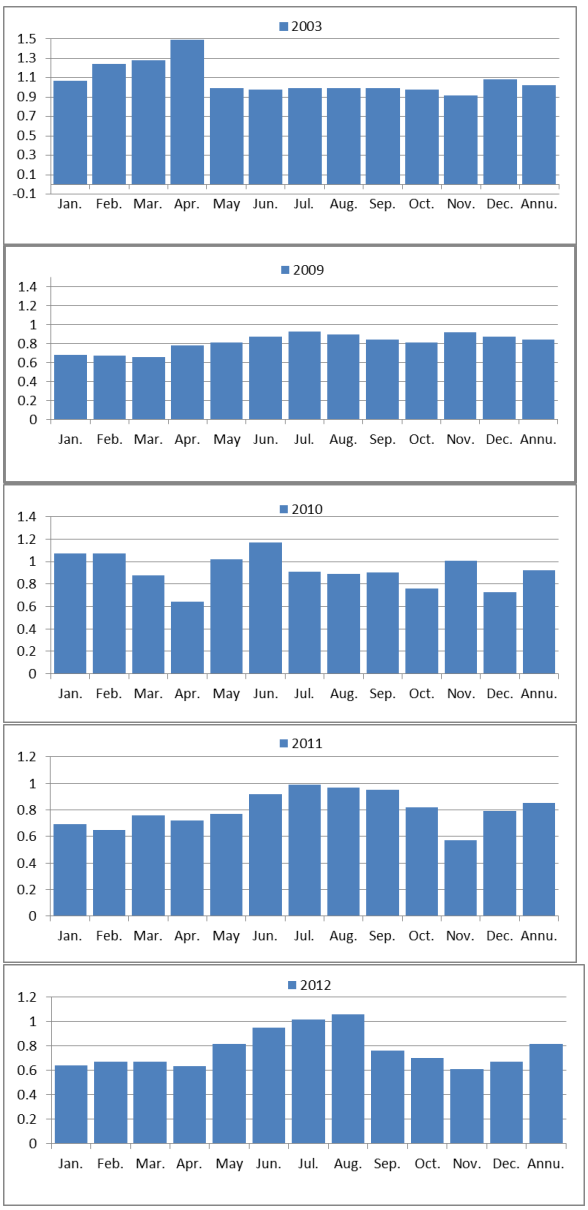

Figure 6. Boiler equivalent efficiency

the value realized over 1.0 while energy input was small.

Figure 7 shows primary energy efficiency limited to the generators. The generation efficiency continued0.4 throughout the years. Since the flow rates of waste hot water were not measured, the values were estimated from a nominal capacity of pumps and operational hours. During 2012, since a modification for BEMS system was made, data for several month was missing. The efficiency including waste heat recovery fluctuate as well as primary efficiency of the system.

DISCUSSIONS

As shown in Figure 5 primary efficiency of the system decreased in spring and autumn. The waste heat from generators was used in heat recovery absorption chiller. The intermediate season, such as spring and autumn, as cooling or heating load for chillers were not sufficient to utilize waste heat, the heat was discharged into atmosphere by cooling towers. The generators were operated by output control of electricity which was decided by contract of the building. The efficiency would be increased if operation of generators was revised in the intermediate season.

From 2011, the operational strategy had been changed. The ordinary chillers had operational priority to heat recovery chillers. Therefore, the amount of heat

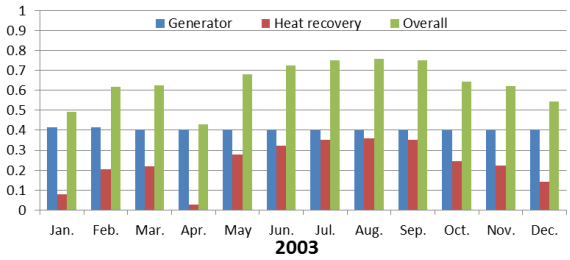

Figure 7-a. Efficiency of co-generation in 2003

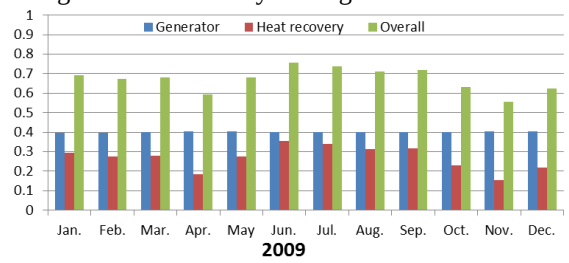

Figure 7-b. Efficiency of co-generation in 2009

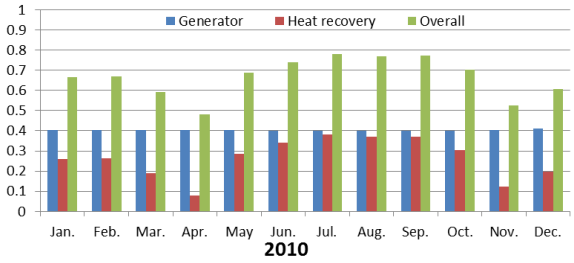

Figure 7-b. Efficiency of co-generation in 2010

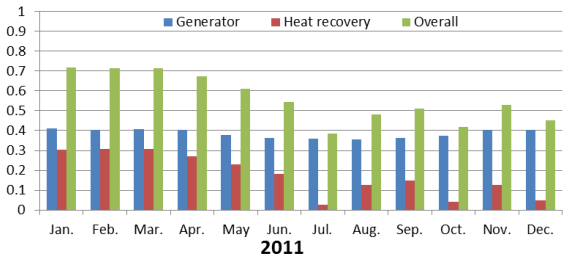

Figure 7-c. Efficiency of co-generation in 2011

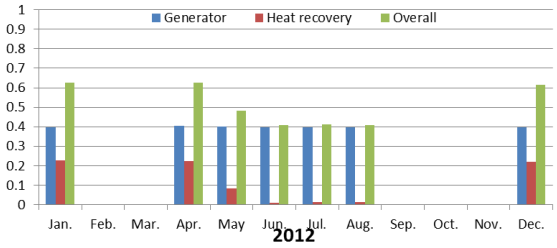

Figure 7-d. Efficiency of co-generation in 2012

recovery was decreased shown in Figure 7-c and 7-d. The reason of change was that COP of heat recovery chillers were lower than ordinary chillers. It was considered that the difference of COP could overcome the amount of heat recovery. In Figure 5, less siginifcance was seen in primary energy efficiency after 2011.

CONCLUSIONS

Energy analysis was conducted using BEMS data of the Osaka gas building. The obtained data was restricted to maintenance purpose. Evaluations were conducted by assuming some values from design specifications.

Primary efficiency for whole year achieved nearly 70 %. However, in the intermediate season, efficiency decreased because the waste heat by output control was not used. Revision of generator operation or utilization of waste heat in intermediate season would be needed to improve the efficiency of the system.

NOMENCLATURES

Q_{DC} : Cooling demand
Q_{DH} :Heating demand
C_S : Gas consumption of whole system
C_P :Gas consumption for chillers
E_P : Electricity consumption for chillers
E_{CGS} : Generated power
Q_{HGS} :Heat recovery
Q_{CGS} : Utilized heat from recovery
Q_{Loss} : Unused heat from recovery
C_{CGS} : Gas consumption of generators
E_s : Electricity consumption of generators
E_D: Electricity Demand
E_G : Purchased electricity
E_T : Electricity consumption for HVAC sytem
k_0:Conversion factor for electricity
k_1:Primary conversion factor for electricity
η_E: Generation efficiency of utitliy (37%)

REFERENCES

Shimoda, Y. et. al. 1998, Synthetic evaluation on ecologilcal District Heating and Cooling system Part 1, Transaction of SHASE, No. 70 pp.59 – 71, 1998. (in Japanese)

Enomoto, H. et. al. 2007, Study on evaluation method of efficiency of cogeneration Part1. *Proceedings of SHASE annual meeting 2007*. B-30, pp.823-826. (in Japanese)

Kawashima, N. et. al 2007, Study on evaluation method of efficiency of cogeneration Part2. *Proceedings of SHASE annual meeting 2007*. B-31, pp.823-826 (in Japanse)

Optimal design of ground source heat pump system integrated with phase change cooling storage tank in an office building

Na Zhu*, Yu Lei, Pingfang Hu, Linghong Xu, Zhangning Jiang

Department of Building Environment and Equipment Engineering, School of Environment of Science and Engineering, Huazhong University of Science and Technology, Wuhan, Hubei 430074, PR China

**Corresponding authors. Tel.: +86 027 87792164x415, E-mail address: bezhuna@hust.edu.cn (N. Zhu)*

Abstract: Ground source heat pump system integrated with phase change cooling storage technology could save energy and shift peak load. This paper studied the optimal design of a ground source heat pump system integrated with phase change thermal storage tank in an office building in Wuhan, China. The performance and economic analysis of this combined system under different thermal storage ratios were analyzed. The optimal operation mode and best storage ratio were obtained for this combined system.

Keywords: ground source heat pump; phase change cooling storage: optimal design; storage ratio

1 Introduction

Geothermal energy is increasingly used through the ground source heat pump (GSHP) in many countries. GSHP provides an efficient and environment friendly way of heating and cooling for buildings. Latent heat storage is particularly attractive since it provides a high energy storage density and has the capacity to store energy at a constant temperature or over a limited range of temperature variation, which is the temperature that corresponds to the phase transition temperature of the material. Phase change material as suitable latent heat storage material used for thermal storage attracts more and more researchers' attention. Thermal storage is an effective way to shift peak load and reduce operation cost.

Zhang et al. [1], Wang et al. [2], Sun et al. [3] and other researchers studied on ground source heat pump system integrated with ice cooling storage technology. He et al. [4] investigated numerically on ground source heat pump system integrated with ice storage technology, and the results showed that the operation cost of the combined system could be reduced by 50% compared with conventional air conditioning system .Han et al. [5] studied ground source heat pump system integrated with solar

heating storage technology, and it is concluded that the system save energy obviously at early and late stages during operation. The energy performance of the combined system could be improved significantly during the medium-term operating compared with conventional heating systems. Kern et al. [6], Hyun-Kap et al. [7] and Kurklu et al. [8] studied on phase change energy storage system. Eduard et al. [9] compared and validated two different mathematical models of packed bed storage with PCM, the results show that the Brinkman equation will be the most useful when free convection play an important role. Huseyin et al. [10] studied energetic performance analysis of a ground-source heat pump system with latent heat storage for a greenhouse heating. Experimental results showed that univalent central heating operation (independent of any other heating system) cannot be met overall heat loss of greenhouse if ambient temperature is very low. There is very few research combined ground source heat pump with phase change thermal storage system in the building.

2 System Design and Modeling

2.1 Load Calculation

A numerical study on a GSHP system integrated with phase change cooling storage tank was carried in an office building located in Wuhan (30.52°N, 114.32°E), China. The total area this office building is 5175 m^2. The heating period is from 1st Dec. to 28th Feb. in winter, and the cooling period is from 1st Jun. to 30th Sep. in summer. The hourly load on architecture standard meteorological year was simulated based on DEST software. Annual dynamic building load is shown in Fig.1. The results are shown in Table 1.

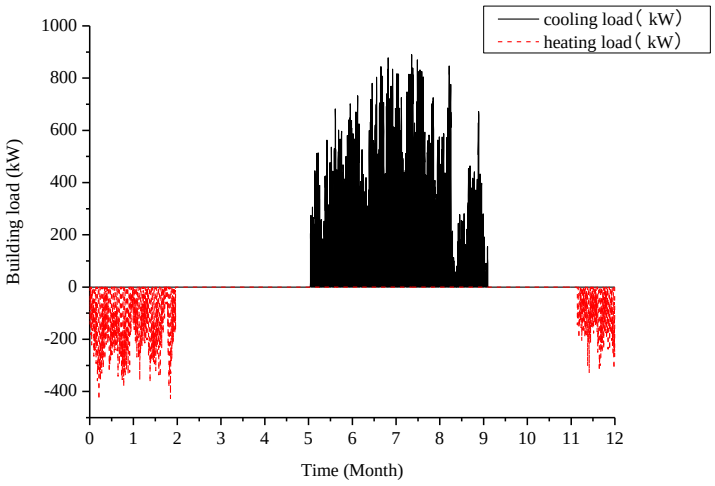

Fig.1. Annual building dynamic load

Table 1. The annual statistical results of dynamic building load

Load type	Value	Ratio of cooling load to heating load
Design cooling load（kW）	1045.46	2.42
Design heating load（kW）	432	
Cumulative cooling load（kWh）	682695	3.6
Cumulative heating load（kWh）	189132	

Fig.1 shows that the cumulative cooling load is 3.6 times the heating load. It is because Wuhan is very hot in summer and cold in winter and is a cooling-dominated area. A single ground source heat pump system can't made the underground soil cold and heat balance. Supplementary cooling technology needs to be used in summer. For the aim of lowering operating cost and shifting peak load, a phase change cooling storage tank integrated into ground source heat pump system is performed without changing conveying system and terminal Forms of the conventional air conditioning system.

2.2 Design calculation of ground heat exchanger and storage tank

This paper uses a ground-coupled heat pump system, the ground heat exchangers as heat source in winter, the cooling tower as cold source in cold storage time, the ground heat exchangers and phase change cooling storage tank were cold source in summer release cold time, Buried pipe adopts vertical single u-shape PE pipe, drilling depth is 100 m, hole spacing is 5 m, the drilling diameter 0.2 m, tube inside diameter 0.032 m, tube external diameter 0.025 m,. According to simulation building annual dynamic load calculation of buried pipe length, the ground heat exchangers as heat source in winter, the ground heat exchangers and cooling tower were cold source in summer. Choose a smaller pipe length as a design value, calculated the number of borehole is 46. However, the ground source heat pump system integrated with phase change cooling storage, without cooling tower provide cold source, because of the ratio of cooling load to heating load is relatively large, under the premise to meet the large load value, so take a summer design pipe length prevail. The number of borehole is 145,126,108,90,72,54 under ration 20%, 30%, 40%, 50%, 60% and 70%

The phase change material is type 47 ($Na_2SO_4 \cdot 10H_2O$ and other salt additives), the phase transition temperature of 8.3℃, phase change latent heat is 95.4 KJ/Kg, cool storage density is 0.0406 m3 / (kW • h).

2.3 Modeling

A numerical model of the ground source heat pump with phase change cooling storage tank have been developed bade on TRNSYS. The ground heat exchangers as heat source in winter. The ground heat exchangers and phase change cooling storage tank were cold source in summer. For cooling storage period at night, heat is dissipated by cooling tower, then the chilled water is transported by cold storage pump to heat pump units, and then the water is cooled to 4-6℃, and finally charge in the storage tank. For cooling release period at daytime, the water from user side goes through cooling storage tank to be cooled to middle temperature, and then to be cooled to set point by chillers. The schematic of composite system is shown in figure 2. The simulation platform of composite system base on TRNSYS is shown in figure 3.

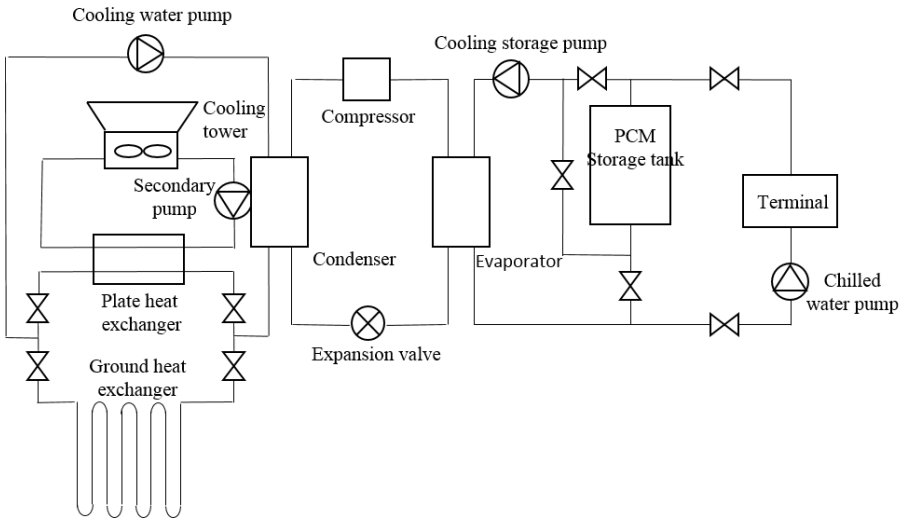

Fig.2. Schematic of composite system

3 Optimization and simulation analysis

3.1 System operation strategy

Operation cost depends on combined system operation strategy. The operation strategy refers to make optimal cooling operation arrangements based on the building load and system characteristics in

the life cycle, including system cooling storage ratio and operation modes in different seasons. Cooling storage includes whole cooling storage and partial cooling storage.

During off-peak hours at night, the chiller will be used for charging cooling when the cooling storage period and operation period of air conditioning systems completely stagger, and stop the chiller while cooling storage meet the requirement of air conditioning. When cooling during the day, cooling storage tank discharges cooling to user side. Refrigerator does not run during this period. All the cooling load of user side is supplied by cooling storage equipment under the whole cooling storage mode. Cooling is stored in a storage tank under partial cooling storage mode during off-peak period at night. During the day, cooling is supplied by cooling storage tank and refrigerator. In general, the refrigerator utilization rate under partial cooling storage mode is higher than whole cooling storage mode, and cooling storage capacity is lower. Considering the system performance and economic factor, partial cooling storage is more appropriate.

Partial cooling storage operation mode includes series and parallel of chiller and cooling storage tank. When chiller and cooling storage tank in parallel, it could take account of the capacity and efficiency of the compressor and cooling storage tank, but the chilled water outlet temperature and water flow control is quite complicated and difficult to maintain at a constant value, and also waste energy. Chiller and cooling storage tank in series includes chiller priority mode and cooling storage tank priority mode. Chiller priority mode is operating chiller firstly when the air conditioning load is greater than the chiller capacity. The rest cooling load is supplemented by cooling storage, while only operating chiller when the air conditioning load is less than the chiller capacity. Cooling storage tank priority is operating cooling storage tank firstly when the air conditioning load is lower than cooling storage capacity, then operating the chiller as complement when the air conditioning load is greater than the storage capacity. This strategy can provide stable and reliable control, and improve the energy efficiency of cooling storage system. Compared with the parallel system, series system is more stable no matter full or partial load operation. Chiller efficiency is higher since higher outlet temperature. It is easier to achieve automatic control of the system.

System operating mode:

1. Summer: Charging cooling in cooling storage tank during night, and opens cooling towers. Discharging cooling during the day, and closes cooling towers, so cooling is provide by ground source heat pump and cooling storage tank.

2. Winter: Heating load is supplied by ground source heat pump systems totally.

3. Remaining season: System stops operating from Mar. 1st to May 31st and Oct. 1st to Nov. 30th.

Base on this project, the operating mode is ground heat pump system integrated with phase change cooling storage tank as partial cooling storage technology. Cooling storage tank operate priority in summer. The optimization ratio of combined system on economy and reliability will be studied in this paper.

3.2 System Optimization

The chillers stop operating or operating less under partial cooling storage mode in peak load, and it could balance the electricity utilization load and improve the power grid load. The air-conditioning electricity consumption is transferred to off-peak period, and it could improve efficiency of electricity utilization and energy efficiency significantly. It could also use cheap electricity at night and save operation cost.

For different cooling storage ratio (the ratio of cool storage tank capacity to total cooling capacity), six different ratios are analyzed in the study, including 20%, 30%, 40%, 50%, 60%, 70%. The calculation time is 20 years and the simulation time step is 1h. The initial soil temperature is 17.3℃. The return water temperature from user side is 10℃ in summer and 40℃ in winter.

The average temperature of soil area during buried pipes showed the similar increasing trend under different cooling storage ratio. Soil temperature increased significantly during the previous 10 years, and tended to stabilized after 10 years. Ground pipe inlet and outlet temperature difference also had the similar trend as above. Choose 30% as an example for analysis within the similar graphics.

The average temperature of soil area during buried pipes and the temperature difference of the inlet and outlet fluid under 30% cooling storage ratio are shown in Fig.3.

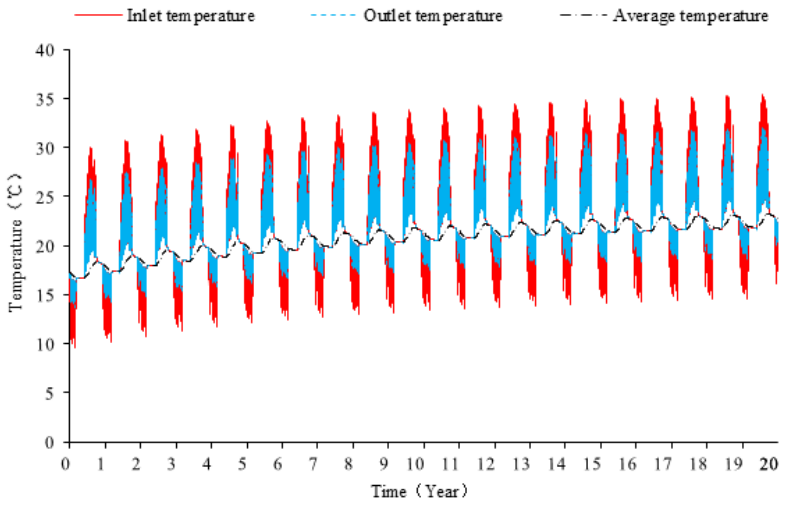

Fig.3. The average temperature of soil and inlet and outlet fluid temperature

Results show that the average soil temperature increased yearly in this region. Soil temperature increases significantly during the previous 10 years, and tends to stabilized after 10 years. After 20 years operation, the average soil temperature increases from the initial 17.3℃ to 23.26℃, and the average annual increases 0.3℃. Ground pipe temperature difference between inlet and outlet changes significantly during the previous 10 years, and tends to stabilized after 10 years. The system operates under different ratio of 20 years, and the maximum soil temperature is shown in Fig.4.

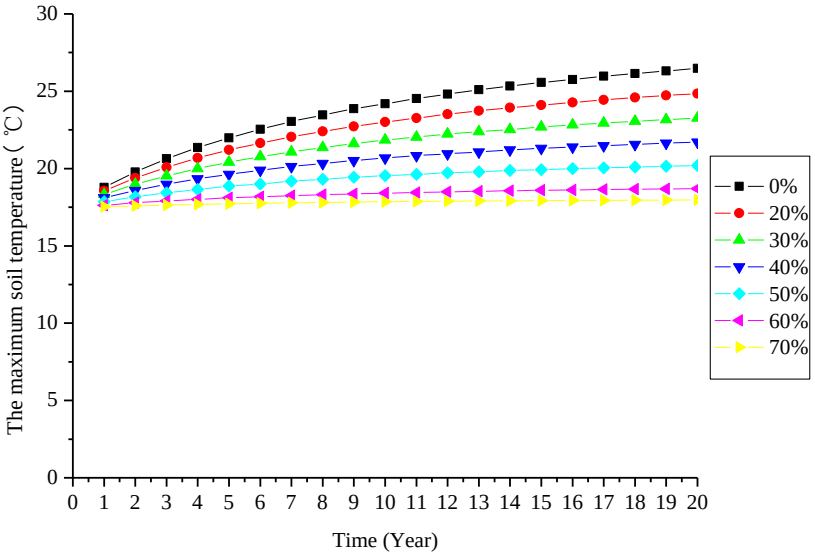

Fig.4. Maximum soil temperature in each storage ratio

Fig.4 shows that with the increase of cool storage rate, maximum average soil temperature decreases with the increase of cooling storage ratio. The initial soil temperature Increased increases

from 17.3℃ to 26.48℃、24.85℃、23.26℃、21.71℃、20.19℃、18.7℃ and 17.97℃ under ration 0%,20%, 30%, 40%, 50%, 60% and 70%, respectively. Storage ratio increased by 0.1 per, The annual average temperature of soil Increased increases 0.46℃、0.38℃、0.3℃、0.22℃、0.14℃、0.07℃ and0.03℃ under ration 0%,20%, 30%, 40%, 50%, 60% and 70%, respectively. The system operates under different ratio of 20 years, and the maximum heat pump units outlet temperature is shown in Fig.5 and the maximum ground pipe outlet temperature is shown in Fig.6

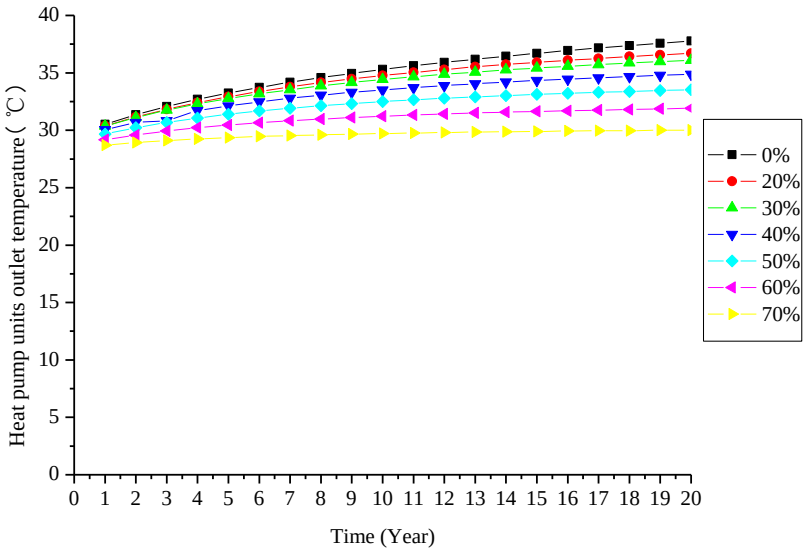

Fig.5. Maximum heat pump units outlet temperature in each storage ratio

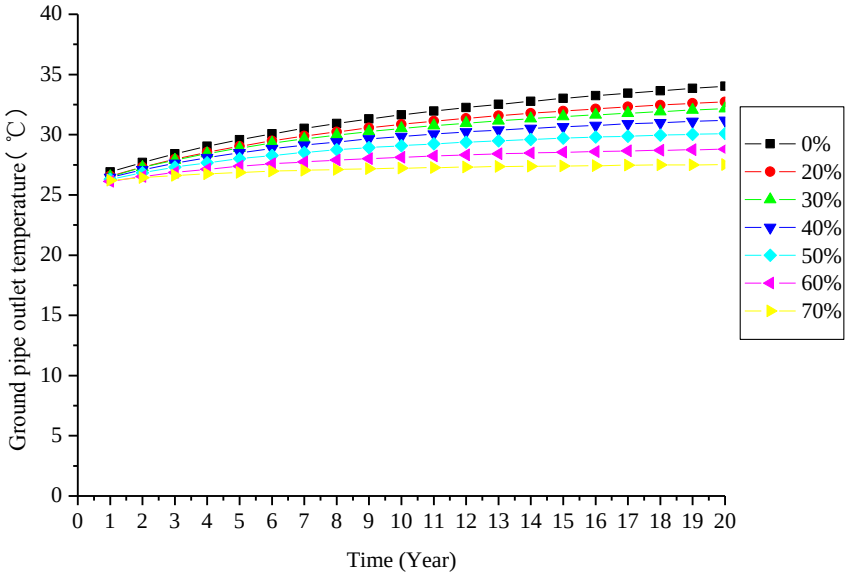

Fig.6. Maximum ground pipe outlet temperature in each storage ratio

Fig.5 and Fig.6 shows that with the increase of cool storage rate, maximum heat pump units outlet and ground pipe outlet temperature decreases with the increase of cooling storage ratio. The temperature increases significantly during the previous 10 years, and tends to stabilized after 10 years. After 20 years operation, the heat pump units outlet temperature increases 7.26℃、6.32℃、5.74℃、4.83℃、3.86℃、2.73℃、1.31℃under ration 0%,20%, 30%, 40%, 50%, 60%,70%. The ground pipe outlet temperature increases 7.12℃、6.17℃、5.63℃、4.74℃、3.79℃、2.69℃、1.31℃ under ration 0%, 20%, 30%, 40%, 50%, 60%， 70%.

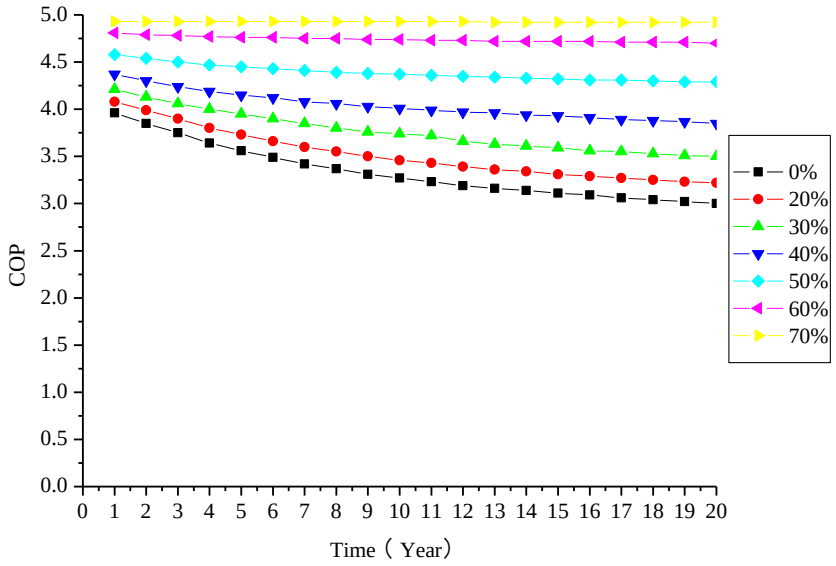

Fig.7. Minimum COP

The minimum COP is shown in Fig.7. Fig.7 shows that with the increase of cool storage rate, The COP decreases with the increase of cooling storage ratio. The COP decline 0.96、0.86、0.71、0.52、0.29、0.11、0.01 under ration 0%,20%, 30%, 40%, 50%, 60%, 70%. After 20 years operation, the COP reduce to 3.5 under ration 0%,20%, 30%， this is not energy-saving. Other cases remained at a high value.

3.3 Energy consumption in life-cycle under different ratios

The calculation time is 20 years and the simulation time step is 1h. The electricity profile of Wuhan is as follow：electricity price is 0.83 RMB/kWh during 7:00-8:00 and 11:00-18:00; it is 0.332 RMB/kWh during 23:00-7:00; it is 1.16 RMB/kWh during remaining time. The system energy consumption in life-cycle under different ratio is shown in table 2. Annual operation cost under different cooling storage ratio is shown in Fig.8. The system energy consumption and annual operation

cost in 20 years operation under optimal ratio compared with the system without cooling storage is shown in Fig.9.

Table 2. The system energy consumption in 20 years operation under different ratio

Cooling storage ratio	Total energy consumption （kWh）	Annual energy consumption （kWh）	Annual operating costs （RMB）	Total operating costs （RMB）	The initial investment （RMB）	Annual cost （RMB）
0%	5187256	259362.8	215271.1	4305422	1212780	275910
20%	4036898	201845	117324	2346478	1530075	193828
30%	3920841	196042	112296	2245918	1387415	181667
40%	3923352	196167	110330	2206598	1293947	175027
50%	4411028	220551	121724	2434483	1617451	202596
60%	4797924	239896	131502	2630039	1940931	228548
70%	5015936	250796	136978	2739568	2102684	242112

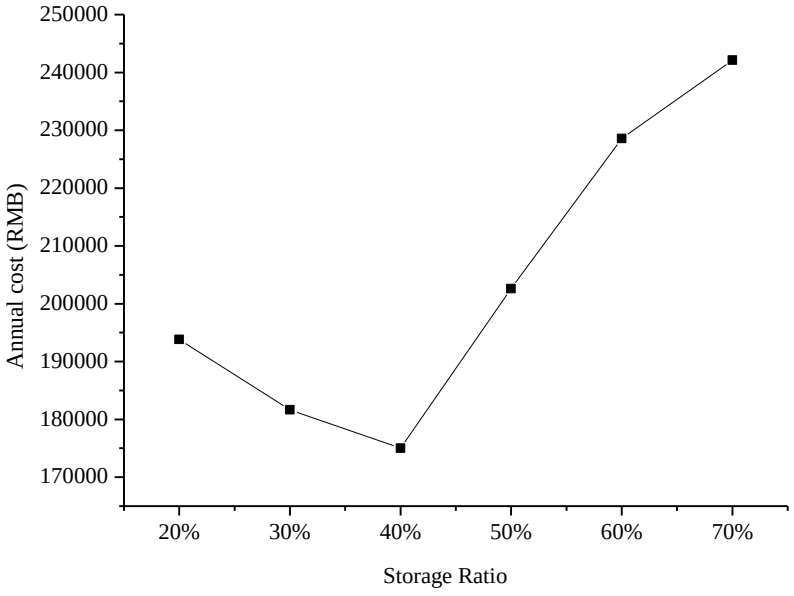

Fig.8. Annual cost under different cooling storage ratio

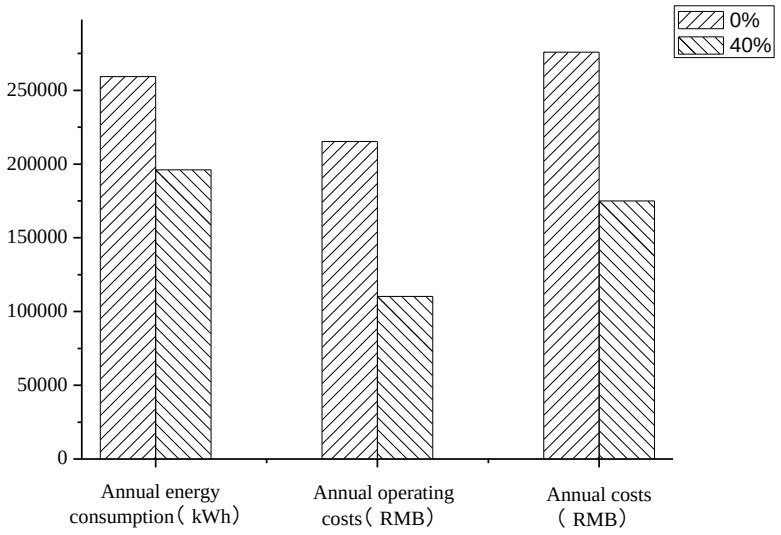

Fig.9. The optimal ratio system compared with the system without cooling storage

Simulation results show that the total energy consumption of the system decreases with the cooling storage ratio and achieves the lowest valuations under cooling storage ratio 30%, and then energy consumption gradually increases. The annual cost reaches minimum value under cool storage ratio 40%. It decreases with the increasing of cooling storage ratio, and then increases with the increasing of cooling storage ratio. Compared with the cooling storage system, the annual operation costs is the largest when there is no cooling storage, while its minimum initial investment. Considering the initial investment and operation costs, it also has the same trend and reached minimum under cooling storage fraction 40%, so the composite system is optimal designed under this ratio.

4 Conclusions

This paper study the performance of ground source heat pump system integrated with phase change cooling storage tank for an office building in Wuhan. Numerical simulation and analysis the composite system have been carried out. A few specific conclusions, which may be useful for optimal design of the combined system, are listed below:

(a) Wuhan is a cooling-dominated area with abundant geothermal energy. Ground source heat pump technology could use renewable energy and the phase change cooling storage technology could shifted peak load and reduce electricity costs. Ground source heat pump system integrated with phase change cooling storage tank is an efficient and environment friendly way of cooling and

heating for buildings. The combined system improves the economy and reliability of the operation performance.

(b) Cooling storage system uses the partial cooling storage and prior cooling mode. The operation mode can make the storage cooling energy release fully and improve the utilization efficiency of cooling storage system. This mode could provide stable and reliable control for the combined system.

(c) With the operation of the system, the average soil temperature increases yearly in this region. Soil temperature increases significantly during the previous 10 years, and tends stabilized after 10 years. The maximum soil temperature decreases with the increasing of cooling storage ratio.

(d) In the system 20 years operation, the energy consumption and operating cost increases with the increasing of cool storage ratio, and then decreases with the increases of cooling storage ratio. Considering initial investment and operation cost, the optimal cooling storage ratio is 40%.

References

[1] X. Zhang. Heat pump technology. Beijing, Chemical Industry Press, 2007.

[2] Y. Wang. Design research of ground source heat pump system integrated with energy storage tank in an office building. Building Science 2010, 26(10): 266-273.

[3] X.F. Sun, Z.H. Zhou. The application of phase change materials in HVAC. Gas & Heat 2006, 26(4): 67-69.

[4] C.F. He, J. Zhu, H.D. Xu. Superiority and application of a combined water-source heat pump and ice storage air conditioning system. HV&AC 2009, 39(10): 116-119.

[5] Z.W. Han, M.Y. Zheng, F.H. Kong, W. Liu. Operation model of solar-assisted ground source heat pump heating system with phase change storage. Renewable Energy Resources 2007, 25(4): 10-14.

[6] M. Kern, R.A. Aldrich. Phase change energy storage in a greenhouse solar heating system. Paper presented at the summer meeting of ASAE and CSAE, pp24-27, University of Manitoba Winnipeg, 1979, 06.

[7] K.S. Hyun. Development of heat pump – PCM latent heat storage system for the greenhouse heating, (I). J Korean Soc Agric Mach 1997, 19(3).

[8] A. Kurklu. Energy storage applications in greenhouse by means of phase change materials (PCM): a review. Renew Energy 1998, 26（1）: 391–399.

[9] O.A. Eduard. Comparative study of different numerical models of packed bed thermal energy storage systems. Applied Thermal Engineering 2013, 50 (1): 384-392.

[10] B. Huseyin. Energetic performance analysis of a ground-source heat pump system with latent heat storage for a greenhouse heating. Energy Conversion and Management 2011, 52(1): 581-589.

A new route for energy efficiency diagnosis and potential analysis of energy consumption from air-conditioning system

Rong-Jiang Ma Nan-Yang Yu
PhD candidate Professor
School of Mechanical Engineering, Southwest Jiaotong University
Chengdu, China

ABSTRACT

Energy consumption of an air-conditioning system reflects the dynamic characters of system in an actual performance. It is extremely important to reduce system energy consumption, while maintains a comfort indoor air condition, by automatic monitoring, and controlling. However, the data collected in a large data repositories become "data disasters", for many operators, it is not possible to detect equipment, design, or operation issues because of data overload. Thus, this paper presents a new route to diagnose the faults of an air-conditioning system and identify the potential energy savings opportunities based on data mining. A case study is implemented to demonstrate the application of the new route and validate its feasibility and effectiveness. The results show that the approach can effectively identify system defaults and reduce the time spent on troubleshooting. It is a powerful and effective tool for diagnosis and potential analysis of energy consumption.

INTRODUCTION

Energy Consumption of Air-Conditioning System

Humanity faces serious energy and environment problems at present. The rapidly growing world energy use has already raised concerns over supply difficulties, exhaustion of energy resources and heavy environmental impacts (Pérez-Lombard et al. 2008). For instance, by increasing greenhouse gas emissions, which are contributed to concentrations in the atmosphere, they having already reached concerning levels in terms of their potential to cause climate change (Arroyo 2006). The international energy agency (IEA) has gathered frightening data on energy consumption trends. During 1984–2004, primary energy has grown by 49% and CO_2 emissions by 43%, with an average annual increase of 2% and 1.8% respectively (Gupta and Chandiwala 2009). Air pollution, acid precipitation and stratospheric ozone depletion are other serious environmental concerns. The severity of climate change impacts is predicted to increase if significant action is not taken to reduce greenhouse gas emissions (Croci et al. 2011). An important action to address energy and environmental challenges lies in the intelligent and efficient use of energy, including reducing energy waste and using low-carbon fuels (Ma et al. 2013).

The global contribution from buildings towards energy consumption, both residential and commercial, has steadily increased reaching figures between 20% and 40% in developed countries (Arroyo 2006). In China, building energy consumption accounts for 19.74% of total energy consumption (Tsinghua University Building Energy Research Center 2013). Among building services, the air-conditioning systems accounts for 50% ~ 60% of energy use (Zhang et al. 2009), and they are the largest energy end use both in the residential and non-residential sector. In other words, the energy consumption of air-conditioning systems accounts for one tenth of the global energy use at least.

Developments of Air-Conditioning System and Major Issues

In 1902, Willis Carrier, the "father of air conditioning", designed a humidity control to accompany a new air-cooling system. He pioneered modern air conditioning (Whitman et al. 2009). After that, to decades of competition with block ice and gas-powered absorption systems, to the rapid spread of space cooling in factories, theaters, offices, houses, automobiles, and entire shopping centers, to the contemporary emergence of cooling load problems and the discovery of the dangers of greenhouse gases and ozone-depleting CFC refrigerants (CFCs) (Kempton and Lutzenhiser 1992).

As a major environmental issue, scientists concluded that released CFCs were depleting the earth's protective ozone layer. Hence many countries, professional organizations and industrial associations made it against the laws or protocols to intentionally vent CFCs into the atmosphere and manufacture CFCs. With sorts of alternative refrigerants were developing and applying to air-conditioning systems, the situation was better with each passing day.

Nevertheless, the status of another major issue is serious enough. As mentioned previously, global warming stemming from the uncontrolled rate of greenhouse gas emissions from energy-consuming process is a major twofold issue, which is the combination of energy and environmental.

An overall objective of energy policy in buildings is to save energy without compromising comfort, health and productivity levels. In other words, the idea is to consume less energy while providing equal or improved building services, that is, being more energy efficient (Pérez-Lombard et al. 2009). Especially important has been the intensification of energy consumption in air-conditioning systems, which has now become almost essential in parallel to the spread in the demand for thermal comfort, considered a luxury not long ago.

Europe developed early building envelope regulations in the late 1970s to reduce heat transfer through envelope elements and to control vapour diffusion and air permeability. This was followed by regulations or best practice recommendations on design, calculation and maintenance of air-conditioning systems and other building thermal services. Significantly, air conditioning equipment was subject for the first time to minimum requirements of energy efficiency (Pérez-Lombard et al. 2009). Until recently, various theories, methods, processes, and practices concerning energy efficiency of air conditioning have continued to develop.

For instance, the principal electrical components of a typical all-air air-conditioning system include: (1) chiller electric driven, (2) condensing water pump, (3) chilled water pump, (4) supply air fan, (5) return air fan, and (6) cooling tower fan. Moreover, the six devices consume most of the energy (electricity) in the system, and soon became the center of a particular focus.

According to the standards, it must be based on the most disadvantageous situation (maximum cooling load) for air-conditioning system design. That is to say, an air-conditioning system must meet the maximum cooling requirements of air-conditioned spaces. Indeed, systems rarely operate with the extreme conditions (maximum cooling load), and most of the time they operate with the partial load. Research data show that the operating time of central air-conditioning systems at 70% load (and below) accounts for 97% of service life (Wang H. Z. et al. 2009; Yang et al. 2005). So it is very meaningful and valuable to study energy efficiency for air-conditioning systems.

STATUS OF ENERGY EFFICIENCY DIAGNOSIS FOR AIR-CONDITIONING SYSTEM

Energy efficiency diagnosis is able to save energy, reduce maintenance costs, extend

equipment life, and improve air-conditioning system control and occupant comfort. In this section, we focus on another critical issue: the current energy efficiency diagnosis methods of air-conditioning system. Summarizing the methods and indicators, the paper also answer to why the introduction of the new route for air-conditioning system.

Energy Efficiency Evaluation and Index System

Most energy (or building) services companies use the energy performance index (EPI) (Pérez-Lombard et al. 2009) as a starting point in energy audits and assess saving opportunities by comparing with existing references. In their final reports or ads, we can find a multiplicity of terms and concepts such as energy performance, energy efficiency, energy rating, benchmarking, baseline, grade, and some acronyms like COP, EER, IPLV, etc. Some of them have nearly similar meaning and usage, which are hard to distinguish. This has frequently led to misleading interpretations by consumers, company staff, and even proficient technicians. Even so, these terms, concepts and indexes have a common purpose: to improve energy efficiency and reduce energy consumption.

Coefficient of performance (COP) (McQuistion et al. 2005) is widely used in the field of air conditioning, and almost is the most important indicator for energy efficiency of an air-conditioning system.

Almost all countries have standards about the limit values of COP, such as "For air-cooled chillers of all sizes, the minimum requirement is COP of 2.8."specified in the ANSI/ASHRAE/IESNA Standard 90.1, *Energy Standard for Buildings Except Low-Rise Residential Buildings* (2010) in the US and "A water-cooled chiller under 528kW has a required minimum COP of 4.0, and a chiller that is over 1163kW has a required COP of 4.2." specified in The People's Republic of China National Standard GB 19577-2004, *The Minimum Allowable Values of The Energy Efficiency and Energy Efficiency Grades for Water Chillers* (2004).

Obviously, COP does not cover various situations, like air-conditioning systems in different regions, orientations, building types, occupants' habits and so on. In order to improve the evaluation of energy efficiency for the systems, other indicators such as IPLV(Cao 2004), SEER (Gu et al. 2005), and DEER (Xiao and Fu 2007) are also used in evaluation of system efficiency. All these indicators provide the basis for energy efficiency diagnosis indeed.

Typical Energy Efficiency Diagnosis Method and Implementation

There is no single ''right way'' to undertake energy efficiency diagnosis. The practical process should shift, adjust, and adapt to each project's needs and context. Therefore many kinds of diagnosis methods are applied to actual projects, but from the overall method, they are similar to each other. Typically and ideally, an energy efficiency diagnosis method includes three phases. First, by looking at the as-built drawings and the energy consumption records of the air-conditioning system, researchers must get the basic information and current status of energy consumption of the system, as well as by learning about the existing problems or troubles and related complaints of the system from the operators. Then, it is necessary to test, analyze and calculate for each existing problem in more detail including the typical condition and various operating conditions of different seasons according to operation records. Finally, the solution and corresponding potential analysis are presented by the summary report. This typical process can be summarized as OTI method (Xue Z. F.2007a; Xue Z. F. 2007b), that is to say, "observation/question → test/calculation → identification/resolution," as shown in Figure 1.

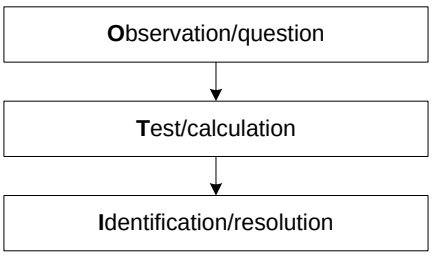

Figure 1 OTI method for energy efficiency diagnosis

This method involves building envelope, fresh air supply, cold and heat source, the transmission and distribution systems, etc., which can be divided into 15 steps for air-conditioning systems in detail, and 5 steps more for whole building. These steps connected to each other, but there is no fixed order. Normally, flexible work according to the specific situation of a system, different seasons, etc., will be carried out for an actual system.

But how to implement energy efficiency diagnosis by using this method? Let's take Step 6 of OTI method to illustrate it. The major contents of Step 6 are listed in Table 1.

Table 1 Diagnosis for COP of chiller (Step 6)

Phase	Job
O	—Whether the chilled water by-pass through a chiller, which is not running? —Is there a chiller correspond to two chilled water pumps? —Check the switch-status of by-pass valve between distributor and collector of chilled water.
T	—Test chilled water-flow of each chiller. —Test and calculate COP of chiller under typi-cal operating modes.
I	—To identify whether each chiller runs efficiently, by testing the typical operating modes and analyzing the operation records.

From the table, we can see that the second and third phase of the process are very important and difficult, especially the latter, and most of the time must be spent on it. At the same time, the indicators mentioned above as the basis of the final conclusion are exploited to evaluate the system. In addition, some methods like artificial neural network (ANN) (Zhao and Magoulès 2012) are used in the measurement and calculation for the value of parameters. That makes this process become more cumbersome and complex.

But generally speaking, although the OTI method is a self-contained system, it is limited to concrete analysis of a specific issue, without common applicable procedure. So to a large extent, the quality of the final result depends on the proficiency of the technicians and investigators in the work.

Summary

The above discussion reviews energy efficiency evaluation and index systems as the basis for diagnosis, presents the typical energy efficiency diagnosis method and implementation, The role of existing evaluation indicators and index systems is just at the level of guideline and standard, which is insufficient for tapping the potential capacity of energy conservation in an air-conditioning system. Present representative energy efficiency diagnosis methods are tedious and complex, and they require a heavy workload to acquire diagnosis results.

DATA MINING AND DATA QUALITY

This section describes the background and requirements of the new route presented in this paper.

Energy consumption of air-conditioning systems is one of the most direct and correct parameters, which reflects the dynamic characters of a system in actual running status. It is important to reduce system energy consumption by automatically monitoring, analyzing, and controlling. Nowadays, more and more air-conditioning systems have achieved

energy consumption data acquisition, and more data are being accumulated in the operation process. These data will provide the foundation for analyzing the operation situation of the system. However, data collected in large data repositories become "data tombs"—data archives that are seldom visited (Han et al. 2012). Therefore, the traditional data analysis methods have some difficulties in dealing with the mass of data, resulting in more and more serious "data disasters" and making it difficult for operation staff to find the abnormal issues of a system efficiently. So it is more impossible to achieve the optimizing control.

Data Mining

Data mining is the application of specific algorithms for extracting patterns from data (Fayyad et al. 1996). Historically the notion of finding useful/interesting patterns in data has been given a variety of names including data mining, knowledge discovery from data (KDD), knowledge extraction, information discovery, knowledge mining from data, data/pattern analysis, data archaeology, data pattern processing, and data dredging. The knowledge discovery process as an iterative sequence comprises the following steps (Han et al. 2012): (1) data cleaning, (2) data integration, (3) data selection, (4) data transformation, (5) data mining, (6) pattern evaluation, and (7) knowledge presentation. In this sequence, steps (1) through (4) are different forms of data preprocessing, where data are prepared for mining.

Research (Kim et al. 2011; Ahmed et al. 2011; Wang Z. et al. 2011; Lian et al. 2006; Rakhshani et al. 2009; Liu et al. 2010; Li X. L. et al. 2010; Seem 2007) in the air-conditioning system or building energy consumption field by using the data mining approach has been yielding some results in recent years. By using this approach, this research has obtained results which are very difficult to be obtained by conventional methods. For example, energy modeling tasks are usually conducted later in the design process due to its time consuming data entry, but the case study in reference (Kim et al. 2011) revealed that data mining based energy modeling helps project teams discover useful patterns to improve the energy efficiency of building design during the design phase. A few researchers like (Ahmed et al. 2011) investigated the impact of connecting building characteristics and designs with their performance by data mining techniques. The derived results show the high accuracy and reliability of these techniques in predicting low-energy comfortable rooms. By using the approach and combining artificial intelligence algorithms, like ANN, a new modeling method for reducing the dimensions of acquired data, aiming to find a strong association, was developed in reference (Wang Z. et al. 2011), and some strategies (Lian et al. 2006, Rakhshani et al. 2009) were developed to detect and diagnose the faults of heating, ventilating, and air conditioning (HVAC) systems. At the same time, the detection/classification of abnormal energy consumption in buildings was researched by using the data mining approach. In Liu et al. (2010) and Li X. L. et al. (2010), the detection/classification method was proposed. Although it can even be used in conjunction with a building-management system to identify abnormal utility consumption and notify building operators in real time, we think, the outlier detection is only the first step that studies energy efficiency and energy conservation of the system. And in these, the causes of generating outlier and the optimization solutions of system operation require analysis and study by the operators and maintenance staff. The burden of this effort has been eased by the work of Seem (2007). The new method uses outlier detection to determine if the energy consumption for a particular day is significantly different than previous energy consumption. Operators should

save time by not having to manually detect faults or diagnose false alarms; also, the new method will reduce operating costs by detecting problems that previously would have gone unnoticed (Seem 2007). But unfortunately, this method obtains the results (e.g., abnormal energy consumption) by comparing the actual energy consumption and normal energy consumption. Thus it does not completely satisfy the requirements of focus field of this paper, for instance, to ensure energy is being used most efficiently, to find out the potential capacity of energy conservation of the actual system.

Energy Consumption Data and Data Quality

Energy waste is often hidden, and some hidden problems that may not obviously affect comfort or environmental quality cause owners to pay much more for energy than necessary. In order to find problems and energy-saving potential and to optimize system operation more precisely and efficiently, it is necessary to put forward some requirements on the quality of the data. Hereafter, electricity-consumption data as the main research object will be discussed. Also, water, gas and other usage data of air-conditioning systems will be analyzed by using the method below.

(1) Data sources. Data can be derived from energy management systems (EMS), data loggers, or monitor sensors, etc.

(2) Accuracy. The data should reflect the real energy consumption of the monitoring components. Monitoring activities should not interfere with the air-conditioning system itself, for these monitoring tools/equipment are usually based on the Non-Intrusive Load Monitor (NILM) approach. More information about the NILM can be found in the references (Hart 1992; Norford and Leeb 1996; Fan et al. 2012).

(3) Completeness. A complete set of data should include the necessary parameters such as amperage, voltage, power factor or power of major energy-using devices for research or practical application. Data loss is not allowed. If any one of the parameters is missing, other parameters at the same time period shall not be used in the data.

(4) Consistency. The format of same type parameter in the system and the intervals of all parameters at the same monitoring time should be consistent.

NEW ROUTE

Overview of New Route

The flow chart is also the achievable functions of the new route as shown in Figure 2. And the whole process is aimed at detecting system problems and finding the energy-saving opportunities.

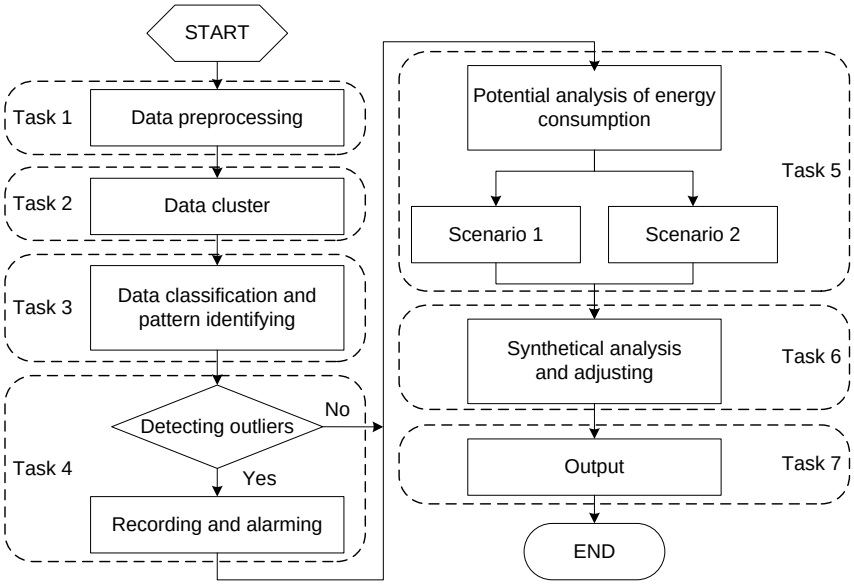

Figure 2 Flow chart of new route

The main tasks are as follows:

(1) Preprocess the data of energy consumption,

(2) Cluster the data and draw clustering figures,

(3) Classify the data of devices and system, and identify pattern of energy consumption (Seem 2005),

(4) Determine whether the energy consumption is abnormal, if "Yes", then take a record and alarm,

(5) In two scenarios, analyze the energy-saving potential of the system,

(6) Synthetically analyze and adjust the results in these two scenarios,

(7) Output the final result.

Data Preprocessing

Data preprocessing techniques can improve data quality, thereby helping to improve the accuracy and efficiency of the subsequent mining process. Data preprocessing is an important step in the knowledge discovery process, because quality decisions must be based on quality data. (Fayyad et al. 1996)

There are four major steps involved in data preprocessing as mentioned above, including many different methods in each step. For actual data preprocessing, every step should meet the requirements of data quality in the previous section and actual quality of the data, then an appropriate method should be chosen.

In the preprocessing step, the data are transformed or consolidated so that the resulting mining process may be more efficient, and the patterns found may be easier to understand (Han et al. 2012). Data normalization is one of strategies for data transformation, and many methods were adopted, such as min-max normalization, z-score normalization, normalization by decimal scaling, and so on. Because the values of energy consumption data are usually large, and exist with frequent variances at different times, so z-score normalization (Cai and Chen 2010) is useful and suitable for data normalization. In z-score normalization, the values for an attribute, A, are normalized based on the mean and standard deviation of A. And A value, v, of A is normalized to v' by computing

$$v' = \frac{v - \overline{A}}{\sigma_A} \quad (1)$$

where $\overline{A}$ and σ_A are the mean and standard deviation of attribute A, respectively.

The missing value of time-series data of

energy consumption, for convenience, will be discarded in the preprocessing step.

Cluster Analysis

Cluster analysis (Han et al. 2012; He et al. 2007) can divide into several categories: partitioning clustering, hierarchical clustering, density-based clustering, and constraint clustering. Partitioning clustering (e.g., k-means, k-medoids, etc.) and hierarchical clustering (e.g., AGNES, DIANA, BIRCH, Chameleon, etc.) are designed to find spherical-shaped clusters, which have difficulties in finding clusters of arbitrary shape. Density-based clustering (e.g., DBSCAN, OPTICS, DENCLUE, etc.) can discover clusters of arbitrary shape, and handle anomalous data effectively. Constraint clustering is commonly used to handle certain requirements in the specific application areas.

Due to the potentially large dataset of energy consumption, there may be noisy data, and we have no prior knowledge on its shape, so DBSCAN (Density-Based Spatial Clustering of Applications with Noise) can be suitable for it.

DBSCAN algorithm steps (Nasibov and Ulutagay 2009) are explained as follows:

(1) Specify ε and *MinPts*,

(2) Find an unclassified core-point p with parameters ε and *MinPts*, mark the point p to be classified, start a new empty cluster C_t and assign p to this cluster,

(3) Find all the unclassified points in the ε-neighborhood of p and call them a set of seeds,

(4) Get a point q in the set of seeds, mark q to be classified, assign q to the cluster C_t, and remove q from the set of seeds,

(5) Check if q is a core-point with parameters ε and *MinPts*, if so, add all the unclassified points in the ε-neighborhood of q to the set of seeds,

(6) Repeat steps (4) and (5) until the set of seeds is empty,

(7) Repeat steps (2)-(6) until no more core points can be found.

where ε is the radius parameter, and *MinPts* is the neighborhood density threshold.

From the results analyzed by DBSCAN algorithm, we can get the preliminary patterns of energy consumption of a system, for example, time-series patterns, "weekday business hours," "weekday off hours," "weekend business hours," and "weekend off hours." Although these results cannot be used directly for energy efficiency diagnosis and potential analysis of energy consumption, that is the necessary basis of the next step.

Data Classification and Pattern Identifying

There are some major classification methods (Kotsiantis 2013): decision tree classifiers, Bayesian classifiers, and support vector machine (SVM), etc. Bayesian classifiers are statistical classifiers, which assume that the effect of an attribute value on a given class is independent of the values of the other attributes. However, this assumption tends to be invalid in many real systems, including air-conditioning systems. The SVM is a highly accurate classification method. Nevertheless, even the fastest SVM still suffers from slow processing, especially when training with massive datasets.

The construction of decision tree classifiers does not require any domain knowledge or parameter setting. The representation of acquired knowledge in tree form is intuitive and generally easy for people to assimilate. In addition, the decision tree classifiers have good accuracy, therefore, the study choose this method to construct the decision tree for patterns of energy consumption.

As a classic algorithm, C4.5 (Polat and Güneş 2009) is widely used to build classification models. C4.5 algorithm steps (Taherkhani 2010) are shown as follows:

(1) Compute gain ratio for each attribute by

$$GainRatio(A) = \frac{Gain(A)}{SplitInfo(A)} \qquad (2)$$

where *Gain* is information gain; *SplitInfo* is split

information, and $SplitInfo(A) = -\sum_{i=1}^{n} p_i \log_2(p_i)$.

(2) Select the attribute with the maximum gain ratio as the splitting attribute of given set and create a node for the splitting attribute and mark the attribute, and then create a branch for each value in the attribute, and partition sample accordingly.

Through steps above, the patterns of energy consumption will be classified and identified for a given dataset. It should be noted that the patterns are more colorful and richer than those in previous subsection. Taking an example for time-series, the patterns were classified by hours, or even minutes, which are selected and adjusted in conformity to the character of practical data, whereas in previous subsection the patterns are classified simply by days.

Outliers Analysis and Energy Consumption

Anomalies Detection

Outlier detection methods (Xue A. R. et al. 2008) can divide into several categories, based on distribution, distance, density, etc. Distribution-based outlier detection methods (e.g., ESD, GESR, etc.) make assumptions of data normality. They assume that normal data objects are generated by a statistical (stochastic) model, and that data not following the model are outliers (Han et al. 2012). Distance-based outlier detection (e.g., k-NN, etc.) takes a global view of the dataset, and such outliers can be regarded as "global outliers." Density-based outlier detection (e.g., LOF, etc.) is useful for global outliers and local outliers.

Given that there may be multiple clusters with different densities, and varieties of position relations between clusters in the dataset of energy consumption, in order to improve the detection accuracy, density-based outlier detection is a good choice. As a classic algorithm, LOF (Breunig et al. 2000) has some nice properties and wide applicability in a real world application.

LOF algorithm steps (Li J.et al. 2008) are expressed as follows:

(1) Search neighborhoods for each object in the dataset, calculate the *MinPts*-neighborhood, and store the distances between the object and its neighbors,

(2) Calculate the local reachability density and local outlier factor (LOF) for each object,

(3) Check every object to determine if it is an outlier according to the pre-set threshold for LOF.

Outliers are not only great energy-saving opportunities, but also the reflection of troubles and faults of a system. So this method will take a record and give an alarm to operators when it finds any outliers.

Potential Analysis and Results

Two scenarios for analysis

This paper analyses the potential capacity of energy conservation under the following two scenarios:

Scenario 1: Study the best running state of system under various operating conditions, without considering the reasonableness of design and device selection;

Scenario 2: Study the best running state of system under various operating conditions, with energy-saving revamping measures.

As one can see, Scenario 1 is the most basic way, which hardly requires money and tunes the system to get it running as well as possible. In addition, the potentials are also very limited, and they are largely affected by the existing system itself. In Scenario 2, it will take the necessary reform measures to improve problem areas, for instance, install the frequency convertor on pump or fan motors, replace the air-cooled chiller with oil-free chiller or water-cooled chiller, etc. which are more energy-efficient than existing facilities. In a word, it costs something in Scenario 2, but saves much more than Scenario 1.

Theoretical basis

Take pumps as an example, η, efficiency parameter, is often used to evaluate the economy of energy consumption. But in fact, it cannot directly reflect the economy level of pump or transport system by itself. Just like the efficiency of auto engines or transmission systems, the values of η cannot be measured directly, and they are not the users' concern. What is more interesting to us is that which can directly and accurately reflect the economic performance of devices or systems, such as fuel consumption per 100 km for cars, and fuel consumption per ton-kilometer for trucks. Some research (Lu 2007; Dong et al. 2008; Lu and Wang 2009) has used engineering attributes to deal with the energy analysis and provided some new concept like K_E, the "energy transport consumption per unit volume (i.e. energy consumption coefficient)" (Dong et al. 2008). The definition (Lu and Wang 2009) is presented as:

$$K_E = \frac{P}{q_V} = \frac{(\rho g H q_V)/\eta}{q_V} = \frac{\rho g H}{\eta} \quad (3)$$

where P is pump shaft power, q_V is transport volume, ρ is density of liquid, g is the gravitational acceleration, H is pump head, η is pump efficiency. And the unit of K_E is J/m^3.

For real-world systems, power consumption of pump system (P_E) is easier to measure than P, the above can be adapted as (Lu and Wang 2009):

$$K_{E,E} = \frac{P_E}{q_V} = \frac{(\rho g H q_V)/(\eta \cdot \eta_M)}{q_V} = \frac{\rho g H}{\eta \cdot \eta_M} \quad (4)$$

where η_M is pump motor efficiency, and the unit of $K_{E,E}$ is kWh/m^3.

As an index for the economic estimation, this concept will be used in the analysis.

Analysis thread and results

Analysis thread for Scenario 1 as follows:

(1) Analyze the data of each pattern of energy consumption, and get the operating characteristic curve,

(2) Analyze the data of each pattern of energy consumption by time-series, and get the attenuation of system and each device,

(3) Study the time and space distribution of data of each pattern of energy consumption, and get the logical relationship between data of each device,

(4) Determine the optimal operating point or range for each pattern of energy consumption based on above works, and as measured by $K_{E,E}$,

(5) Calculate the difference between actual operating data and the optimal data of corresponding patterns, and get the energy-saving potential of devices and systems.

The analysis thread for Scenario 2 is similar to above, except that it will call the data of revamping measure database in step (4).

Before the final result comes out, we need to synthetically analyze and adjust the results of two scenarios accounting for variations in weather, space use, or other variables from year to year.

METHOD VALIDATIONS

It is known from analysis in the second section that we still lack a systematic method for energy efficiency diagnosis of air-conditioning systems, so we proposed the new route before that. This section selected one case to investigate the application of the new route mentioned at the previous section, in order to validate its feasibility and effectiveness.

Case Description

As described in the above sections, the electricity of pumps was a part of air-conditioning system energy consumption, which was shown in Figure 3. We can see that the pumps are intermittent, running in 0:00 to 06:00 and 22:00 to 0:00, the rest of the time running continuously. Note that this pump electricity was simulated by using "RefBldgLargeOfficeNew2004_Chicago.idf" on July 21 in the Energyplus V8.0.0 (http://apps1.eere.energy.gov). The "timestep" was set to 60 times per hour. This study selected

SPSS Clementine 12.0 (http://www.SPSS.com) to preprocess and classify the data. In addition, ELKI 0.6.0 (http://elki.dbs.ifi.lmu.de) was used to do cluster analysis and outlier analysis for all the data.

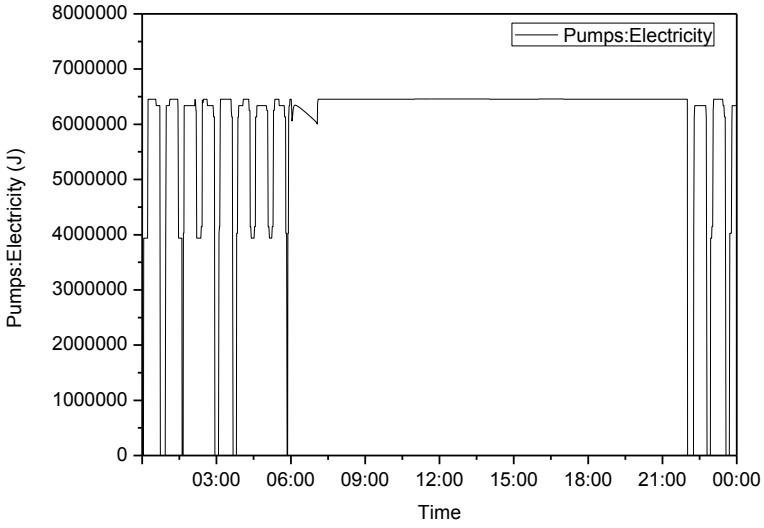

Figure 3 Electricity consumption of pumps in July 21st

Validation Process and Results

According to the method shown in the previous section, the energy consumption data were first preprocessed before the cluster analysis. To find the potential energy consumption pattern for an air-conditioning system, the cluster analysis needs to extract the feature vector from the time series data of energy consumption. This important feature vector shows the system energy consumption and was represented as:

$$\boldsymbol{C}=(C_{avg},\ C_{max}) \qquad (5)$$

where C_{avg} and C_{max} are the averaged and maximum energy consumption per quarter of an hour, respectively.

Figure 4 shows the results of cluster analysis utilizing the method presented in the previous section. From this figure, we can find that there are three patterns for system energy consumption, which are system halt and underload condition and constant load condition. Here these two conditions were named Cluster A and Cluster B, respectively.

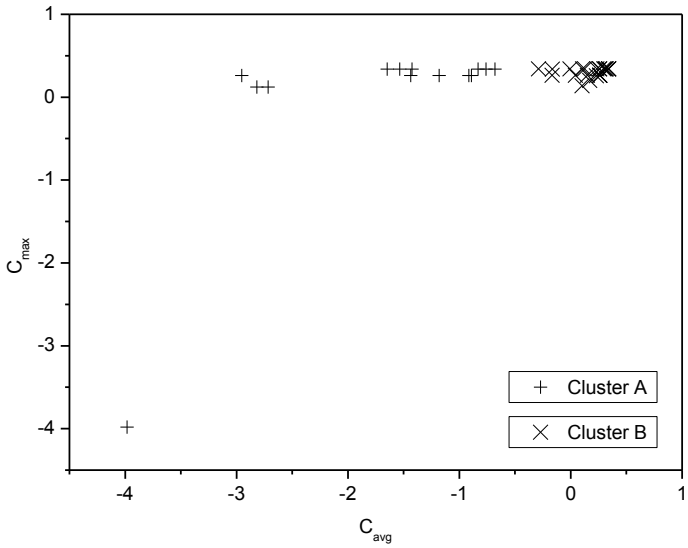

Figure 4 Cluster analysis results

To easily analyze the criterion of energy consumption pattern, this study constructed one new attribute: energy consumption label, and brought results of the cluster analysis into the case data. These case data were then classified by using the method mentioned in the previous section and applied to obtain the decision tree (Figure 5) of energy consumption pattern.

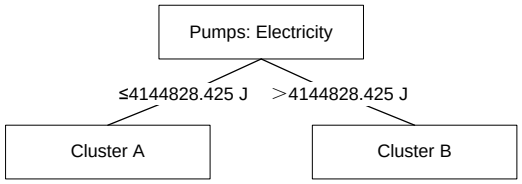

Figure 5 Decision tree of energy consumption pattern

The conclusion was presented as:

(1) If "Pumps: Electricity"≤4144828.425 J (based on 109 training data), this energy consumption pattern is Cluster A with confidence level of 100%.

(2) If "Pumps: Electricity"＞4144828.425 J (based on 891 training data), this energy consumption pattern is Cluster B with confidence level of 100%.

To validate the effect of outlier analysis, we assumed one abnormal point at one moment between 8:01 to 22:00, such as the decrease of motor efficiency. According to the decision tree of energy consumption pattern, the entire patterns are Cluster B at this moment. In addition, to estimate the abnormal moment as detailed as possible, the energy consumption data at abnormal moment and normal moment with the same pattern (Cluster B) were analyzed by using the method mentioned in the previous section. Figure 6 shows the local outlier factor for all the data between 8:01 to 22:00. From this figure, we can find that the majority of LOF values were around 1, while the LOF value at 16:33 was 35.25. In fact, the motor efficiency at this moment decreased from 90% to 89%, resulting in abnormal energy consumption. Therefore, this special point was exactly the outlier which was characterized by the abnormal energy consumption.

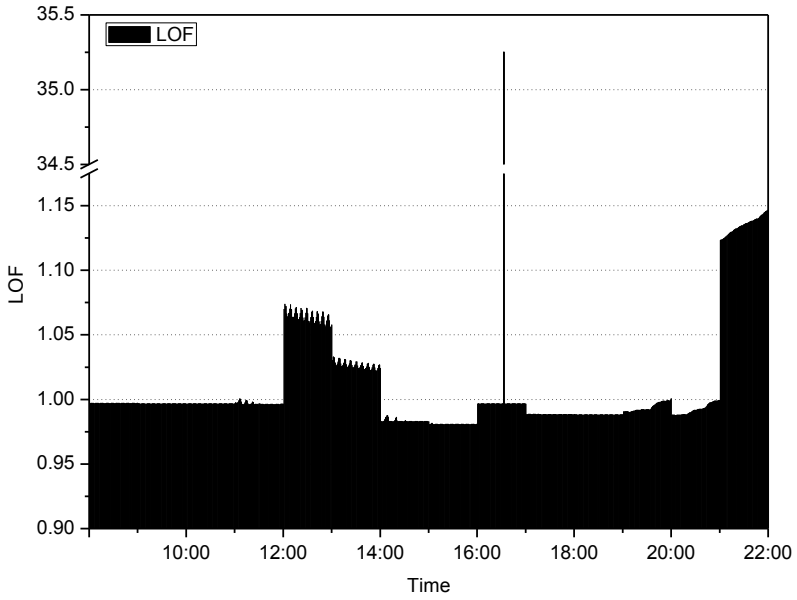

Figure 6 The LOF values of energy consumption data between 8:01 to 22:00

Discussion

For the potential analysis of energy consumption conservation, the more variable and more substantial data are required, such as data warehouse. It should be noted that the energy consumption difference between the motor efficiency with the value of 89% and 90% at 16:33 was considered as basic energy-saving potential. Due to lack of more data and collision with the main object of this research, this paper will not investigate the validation more deeply. Further study will focus on more detailed application research.

CONCLUSIONS

In this paper, we reviewed the major issues and status of energy efficiency diagnosis for air-conditioning systems. The role of existing evaluation indicators and index systems is just at the level of guideline and standard, and it is insufficient for tapping the potential capacity of energy conservation in air-conditioning systems. Although efforts have been made to develop energy efficiency diagnosis methods, including expert diagnosis systems and knowledge-based technologies, these typically rely on users or domain experts to manually input knowledge into knowledge bases. Unfortunately, the manual knowledge input procedure is prone to biases and errors and is extremely costly and time consuming.

Although many buildings use a sophisticated system (e.g., EMS) to manage a wide and varied range of building systems, which can collect and store massive quantities of energy consumption data, facility operators can be overwhelmed with the quantity of data. For many operators, it is not possible to detect equipment, design, or operation problems because of data overload. Data mining, which has benefited from the development of computer and information technology, provides a basis for using the data.

Based on these understandings, we presented a new route for solving the energy efficiency diagnosis and potential analysis of energy consumption using the data mining approach, and introduced the main tasks, implementation methods and some requirements. We then selected one case to investigate the application of the new route, and the results show that the route is feasible and applicable in air-conditioning systems.

At last, for this route, we recognize that there is still a long way to investigate, improve, and practically apply. Even so, we still believe that this approach advances a brand-new research method and is of great project application value in bringing about a leap of energy efficiency of air-conditioning systems in a real sense.

ACKNOWLEDGMENTS

Authors would like to thank Dr. Ji-Ying Liu for his advice and constructive discussions.

CONFLICT OF INTEREST

Authors declare that we do not have any commercial or associative interest that represents a conflict of interest regarding the publication of this article.

REFERENCES

Ahmed, A., Korres, N. E., Ploennigs, J., Elhadi, H., & Menzel, K. (2011). Mining building performance data for energy-efficient operation. *Advanced Engineering Informatics, 25*(2), 341-354, doi:10.1016/j.aei.2010.10.002.

ANSI/ASHRAE/IESNA Standard 90.1, Energy standard for buildings except low-rise residential buildings (2010). (Vol. 90.1). Atlanta, USA: ASHRAE, Inc.

Arroyo, V. (2006). Agenda for climate action. Arlington, VA, USA: Pew Center on Global Climate Change.

Breunig, M. M., Kriegel, H.-P., Ng, R. T., & Sander, J. (2000). LOF: identifying density-based local outliers. *SIGMOD Rec., 29*(2), 93-104, doi:10.1145/335191.335388.

Cai, W. L., & Chen, D. X. (2010). Influence of date normalization methods on k-nearest neighbor classifier. *Computer engineering*(22), 175-177.

Cao, Q. (2004). Disccussion on meanings of IPLV. *Construction Machinery for Hydraulic Engineering & Power Station*(2), 9-10.

Croci, E., Melandri, S., & Molteni, T. (2011). Determinants of cities' GHG emissions: a comparison of seven global cities. *International Journal of Climate Change Strategies and Management, 3*(3), 275-301.

Dong, Y., Yan, G. J., & Lu, Z. D. (2008). Energy efficiency analysis and evaluation for the pump fluid system. *China mechanical engineering, 19*(14), 1687-1690.

Fan, Y. C., Liu, X. J., Lee, W. C., & Chen, A. L. P. Efficient Time Series Disaggregation for Non-intrusive Appliance Load Monitoring. In *Ubiquitous Intelligence & Computing and 9th International Conference on Autonomic & Trusted Computing (UIC/ATC), 2012 9th International Conference on, 4-7 Sept. 2012 2012* (pp. 248-255). doi:10.1109/UIC-ATC.2012.122.

Fayyad, U. M., Piatetsky-Shapiro, G., Smyth, P., & Uthurusamy, R. (1996). *Advances in knowledge discovery and data mining*: AAAI/MIT Press.

Gu, B., Wang, P., & Xi, D. M. (2005). *SEER standard calculation based on weather parameters for air-conditioner in China.* Paper presented at the Chinese Association of Refrigeration (CAR) Kunming, China.

Gupta, R., & Chandiwala, S. (2009). *A critical and comparative evaluation of approaches and policies to measure, benchmark, reduce and manage CO_2 emissions from energy use in the existing building stock of developed and rapidly-developing countries - case studies of UK, USA, and India.* Paper presented at the 5th Urban Research Symposium: Cities and Climate Change - Responding to an Urgent Agenda, Marseille, France, 28-30 June

Han, J., Kamber, M., & Pei, J. (2012). *Data mining: concepts and techniques*. Singapore: Elsevier Inc.

Hart, G. W. (1992). Nonintrusive appliance load monitoring. *Proceedings of the IEEE, 80*(12), 1870-1891, doi:10.1109/5.192069.

He, L., Wu, L. D., & Cai, Y. C. (2007). Survey of clustering algorithms in data mining. *Application research of computers, 24*(01), 10-13.

Kempton, W., & Lutzenhiser, L. (1992). Air-Conditioning - The Interplay of Technology, Culture and Comfort - Introduction. *Energy and Buildings, 18*(3-4), 171-176, doi:10.1016/0378-7788(92)90011-5.

Kim, H., Stumpf, A., & Kim, W. (2011). Analysis of an energy efficient building design through data mining approach. *Automation in Construction, 20*(1), 37-43, doi:10.1016/j.autcon.2010.07.006.

Kotsiantis, S. B. (2013). Decision trees: a recent overview. [Article]. *Artificial Intelligence Review, 39*(4), 261-283, doi:10.1007/s10462-011-9272-4.

Li, J., Yan, B. P., & Li, J. (2008). Memory-effect-based local outlier detection algorithm. *Computer engineering, 34*(12), 4-6.

Li, X. L., Bowers, C. P., & Schnier, T. (2010). Classification of Energy Consumption in Buildings With Outlier Detection. *Industrial Electronics, IEEE Transactions on, 57*(11), 3639-3644, doi:10.1109/TIE.2009.2027926.

Lian, Z. W., Hou, Z. J., Yao, Y., & Yuan, X. J. (2006). Data mining based sensor fault diagnosis and validation for building air conditioning system. *Energy Conversion and Management, 47*(15-16), 2479-2490, doi:10.1016/j.enconman.2005.11.010.

Liu, D., Chen, Q., Mori, K., & Kida, Y. (2010). A Method for Detecting Abnormal Electricity Energy Consumption in Buildings. *Journal of Computational Information Systems, 6*(14), 4887-4895.

Lu, Z. D. (2007). New energy efficiency analysis and evaluation for the design and implementation of pump and fan systems. *Energy conservation technology, 25*(02), 182-189.

Lu, Z. D., & Wang, L. W. (2009). *Energetics and economy analysis of pump and fan systems*. Beijing, China: National defense of industry press.

Ma, R. J., Yu, N. Y., & Hu, J. Y. (2013). Application of Particle Swarm Optimization Algorithm in the Heating System Planning Problem. [Article]. *Scientific World Journal*, doi:10.1155/2013/718345.

McQuistion, F. C., Parker, J. D., & Spitler, J. D. (2005). *Heating, Ventilating, and Air Conditioning Analysis and Design* (6ed.). NJ, USA: John Wiley & Sons, Inc.

Nasibov, E. N., & Ulutagay, G. (2009). Robustness of density-based clustering methods with various neighborhood relations. *Fuzzy Sets and Systems, 160*(24), 3601-3615, doi:10.1016/j.fss.2009.06.012.

Norford, L. K., & Leeb, S. B. (1996). Non-intrusive electrical load monitoring in commercial buildings based on steady-state and transient load-detection algorithms. *Energy and Buildings, 24*(1), 51-64, doi:10.1016/0378-7788(95)00958-2.

The People's Republic of China National Standard GB 19577-2004, The minimum allowable values of the energy efficiency and energy efficiency grades for water chillers (2004). Beijing, China: China Standards Press.

Pérez-Lombard, L., Ortiz, J., González, R., & Maestre, I. R. (2009). A review of benchmarking, rating and labelling concepts within the framework of building energy certification schemes. *Energy and Buildings, 41*(3), 272-278, doi:10.1016/j.enbuild.2008.10.004.

Pérez-Lombard, L., Ortiz, J., & Pout, C. (2008). A review on buildings energy consumption information. *Energy and Buildings, 40*(3),

394-398, doi:10.1016/j.enbuild.2007.03.007.

Polat, K., & Güneş, S. (2009). A novel hybrid intelligent method based on C4.5 decision tree classifier and one-against-all approach for multi-class classification problems. *Expert Systems with Applications, 36*(2, Part 1), 1587-1592, doi:10.1016/j.eswa.2007.11.051.

Rakhshani, E., Sariri, I., & Rouzbehi, K. Application of data mining on fault detection and prediction in Boiler of power plant using artificial neural network. In *Power Engineering, Energy and Electrical Drives, 2009. POWERENG '09. International Conference on, 18-20 March 2009 2009* (pp. 473-478). doi:10.1109/POWERENG.2009.4915186.

Seem, J. E. (2005). Pattern recognition algorithm for determining days of the week with similar energy consumption profiles. *Energy and Buildings, 37*(2), 127-139, doi:10.1016/j.enbuild.2004.04.004.

Seem, J. E. (2007). Using intelligent data analysis to detect abnormal energy consumption in buildings. *Energy and Buildings, 39*(1), 52-58, doi:10.1016/j.enbuild.2006.03.033.

Taherkhani, A. Recognizing Sorting Algorithms with the C4.5 Decision Tree Classifier. In *Program Comprehension (ICPC), 2010 IEEE 18th International Conference on, June 30 2010-July 2 2010 2010* (pp. 72-75). doi:10.1109/ICPC.2010.11.

Tsinghua University Building Energy Research Center. (2013). *2013 Annual report on China building energy efficiency*. Beijing, China: China Architecture & Building Press.

Wang, H. Z., Wang, H. M., & Lin, W. (2009). Energy-saving research on central air-conditioning system. *Energy Engineering*(03), 61-64.

Wang, Z., Han, N., & Wang, Y. (2011). *Studies on Neural Network Modeling for Air Conditioning System by Using Data Mining with Association Analysis.* Paper presented at the Proceedings of the 2011 International Conference on Internet Computing and Information Services (ICICIS 2011), 2011

Whitman, W. C., Johnson, W. M., Tomczyk, J. A., & Silberstein, E. (2009). *Refrigeration & air conditioning technology* (sixth ed.). Delmar: Cengage Learning.

Xiao, Y. M., & Fu, X. Z. (2007). *Limit value on design energy efficiency ratio of central air conditioning project in public buildings.* Paper presented at the Academic annual conference for HVAC and thermal power of southwestern China, Chengdu, China,

Xue, A. R., Yao, L., Ju, S. G., Chen, W. H., & Ma, H. D. (2008). Survey of outlier mining. *Computer science, 35*(11), 13-18+27.

Xue, Z. F. (2007a). *Building energy efficiency technology and application*. Beijing, China: China Architecture & Building Press.

Xue, Z. F. (2007b). *Energy efficiency diagnosis and refit for existing buildings*. Beijing, China: China Architecture & Building Press.

Yang, C. Z., Liu, G. D., & Li, N. P. (2005). *Engineering design method and system analysis of HVAC.* Beijing, China: China Architecture & Building Press.

Zhang, Y. B., Bai, X. L., Tian, Z. H., & Wu, L. J. (2009). Study on operating dynamic energy efficiency of HVAC systems. *Refrigeration & Air Conditioning, 23*(4), 16-19+23.

Zhao, H.-x., & Magoulès, F. (2012). A review on the prediction of building energy consumption. *Renewable and Sustainable Energy Reviews, 16*(6), 3586-3592, doi:10.1016/j.rser.2012.02.049.

APPLICATION OF EXPERT SYSTEMS TO INDUSTRIAL UTILITY EQUIPMENT OPTIMISATION

SEÁN HAYES
RESEARCH ENGINEER

KEN BRUTON
I2E2 RESEARCHER

DOMINIC O'SULLIVAN
LECTURER & PRINCIPAL INVESTIGATOR

DEPARTMENT OF CIVIL & ENVIRONMENTAL ENGINEERING

UNIVERSITY COLLEGE CORK, IRELAND

ABSTRACT

Expert systems are computer systems which are capable of imitating the reasoning of a human expert within a particular area of knowledge. This reasoning is used to make decisions which solve problems in a particular domain. Applications of expert systems to industrial utility equipment have included fault detection and diagnosis (FDD), automated commissioning and optimisation. Substantial work has been carried out to date in the application of expert systems to the optimisation of HVAC and refrigeration equipment. This paper outlines other industrial technologies which display potential for deployment of remotely based expert systems tools for whole system improvement of operation. An analysis of the suitability of different expert system approaches toward identification of opportunities for improvement in each technology is detailed.

1 INTRODUCTION

Expert systems have been used in the past to solve problems for industrial utilities, with applications including automated fault detection and diagnosis (AFDD) (Bruton *et al* 2014), automated commissioning (Choinière 2008) and optimisation (Choinière 2008).

For an expert system to fault find or optimise an item of equipment a multi stage process is involved comprising; data extraction from existing systems, fault finding or optimisation through rule based or model based approaches, and typically some feedback or fault correction control action.

The range of Building Management Systems (BMS), Supervisory Control and Data Acquisition Systems (SCADA) and Programmable Logic Controllers (PLC) that exist in an industrial facility, coupled with the differing ability of each to archive data drawn from equipment, has led to the development of cloud-based data-extraction processes for analysis with expert systems (Bruton *et al* 2014). Remotely based systems present a number of key considerations including security of both facilities and data (Igure *et al* 2006).

The key industrial utilities examined in this paper as showing potential for deployment of expert system tools are Boilers, HVAC, Air Compressors and Chillers. These technologies have been chosen as many of the opportunities for improvement identified by human experts in the course of review are generic and repeatable. Improvement of these utilities using expert system tools will lead to continued energy and maintenance savings, along with benefits regarding enhanced operation, control and diagnostics. Furthermore expert system tools lend themselves to measurement and verification of the energy performance of utility equipment.

Section 2 of this paper presents some of the primary objectives which expert system implementations aim to achieve. This is followed by a discussion of previous applications of expert systems to industrial utilities and other relevant areas, categorised by the approach taken. The merits and drawbacks of each approach are discussed.

Section 3 of this paper discusses various utilities in modern industry which are typically managed locally; presenting opportunities for improvement using expert system approaches. Some typical modes of equipment failure and/or increased energy consumption are presented, which show potential for improvement using an expert system implementation.

Section 4 of this paper outlines future work to be carried out regarding the application of expert systems to industrial optimisation, and the benefits achievable by these applications.

2 PREVIOUS APPLICATIONS OF EXPERT SYSTEMS TO INDUSTRIAL UTILITIES

Expert System Applications: Objectives

When an expert system is deployed with the aim of improving the operation of utility equipment, the

higher level focus and objective can take several forms. In this paper, the objectives referred to are AFDD, Commissioning, and Optimisation.

AFDD is taken in the context of this paper to refer to the automatic recognition of when an issue of concern, or fault, is present in a physical system. AFDD furthermore identifies the cause which effected this fault condition. In (Bruton *et al* 2014), a rule based expert system tool for a HVAC system was developed and deployed in industry, with a key goal or focus being AFDD.

Commissioning in the context of this paper is taken to refer to a process for achieving, verifying, and documenting that the performance of systems meets defined objectives and criteria ("The Commissioning Process" 2005). In (Pacas and Villwock 2008), a model based expert system using a frequency response analysis method was developed for a primary purpose of commissioning electrical drives.

In the context of this paper, optimisation refers to achieving the goal of best possible operation of a system with respect to some defined criteria (e.g. minimal energy consumption), under a given set of circumstances or constraints. In (Zhang *et al* 2011), a decision support system (DSS), with a model based expert system reasoning mechanism was developed and trialled at an iron and steel enterprise. The objective of this system was to optimise the blend of ore for producing iron in blast furnaces, with the criteria to be optimised being lowest cost.

Expert System Applications: Methods

Industrial utilities have been shown in the past to be suitable for problem solving using expert systems. Methods used by expert system implementations include rule-based systems (Bruton *et al* 2014); model-based systems (Afgan *et al* 1998); neural networks (Palau *et al* 1999), artificial immune systems (Wojdan and Świrski 2007), and signed directional graphs (SDG) (Lee *et al* 1997). In other relevant areas requiring system improvement, methods used have included Bayes belief networks (Lee 2001) (automotive FMEA).

Rule-Based Systems.

In (Bruton *et al* 2014), an AFDD tool was developed using a rule-based approach, with the intended goal of detecting faults and their causes in Air Handling Units (AHUs). This detection of faults allows for on-going commissioning of an AHU, removing potential degradation in performance. Degradation in the performance of an AHU can go un-noticed for significant periods of time, during which desired supply air conditions are maintained. Despite achieving these desired conditions, the conditions of operation may give rise to energy wastage.

An example of this form of energy wastage which could occur in an AHU would be the continuous operation of a frost protection setting on a heating coil. Allowing excessively low temperature air to pass through the initial stage of an AHU can cause issues within the unit, including coil tube failure. To prevent this occurrence, the initial stage of an AHU often includes a frost heating coil, which serves to heat the incoming air to a specified minimum temperature.

In practice, an operator may be unwilling to rely on the ability of the frost coil valve controller to react quickly enough to prevent excessively low temperature air entering the AHU. A means to remove this risk is to manually apply a minimum open setting to the frost coil valve. This manual setting is typically applied if the unit is to be unsupervised during a period of expected cold weather. As the operator may be responsible for many other aspects of plant operation, this manual setting may be forgotten about, and remain in place. While desired delivered air conditions are maintained, heating energy wastage takes place due to the continuous, potentially unnecessary (if no heating is required) operation of the frost coil. If the minimum open setting is allowed to remain during periods of hot weather, energy wastage may also occur at the cooling coil of the AHU, to counteract the frost coil. This degradation in AHU performance, caused by human error, can be flagged by an AFDD tool, removing energy wastage.

The rule-based approach of (Bruton *et al* 2014) began with the usage of the 28 previously defined AHU performance assessment rules (APAR) (House *et al* 2001). These expert rules require 11 data measurements (e.g. supply air temperature, return air temperature) for the AHU to be assessed. By calculations on the retrieved data, the 28 rules are assessed as either True or False. If any rule is found to be True, a fault in operation is defined. This fault can then be attributed to a limited number of component failures.

(Bruton *et al* 2014) expanded on the APAR rules, to incorporate additional data measurements where available, allow for alternative configurations of AHUs, and to calculate virtual data measurements in the case of poorly instrumented AHUs. The output from the calculation of rules was altered from True/False to a numerical value, to allow for determination of the degree of a fault, and to predict potential future failures.

The key advantage of rule-based expert systems is their efficiency when assessing a system which operates within a defined set of conditions (Angeli

2010). Software is commonly written using IF-THEN-ELSE statements, which lend themselves to the implementation of defined rule sets. If the original system is required to be altered, e.g. to incorporate new rules, an expert working with a software engineer can relatively easily re-structure the expert system, provided software is structured and specified in accordance with normal procedures (e.g. Unified Modelling Language (UML).

A drawback of rule-based expert systems is the potential for an incomplete rule base (Bernard 1988). A rule-based expert system is incapable of detecting where the rule base may be incomplete, or of noticing where the expert system itself is making errors in calculation, which could be learnt from (Widman and Loparo 1990). Novel situations cannot be dealt with effectively (Angeli 2010), and require modification to the original expert system.

Rule-based systems have also been applied to steam boilers (Cantú-Ortiz and García-Espinosa 1992), chillers (Dexter and Pakanen 2001), and air compressors (Batanov *et al* 1993).

Model-Based Systems.

In (Afgan *et al* 1998), an expert system was developed to detect tube leakage in a power plant boiler using a model-based approach. Tube leakage is cited as the most probable cause of power plant boiler failure.

As the tubes of a boiler are located internally, they are inaccessible for inspection during normal operation. A power plant boiler is typically of water tube type. This configuration of boiler is comprised of vertical tubes containing water, adjacent to fuel burners. The heat applied by the fuel burners causes the water to boil, and steam to rise to a steam drum.

Boiler tubes are subjected to extreme temperature gradients through their surfaces. While the materials used in construction are typically designed to allow for certain temperature gradients, inadequate operation and maintenance of the boiler can cause mechanical failure of the tubes. If a tube ruptures, the water/steam within will pass from the water side to the fire side of the boiler. This type of failure typically results in downtime, to allow for tube replacement.

Boiler tube failure is typically detected at a stage when there is an imminent risk of an accident, and urgent action is required (Afgan *et al* 1998). If boiler tube failure can be detected in advance, the benefits will include minimising the damaging effects of leakage, and improved maintenance planning.

(Afgan *et al* 1998) developed an expert system, which used heat flux measurements within the fire side of the boiler to detect when internal tube failure was present. When boiler tubes fail, the pattern of heat flux in the boiler will change, due to the lower temperature of the water/steam with respect to the normal fire side temperature. The value of heat flux at each point in the boiler relative to the value with no leak present (standard operation) was defined as the relative heat flux. If this relative heat flux was lower than a predetermined set point, it was indicative of a leak at that location.

By arranging heat flux sensors in a grid on the boiler walls, a heat flux pattern could be obtained. Heat flux patterns were stored in the knowledge base of the expert system, using an object oriented structure. A leakage class was defined, with two major sub-classes: Case and Sensor. The Case class defined the location and intensity of the tube leakage. The Sensor class defined the pattern of readings of the heat flux sensors.

By storing the information regarding heat flux patterns and leakages in the knowledge base, new instances of leakage could be attributed to a specific location and intensity. However, as the actual values defined in previous cases were usually different to those encountered in new instances, a fuzzification of the diagnostic variables drawn from sensor readings was required. This fuzzification was used to draw semantic variables from the diagnostic variables obtained from sensors, to allow inference of likely tube failure.

In order to obtain a confidence level for the diagnostic variables with regard to the sensitivity in detecting a minimum level of leakage, three-dimensional mathematical modelling was used. A previously defined model (Carvalho *et al* 1987) defined the expected heat flux in the boiler, and was compared to actual measurements taken in an operational boiler for validation of results (Coelho and Carvalho 1995).

While this particular expert system focussed on one single point of failure within a boiler, it demonstrates an advantage of model-based systems in its accuracy. The equations used in the model for sensitivity analysis regarding flow, combustion, and heat transfer allow confirmation that the expert system will detect a minimum level of leakage. The compilation of a detailed object oriented knowledge base of potential leakage locations and intensities will in theory encompass all potential future leakage incidents.

A drawback of this expert system is the detailed level of calibration which is required for each application. The sensitivity analysis which was carried out to ensure the expert system could detect a minimum level of leakage required an extensive mathematical model of the boiler in question to be run. This would be difficult to repeat across varying

ranges of boilers, due to differing geometries and configurations of different boiler types. It would therefore not lend itself to a "plug-and-play" solution.

The expert system, while useful for determining the location and intensity of tube failures, defines both location and intensity in the knowledge base and diagnostic variable as discrete parameters. Intensity is defined as a mass flow rate of steam of Low, Medium, or High (each with corresponding discrete values). Location is determined according to a 3*3 grid on each wall of the boiler. While this is sufficient for leakage detection, it could be argued that the level of mathematical modelling required for the sensitivity analysis was extremely intensive for a relatively low resolution result. It is clear that due to expected deviations between model-predicted values and actual diagnostic variables, fuzzification of variables is required to obtain meaningful semantic results.

(Soyguder and Alli 2009) used fuzzy modelling as one technique, in conjunction with artificial neural networks, in the development of an expert system for HVAC humidity and temperature control. (Grimmelius *et al* 1995) used a regression analysis model to predict healthy behaviour of a compression refrigeration plant, as part of a failure diagnosis expert system. This expert system again required fuzzification of variables to allow the recognition of failure modes. The more simplistic regression analysis modelling approach taken by (Grimmelius *et al* 1995) did not allow for complete modelling of the system, e.g. fault recognition during transient operation was not possible. Neural networks were used for system modelling of an air compressor in (Kim and James Li 1995). While not explicitly an expert system, the modelling obtained using neural networks allowed for fault diagnosis of common issues regarding the air compressor.

Neural Networks.

(Tassou and Grace 2005) developed an expert system for fault diagnosis of a refrigeration system, specifically regarding refrigerant leak detection. In this paper artificial neural networks (ANNs) were used to predict the expected values of key parameters pertaining to the chiller in question.

In a refrigeration unit or chiller, maintaining the optimum level of refrigerant is crucial for effective system performance. Due to the refrigerant pressure being higher than atmospheric pressure, there is a potential for refrigerant to leak, reducing the level of refrigerant in the system. In addition, failure of key control instrumentation can cause refrigerant to build up and overcharge in the system.

If refrigerant is lost from a chiller, the consequences include a reduction in coefficient of performance (COP), increased maintenance costs, and the potential for system failure (Tassou and Grace 2005). It is noted that leak detection systems are available which use refrigerant sensors, however they display a number of inherent drawbacks. A crucial drawback of refrigerant sensor based systems is their inability to detect slow refrigerant leaks, which is cited by (Tassou and Grace 2005) as the most common case of refrigerant loss.

(Grimmelius *et al* 1995) were mentioned previously as developers of a model-based expert system for failure diagnosis in chillers. (Tassou and Grace 2005) cited model-based efforts such as this as being capable of accurate predictions of system performance. However, it is noted that this method requires a new approach for individual units, and is therefore difficult to propose on a broad scale.

(Tassou and Grace 2005) used a test rig chiller which was instrumented to measure temperatures, pressures, and flows at key points in the refrigeration circuit (e.g. condenser inlet, evaporator outlet, etc.). The key parameters of coolant inlet temperatures to the evaporator and condenser were used as the primary input data to the expert system. A fault-free operation of the chiller was then performed to allow for training of the ANNs. Ten ANNs were used in the prediction module, correlating to ten prediction parameters. The ANNs were trained using the primary input parameters, and the observed conditions of ten parameters within the refrigeration system. Following this training, the ANNs were capable of predicting the expected fault-free values of the ten parameters throughout the chiller.

Following this training period, the predicted values for the ten parameters were available in the knowledge base of the expert system for a range of operational coolant inlet temperatures. Comparing actual observed values during operation for the ten parameters, and those predicted by the ANNs, enabled the calculation of residuals. These residuals were assigned semantic values ranging from Low to High, and formed a residual pattern.

The expert system included a rule set which was able to diagnose the condition of the refrigerant level based on the residual pattern observed. These rules allowed for detection of both under and over charge of refrigerant, which is not readily implemented using sensor based systems.

It was recognised that during implementation of this expert system in the field, a training period for the ANNs during fault-free operation would be required. Since it may be unknown whether the chiller in question is indeed running in fault-free operation, a validation procedure was proposed. This concerned monitoring the degree of sub cooling and superheat of the refrigerant, and comparing these parameters to normal acceptable limits.

In this work, the expert system was concerned with FDD for refrigerant leakage only. Therefore the two critical predicted values were compressor discharge pressure and evaporator coolant temperature. It was acknowledged however that by developing rules which could detect other faults, based on the other key predicted parameters, a more comprehensive chiller FDD system could be developed.

This expert system approach has the key advantage of being readily deployable across a large population of installed equipment in industry. Its ability to train itself to predict the expected parameters for an individual chiller, removes the issue of individuality between equipment types which arises when taking a model based approach.

However, it is noted that this approach is extremely suitable for deployment on refrigeration equipment, but may not be so for other categories of industrial utility. The vapour compression refrigeration cycle is relatively generic between chillers, and it is likely that the required parameters for expert system training and operation would be present on the majority of installed equipment. Where the required instrumentation is not installed, pressure, temperature and flow measurement sensors are in general readily possible to be fitted after market.

For other categories of industrial utility however, generic characteristics are not always the case. Air compressors, for example, have many different configurations (e.g. screw, reciprocating, centrifugal) each of which is significantly different in operation. A generic set of parameters which can be trained on, and then used for residual calculation with an ANN based expert system may therefore not be as readily repeatable across other categories of utility. For this reason, future FDD applications to chillers using ANNs may be restricted from generic rollouts due to different compressor types within the chiller.

A neural network approach for evaluating biomass boiler behaviour, specifically with regard to fouling, was presented by (Romeo and Gareta 2006). This paper is indicative of a general trend for neural network applications to focus on one single aspect of utility operation, rather than a comprehensive system wide approach.

An FDD system for an AHU was proposed using general regression neural networks in (Lee *et al* 2004). This paper again used residuals generated with neural networks, and an expert rule set, to identify subsystem level faults in AHUs. The comprehensive rule set was able to identify faults including stuck coil valves, fouled coils, leaking valves, stuck dampers, and a decrease in fan performance.

(Kim and James Li 1995) presented a fault diagnosis tool for screw compressors which used neural networks to generate indications of common compressor failures. While not explicitly an expert system, the neural network approach was used not only to diagnose faults, but was also able to indicate the severity of issues which arose.

The approaches of expert system applications to industrial utilities discussed in this section are summarised in **Table 1**.

Table 1: Summary of approaches of expert system applications to industrial utilities

Industrial Utility	Expert System Approach		
	Rule Based	Model Based	Neural Networks
Boilers	(Cantú-Ortiz and García-Espinosa 1992)	(Afgan *et al* 1998)	(Romeo and Gareta 2006)
HVAC	(Bruton *et al* 2014)	(Soyguder and Alli 2009)	(Lee *et al* 2004)
Air Compressors	(Batanov *et al* 1993)	(Kim and James Li 1995)	(Kim and James Li 1995)
Chillers	(Dexter and Pakanen 2001)	(Grimmelius *et al* 1995)	(Tassou and Grace 2005)

3 INDUSTRIAL UTILITIES WITH POTENTIAL FOR IMPROVEMENT USING EXPERT SYSTEMS

For the purposes of this paper, four utilities will be discussed, namely: Boilers, HVAC, Air Compressors and Chillers. These utilities are typically managed at site level, with operator supervision of building management systems (BMS), supervisory control and data acquisition systems (SCADA), or local control panels.

While operator expertise is generally capable of reacting to faults and performing corrective measures, guidance using expert systems will improve operation and reduce downtime. The move toward condition based maintenance (CBM) of utilities from planned maintenance systems (PMS) can be assisted by expert systems detecting when utility components' performance is below expected norms.

Boilers

Steam systems are common across a vast range of industries, including food and beverage, oil refining, chemical production, pharmaceuticals, primary metal processing, and pulp and paper. Thirty-seven percent of fossil fuels burnt in industry is attributable to steam production (Einstein *et al* 2001).

Steam boilers can take various forms, with one of the most common types used in industry today being the package boiler. A package boiler is a boiler which is shipped to a facility pre-assembled, and only requires connections for fuel, electricity and feed water.

Package boilers are often run with less than optimal operating characteristics. This may be due to equipment wear and tear, poor operational methodology, or a lack of maintenance. In general, poor operation of a boiler will result in a reduction in efficiency, increasing energy consumption. In drastic cases, poor boiler operation may result in equipment failure, and may pose a risk to site safety.

Many of the issues which arise leading to ineffective boiler operation are common across industry. These issues are not typically picked up until a comprehensive energy review or audit takes place. The implementation of an expert system to highlight these issues before they impact on energy consumption would allow for increased energy efficiency and improved operation.

As previously discussed in **Section 2**, boiler tubes can rupture or fail, causing leakage between the water side and fire side of the boiler. Operational means by which failure can occur include chemical corrosion, erosion, mechanical fatigue, and material failure (Bamrotwar and Deshpande 2014). Boiler tube failure can lead to boiler shut down, and serious safety concerns. The ability to detect and supply prognostics for boiler tube failures would reduce downtime and maintenance.

Boiler blow down is typically used to control the level of dissolved solids within the boiler water. By steam generation in the boiler, the level of dissolved solids increases over time. Surface blow down operates by removing boiler water in order to achieve a desired level of total dissolved solids. However, in practice blow down is often observed to be excessive, representing an unnecessary loss of energy from the boiler. An expert system implementation could recognise excessive levels of blow down, and diagnose the reason, which could be related to feed water conductivity, or component issues.

A boiler should ideally be fed with water that is free of oxygen. Oxygen present in boiler feed water accelerates the rate of corrosion of internal boiler water side surfaces. In practice, oxygen is typically removed using a mechanical de-aerator. This de-aerator operates by sparging steam through the boiler feed water before it enters the feed tank. The steam supply is typically regulated to maintain a feed tank temperature of approx. 105 °C. In practice, boiler feed water may be at a lower temperature than this, but the operation of the steam boiler will remain as expected. Highlighting drops in de-aerator performance using an expert system implementation will reduce energy consumption and decrease corrosion within the boiler.

Boilers are typically tuned at commissioning to have a certain level of excess O_2 in the exhaust gases. This level, which varies according to the fuel burnt, is indicative of overall combustion efficiency. Over time, boiler fouling and deviations from original operating conditions can cause this excess O_2 level to drift from its ideal level, causing a drop in efficiency. While automatic combustion tuning systems can modulate dampers in the boiler to maintain the desired O_2 level, an expert system implementation could establish the root cause of a drift, allowing rectification in a way that does not impact on other operational characteristics of the boiler.

These are a few characteristic issues which commonly arise during steam boiler operation. Due to the measurability of the parameters involved in each case, they lend themselves to being diagnosed using an expert system implementation.

HVAC

HVAC is a utility which is common across industrial, commercial, and office environments. In clean environments such as the pharmaceutical industry, HVAC can be critical to ensuring product quality and safety. In a report on reducing HVAC energy usage in industry (SEAI 2010), of the nine companies involved in the study, on average HVAC accounted for 35% of site electrical usage, and 60% of site thermal usage. This demonstrates that HVAC is a significant energy user in industry, and should be focussed on with regard to improving energy performance. (Pérez-Lombard *et al* 2008) cites HVAC as accounting for 10-20% of total energy consumption in developed countries.

As with other industrial utilities, degradation in performance is often noted in HVAC systems. This degradation in performance invariably leads to increased energy consumption, which is typically rectified following individual health assessments of AHUs, to ensure individual components are operating as expected. Expert system approaches to HVAC have been able to diagnose areas of poor performance, and failed components, through intelligent assessment of key monitored parameters (Bruton *et al* 2014).

HVAC serves to provide air at a condition which is desirable for the space served. In order to achieve this condition, invariably some heating and/or cooling must take place within the AHU. This is typically achieved using heating and cooling coils, which are supplied with steam/hot water and chilled water. The valves which control the flow of the heating/cooling medium can over time deteriorate in condition, and may leak or become stuck open. Modulation of the amount of fresh air which is drawn by an AHU can also be used for temperature control. The quantity of fresh air used is typically regulated by modulating dampers, which over time can leak, allowing fresh air to be used when it is not required. If either of these leakage cases occurs, energy consumption of the AHU will unnecessarily increase, but the desired supply air condition may be maintained. FDD tools using an expert system approach can identify when valves or dampers leak or pass, and highlight this issue in order that increased energy consumption does not go unnoticed for extended periods.

For quality requirements, air is normally filtered during conditioning. Over time, the filters used can become clogged, which increases the electrical load on a variable speed drive (VSD) fan drawing air into the AHU. At many facilities, filter replacement is carried out on a scheduled basis, based on expected service life of a filter. While this practice normally ensures that filters will be replaced before becoming clogged, it does not take into account the condition of the filter at the time of the replacement. Ambient air conditions can have an effect on how rapidly the filter clogs, and this can be detected by a differential pressure sensor across the filter. An expert system implementation could diagnose when a filter is clogged, and issue an alert for replacement. Diagnosis could be based on differential pressure measurement across the filter, or by electrically fingerprinting the AHU VSD fan to allow for detection of an increase in load from the relevant electrical distribution board.

Air Compressors

Compressed air is a common utility in many areas of industry, particularly in the manufacturing sector. It is recognised as an expensive form of energy delivery, as the majority of the energy required for generation is lost as heat of compression. Compressed air has been cited as accounting for 10% of industrial electricity usage in the EU (Saidur *et al* 2010).

Many different configurations of compressor are common in industry, the most common of which are centrifugal, screw, reciprocating and scroll. A common means for improved energy efficiency in compressed air plants is heat recovery, which can tend to take first priority in energy reviews. There are however, numerous operational improvements which can be undertaken to reduce the energy consumption of a compressed air system.

In a typical compressed air system, accepted normal practice for compressed air leaks is approximately 10%. However in many facilities the level of leakage can account for 25% of compressor output (Kaya *et al* 2002). While many facilities undertake periodic compressed air leak detection exercises, these are typically schedule based. A comprehensive expert system implementation for a compressed air system would balance compressor output with system flows, and advise when leakage rates were too high and possible locations. This would enable leakage detection exercises to be carried out more efficiently, with efforts concentrated on areas with expected highest loss.

Mechanical and/or electrical failure of compressor components is a key cause for deviations from normal operation, and increased maintenance requirements and energy consumption. It can often be difficult to determine without a complete overhaul of the compressor which is the exact point of failure (Chen and Ishiko 1990). An example given in (Batanov *et al* 1993) of a compressor failing to start has many possible causes, including damaged transformers, circuit breakers, and incorrectly configured control switches. The expert system described uses a set of 154 rules to effectively manage the maintenance requirements of an air compressor.

Chillers

Refrigeration systems in industry are widespread, with chilled water used for both process needs and HVAC cooling. Refrigeration systems can account for a large proportion of total energy usage in a facility, particularly in industries such as cold storage (90%), retail (70%) and ice cream manufacturing (70%) (“Refrigeration Systems” 2011).

Due to the varying types of compressor normally installed in a chiller, the configuration of a refrigeration system can vary as with compressors. A survey of common faults in chillers was carried out in (Comstock *et al* 2002), encompassing centrifugal and screw chillers (water and air cooled). The faults in this paper were categorised at system or subsystem level.

As discussed previously, refrigerant leak from a chiller can have consequences impacting on service life of equipment and energy consumption. (Tassou and Grace 2005) proposed an expert system implementation which is able to identify refrigerant leakage in situations where normal, refrigerant sensor based leakage detection systems would not. As refrigerant leakage is a leading cause of chiller issues,

expert systems implementations should include allowance for leak detection.

The fouling of a heat exchanger on the evaporator or condenser of a chiller will cause a reduction in heat transfer, giving a reduction in system COP. The ability to detect degradation in heat exchanger performance would allow for action to be taken to clean the heat exchangers, and highlight when water quality may be a concern.

Slow, degradational faults on chillers such as these, as opposed to immediate mechanical or electrical failure of components, are more suited to detection and diagnosis using an expert system implementation. (Comstock *et al* 2002) cited this degradation category of faults as representative of 42% of service calls made and 26% of service costs in a sample study of chiller services. The ability to provide prognostic information regarding these faults would assist in reducing downtime, and more effectively planning maintenance. In the case of faults such as fouled heat exchangers, the chiller may be able to provide the desired output, but will have a higher electrical power requirement. Detecting fouling and other energy impacting faults would reduce total energy usage.

4 CONCLUSIONS AND FUTURE WORK

This paper discussed three approaches taken when applying expert systems to the improvement of industrial utility equipment operation. It is concluded that each has its merits and drawbacks.

Rule based systems are efficient when operating within a defined domain, but do not allow for novel situations not accounted for in the rule set. Model based systems address this issue by normally providing an all-encompassing physical model of a system. This however is more difficult to deploy across large ranges of industrial equipment, due to the individual nature of modelling required. Work carried out in the area of machine learning models for fault diagnosis (Murphey *et al* 2006) attempts to address this individuality issue by automatically learning about the system in question.

Neural networks based systems attempt to address some of the issues presented by rule based and model based systems, as they are capable of characterising an individual piece of equipment using a training period and a defined list of variables. They do however need to be supported by a rule set to distinguish between residual patterns, which could present the same issue as with rule based systems.

It is the intention of the authors to develop an expert system for industrial utility optimisation using as diverse an approach as possible, drawing from the benefits of all methods. It is acknowledged that many neural network applications focus on one single aspect of equipment operation, and it is envisaged that incorporating neural networks from previous works together into a more complete system would allow for whole system improvements in energy performance. It is also noted that the majority of expert system implementations focus on individual pieces of primary equipment as their highest level. Development of an expert system which takes into consideration parameters from associated auxiliaries of the primary equipment (e.g. considering the pumps associated with a chiller), might allow for whole facility improvements, and may highlight issues which impact on decisions made regarding improvements in the primary plant.

5 REFERENCES

Afgan, N., Coelho, P.J., Carvalho, M.G. (1998) "Boiler tube leakage detection expert system," *Applied Thermal Engineering*, 18(5), 317–326.

Angeli, C. (2010) "Diagnostic Expert Systems: From Expert's Knowledge to Real—Time Systems," in Sajja, P.S. and Akerkar, R., eds., *Advanced Knowledge Based Systems: Models, Applications And Research*, 50–73.

Bamrotwar, S.R., Deshpande, V.S. (2014) "Root Cause Analysis and Economic Implication of Boiler Tube Failures in 210 MW Thermal Power Plant," *Journal of Mechanical and Civil Engineering*, 2014, 6–10.

Batanov, D., Nagarur, N., Nitikhunkasem, P. (1993) "EXPERT-MM: A knowledge-based system for maintenance management," *Artificial Intelligence in Engineering*, 8(4), 283–291.

Bernard, J. (1988) "Use of a rule-based system for process control," *Control Systems Magazine, IEEE*.

Bruton, K., Raftery, P., O'Donovan, P., Aughney, N., Keane, M.M., O'Sullivan, D.T.J. (2014) "Development and alpha testing of a cloud based automated fault detection and diagnosis tool for Air Handling Units," *Automation in Construction*, 39, 70–83.

Cantú-Ortiz, F.J., García-Espinosa, M.A. (1992) "An expert system for diagnosing problems in boiler operations," *Expert Systems with Applications*, 5(3–4), 323–336.

Carvalho, M.G.M.S., Durão, D.F.G., Pereira, J.C.F. (1987) "Prediction of the flow, reaction and heat transfer in an oxy-fuel glass furnace," *Engineering Computations*, 4(1), 23–34.

Chen, J.-G., Ishiko, K. (1990) “Automobile air-conditioner compressor troubleshooting — An expert system approach,” *Computers in Industry*, 13(4), 337–345.

Choinière, D. (2008) “DABO: A BEMS Assisted On-Going Commissioning Tool,” in *National Conference on Building Commissioning*.

Coelho, P.J., Carvalho, M.G. (1995) “Evaluation of a three-dimensional model for the prediction of heat transfer in power station boilers,” *International Journal of Energy Research*, 19(7), 579–592.

Comstock, M., Braun, J., Groll, E. (2002) “A survey of common faults for chillers.,” *ASHRAE Transactions*.

Dexter, A., Pakanen, J. (2001) “Demonstrating Automated Fault Detection and Diagnosis Methods in Real Buildings Proceedings of VTT Symposium: 217,” *VTT Building Technology*.

Einstein, D., Worrell, E., Khrushch, M. (2001) “Steam systems in industry: Energy use and energy efficiency improvement potentials.”

Grimmelius, H.T., Klein Woud, J., Been, G. (1995) “On-line failure diagnosis for compression refrigeration plants,” *International Journal of Refrigeration*, 18(1), 31–41.

House, J.M., Vaezi-Nejad, H., Whitcomb, J.M. (2001) “An expert rule set for fault detection in air-handling units / Discussion,” in *ASHRAE Transactions*, American Society of Heating, Refrigeration and Air Conditioning Engineers, Inc.: Atlanta, 858.

Igure, V.M., Laughter, S. a., Williams, R.D. (2006) “Security issues in SCADA networks,” *Computers & Security*, 25(7), 498–506.

Kaya, D., Phelan, P., Chau, D., Ibrahim Sarac, H. (2002) “Energy conservation in compressed-air systems,” *International Journal of Energy Research*, 26(9), 837–849.

Kim, T., James Li, C. (1995) “Feedforward neural networks for fault diagnosis and severity assessment of a screw compressor,” *Mechanical Systems and Signal Processing*, 9(5), 485–496.

Lee, B.H. (2001) “Using Bayes belief networks in industrial FMEA modeling and analysis,” *Annual Reliability and Maintainability Symposium. 2001 Proceedings. International Symposium on Product Quality and Integrity (Cat. No.01CH37179)*, 7–15.

Lee, G., Mo, K.J., Yoon, E.S. (1997) “The methodology for knowledge base compression and robust diagnosis: Application to a steam boiler plant,” *Expert Systems with Applications*, 12(2), 263–274.

Lee, W.-Y., House, J.M., Kyong, N.-H. (2004) “Subsystem level fault diagnosis of a building’s air-handling unit using general regression neural networks,” *Applied Energy*, 77(2), 153–170.

Murphey, Y., Masrur, M.A.M., Chen, Z., Zhang, B. (2006) “Model-based fault diagnosis in electric drives using machine learning,” *IEEE/ASME Transactions on Mechatronics*, 11(3), 290–303.

Pacas, M., Villwock, S. (2008) “Development of an expert system for identification, commissioning and monitoring of drives,” *2008 13th International Power Electronics and Motion Control Conference*, 2248–2253.

Palau, A., Velo, E., Puigjaner, L. (1999) “Use of neural networks and expert systems to control a gas/solid sorption chilling machine,” *International Journal of Refrigeration*, 22(1), 59–66.

Pérez-Lombard, L., Ortiz, J., Pout, C. (2008) “A review on buildings energy consumption information,” *Energy and Buildings*, 40(3), 394–398.

Refrigeration Systems [online] (2011) *Carbon Trust*, available: http://www.carbontrust.com/media/13055/ctg046_refrigeration_systems.pdf.

Romeo, L.M., Gareta, R. (2006) “Neural network for evaluating boiler behaviour,” *Applied Thermal Engineering*, 26(14-15), 1530–1536.

Saidur, R., Rahim, N.A., Hasanuzzaman, M. (2010) “A review on compressed-air energy use and energy savings,” *Renewable and Sustainable Energy Reviews*, 14(4), 1135–1153.

SEAI (2010) *Energy Agreements Programme HVAC Special Working Group Spin III Report*.

Soyguder, S., Alli, H. (2009) “An expert system for the humidity and temperature control in HVAC systems using ANFIS and optimization with

Fuzzy Modeling Approach," *Energy and Buildings*, 41(8), 814–822.

Tassou, S.A., Grace, I.N. (2005) "Fault diagnosis and refrigerant leak detection in vapour compression refrigeration systems," *International Journal of Refrigeration*, 28(5), 680–688.

"The Commissioning Process" (2005) *ASHRAE Standard*, (GUIDELINE 0), 1–64.

Widman, L.E., Loparo, K.A. (1990) "Artificial Intelligence, Simulation, and Modeling," *Interfaces*, 20(2), 48–66.

Wojdan, K., Świrski, K. (2007) "Immune Inspired Optimizer of Combustion Process in Power Boiler," in Okuno, H. and Ali, M., eds., *New Trends in Applied Artificial Intelligence SE - 102*, Lecture Notes in Computer Science, Springer Berlin Heidelberg, 1022–1031.

Zhang, R., Lu, J., Zhang, G. (2011) "A knowledge-based multi-role decision support system for ore blending cost optimization of blast furnaces," *European Journal of Operational Research*, 215(1), 194–203.

Implemented Continuous Commissioning® Measures for Schools, Hospitals, and Office Buildings in the U.S.

Sukjoon Oh
Graduate Assistant Researcher

James B. Watt
Associate Director

David E. Claridge
Professor/Director

Charles H. Culp
Professor/Associate Director

Jeff S. Haberl
Professor/Associate Director

Meet Shah
Research Engineering Associate

Energy Systems Laboratory, Texas Engineering Experiment Station
College Station, TX

ABSTRACT

This study presents an overview of 32 projects (i.e., 126 buildings) conducted in the U.S. regarding Continuous Commissioning[1®] (CC®) over the last 10 years. It includes the projects of 43 schools, 68 hospitals, 4 office, and 11 other buildings. In this study, we estimated the implemented CC® measures that were applied to the existing buildings of the projects in schools, hospitals, and office buildings (i.e., 115 buildings). We categorized the CC® measures by system and measure type using the standard annotation. The rankings of the measures were analyzed. This study shows that the five most frequent CC® opportunities through the projects are: Air Handling Unit (AHU) operation, AHU maintenance, AHU supply air temperature (SAT) cooling and heating setpoint adjustment, and Chilled Water (CHW) system operation.

INTRODUCTION

Saving building energy and improving occupant comfort is an important issue for today's building managers. One of the most effective methods is to tune and optimize HVAC systems for saving building energy as well as improving comfort. This method can be achieved by properly managing the existing HVAC systems or by controlling the operations of advanced HVAC systems such as variable air volume Air Handling Unit (AHU) systems, high efficiency chillers and boilers, and Building Automation Systems (BAS) (Liu et al. 2002).

The Energy Systems Laboratory (ESL), a division within the Texas A&M Engineering Experiment Station (TEES), has conducted CC® projects for existing buildings in various climates over 10 years in order to save building energy and improve occupant comfort. This paper describes the implemented CC® of 32 projects (i.e., 126 buildings) based on the final reports of the projects other than the reports of retrofit and ongoing projects. This paper provides the frequency of the implemented CC® measures by system and measure type, with the intention that if we know the frequency of the implemented CC® measures by specific type, we can more easily find where energy saving opportunities are obtained and better account for the opportunities in other buildings with similar situations. Specific examples of the most frequent CC® opportunities are also discussed in this study.

Table 1 shows the building type, number, conditioned square feet, savings per year, and savings per year by square feet of the 32 projects. The achieved savings[2] were calculated during the first year period after the CC® measures were implemented. The projects for school buildings accounted for approximately 40% of the total savings achieved through CC®. Table 2 shows the same categories above, however the projects were categorized by specific location and climate. The total conditioned area of 32 projects was 9,524, 849 ft^2, and the total savings per one year after the CC® measures were implemented was $ 2,740,563. The savings per year by square feet was $ 0.29. Overall, approximately 80% of the total achieved savings through CC® was obtained from the projects in Texas.

Table 1. Achieved Energy Savings by Building Type

Building Type	# of Buildings	Conditioned Square Feet	Savings $/ Year	Savings$/ Year,Sqft
Schools	43	4,526,962	1,112,604	0.25
Hospitals	68	3,554,897	960,863	0.27
Offices	4	187,506	143,465	0.77
Other (Courthouse, Research center, Cultural center, etc.)	11	1,255,484	523,631	0.42
Grand Total	**126**	**9,524,849**	**2,740,563**	**0.29**

[1] Continuous Commissioning® and CC® are Registered Trademarks of the Texas Engineering Experiment Station. Contact the Energy Systems Laboratory, Texas A&M University for further information.

[2] The achieved savings were calculated using the electricity and gas unit cost of the year when the projects were completed.

Table 2. Achieved Energy Savings by Location and Climate

State	City	ASHRAE Climate Zone	Building Type	# of Buildings	Conditioned Square Feet	Savings $/ Year	Savings $/ Year,Sqft
TX	Austin	2A (Hot & Humid)	School	15	1,765,264	265,703	0.15
			Office	3	106,550	72,119	0.68
			Other	7	604,020	375,301	0.62
TX	Brenham	2A (Hot & Humid)	Hospital	30	362,249	48,888	0.13
TX	College Station	2A (Hot & Humid)	School	1	61,658	61,828	1.00
TX	Corpus Christi	2A (Hot & Humid)	School	13	826,300	127,587	0.15
TX	Dallas	3A (Warm & Humid)	Office	1	80,956	71,346	0.88
TX	Kerrville	3B (Warm & Dry)	Hospital	18	316,700	179,600	0.57
TX	Laredo	2B (Hot & Dry)	School	3	408,000	276,434	0.68
TX	Lubbock	3B (Warm & Dry)	School	6	800,000	132,012	0.17
TX	Prairie View	2A (Hot & Humid)	School	3	278,291	112,464	0.40
TX	San Antonio	2A (Hot & Humid)	Hospital	5	1,468,592	329,437	0.22
TX	Terrell	3A (Warm & Humid)	Hospital	13	499,356	159,386	0.32
TX Subtotal				118	7,577,936	2,212,105	0.29
CA	Edwards	3B (Warm & Dry)	Other	3	281,464	41,500	0.15
GA	Fort Benning	3A (Warm & Humid)	Hospital	1	398,000	69,552	0.17
MN	Minneapolis	6A (Cold & Humid)	Hospital	1	510,000	174,000	0.34
PA	State College	5A (Cool & Humid)	School	1	37,449	86,000	2.30
UT	Salt Lake City	5B (Cool & Dry)	School	1	350,000	50,576	0.14
			Other	1	370,000	106,830	0.29
Other Subtotal				8	1,946,913	528,458	0.27
Grand Total				**126**	**9,524,849**	**2,740,563**	**0.29**

CC® MEASURE CATEGORY

Approximately 40 types of CC® measures were applied to the 32 projects (i.e., 126 buildings) as shown in Table 1 and 2 to save building energy and improve occupant comfort. In general, most commissioning measures are categorized by non-standard groups. However, a standard grouping is necessary to better understand and apply commissioning measures. Therefore, this paper presents standard annotations to categorize the implemented CC® measures.

First, the implemented CC® measures were categorized by two types: system and measure type. The system type consists of Air-Side HVAC System, Water-Side Central Plant, and other. Table 3 shows the sub-levels of the system types. The section called "other" mainly contains Fan Coil Unit and Heat Recovery Unit. The categorization of Table 3 was then applied to Figures 1, 3, and 5 for schools, hospitals, and office buildings.

Table 3. Categorization by System Type

1st Level System Type	2nd Level System Type	3rd Level System Type
Air-Side HVAC System	Single Zone (SZ) AHU	Constant Air Volume (CAV)/ Variable Air Volume (VAV)
	Multi Zone (MZ) AHU	Single Duct (SD) CAV/ SD VAV/ Dual Duct (DD) CAV/ DD VAV
	Terminal Box	CAV/VAV
Water-Side Central Plant	Chilled Water (CHW) System	N/A
	Heating Hot Water (HHW) System	N/A
	Steam HW System	N/A
	Domestic Hot Water (DHW)	N/A
Other	N/A	N/A

The other approach for categorizing the implemented CC® measures is by measure type that uses standard annotations. As the 1st level of measure type, the CC® measures were sorted by three categories: Operation, BAS Control/Optimization, and Maintenance. Table 4 describes each 1st level measure type. The standard annotation was used for the 2nd level measure type of BAS Control/Optimization. This BAS Control/Optimization section has many variables, so the standard annotation is helpful to understand the implemented CC® measures.

Table 4. Categorization by Measure Type

1st Level Measure Type	General Description for the 1st level	2nd Level Measure Type
Operation	Turn off system or reduce system quantity/volume or change operation	N/A
BAS Control/ Optimization	Optimize sequence of operation to take advantage of variable loads	**Standard Annotation**
Maintenance	Restore or repair components of systems to correct operation	N/A

In order to categorize the 2nd level measure type of BAS Control/Optimization with a standardized approach, additional process variables were used. Process variables consist of how to apply the CC® measures to control building systems to save energy and improve occupant comfort. Table 5 indicates the process variables of standard annotations. Table 6 shows the examples of the standard annotations used in Figures 2, 4, and 6. The standard annotations are created based on each process variable.

Figures 1 to 6 show the frequency of the implemented CC® measures of schools, hospitals, and offices [3] using the system (i.e., Table 3) and the measure (i.e., Table 4) type. Figures 1 and 2 show the frequency of the CC® measures implemented in 43 school buildings. CHW, SD VAV, and SD CAV systems, except "other", were the top three systems where CC® measures were implemented (see Figure 1). AHU operation, AHU maintenance, and AHU supply air temperature (SAT) cooling setpoint adjustment (i.e., indicator c) were the top three measures for the school buildings (see Figure 2). The fourth top measure was supply water flow cooling setpoint adjustment of CHW system (i.e., indicator t), and the fifth top measure was supply air pressure cooling &

[3] In this study, other type buildings were excluded for the categorizing analysis of the CC® measures.

Table 5. Process Variables for Standard Annotations

System Type	Process Sensor Location	Process Sensor Medium	Process Sensor Type	Process Function	Modify the _____ Setpoint for the Process Variable	If Applicable, Add _____
AHU/ Terminal Unit/ CHW System/ HHW System/ DHW System/ Heat Pump/ Heat Recovery Unit	Outside/ Preheat Coil Leaving/ Supply/ Reheat Coil Leaving/ Space/ Return/ Exhaust	Air/ Water	Flow/ Temperature/ Pressure/ Humidity	Cooling/ Heating/ Cooling&Heating/ Preheat/ Reheat/ Bypass/ Economizer/ Dehumidification/ Ventilation	Min/ Operation/ Lockout	Setpoint Adjustment/ Control Sequence Optimization

Table 6. Examples of Standard Annotations

Indicator	System Type	Process Sensor Location	Process Sensor Medium	Process Sensor Type	Process Function	Modify the _____ Setpoint for the Process Variable	If Applicable, Add ____	Standard Annotation
c	AHU	Supply	Air	Temperature	Cooling	Operating	Setpoint Adjustment	AHU Supply Air Temperature Cooling Operating Setpoint Adjustment
i	AHU	Outside	Air	Flow	Ventilation	Operating	Setpoint Adjustment	AHU Outside Air Flow Ventilation Operating Setpoint Adjustment
p	Terminal Unit	Space	Air	Temperature	Cooling & Heating	Operating	Setpoint Adjustment	Terminal Unit Space Air Temperature Cooling & Heating Operating Setpoint Adjustment
r	Terminal Unit	Space	Air	Flow	Reheat	Lockout	N/A	Terminal Unit Space Air Flow Reheat Lockout
v	CHW System	Supply	Water	Flow	Cooling	Operating	Control Sequence Optimization	CHW System Supply Water Flow Cooling Operating Control Sequence Optimization

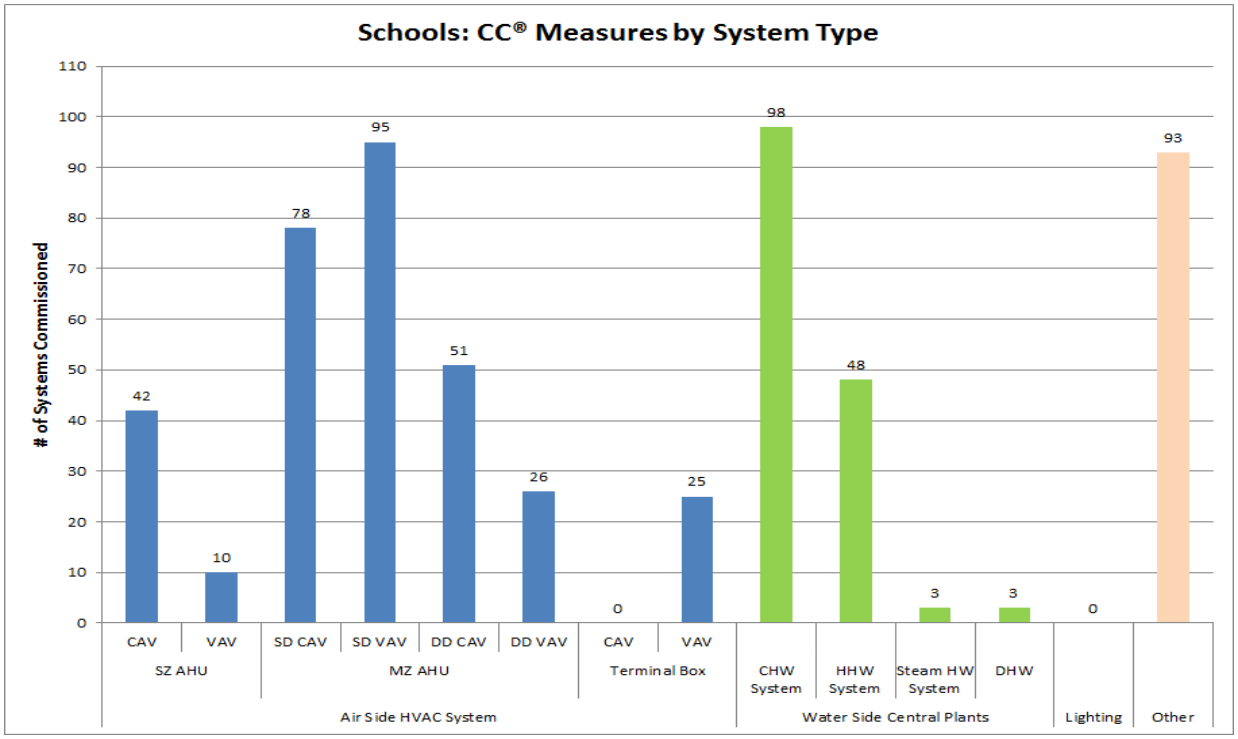

Figure 1. CC® measures by System Type in Schools

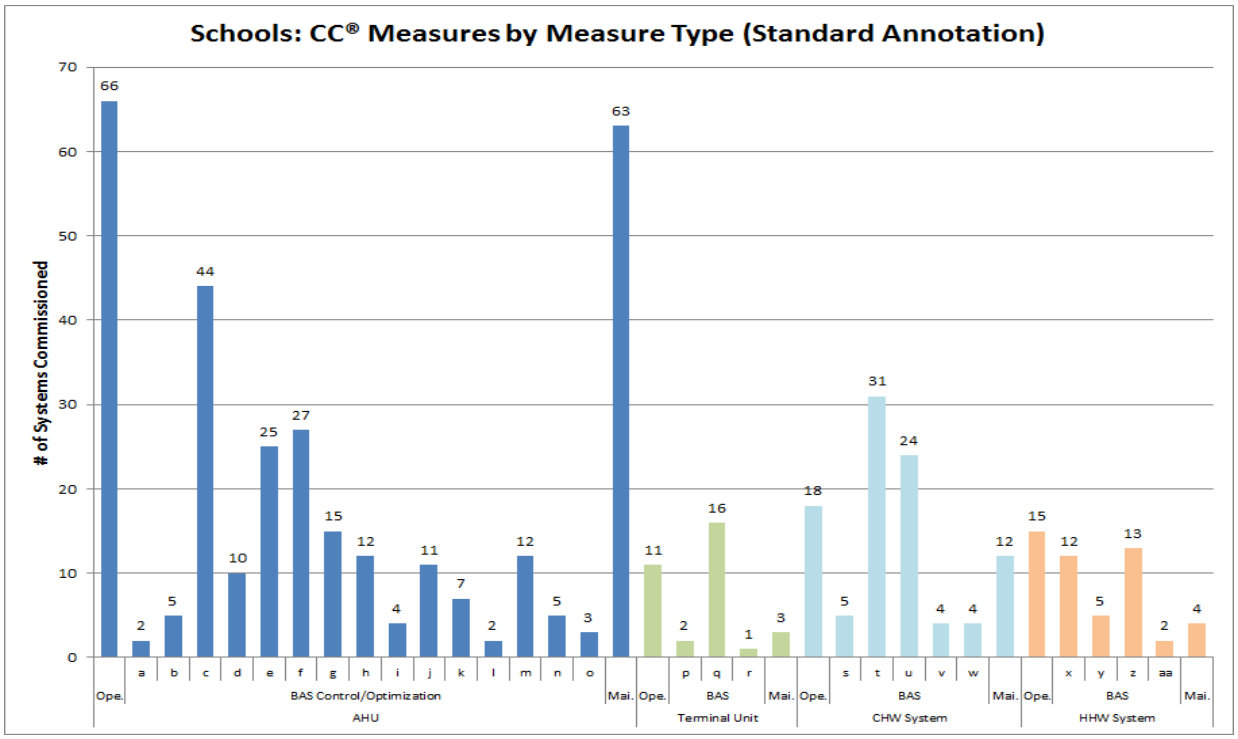

Figure 2. CC® measures by Measure Type in Schools

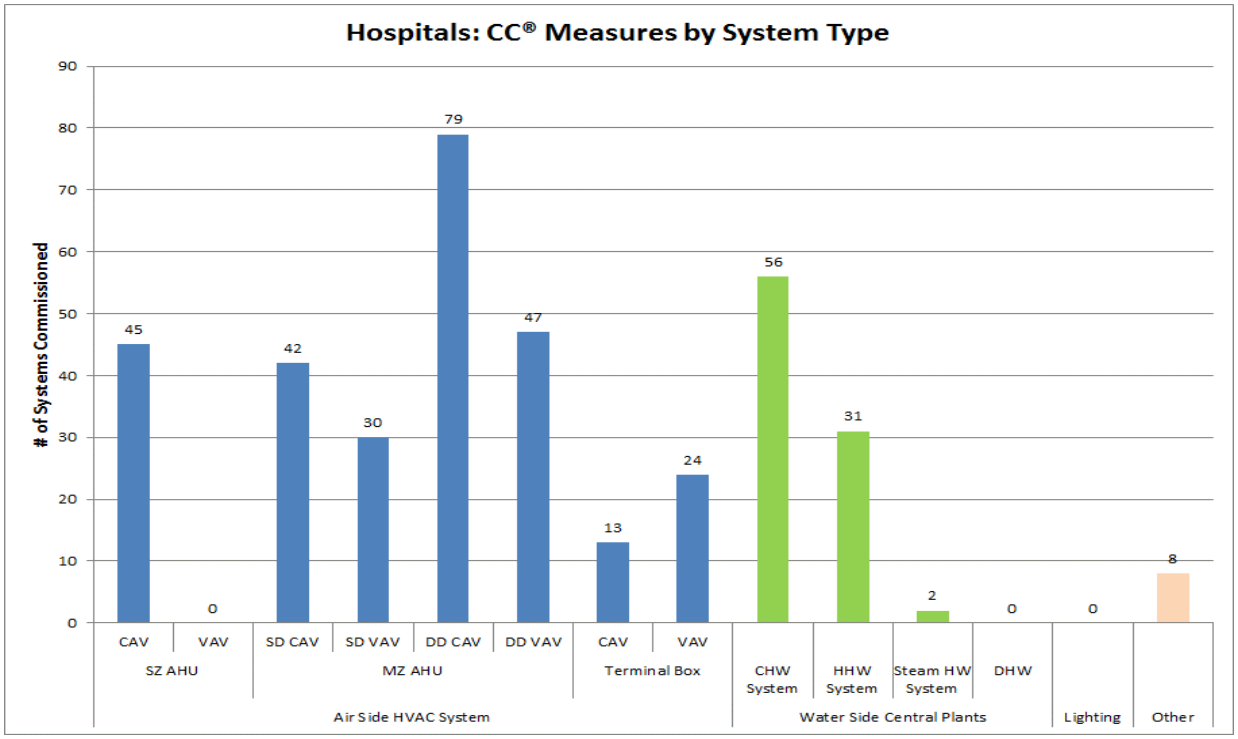

Figure 3. CC® measures by System Type in Hospitals

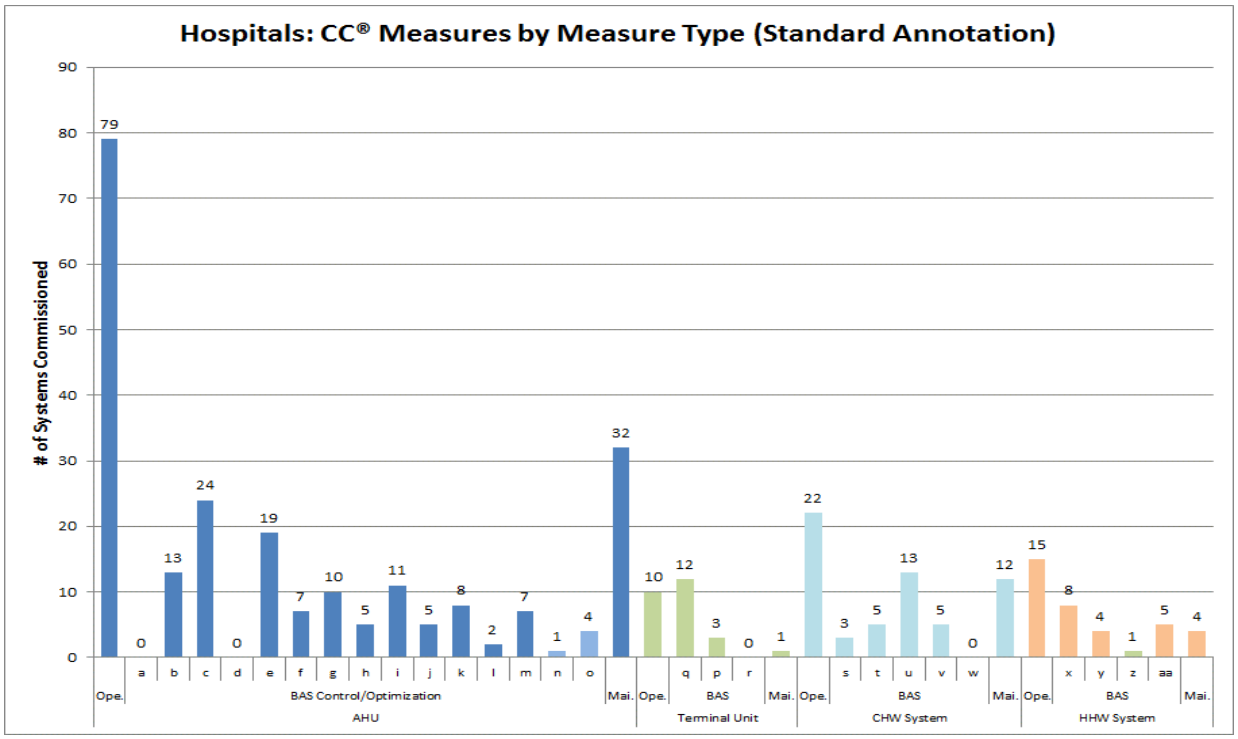

Figure 4. CC® measures by Measure Type in Hospitals

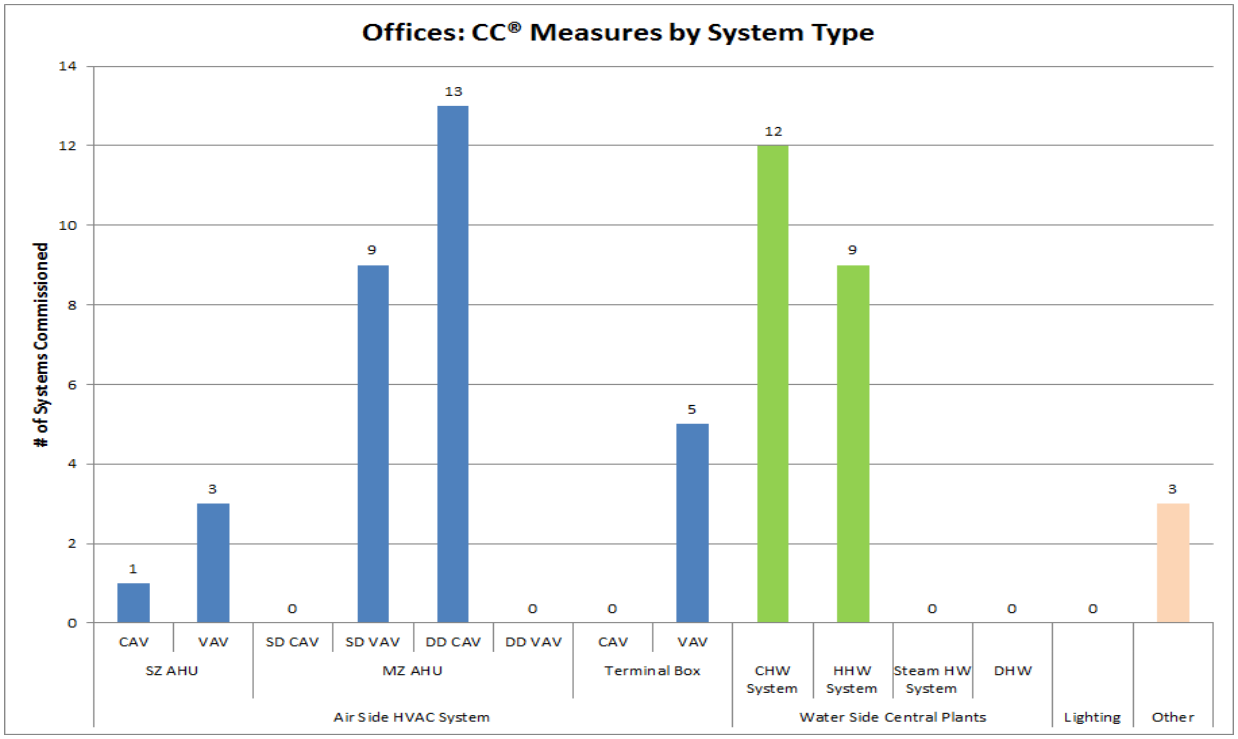

Figure 5. CC® measures by System Type in Offices

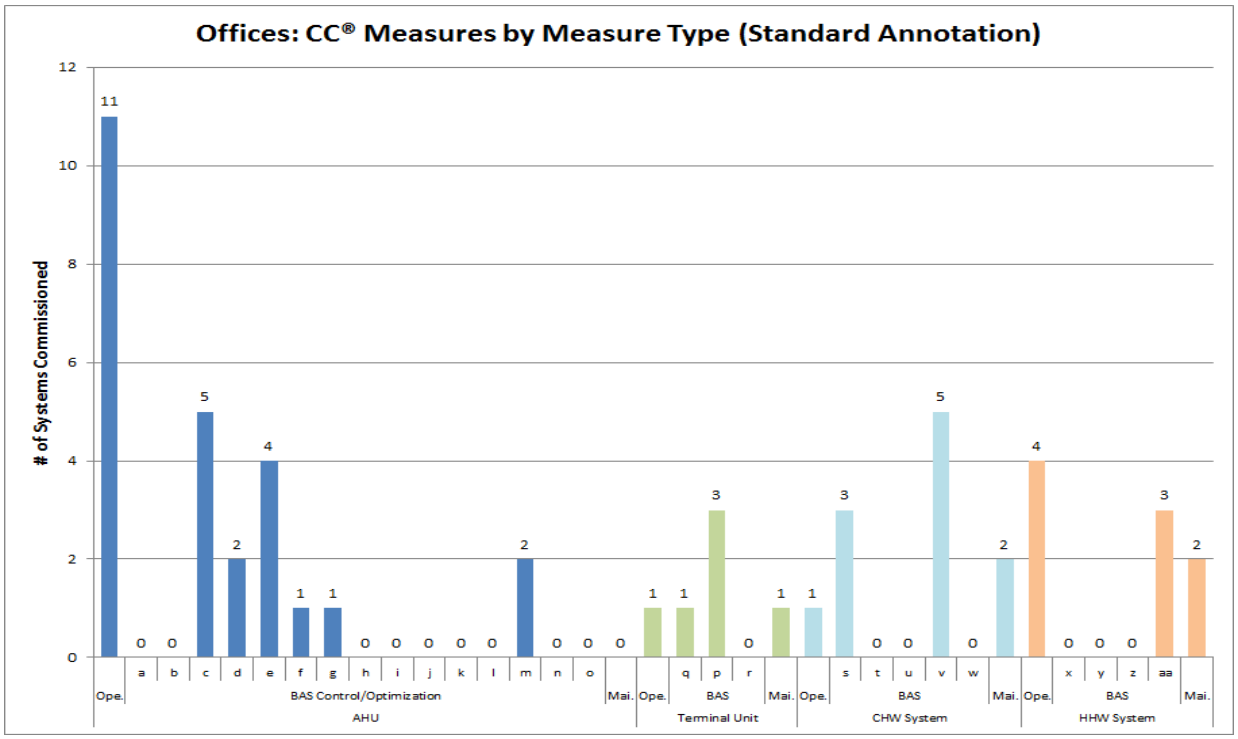

Figure 6. CC® measures by Measure Type in Offices

heating setpoint adjustment of AHU system (i.e., indicator f).

Figure 3 and 4 show the frequency of the CC® measures implemented in 68 hospital buildings. DD CAV, CHW, and DD VAV systems were the most frequent systems of CC® measures that were implemented (see Figure 3). AHU operation, AHU maintenance, and AHU supply air temperature cooling setpoint adjustment (i.e., indicator c) were the top three measures for the hospital buildings (see Figure 4), which is the same with the top three measures of the school buildings. The fourth measure was the operation of the CHW system, and the fifth was AHU supply air temperature heating setpoint adjustment (i.e., indicator e).

Figure 5 and 6 show the frequency of the CC® measures implemented in four office buildings. DD CAV, CHW, SD VAV, and HHW systems were the top three systems where CC® measures were implemented. SD VAV and HHW systems had the same frequency of occurrence (see Figure 5). AHU operation, AHU supply air temperature cooling setpoint adjustment (i.e., indicator c), and supply water flow cooling control sequence optimization for CHW system (i.e., indicator v) were the top three measures for the office buildings (see Figure 6). AHU supply air temperature heating setpoint adjustment (i.e., indicator e) and HHW system operation shared the fourth position.

THE MOST FREQUENT CC® MEASURES

The total of the CC® measures implemented in all the school buildings in this study was 491, the total in hospital buildings was 346, and the total of the office buildings was 50. Among the overall CC® measures (i.e., 887), AHU operation, AHU maintenance, and AHU supply air temperature cooling setpoint adjustment (i.e., indicator c) were the top three measures. The fourth was supply air temperature heating setpoint adjustment (i.e., indicator e), the fifth was CHW operation. Figure 7 shows the percentage of top five CC® measures implemented in the schools, hospitals, and office buildings.

The top five measures account for 47% of the total implemented measures. The examples of the most frequent CC® measures are included in the following sections.

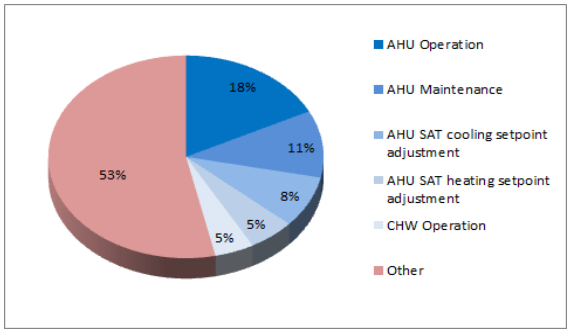

Figure 7. Top Five Implemented CC® measures

AHU Operation

In many projects, AHUs operated during unoccupied periods. This caused an unnecessary increase of overall energy use. Therefore, AHUs were turned off or AHU schedules were changed based on operation schedules. For example, an occupied/unoccupied schedule was obtained from a site visit. After that, the schedule was modified based on the survey, and it was then implemented in the control program of BAS. During an unoccupied period, the fans and cooling and heating coil valves were shut down.

AHU Maintenance

The major CC® measures that were conducted usually identified and repaired AHU malfunctions. Examples include wrong temperature, humidity, and static pressure sensors, which were calibrated or replaced for proper AHU operation without erroneous readings. In some cases, fan pulleys and belts were replaced to increase air flow and improve static pressure.

AHU SAT cooling and heating setpoint adjustment

The 3rd and 4th most frequent CC® measures were to adjust AHU SAT cooling and heating setpoints. In such cases, there were existing DDC controllers that maintained cooling and heating temperature. However, resetting cooling and heating coil temperature based on outside air temp (OAT) was a more efficient measure to maintain room comfort and reduce waste of cooling and heating energy. For example, a cooling coil temperature was reset according to a room temperature when OAT is below 60°F, and it was maintained at 55°F when OAT is above 60°F. Therefore, these strategies were applied

to many projects to save cooling and heating energy for AHUs.

CHW Operation

The 5th most frequent CC® measure was to turn on and off a chiller using an occupancy schedule. This approach was explained at the above section of AHU operation. In the same way, a chiller was turned off based on an occupied/unoccupied schedule. For example, a new control program was written in the BAS language to turn a chiller off when all the AHUs were off (i.e., an unoccupied period).

SUMMARY

Over the last 10 years, the ESL has conducted CC® projects for hundreds of existing buildings in the U.S in order to save energy and improve occupant comfort. This paper describes the implementation of CC® measures in 115 buildings based on the final reports of the projects on file at the ESL. A standard grouping was applied to better understand and make use of commissioning measures. The implemented CC® measures for schools, hospitals, and office buildings were categorized using the standard annotation (i.e., grouping).

The five most frequent CC® opportunities used in schools, hospitals, and office buildings were: Air Handling Unit (AHU) operation, AHU maintenance, AHU supply air temperature cooling and heating setpoint adjustment, and Chilled Water (CHW) system operation. These measures account for 47% of the total implemented measures.

FUTURE WORK

Additional analysis is required to better represent implemented CC® measures in order to allow building operators to use the CC® opportunities in other buildings with similar conditions. Additional standard annotations, histograms by ambient temperature and energy use, and cost analysis by measure will be needed to expand this study into more buildings.

REFERENCES

Mills, E., N. Bourassa, M.A. Piette, H. Friedman, T. Haasl, T. Powell, and D. Claridge. 2005. The cost-effectiveness of commissioning new and existing commercial buildings: Lessons from 224 buildings. *Proceedings of the 2006 National Conference on Building Commissioning*, *Portland Energy Conservation, Inc., New York, NY.*

Mills, E., and P. Mathew. 2009. Monitoring-based commissioning: Benchmarking analysis of 24 UC/CSU/IOU projects. Report LBNL-1972E. Berkeley, CA: Lawrence Berkeley National Laboratory.

Mills, E. 2011. Building commissioning: A golden opportunity for reducing energy costs and greenhouse gas emissions in the United States. *Energy Efficiency* 4(2):145-173.

BIBLIOGRAPHY

Liu, M., D.E. Claridge, and W.D. Turner. 2002. Continuous commissioning guidebook for federal energy managers. www1.eere.energy.gov/femp/pdfs/ccg03_ch1.pdf

Portland Energy Conservation, Inc (PECI). 2007. A retrocommissioning guide for building owners. http://www.peci.org/sites/default/files/epaguide_0.pdf

Effinger, J., H. Friedman, C. Morales, E. Sibley, and S. Tingey. 2009. A study on energy savings and measure cost effectiveness of existing building commissioning. www.peci.org/sites/default/files/annex_report.pdf

Watt, J.B. 2010. Retro-commissioning K-12 schools: real results for real market transformation. *Proceedings of World Energy Engineering Congress 2010, Washington, DC.*

Diagnosis of Effectiveness of HVAC System and Energy Performance of Osaka-Gas Building through Retro-Commissioning
Part 1 Outline of HVAC Systems and Diagnosis of Energy Efficiency of Air Systems.

Toshiomi Hatanaka
Osaka Gas Co., Ltd.
Osaka, Japan

Ko-ichiro Aoki
Manager
Osaka Gas Co., Ltd.
Osaka, Japan

Norio Matsuda
Building Service
Commissioning Association
Nagoya, Japan

Motoi Yamaha
Professor
Chubu University
Kasugai, Japan

Hideki Tanaka
Designated professor
Nagoya University
Nagoya, Japan

Nobuo Nakahara
Nakahara Laboratory,
Environmental Syst.-Tech
Nagoya, Japan

1.ABSTRACT

The south part of Osaka-Gas Building was built in 1933 and the north annex was built in 1966, both of which were equipped with complete HVAC systems using centrifugal chillers. The original HVAC system of the latter was induction unit system for the perimeter and dual-duct system for the interior. The present energy plant consists of gas-fired absorption and cogeneration systems. Both parts of HVAC as well as energy plant system experienced several times of retrofits for energy conservation. Present three papers introduce some of the results of retro-commissioning process to identify actual figures of operation, controls and maintenance for raising energy efficiency using actual measurements, theoretical system analyses and HVAC system simulations.

2. INTRODUCTION

In case of the initial commissioning, verification items are specified based on the Owner's Project Requirement (OPR), the performance is verified in each process, and finally results are checked whether the performance defined in the OPR is achieved or not through functional performance tests.

In contrast, the retro-commissioning includes a process for commissioning the performance of the existing building systems. After the performance was evaluated in light of the verification purposes, improvement plans are developed and implemented as needed, and the results are checked.

In the retro-commissioning, items and scope to be evaluated shall be defined beforehand, as a part of the OPR, because the purposes of retro-commissioning will vary widely such as: improvement of control or operational methods of equipment and sub-systems, improvement of the system itself, and renewal or renovation of equipment, which seek for direct effects, and/or such as; introducing or upgrading continuous monitoring system, favorably with fault detection and diagnosis system to identify system and equipment performance, which seeks for broader effects. Thus the area to be evaluated should be determined in accordance with the commissioning purposes.

The guideline how to proceed commissioning process and how to specify equipment performance have been established elsewhere as in SHASE, however, standardizing how to define and how to proceed the verification process for existing system performance are difficult, because whichever system has its own design philosophy despite of the lack of detailed documentations.

The present paper describes, the outline of the retro-commissioning process of a memorial kind of building, situated in Osaka, with complicated system combination coming from its historical character, which had been brought up with the growth of HVAC technology itself since 1930s.

3. OUTLINE OF BUILDING AND EQUIPMENT

3-1. Outline of Osaka-Gas Building

(1)Outline of building

Address : Hirano-machi, Chuo-ku, Osaka City
Use : Office building
Structure: Steel-reinforced concrete, reinforced concrete
Number of floors: Eight floors above ground and two floors below ground
Total floor area : Total of south and north parts: about 46,987 m^2
South part: 18,422 m^2 (built in 1933)
North part: 28,475 m^2 (extended in 1966)

(2)Outline of HVAC system. The south part of the building was originally equipped with complete air conditioning system installed by TOYO Carrier Corporation, despite the fact that it was built as early as in 1933. The entire building, which comprises offices, an auditorium, dining rooms, and a showroom, was air-conditioned with temperature and humidity control devices. Also installed were the heating radiators for the perimeter area. The energy plant consisted of the turbo refrigerating machine and gas-fired boilers, both of which were made in USA.

In 1966, the north annex building was completed, the air conditioning systems of which were the state-of-the art in those times, that is, induction unit systems for the perimeter zone and dual-duct systems for the interior zone. The energy plant was again the turbo refrigerators and gas-fired boilers, but with cold water thermal storage tank. After the oil crises from 1973, energy un-efficiency of the north annex HVAC system was clarified and various kind of renovations for energy saving were implemented by stages.

Also promoted were changeover of energy source to gas from electricity, natural as gas supplier, such as; introduction of CGS, introduction of absorption type cooling and heating machines, integration of energy plant of the north and south, removal of heat storage tanks.

Radiators and induction units in the perimeter zone were changed to four-pipe fan-coil units with primary air, dual-duct system for interior zones were renovated as VAV system, ventilation demand control based on CO_2 concentration were also introduced.

4. APPLICATION OF RETRO-COMMISSIONING TO OSAKA-GAS BUILDING

4-1. Outline of retro-commissioning processes

The retro- commissioning consists of six phases to be followed as shown in Figure 4.1.

4-2. Retro-commissioning plan

(1)Set-up the project and define objectives

Osaka-Gas Building is historical architecture, the south part of which was built 80 years ago. The systems have been changed and the apparatuses have been renewed many times. Few people can understand the design concept of the building systems at the time of construction or system retrofits, which is typical of old architecture.

The objective of the project is to confirm the validity of retro-commissioning, to clarify problems concerning equipment management and operation and to identify performance of equipment and subsystems by analyzing the actual operation status, in order for the building owner to make decision for further actions.

(2) Study and development of working plan

i) Scope of application of the process. The process includes a part of the *Planning phase* and the *Inspection phase* in Figure 4.1, but does not include on-site detailed measurement. It also does not include an implementation phase and subsequent phases.

The process should include air side system, water distribution system and energy plant as the object of commissioning, however, due to the insufficient data, detailed measurements and analyses on energy plant and water system was postponed to the 2nd stage.

ii) Commissioning team and work sharing. The commissioning management team, CMT, independent

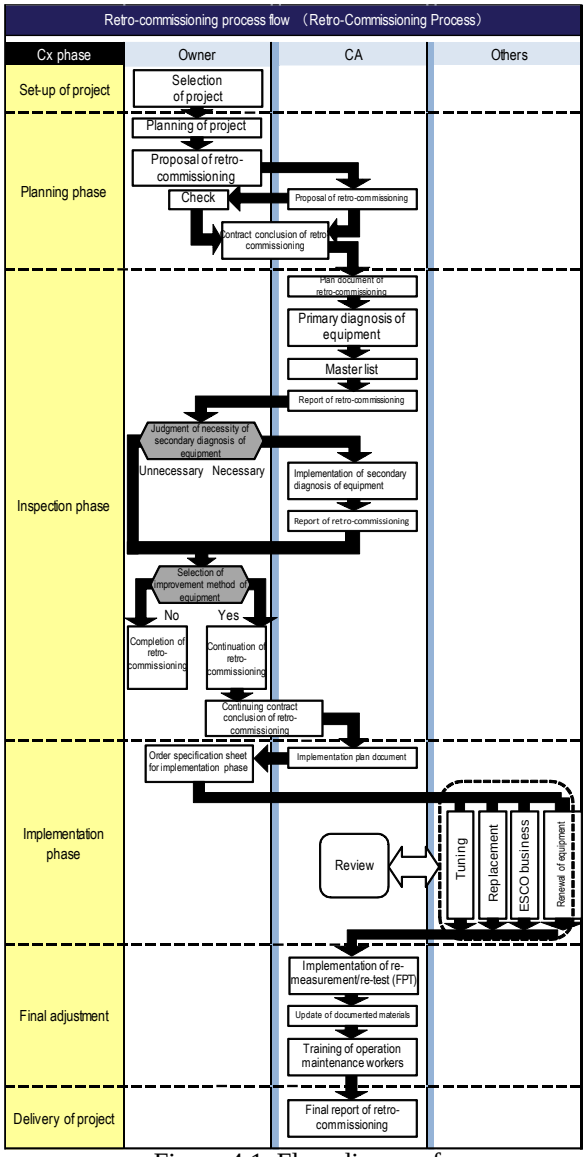

Figure 4.1 Flow diagram for retro-commissioning process

from building management and O&M, was set up mainly by BSCA. The CMT drew up commissioning documents for the project, reviewed materials relevant to the system and equipment stored by the building manager, and clarifies the characteristics of the system constitution and operational problems. The CMT also proposes performance improvement plans and makes reports based on analyses of provided BEMS data and actual measurement data by its own.

(3)Performance verification process. The performance verification process is shown in Figure 4.2. Energy conservation measures were extracted based on ⅰ) macro analyses using BEMS data, ⅱ) additional actual measurement data analyses and ⅲ) HVAC system simulations using LCEM tool. The detailed air-conditioned state analyses and the mixing energy loss analyses for a representative HVAC system, AC-22, were carried out and details are given in the present paper.

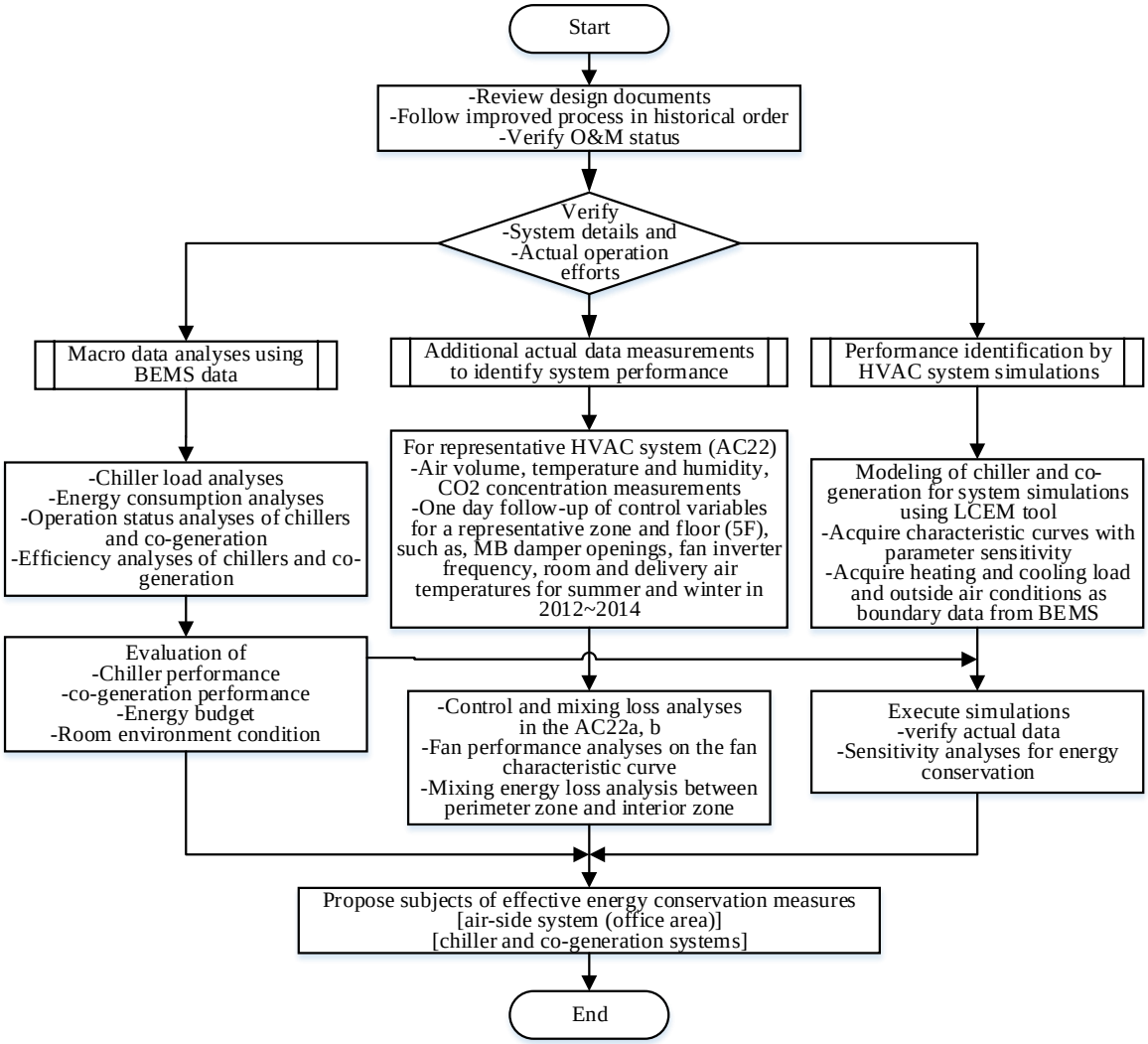

Figure 4.2 Performance verification process (1)

5. IDENTIFYING SYSTEM OPERATION

5-1.Detail of Air-Conditioning System and Controls for the Office Area of the North Building

Main outside air for the entire parts of the building is drawn through outside air shafts situated in the north part, treated by coils and air washers before being introduced to each air conditioning unit. Recirculated air from the interior zone of standard floors return via return air louvers on each floor and each shaft situated in the south and north parts to each air conditioning unit. The demand control by CO_2 concentration is incorporated into the return air system to minimize the amount of outside air. An exhaust air fan is installed to enable total outside air operation as the economizer at the intermediate seasons, which is currently not in use.

As with the south part, the perimeter zone in the office area adopts four-pipe fan coil units together with the primary conditioned air, rich in the outside air, using the primary-air ducts for the past induction units. In the interior zone, the past dual-duct system with mixing boxes are in use as VAV system. Fans were originally suction vane-controlled, which is currently fixed and fans are inverter-controlled. .

Flow diagrams of AC-22 for the north part office area are shown in Figure 5.1

5-2. System operation in summer

The AC-22a, the cold deck, is in operation, while AC-22b, the hot deck, is off operation. Part of the return air to AC-22b is drawn to AC-22a through the bypass damper between AC-22a and AC-22b, mixed with the outside air supplied from AC-24 after primary processing and cooled by the cooling coil before supplied to the office interior zones. The air volume is controlled with the reference point temperature in the interior zone using the cold air damper before the mixing box and supplied from the breeze-line outlets.

5-3. System operation in winter

The outside air taken into AC-24 is humidified with the air washer, mixed with the return air through VD1, 50% open, and further humidified and cooled by water spray in AC-22a before supplied to the office interior zones. The AC-22b heats and humidifies (with steam when in use) the return air and supplies warm air. The VD2 shall be shut but is stick open to 100%.

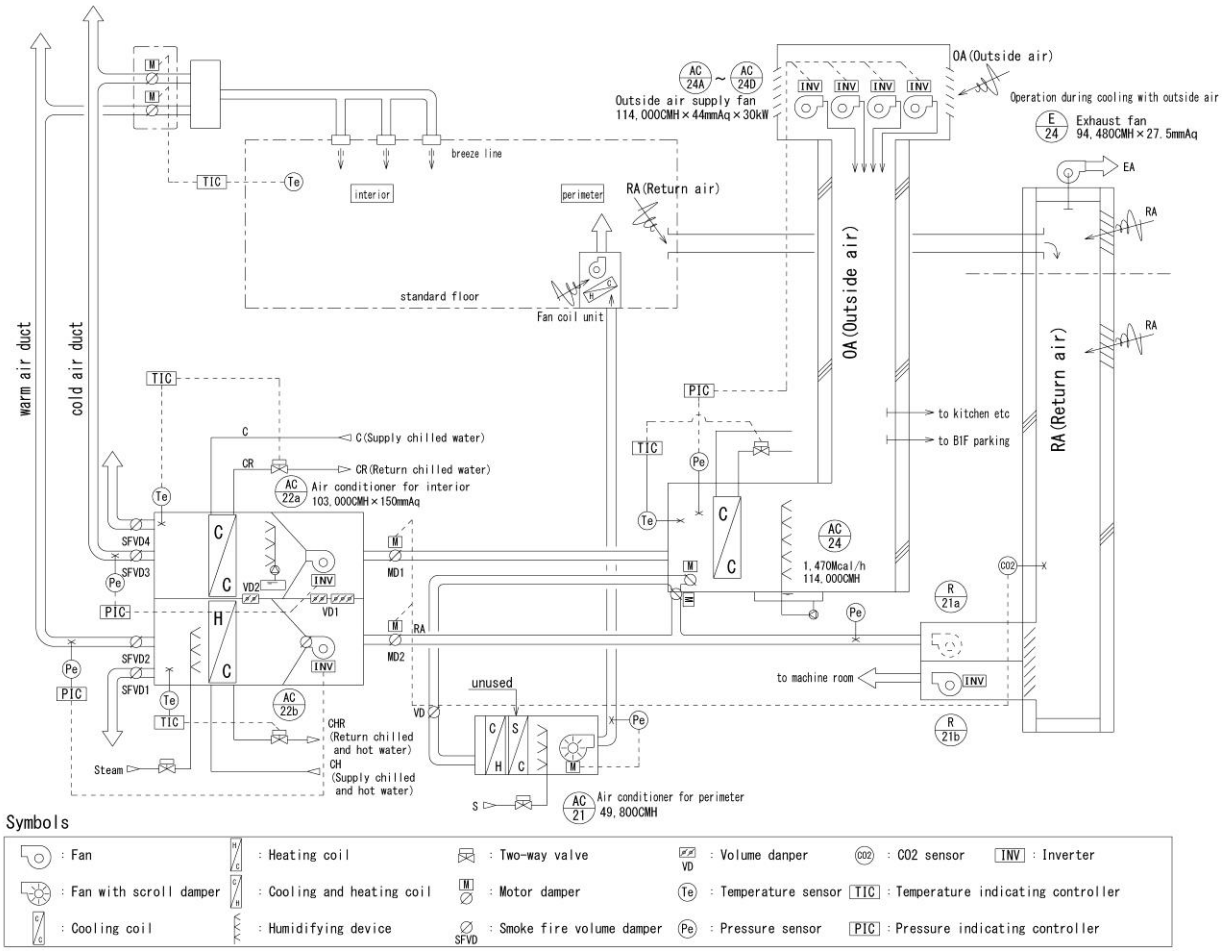

Figure 5.1 Flow diagram of duct system in north part.

6. EVALUATION OF ENERGY LOSS BY MIXING IN AC-22 BY ACTUAL MEASUREMENTS AND PROCESS ANALYSIS

6-1 Measurement data in summer and winter in FY 2013

Table 6.1 shows the measurement data of AC-22a and AC-22b. Both fans have the same specification with the performance curve as shown in Figure 6.1 with plotting for the estimated operating points.

Table 6.1 AC-22 simple measurement data in FY 2013

	At 11:00 on Tuesday, August 27, 2013 (in summer)		At 11:00 on Friday, January 17, 2014 (in winter)	
	AC-22a	AC-22b	AC-22a	AC-22b
INV Output	97% (58.2Hz)	Stopped	84% (50.4Hz)	70% (40.8Hz)
Air volume at the outlet duct	87,848 m^3/h		56,968 m^3/h	42,635 m^3/h
Power consumption	70.0kW		46.8kW	20.6kW
Outlet static pressure	854Pa		798Pa	802Pa
5F MD cold air damper position	9% open		100% open	0%
Outlet temperature	12.4℃		13.4℃	36℃

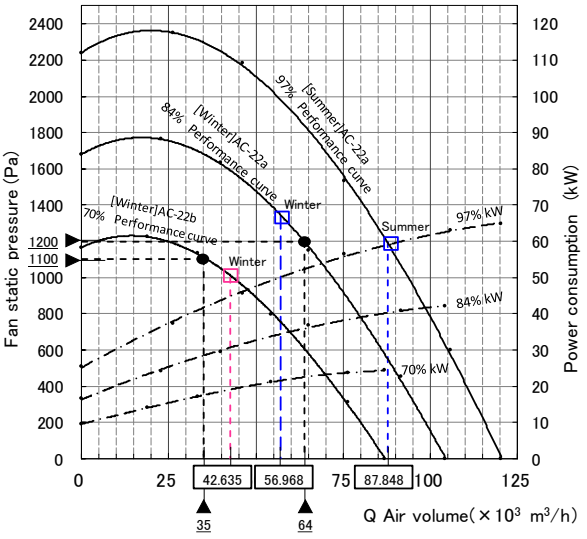

Figure 6.1 Operating points of AC-22a and AC-22b in FY 2013

Note 1: Circles (●) in Figure 6.1 represent operating points of the fans alone. Triangles (▲) represent operating air volumes calculated based on the fan's static pressure.

Note 2: Numbers in boxes ○○○ represent air volume measurement values at the outlet of AC-22.

6.2 Some measured process variables around AC-22 in winter

Figure 6.2 shows one day record of the delivery temperatures and fan inverter outputs of AC-22a and AC-22b, and supply air temperatures from breeze-line outlet on the 5th floor on Friday, January 17, 2014.

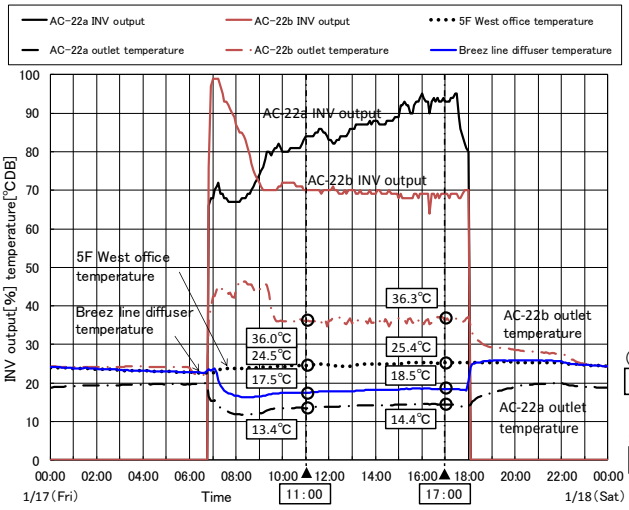

Figure 6.2 Delivery temperatures and inverter outputs of AC-22a, b and breeze-line outlet temperature on 5F

(1) AC-22 inverter output. The AC-22a inverter output is 70% just after start-up, and constantly increases to approximately 93% in the evening. The AC-22a outlet air temperature also increases gradually. On the contrary the AC-22b inverter output is stable at 70% throughout the day after 9:00.

(2) AC-22 outlet static pressure. The outlet static pressure of AC-22a and AC-22b that was recorded otherwise was stable at 800 Pa throughout the day.

(3) AC-22 power consumption. The inverter output almost matches the power consumption

Table 6.2 AC-22 operation status on January 17, 2014

	11 : 00		17 : 00	
	INV Output %	Power consumption kW	INV Output %	Power consumption kW
AC-22a	84	46.8	93	66.0
AC-22b	70	20.6	69	12.7

(4) AC-22 outlet temperature. The AC-22a outlet temperature is approximately 12–15°C during the daytime and approximately 19–20°C during the nighttime (fans are off operation.). The AC-22b outlet temperature is 43–46°C at the time of start-up, and is stable at approximately 36°C from 10:00.

(5) Cold air and warm air mixing damper (MD). The cold air MD opening at the time of start-up is unknown, but is almost 100% throughout the day. The warm air MD opening at the time of start-up is open 40% during 6:00–7:00, and is closed (opening: 0%) for the rest of the day. (Here, the damper opening refers to the controller output. Actually, it was disclosed that the minimal opening had been preset.)

6-3. Mixing inside AC-22 due to bypass dampers

The air volumes through the by-pass dampers VD1 and VD2 in AC-22 are estimated by calculating the air volumes of fans alone (derived from fan operating points based on the operating static pressure at the respective parts). Circles (●) shown in Figure6.1 represent operating points of AC-22a and AC-22b alone.

- [AC-22a] 64,000 m^3/h × 1,200 Pa
- [AC-22b] 35,000 m^3/h × 1,100 Pa

Figure 6.3 shows the AC-22 internal bypass air volume.

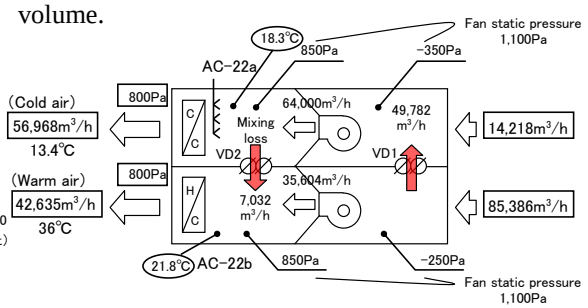

Figure 6.3 Air volumes at 11:00 on January 17, 2014

6-4. Evaluation of the energy loss by mixing

(1) Presumption of the balance of air volumes by measurement. In winter, the interior zones of office space of the typical floor as of the 5th floor need to be cooled, while the cafeteria on B2F and the bank on 1F need to be heated. As the minimal opening was preset at 10% for the control sequence of mixing dampers, the mixing energy loss between cold air and warm air stably exists, which causes excessive air to be fed to both AC-22a and AC-22b and excess heat and fan power are consumed.

Figure 6.4 shows the identified temperatures and air volumes around AC-22 at 11:00 on January 17, 2014.

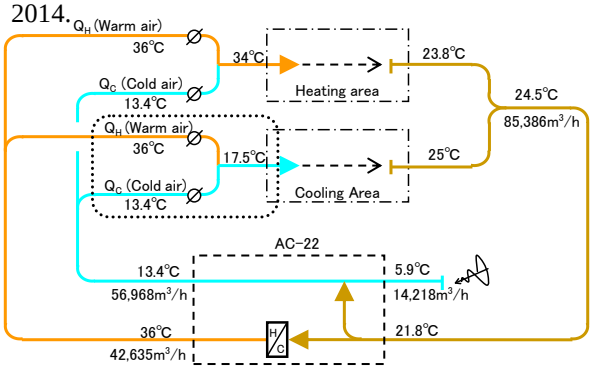

Figure 6.4 Temperatures and air volumes in the AC-22 system at 11:00 on January 17, 2014

Based on Fig. 6.4, the cold air/warm air ratio in the cooling/heating areas is as follows:

Cooling supply area: $Q_H = 0.22Q_C$

Heating supply area: $Q_C = 0.10Q_H$

Figure 6.5 shows the overall air volume balance calculated based on the above relational expression and cold/warm air fan outlet volume.

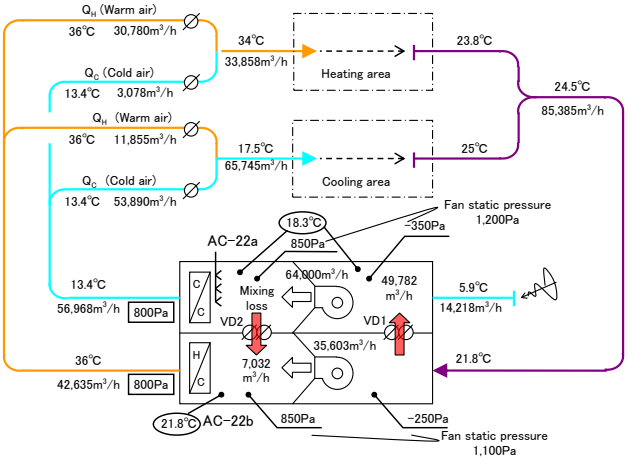

Figure 6.5 Air volume balance of cold air and warm air at 11:00 on January 17, 2014

(2) Presumption of air and heat balance in case of no mixing of cold and warm air. Based on the actual heat and air balance as shown in Figure 6.5, the air volume necessary to treat the net cooling and heating load when the breeze-line supply air temperature were assumed to be kept at the AC22 delivery temperature without any mixing is as follows:

• Cooling area:

65,745 × (25 − 17.5)/(25 − 13.4) = 42,508 m^3/h

Excess air volume: 56,968 − 42,508 = 14,460 m^3/h.

• Heating area:

33,858 × (34 − 23.8)/(36 − 23.8) = 28,308 m^3/h

Excess air volume: 42,635 − 28,308 = 14,327 m^3/h.

Furthermore, if the by-pass air through the VD2 could be completely eliminated, an ideal heat and air balance without mixing loss is estimated as figure 6.6

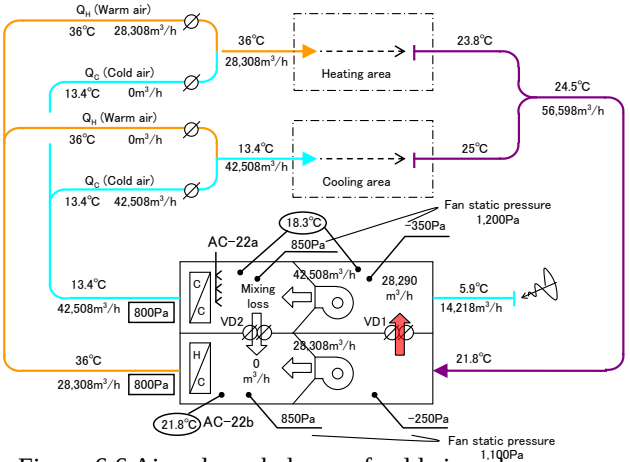

Figure 6.6 Air volume balance of cold air and warm air in case of no mixing

(3) Thermal energy loss by mixing. Because the economizer operation was applied, no energy was originally consumed for the cooling side, so that the thermal energy loss occurs only on the heating side. The difference of the heating energy between Figure6.5 and Figure 6.6 serves as the thermal energy loss due to the mixing of the cold air and warm air in this system as a whole.

• Amount of present heating:

(36°C – 21.8°C) × 42,635 m^3/h ×1.2 kg/m^3 × 1.006 kJ/kg ÷ 3,600 s/h = 203.0 kW

• Amount of heating when there is not mixture:

(36°C – 21.8°C) × 28,308 m^3/h ×1.2 kg/m^3 × 1.006 kJ/kg ÷ 3,600 s/h = 134.8 kW

• Thermal energy loss by the mixture

= Difference of the quantity of heating = 68.2kW

(4) Fan power energy loss by mixing. Amount of power consumption equivalent to the amount of air volume differences becomes the excessive energy loss. Supposing the fan efficiency × motor efficiency is 0.5,

• AC-22a fan :

14,460 m^3/h/3600 × 1,200 Pa/0.5 = 9.6 kW

• AC-22b fan :

14,327 m^3/h/3600 × 1,100 Pa/0.5 = 8.8 kW

• The total : 18.4kW

(5) Primary energy loss by mixing. Assuming the comprehensive primary system COP, which is defined as the heating and cooling load versus total primary energy consumed for HVAC system, is 0.7, primary energy mixing loss is estimated as follows.

• Primary thermal energy loss :

68.2kW/0.7=97.4kW×3.6MJ/kW=350.7MJ/h

• Primary energy loss of fan power consumption :

18.4kW×9.97MJ/kW=183.4MJ/h

• The total : 534.1MJ/h

However, it should be noted that this calculation is based on the heat/air balance on the representative day and time in winter (at 11: 00 on January 17, 2014). Although the energy loss during a specific period cannot be directly calculated, this analysis shall offer a valuable information concerning specific character of mixing energy loss of the dual-duct system for retrofit.

7. ENERGY MIXING LOSS BETWEEN INTERIOR AND PERIMETER ZONES AT SIMULTANEOUS HEATING AND COOLING

In the above-mentioned air-conditioning system, although the office area in the north part was air-conditioned, it was pointed out at the first stage of commissioning in FY 2012 that extensive mixing loss might be incurred in this area in winter between the interior zone and perimeter zone. This phenomenon is very popular but not well recognized, then authors are to analyze and evaluate the mixing loss hereafter.

7-1. Temperature measurement in the interior zone and the air-conditioning system on the typical floor

To analyze and evaluate the mixing loss in the interior zone and perimeter zone on the typical office floor, the temperature was measured in the west office area on 5F of the north part building for a week, i.e., from Tuesday, January 14 to Monday, January 20, 2014. Figure 7.1 shows the measurement data on Friday, January 17, 2014 (the representative day for

measurement). Figure 7.2 shows the measurement points.

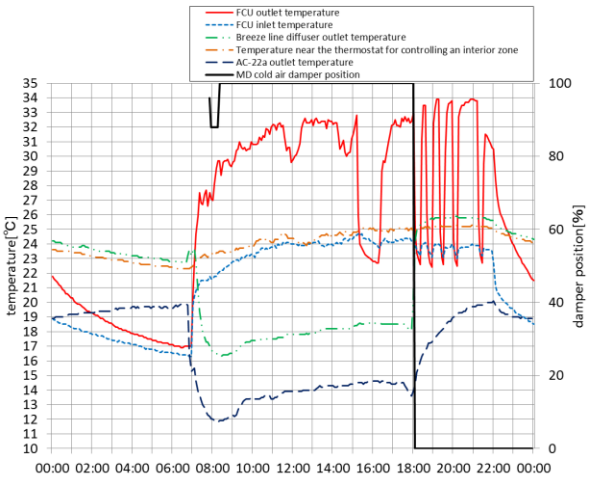

Figure 7.1 Temperature measurement on Friday, January 17, 2014 in the west office area on 5F of the north part

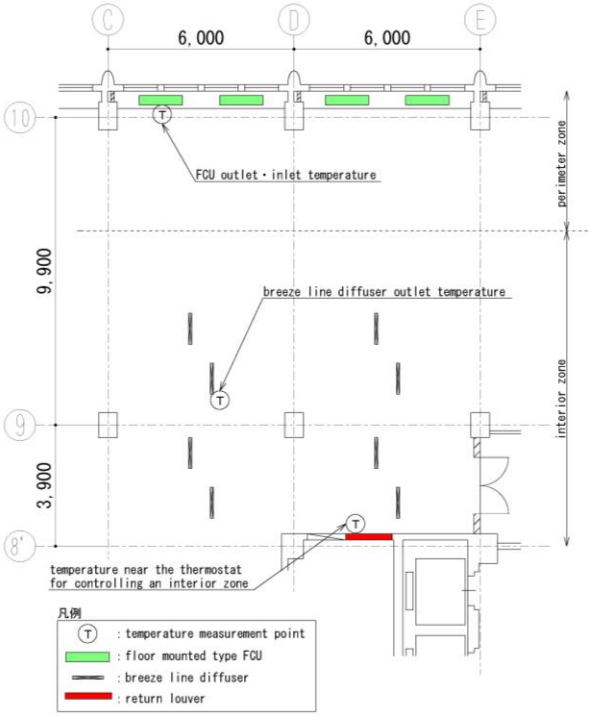

Figure 7.2 Temperature measurement points in the west office area on 5F of the north part

7-2. Definition of the mixing energy loss

When cold air is mixed with warm air at the boundary of the interior and perimeter zones, the load processing capacity is mutually offset and lost. This phenomenon is referred to as the mixing energy loss between the interior zone and perimeter zone.

Equation (1) shows the definition of the mixing loss ratio (MLR). Figure 7.3 shows the schematic diagram of the mixing energy loss.

$$MLR = \{(|Q_P| - |H_P|) + (Q_I - H_I)\} / (|H_P| + H_I), \quad (1)$$

H: Real heat load (subscript I: interior cooling load (+), P: perimeter heating load (-))
Q: Actual heat supply/removal (subscript I: interior cold heat (+), P: perimeter warm heat (-))

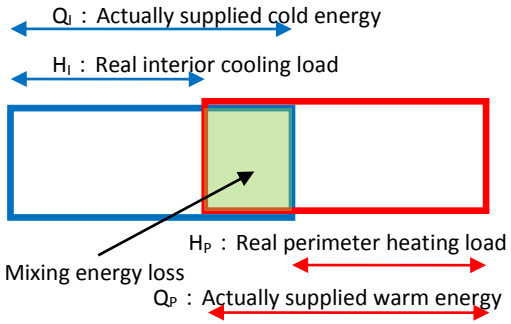

Figure 7.3 Mixing energy loss

7.3 Estimation of the status of mixing loss

Figure 7.1 shows that, during the measurement period, the perimeter zone is heated by FCU and AC-21, while the interior zone is cooled by AC-22a. The MD cold air is open 100% except during the start-up of the air-conditioning system. As discussed below, the interior room temperature was higher than the SP value and cooling capacity arrived at the high limit, while the perimeter zone temperature was closer to the SP value and abundant heating capacity even heated up the interior zone. Thus, it is evident that the mixing energy loss between the interior cold air and perimeter warm air took place and further, as the result of saturated cooling capacity, warmed up the interior zone above SP. Meanwhile, it should be noted that this is another story than the mixing phenomenon as introduced in the previous chapter.

7-4. Temperature control in the interior and perimeter zones

It has been reported in literature that the preset temperature in the interior and perimeter zones serves as a very important factor in calculating the mixing loss.[1) 2)] Table 7.1 below shows the preset temperatures for the interior and perimeter zones that were used for the study.

Table 7.1 Preset temperatures in each zone

	Set value	Remarks
Preset temperature in the interior zone	22.5 ºC	Check the set value of MD (mixing dampers) from the central monitor.
Preset temperature in the perimeter zone	24 ºC	Visual check of the set value of the northwestern FCU, the temperature of which were measured.

As shown in Figure 7.1, the inlet temperature of the FCU during operation is almost 24°C in the perimeter zone, which is almost the same as the preset temperature in the perimeter zone. Meanwhile, the temperature in the interior zone (in the vicinity of the thermostat for mixing damper control) is 24–25°C, which is approximately 1.5–2.5°C higher than the preset temperature. On the same day, the MD in this

area was open 100% on the cold air side and 0% on the warm air side, which means the cooling capacity was at the maximum determined by the air volume and outlet air temperature difference. The heating preset temperature prevailed and raised the temperature in the interior zone, too, due to the excessive capacity in the perimeter zone by FCU and primary air. Thus, the cooling capacity limit prevented further mixing loss.

The temperature in the interior zone (which is used in the mixing loss estimation equation as described below) is the preset temperature that determines the cooling output (i.e., a mixing loss factor). Thus, if the preset temperature were 24°C, there would not be cooling needs to this extent, and mixing loss must have been prevented. With this in mind, 22.5°C was set as the preset temperature for the interior zone in the estimation equation.

7-5. Estimation of the mixing loss ratio (MLR)

The mixing loss is basically determined by the preset temperature difference between the interior and perimeter zones. There are some other relevant factors including the zone air change rate. According to a study conducted by Nakahara et al., [1)2)] the mixing loss ratio can be estimated using various significant factors (P: Depth-length, P: Outlet direction, I: Outlet air volume (air change rate), I-P: Preset temperature difference, Depth of hanging wall, Outlet Ar. number, I Thermostat position, wall or ceiling). The conditions of the full-scale experiment model used in the study by Nakahara et al. are not fully equivalent to those of the objective floor of the present building, but it has sufficient similarity except that the cooling capacity reached the limit in the present case. As no other applicable reference is found, this estimation table has been used.

Table 7.2 shows the substitution results using factor effect values for respective significant factors (based on the effect estimation table of the mixing loss ratio). According to Table 7.2, the mixing loss ratio (MLR) in winter is as follows:

MLR = +23 (−2) = 21% (± 27%)

where (−2 ± 27%) represents the average value ± confidence limit.

8. IMPROVEMENT MEASURES FOR OPTIMIZATION

8-1. Improvement measures for optimization around AC-22

(1) Preventing mixing thermal energy loss. By preventing mixture at the dual duct mixing dampers, and at the bypass-damper for the cold and warm air in AC-22, mixing thermal energy loss will be reduced by 68.2kw. However, outside air demand control should be carefully examined with this measure.

(2) Reducing excessive fan power consumption due to mixing. The minimum opening policy of mixing dampers to allow mixing of warm and cold air shall be examined to reduce bypassed air. Inside AC-22 VD2 bypass damper shall be completely closed to reduce air volume and fan power and to reduce excessive outside-air heating load. The power consumption can be reduced by 18.4 kW (total of AC-22a and AC-22b) in winter.

(3) AC-22 internal mixing loss. As shown in Figure 6.3, AC-22b internal mixing loss is attributed to the mixing of AC-22a fan outlet air (18.3°C) and AC-22b outlet air (21.3°C). The internal mixing loss can be reduced by 7.1 kW by closing VD2. (This effect is, however, included in the 68.2kW of item (1))

(4) Effective utilization of outside air (cold air) in the intermediate season as economizer. The cold/cool outside air supplied to the office floors is balanced with the exhaust air volume from the restrooms and kitchenettes, etc. Because these exhaust air volume are constant, it was difficult to increase the outside air volume. However, the E-24 fan is installed perhaps for this purpose, shall be then operated in the intermediate

Table 7.2 Factor effect of the mixing loss ratio (value substitution)

Factor		Factor level	Mixing loss ratio
A	P : Depth	Estimated at about 4.5 m	15
C	P : Outlet direction	P Outlet direction : 0º	4
F	I : Outlet air volume (air change rate)	Air volume in the interior is estimated at the rated value (8,230 m^3/h), as MD opening on the cold air side is 100%. Air change rate in the interior is about 5 times/h.	-8
G	I-P : Preset temperatures difference	-1.5ºC (I: 22.5ºC, P: 24ºC)	44
B × D Length of hanging wall × P Outlet Ar number		Hanging wall: None, Ar number: middle	-18
B × H Length of hanging wall × I thermostat position		Hanging wall: None I thermostat position: Wall	-22
C × D P Outlet direction × P outlet Ar number		P Outlet direction: 0ºC P Outlet Ar number: middle	8
		Total factor effect	23 (%)

season as the economizer, depending on the cold air requirements. When there are needs for cooling and outside air has less enthalpy than recirculated air, the outside air volume shall be increased. The control algorithm is available elsewhere as outside air cooling. An inverter is already installed to the E-24 fan to ensure this control.

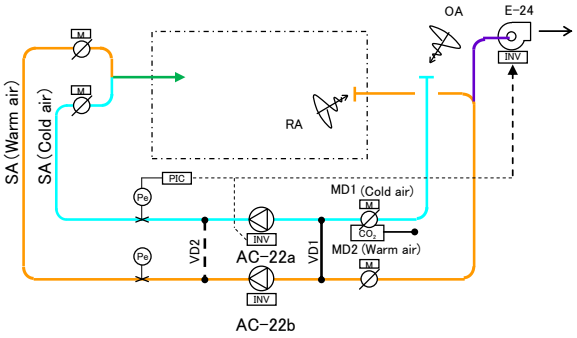

Figure 8.1 Conceptual image of control

(5) Re-installing the return fan and reducing the outlet static pressure settings for AC-22a and AC-22b.

It should be noted that the return fan became out of order several years ago and removed as shown in Figure 5.1, while the outside air is sent by plural OA fans. In winter, the operating pressure of AC-22 system is shown in Fig. 8-2. The suction pressure of AC-22b is -250Pa, higher than that of AC22a by 100 Pa, the resistance of the damper VD1, in order to pass the return air from AC-22b to AC-22a. The negative pressure was caused by removal of the return fan, R-21a (145,590m^3 × 300Pa × 30kW), and resistance of MD1 becomes 380Pa to perform the pressure balance, resulting in the useless energy loss. The effect of energy saving by re-installing the return fan R-21a is calculated as follows. As corrected values are shown in Figure 8.2, pressure balance is corrected as for the resistance of MD1 to become as small as 80Pa. Supposing the same efficiency for the reinstalled fan and motor as AC22 fans, the fan power consumption before and after reinstallation is as follows.

Before (present condition)

- AC-22a fan :
  64,000 m^3/h/3600 × 1,200 Pa/0.5 = 42.7 kW
- AC-22b fan :
  35,603 m^3/h/3600 × 1,100 Pa/0.5 = 21.8 kW
- The total : 64.5kW

After (future condition)

- AC-22a fan :
  64,000 m^3/h/3600 × 900 Pa/0.5 = 32.0 kW
- AC-22b fan :
  35,603 m^3/h/3600 × 800 Pa/0.5 = 15.8 kW
- R-21a fan :
  85,385 m^3/h/3600 × 300 Pa/0.5 = 14.2 kW
- The total : 62.0kW

Reduction of the fan power consumption becomes 2.5kw. (= 64.5 – 62.0) However, this value changes with the amounts of introduced outdoor air and becomes larger if high efficient fan and motor are used.

In addition to energy saving effect, pressure balance of the relevant air-conditioning systems connected in parallel to the common outside air shaft and return air shaft is improved and controllability of each duct-fan system, will be stabilized as the byproduct.

Moreover, although the outlet static pressure is preset at constant value of 800 Pa for now, if optimal pressure setting control is introduced depending on the air- conditioning load change and resulting air volume change, far more energy saving will be realized. Thus, the reduction of fan power consumption of AC-22 systems is aimed at by carrying out these two methods.

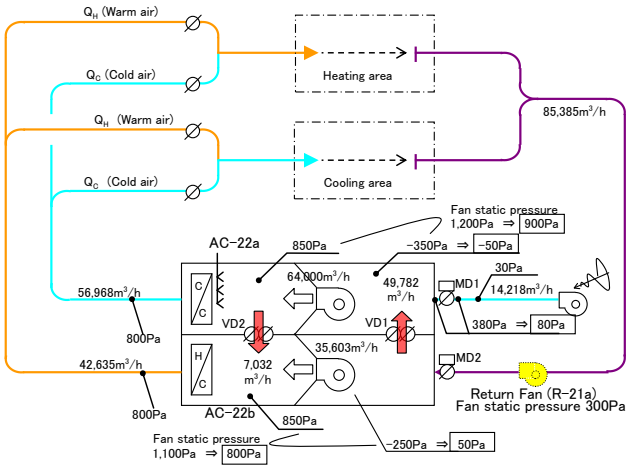

Figure 8.2 Static pressure and air volumes in the AC-22

Note 1: Numbers in boxes ○○○ numerical value after re-installing the return fan.

8-2. Improvement measures to minimize the mixing energy loss between the interior and perimeter zones.

In Chapter 7, the mixing loss ratio was estimated as 21%. To reduce the mixing loss ratio, it is necessary to either reduce the difference in room temperature settings between the interior and perimeter zones or reverse the settings (i.e., lower the preset temperature in the perimeter zone than that of the interior zone), as is evident from Table 2 and its original estimation table[1) 2)].

Apart from the estimation table, it was observed that the interior cooling capacity reached to the upper limit with fully opened cooling damper and resulted raised room temperature. This suggest that limiting the excessive heating and cooling capacity is an effective measure to limit the mixing energy loss. To limit the interior cooling capacity optimal supply temperature setting control is effective. To reduce the perimeter heating capacity, most effective way in this case will be reduce primary air supply by AC-21, which has too excessive heating capacity and uncontrollable at the terminal.

Another most effective solution to exclude mixing energy loss would be to eliminate the need for simultaneous cooling and heating with the use of perimeter-less system. In realistic viewpoint, however, it is difficult to switch to the perimeter-less

system in the existing Osaka-Gas Building. Described below are feasible solutions.

1) Reducing the excessive air conditioning capacity in the perimeter zone. a) Minimizing the primary air volume in the AC-21 system. The primary air of the AC-21 system not only introduces outside air and serves as a heat source but also humidifies rooms. An investigation must be conducted before stopping the primary air. b) Reducing the maximum capacity of FCU and AC-21 through the cascade control of the hot water supply temperature based on the outside air temperature. This solution can curb the excess mixing loss.

2) Lowering the preset temperature in the perimeter zone to the extent that the occupied zone is not affected, and raising the preset temperature in the interior zone taking the same care for comfort.

3) Change the mixing damper control schedule to eliminate minimum opening preset to exclude stable mixing of warm and cold air.

4) Introducing optimal delivery air temperature setting control for the AC-22a and b to limit excessive cooling effect and limit the mixing loss capacity.

5) Reducing the outlet volume of cold air in the interior zone in the vicinity of the perimeter zone, and preventing direct mixing loss with the perimeter zone

6) Lowering the cold air ventilation temperature from the current level to reduce the air change rate

7) Setting up control sensors at appropriate locations so that they can correctly detect the room temperature.

9. DISCUSSION

The commissioning process has been applied for the existing Osaka-Gas Building as a case study of research subject how to proceed retro-commissioning for the old and memorial kind of building with long history of building annex and several times of retrofits for energy conservation. The project was performed for two and a half years up to the former half of the inspection phase of retro-commissioning process. One of the principal works were to determine the performance of the current system, identify problems, review solutions, present the possibilities of optimizing the operation method, and to help achieve energy conservation in the future.

The inspection phase started in August 2012. After conducting hearings, scrutinizing the drawings, and performing on-site inspections, authors identified the performance based on the BEMS data as shown in the Part-2, analyzed the operating status of air and heat source systems based on added actual measurements, and then examined energy-saving effect of several ways of retrofit based on simulation study as shown in the Part 3.

Figure 9.1 shows the performance verification process flow in this study. Figure 9.1 shows the long-term improvement strategy for the air system and the basic concept of grading-up the energy plant now under consideration. Some energy-saving measures require extensive modification. Continuous renovation plans will be formulated in collaboration with the operation staff as the continuous commissioning process, that is, the combination of on-going commissioning by O&M +FM and re-commissioning by the third party.

This study is one of the result of research works by (NPO) Building Services Commissioning Association on the useful application of the commissioning process. Authors acknowledge the building owner and O&M staff of the Osaka Gas Building and member of the research committee for their assistance.

ABBREVIATION

- BEMS : Building and Energy Management System
- BSCA : Building Services Commissioning Association
- CGS : Cogeneration System
- CMT : Commissioning Managing Team
- FCU : Fan Coil Unit
- FM : Facility Management
- LCEM : Life Cycle Energy Management
- O&M : Operation & Maintenance
- SHASE : The Society of Heating, Air-Conditioning and Sanitary Engineers of Japan
- VAV : Variable air volume

REFERENCES

1)-Nakahara, N. and Ito, H.: PREDICTION OF MIXING ENERGY LOSS IN A SIMULTANEOUSLY HEATED AND COOLED ROOM: PART 1- EXPERIMENTAL ANALYSES OF FACTORIAL EFFECTS, ASHRAE TRANSACTIONS, 1993. V. 99, Pt. 1

2)-Nakahara, N. and Ito, H.: PREDICTION OF MIXING ENERGY LOSS IN A SIMULTANEOUSLY HEATED AND COOLED ROOM: PART 2- SIMULATION ANALYSES ON SEASONAL EFFECTS, ASHRAE TRANSACTIONS, 1993. V. 99, Pt. 2

3)-Matsuda,N. Hatanaka,T. Aoki,K. Tanaka,H. et al. :Performance verification of an existing building which has the cogeneration system : Part.1 The way of application and evaluation of the Commissioning Process for existing system, Part.2 Performance verification of the energy system by BEMS data, Part.3 Evaluation of Operating Performance and Energy Efficiency for Air-conditioning System, Part.4Performance evaluation with system simulation by using BEMS measured data, The Society of Heating, Air-Conditioning and Sanitary Engineers of Japan, 2013.9

4) -Hatanaka.T. Aoki,K. et al., : Performance verification of an existing building which has the cogeneration system : Part.5 The evaluation and the measure against mixing loss between the zones of a north building standard floor, Part.6 The Mixed Energy Loss of the AC-22 Perimeter Air in the HVAC system for a typical Office Floor and the Countermeasures, The Society of Heating, Air-Conditioning and Sanitary Engineers of Japan, 2014.9

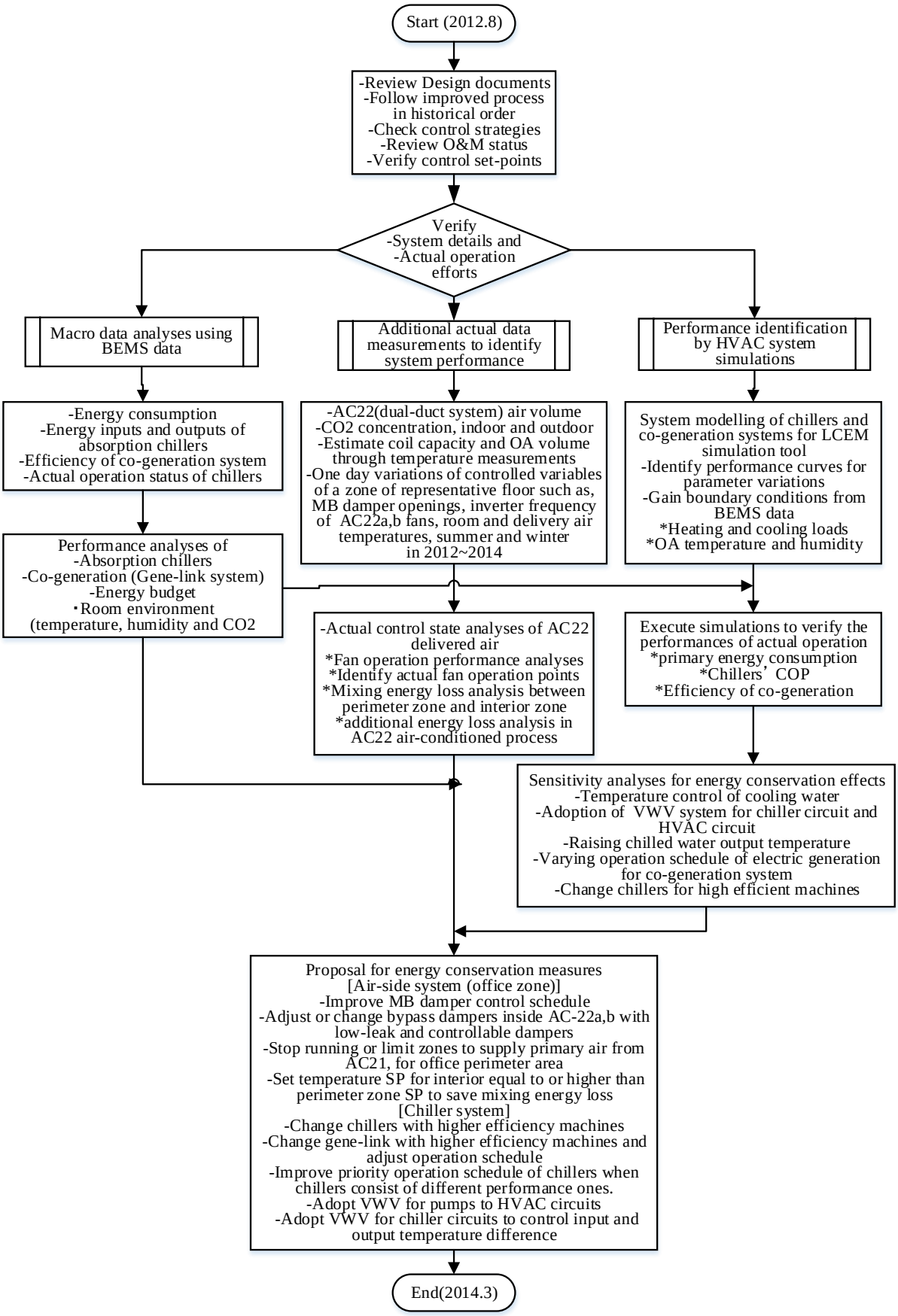

Figure 9.1 Performance verification process(2)

Modeling to predict positive pressurization required to control mold growth from infiltration in a building in College Station, Texas

Wei-Jen Chen
Research Student

David E. Claridge
Ph.D., P.E.
Leland Jordan Professor

Energy Systems Laboratory, Texas A&M Engineering Experiment Station
College Station, TX

ABSTRACT

Commercial buildings are generally designed to operate at a positive pressure to limit the danger of mold growth, material deterioration and other condensation related problems from infiltration in hot and humid climates. Pressurization to limit the entry of untreated outside air also limits discomfort due to humidity from this untreated air. This paper focuses on infiltration modeling to predict the influence of pressurization level on the risk of mold growth. In this model, walls are treated differently depending on their height and the direction they face. Local weather data is utilized to generate the outside pressure field. The simulated results indicate that for an unpressurized building with 3 meter high walls in College Station, TX, only walls on the southwest side risk mold growth due to infiltration if the indoor temperature set-point is at 24°C. When the set-point temperature is lowered to 22°C, walls facing all directions risk mold growth. The model also indicates that 1 Pa positive pressurization should theoretically eliminate the risk of mold growth on all walls for the leakage characteristics considered assuming a 24°C indoor temperature set-point.

INTRODUCTION

One of the major benefits of building pressurization is to limit the danger of mold growth in building envelopes. Since excessive pressurization during the cooling season usually means extra energy consumption, a method to quantify the required minimum pressure level is desirable. To achieve this goal, the location that theoretically has the most severe mold growth potential should be identified first.

Research (Viitanen 1997, Nielsen, Holm et al. 2004, Johansson, Ekstrand-Tobin et al. 2012) indicates that relative humidity (RH) and temperature are two key factors involved in mold growth. Critical RH and temperature conditions are required to create favorable conditions for mold growth. According to psychometric principles, the RH of air goes up when temperature of air goes down if the moisture content of the air is constant. This occurs with infiltrating air when the outside air temperature is higher than indoor air temperature. Likewise, it happens to exfiltrating air when the temperature relationship is reversed. Hence, in hot and humid climates, mold

growth and condensation will most likely occur on a building envelope layer that is in contact with the inner space or close to the inner wall surface (where moist infiltrated air reaches its highest RH).

Hukka and Viitanen (1999) proposed a mathematical model to predict mold growth on wooden material, using critical RH as the key factor. Conditions with RH exceeding critical RH are considered favorable for mold growth, otherwise they are unfavorable for mold growth. Critical RH varies with different materials and temperature range. For a gypsum board at 22°C, critical RH is estimated between 89% to 95%. (Johansson, Ekstrand-Tobin et al. 2012) In this paper, 89% is selected to represent the worst case scenario.

Under this model, mold growth intensity is categorized into seven levels called the "mold index M" where, M=0 – 6. A detailed definition of each mold index level is listed in Table 1. Under conditions favorable for mold growth, the following equation applies:

$$\frac{dM}{dt} = \frac{1}{7 * \exp(-0.68 \ln T - 13.9 \ln RH + 0.14W - 0.33SQ + 66.02)} * k_1 k_2$$

(Per day)

Where:

T is temperature (°C)

RH is relative humidity

k_1 is intensity of growth

k_2 is calculated based on M_{max}

W is a wood species factor

SQ is a surface quality factor

For unfavorable mold growth conditions, the following equation is applied:

$$\frac{dM}{dt} = \begin{cases} -0.00133, \text{when } t - t_1 \leq 6h \\ 0, \quad \text{when } 6h < t - t_1 \leq 24h \\ -0.000667, \text{when } t - t_1 > 24h \end{cases}$$

(Per hour)

Where:

t is the time (h) from the moment t_1 when the conditions changed from favorable to unfavorable conditions.

This model is then expanded to cover other building materials (Viitanen, Viitanen et al. 2010) (Viitanen, Ojanen et al. 2011). The declining model for unfavorable condition is multiplied by a relative coefficient C_{mat} for materials different from the pine wood tested originally. This model is utilized to predict mold growth, and the results will be presented in terms of the mold index.

Typically indoor RH is controlled within a range that is unfavorable for mold growth, which means that for building envelope, exfiltration is risk free of mold growth. To find out when exfiltration will occur, both outside and indoor pressure field must be generated first.

Outside pressure field is mainly affected by two factors: stack effect and wind effect, by assigning outside ground level as reference point, stack effect is calculated by the following equation:

$$P(h) = 0 - \rho g h$$

Where:

$P(h)$ is outside pressure (Pa.) at height h (meters)

ρ is the density of air (kg/m^3)

g is gravity constant $(9.81\mathrm{m}/s^2)$

Wind effect is calculated by the following equation: (Sherman 1980)

$$\Delta P_{\mathrm{j}}^{\mathrm{w}} = \mathrm{C_j} * \frac{1}{2}\rho V^2$$

Where:

$\Delta P_{\mathrm{j}}^{\mathrm{w}}$ is the exterior pressure rise due to the wind for the jth face

ρ is the density of air (kg/m^3)

V is the actual wind speed (m/s)

$\mathrm{C_j}$ is the shielding coefficient for the jth face.

For V, Following equation is applied:

$$\mathrm{V} = \mathrm{V_o}\alpha\left[\frac{\mathrm{H}}{10}\right]^{\gamma}$$

Where:

V is the actual wind speed

$\mathrm{V_o}$ is the wind speed measured at the nearest 10 meter high weather station

α and γ are constants that depend on terrain class.

Assuming Class III terrain (rural areas with low buildings, trees, etc.), $\alpha = 0.85$ and $\gamma = 0.2$ are applied.

For shielding coefficient (or pressure coefficient), the following equation is applied with typical values $\mathrm{C_p}(1) = 0.6, \mathrm{C_p}(2) = -0.3, \mathrm{C_p}(3) = \mathrm{C_p}(4) = -0.65$ (ASHRAE 2009):

$$\begin{aligned} C_p(\phi) = 1/2\{&[C_p(1) + C_p(2)](\cos^2\phi)^{1/4} \\ &+ [C_p(1) - C_p(2)](\cos\phi)^{3/4} \\ &+ [C_p(3) - C_p(4)](\sin^2\phi)^2 \\ &+ [C_p(3) - C_p(4)]\sin\phi\} \end{aligned}$$

where

$C_p(1)$ = pressure coefficient when wind is at 0°
$C_p(2)$ = pressure coefficient when wind is at 180°
$C_p(3)$ = pressure coefficient when wind is at 90°
$C_p(4)$ = pressure coefficient when wind is at 270°
ϕ = wind angle measured clockwise from the normal to wall 1

Indoor pressure field is also affected by stack effect; however, when the building achieves steady state, the infiltration/exfiltration flow should be equal. The flow through a leakage path is calculated by the following equation (Sherman 1980):

$$Q = C(\Delta P)^n$$

Where:

Q is the air flow (m^3/sec)

C is the flow coefficient

n is the pressure exponent

ΔP is the pressure difference (Pa.)

While C and n should be determined by experiment, in this paper, leakage area is assumed evenly distributed on walls, C and n are assumed constant and n is assumed 0.65. Under these assumptions, ΔP can be determined as well as the indoor pressure field. After both outside and indoor pressure fields are available, the infiltration or exfiltration condition at a specific wall/roof section can be determined.

When a section is determined to be under infiltration condition, RH of infiltration air is then calculated as its temperature reaches indoor temperature; for example, assuming indoor temperature is 24°C,

saturation vapor pressure at 24°C is then calculated by the following equation (Wagner and Pruß 2002):

When T>0°C

$$\ln\left(\frac{p_\sigma}{p_c}\right) = \frac{T_c}{T}(a_1\vartheta + a_2\vartheta^{1.5} + a_3\vartheta^3 + a_4\vartheta^{3.5} + a_5\vartheta^4 + a_6\vartheta^{7.5}),$$

with $\vartheta = (1 - T/T_c)$, $T_c = 647.096$ K, $p_c = 22.064$ MPa, $a_1 = -7.859\,517\,83$, $a_2 = 1.844\,082\,59$, $a_3 = -11.786\,649\,7$, $a_4 = 22.680\,741\,1$, $a_5 = -15.961\,871\,9$, and $a_6 = 1.801\,225\,02$.

When T<0°C

$$\ln\left(\frac{p_{subl}}{p_n}\right) = -13.928\,169(1 - \theta^{-1.5}) + 34.707\,823\,8(1 - \theta^{-1.25}), \quad (2.21)$$

with $\theta = T/T_n$, $T_n = 273.16$ K, and $p_n = 0.000\,611\,657$ MPa.

Infiltration vapor pressure is then calculated by the following equation:

$$P_w = P_s * RH$$

Where:

P_w is vapor pressure

P_s is saturation vapor pressure

RH of infiltration air at 24°C is then calculated by the following equation:

$$RH_{24°C} = P_w / P_{s@24°C}$$

Either declining or increasing mold growth is then applied to calculate mold level change.

MODEL DESCRIPTION

The building is assumed to be a square structure 3 meters high, facing South-East. The material of the target layer is assumed to be gypsum board, which has critical RH of 89% (Johansson, Ekstrand-Tobin et al. 2012). The third Typical Meteorological Year data set (TMY3) from Easterwood Airport (College Station, TX) is utilized to calculate the outside pressure field. Figure 1 represents the flow chart for how the mold index level change is calculated.

The building envelope is divided into 9 sections, Top South West, Top South East, Top North West, Top North East, Bottom South West, Bottom South East, Bottom North West, Bottom North East, and Roof; all sections are assumed to have the same specific leakage area, but the floor is assumed airtight.

The hourly mold index level changes throughout the year are summed up to show the predicted mold index level change for a year, as well as infiltration time percentage (hours of infiltration within a year divided by 8760). Conditions for both 22°C and 24°C are simulated.

The building operation schedule is assumed to be operating 24/7 for both settings.

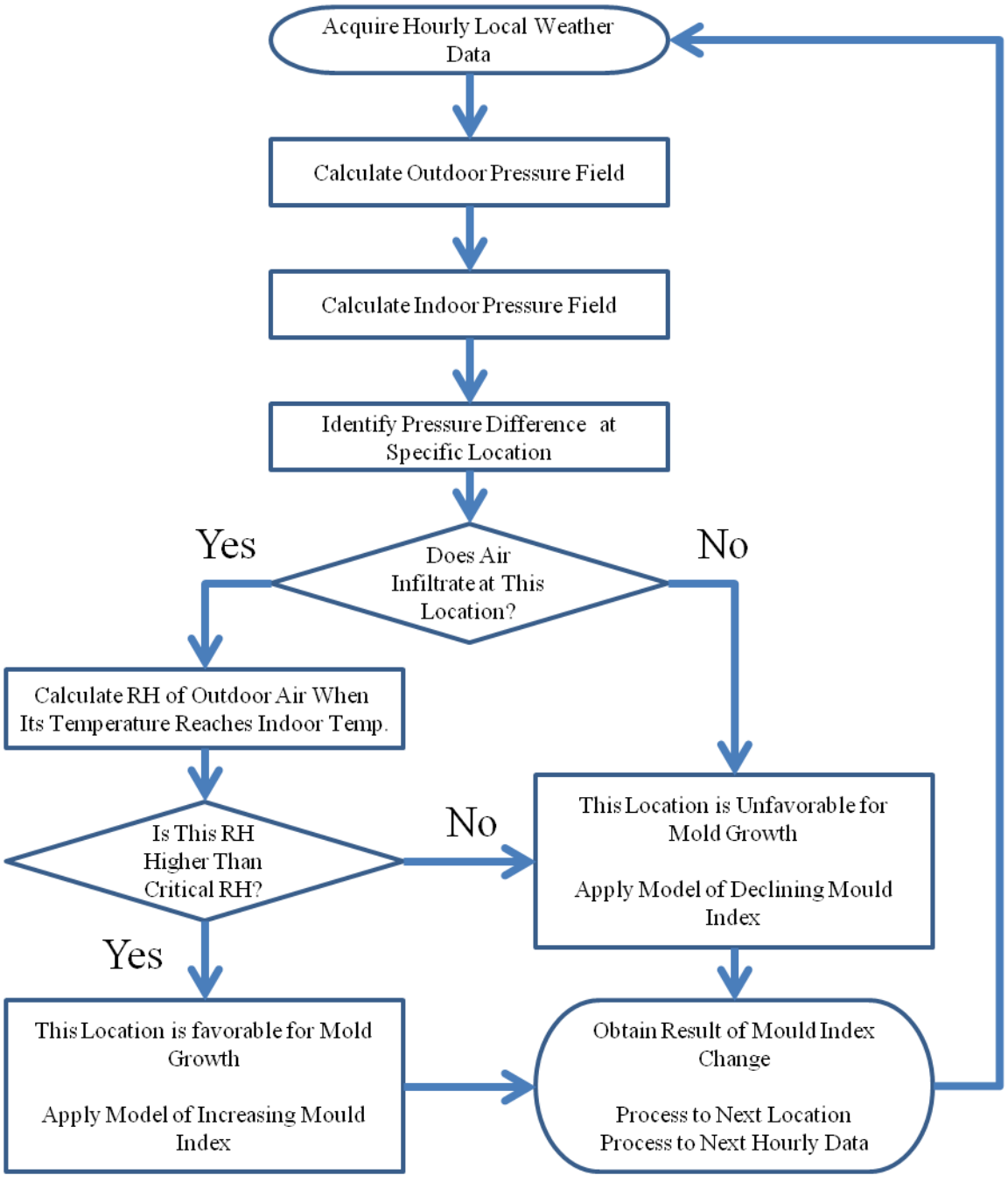

Figure 1. Flow chart of the model

Table 1. Mould Index for Experiments and Modeling. New determinations for index levels 3 and 4 are presented using bold fonts.

Index	Description of the growth rate
0	No growth
1	Small amounts of mould on surface (microscope), initial stages of local growth
2	Several local mould growth colonies on surface (microscope)
3	Visual findings of mould on surface, < 10 % coverage, or, **< 50 % coverage of mould (microscope)**
4	Visual findings of mould on surface, 10 - 50 % coverage, or, **>50 % coverage of mould (microscope)**
5	Plenty of growth on surface, > 50 % coverage (visual)
6	Heavy and tight growth, coverage about 100 %

Table 1. Mold Index (Viitanen, Ojanen et al. 2011)

RESULTS

Three types of results will be presented. Infiltration time percentage is the percentage of time a specific section of wall is under infiltration condition. Each section will have three results that represent unpressurized, 1 Pa positive pressure, and 2 Pa positive pressure conditions, respectively.

Mold index level change is the net change of mold index for whole year at specific sections. There are also results under different pressurization levels.

Risky infiltration time is the percentage of time during each month that infiltration is favorable for mold growth. The result is available for both 22°C and 24°C indoor temperatures.

For indoor temperature at 24°C, the results of infiltration time percentage, mold level change per year, and risky infiltration time percentage are shown as Figure 2, Figure 3 and Figure 4. For indoor temperature at 22°C, the results are shown as Figure 5, Figure 6 and Figure 7.

As expected, higher indoor temperatures induce more infiltration through the bottom portions of walls. The maximum infiltration time percentage occurs on the bottom SW wall, which is 69.0% at 24°C indoor temperature and 63.3% at 22°C, 2 Pa positive pressurization can reduce the values to 21.9% and 20.6%, respectively.

Under unpressurized conditions, only the SW side wall risks mold growth for 24°C indoor temp., but all side walls risk mold growth when it is 22°C. 1 Pa pressurization is enough to make the whole year mold index change on all walls negative for 24°C, but for 22°C, 2 Pa pressurization is required to achieve this protection.

It may also be noted that infiltration is risk free from November to April for 24°C indoor temperature, but this period is shortened to December to March for 22°C set-point. June has the highest risky infiltration times, which are 77.9% and 94.3%, respectively.

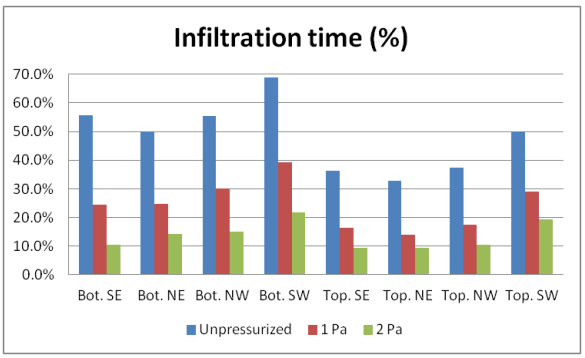

Figure 2. Infiltration time (%) (Indoor=24°C)

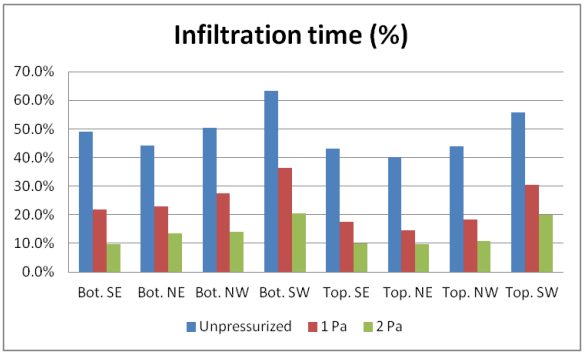

Figure 5. Infiltration time (%) (Indoor=22°C)

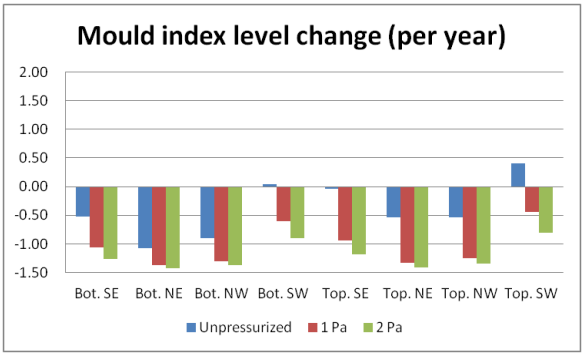

Figure 3. Mold index level change (Indoor=24°C)

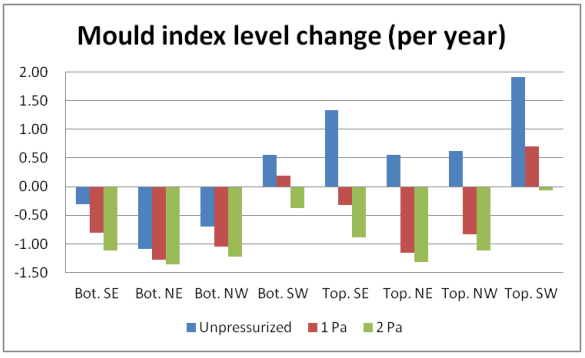

Figure 6. Mold index level change(Indoor=22°C)

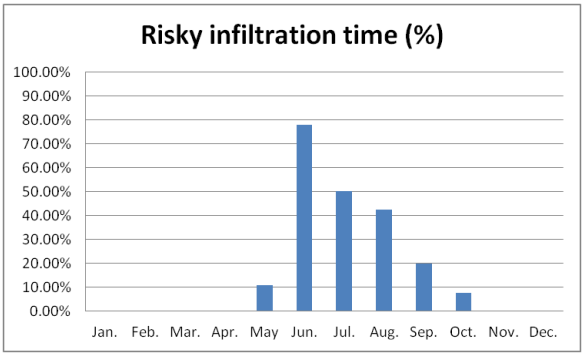

Figure 4. Risky infiltration time (Indoor=24°C)

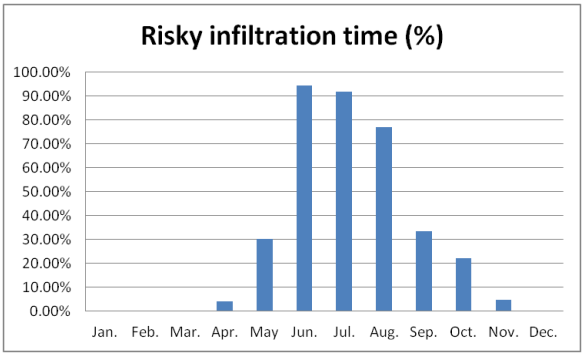

Figure 7. Risky infiltration time (Indoor=22°C)

CONCLUSIONS

Positive pressurization and higher indoor temperature set-points both were found capable of eliminating mold growth in for the configurations modeled. Pressurization is not necessary during colder months to control mold growth, but is quite necessary from June to August. A higher indoor temperature set-point requires lower positive pressurization to become theoretically risk free of mold growth, but for the assumptions modeled, 2 Pa is sufficient for a building that has a set-point as low as 22°C if the target material is assumed to be gypsum board.

REFERENCES

ASHRAE (2009). "ASHRAE Handbook–Fundamentals." Atlanta, GA.

Hukka, A. and H. A. Viitanen (1999). "A mathematical model of mould growth on wooden material." Wood Science and Technology **33**(6): 475-485.

Johansson, P., A. Ekstrand-Tobin, T. Svensson and G. Bok (2012). "Laboratory study to determine the critical moisture level for mould growth on building materials." International Biodeterioration & Biodegradation **73**: 23-32.

Nielsen, K. F., G. Holm, L. Uttrup and P. Nielsen (2004). "Mould growth on building materials under low water activities. Influence of humidity and temperature on fungal growth and secondary metabolism." International Biodeterioration & Biodegradation **54**(4): 325-336.

Sherman, M. (1980). Infiltration-pressurization correlation: Simplified physical modeling. The American Society of Heating, Refrigeration and Air Conditioning Engineers, Denver, CO, June 22-26, 1980.

Viitanen, H. (1997). "Modelling the Time Factor in the Development of Mould Fungi - the Effect of Critical Humidity and Temperature Conditions on Pine and Spruce Sapwood." Holzforschung **51**(1): 6-14.

Viitanen, H., T. Ojanen, R. Peuhkuri, J. Vinha, K. Lähdesmäki and K. Salminen (2011). "Mould growth modelling to evaluate durability of materials". Proceedings of the 12th DBMC International Conference on Durability of Building Materials and Components, Porto, Portugal.

Viitanen, H., J. Viitanen, K. Vinha, T. Salminen, R. Ojanen, L. Peuhkuri, K. Paajanen and Lahdesmaki (2010). "Moisture and Bio-deterioration Risk of Building Materials and Structures." Journal of Building Physics **33**(3): 201-224.

Wagner, W. and A. Pruß (2002). "The IAPWS formulation 1995 for the thermodynamic properties of ordinary water substance for general and scientific use." Journal of Physical and Chemical Reference Data **31**: 387.

Performance evaluation of a ground source heat pump system based on ANN and ANFIS models

Weijuan SUN [a], Pingfang HU[a,*], Fei Lei[a], Na Zhu[a], Jiangning Zhang[a]

[a]Huazhong University of Science and Technology, Wuhan 430074, P. R. China

Abstract: The aim of this work is to calculate the heat pump coefficient of performance (COP) and the system COP of a ground source heat pump (GSHP) system based on an artificial neural network (ANN) model and (adaptive neuro-fuzzy inference system (ANFIS) model. In order to get the training and test data, a GSHP system of an office building in China was monitored in the summer of 2013, and the system uses a GSHP unit and a water chiller unit as the cooling source. To calculate the heat pump COP, the water temperature entering/exiting the condenser and the water temperature entering/exiting the evaporator of the GSHP unit were used as input layer of ANN and ANFIS models. While six parameters including the water temperature entering/exiting the condensers of two units and the water temperature entering/exiting the user side were used as the input layer. Some statistical methods were adopted to evaluate the accuracy of the calculation models. The results show that the models provide high accuracy and reliability for calculating performance indexes of GSHP system with fewer parameters.

Keywords: Artificial neural network ANFIS Ground source heat pump COP

1. Introduction

GSHP uses the low grade energy stored in the shallow level of the earth to heat or cool the building. It has been applied to real projects widely these years thanks to its high energy efficiency, energy-saving, environment-friendly and the ability to use the low level energy [1]. Calculation of the real-time evaluation indexes is important for system evaluation, system optimization and fault diagnosis of the GSHP system. But for most of the GSHP projects which have been put in operation, the monitoring system has't been installed. It is hard to get all the parameters needed when we calculate the evaluate indexes such as coefficient of performance（COP） because of the lack of the measuring device in the system or the diagnosis of the sensors or other reasons.

Some authors have tried calculating the evaluation indexes of some system or equipment with low cost parameters while ANN and ANFIS are used frequently in the researches. Artificial neural network is an information processing idea that is inspired by the way of biological nervous systems, such as the brain, processing information[2]. It can tackle complex problems in actual situations with the advantages of of learning ability, memory simulating and nonlinear approximation. ANFIS is created combining neural networks and fuzzy models, it has the advantages of the fuzzy processing, self learning and the nonlinear approximation.

H.M. Ertunc calculated the winter COP of a horizontal GSHP based on ANN model using the

*Corresponding author. Tel: +86 27 87792165-415; fax: +86 278792101; E-mail address: pingfanghu21@163.com, pingfanghu@hust.edu.cn (P.Hu)

air temperature leaving/entering the condenser, the water temperature leaving/entering the evaporator and the ground temperature as the input layer parameters[3]. Haslinda [4] built an ANN model for a standard air-conditioning system of a passenger car to calculate the cooling

Nomenclature

ρ	water density (kg/m^3)
c	specific heat capacity of water ($kJ/(kg \cdot K)$)
m_g	water mass flow on the evaporator side of the GSHP unit (m^3/h)
m_{ls}	water mass flow on the load side of air conditioning system (m^3/h)
$T_{gevap,i}$	evaporator inlet water temperature of the GSHP unit (^{o}C)
$T_{gevap,o}$	evaporator out water temperature of the GSHP unit (^{o}C)
$T_{gcond,i}$	condenser inlet water temperature of the GSHP unit (^{o}C)
$T_{gcond,o}$	condenser outlet water temperature of the GSHP unit (^{o}C)
$T_{cevap,i}$	evaporator inlet water temperature of the chilled water unit (^{o}C)
$T_{cevap,o}$	evaporator out water temperature of the chilled water unit (^{o}C)
$T_{ccond,i}$	condenser inlet water temperature of the chilled water unit (^{o}C)
$T_{ccond,o}$	condenser outlet water temperature of the chilled water unit (^{o}C)
W_g	power consumed by the GSHP unit (W)
W_c	power consumed by the chilled water unit (W)
$W_{l,p}$	power consumed by the water pump on load side (W)
$W_{gss,p}$	power consumed by the water pump on ground source side (W)

$W_{cts,p}$ power consumed by the water pump on cooling tower side (W)

$T_{l,i}$ inlet water temperature on the load side (W）

$T_{l,o}$ outlet water temperature on the load side (W）

capacity, compressor power input and the coefficient of performance (COP) of the automotive air-conditioning (AAC) system. The input layer parameters of ANN model are the compressor speed, air temperature at evaporator inlet, air temperature at condenser inletand air velocity at evaporator inlet. Arzu S [5] calculated the COP of a single stage vapor compression refrigeration system with inner heat exchanger based on ANN model and ANFIS model using the evaporator temperature, condenser temperature, sub cooling temperature, superheating temperature and cooling capacity. ZHAO Jing [6,7] made a post evaluation before the renovation of a central air-conditioning system of a large-scale public building and a prediction evaluation after the retrofit scheme is determined. The prediction evaluation model was built based on Back-Propagation Artificial Neural Network by the use of MATLAB Neural Network Toolbox.

ANN and ANFIS are applied in many fields. In the HVAC area, they have been used in load prediction, energy management and controlling system, fault diagnosis, system identification and other aspects [8].The aim of this thesis is to calculate the heat pump COP and the system COP of the GSHP based on ANN and ANFIS model through a low number set of data. For getting the training and test data, a GSHP system of an office building in China was tested in the summer of 2013.

2. System description and monitoring data analysis

2.1 System description

In this study, a GSHP system of an office building was monitored for a cooling season in summer of 2013. The office building was located in Shaoxing China. The cooling load and heating load of the office building (air conditioning area: 7320 m^2) were 618 kW and 403kW at design conditions, respectively. The schematic diagram of the air conditioning system for cooling mode is illustrated in Fig1. Two heat pumps were were selected as the cooling source according to the heating and cooling load, one is a total heat recovery GSHP unit (cooling capacity: 315kW; heating capacity: 343.7kW; COP: 5.78 and 4.48 in cooling season and heating season respectively) and the other on is a water chiller unit (cooling capacity: 307kW; heating capacity: 326kW; COP: 5.45 and 4.32 in cooling season and heating season respectively). Two units can run simultaneously or run by itself depending on the requirement. The total recovery GCHP unit supplies domestic hot water. The total heat recovery GSHP unit rejected heat to the ground by means of buried pipes while the water chiller unit dissipate heat through cooling tower.

Moreover, the air conditioning system includes three water pumps on source side, a water pump on cooling tower side, three water pimps on user side, two hot water pumps and a heat insulating water tank. 140 boreholes were designed. The drilling diameter, borehole spacing and the borehole depth were 150mm, 4m and 50m respectively. Single-U, double-U and three-U heat exchangers were selected and the outer diameter of pipe is 32mm.

The water return from air conditioning terminal releases heat to the refrigerating fluid in the evaporator of the GSHP unit or the water chiller unit and then goes back to the air conditioning terminal to cooling the house. The circulating water from the buried pipes extract the heat from the refrigerating fluid in the condenser of the GSHP unit and reject the heat to ground. The cooling water from the cooling tower absorb heat from the refrigerating fluid in the condenser of the water chilled unit and is cooled by cooling tower.

Some measuring devices were installed in the system to get running data. The water temperatures entering and existing condenser , evaporator and the air conditioning terminal were measured by temperature sensors. The flow rate of water entering and existing condenser , evaporator and the air conditioning terminal were measured by flow sensors. Both the temperature sensors and flow sensors were installed with wireless transmitting module which can transmit the data collected. Wireless smart electric meters were used to measure the power consumed by cooling tower, GSHP unit, water chilled unit and water pumps, the data also transmitted by wareless transmitting module. The wireless signal acquisition module collect data from wireless transmitting module and supply them to the local sever through internet or local area network. Then we can get the data from the monitoring platform of local sever.

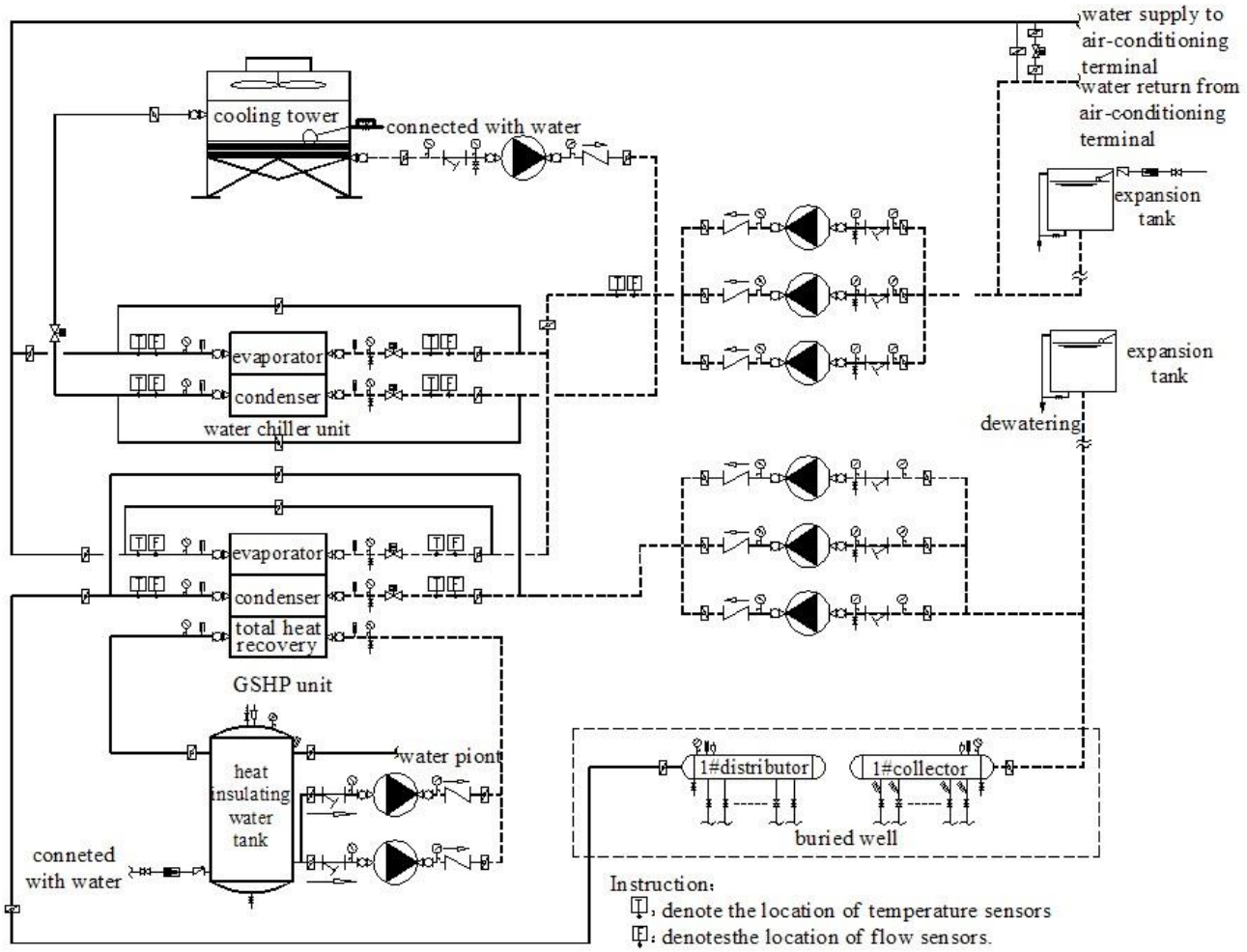

Fig.1. Schematic diagram of the air conditioning system for cooling mode

2.2 Monitoring data analysis

The GSHP in Shaoxing was monitored every 15 minutes during normal office hours from June 1st to June 27st, 2013. We had obtained 729 data patterns total in these 27 days. The COP of GSHP unit was obtained by Eq.(1) and the COP_s of the GSHP air conditioning system was calculated by Eq.(2) to verify the results from ANN and ANFIS approach.

$$COP = \frac{Q_{g,\ cl}}{W_g} \tag{1}$$

Where the cooling capacity of the GSHP unit $Q_{g,cl}$ is defined as Eq.(2)

$$Q_{g,\ cl} = \rho c m_g (T_{gevap,i} - T_{gevap,o}) \tag{2}$$

$$COP_s = \frac{Q_s}{W_g + W_c + \sum W_{i,p}} \tag{3}$$

Where Q_s is the cooling capacity of the airconditioning system defined as Eq.(4) and $\sum W_{i,p}$ is the total power consumed by all the water pump defined as Eq.(5)

$$Q_s = \rho c m_{ls} (T_{ls,o} - T_{ls,i}) \tag{4}$$

$$\sum W_{i,p} = W_{ls,p} + W_{gss,p} + W_{cts,p} \tag{5}$$

During the monitoring period, the GSHP unit was running all the time but the chilled water unit was intermittent running. The measured running data values of the GSHP air conditioning system are given in Figs. 2-4. Fig.2 shows the variation of $T_{gevap,i}$, $T_{gevap,o}$, $T_{gcond,i}$ and $T_{gcond,o}$ of the GSHP unit with its COP. We can see that $T_{gevap,i}$, $T_{gevap,o}$, $T_{gcond,i}$ and $T_{gcond,o}$ variate in 9.6~17.1ºC, 8.0~14.3ºC, 28.9~40.7ºC and 25.7~37.2ºC. COP of the GSHP unit is between 2.5~5.4. The mean difference of $T_{gevap,i}$ and $T_{gevap,o}$ is 2.33ºC , for $T_{gcond,i}$ and $T_{gcond,o}$, it is 2.72ºC. COP of the GSHP unit shows an opposite direction of changing trend approximately with the changing trend of $T_{gcond,i}$ and $T_{gcond,o}$. It indicates that in a certain range, the lower of the output water temperature of ground source well, the higher of GSHP unit COP which means the better operation performance of the GSHP unit. Fig. 3 hows the variation of $T_{cevap,i}$, $T_{cevap,o}$, $T_{ccond,i}$, $T_{ccond,o}$ and W_c of the chilled water unit. The power consumed by the chilled water unit means that the running state of this unit is off. Fig.4 shows the variation of $T_{l,i}$, $T_{l,o}$ and the system COP_s. We can see

that $T_{l,i}$ and $T_{l,o}$ variate in 8.2~14.3ºC, 9.5~17.0ºC. The system COP_s is between 1.3~4.0. The mean difference of $T_{l,i}$ and $T_{l,o}$ is 2.1ºC.

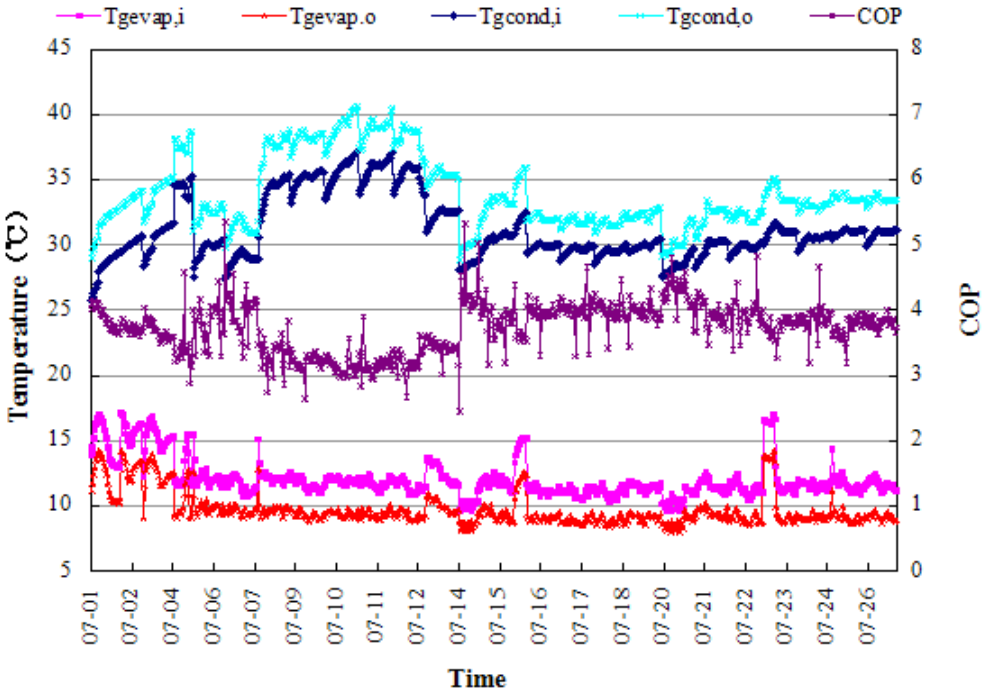

Fig.2. The variation of water temperature, COP of GSHP unit

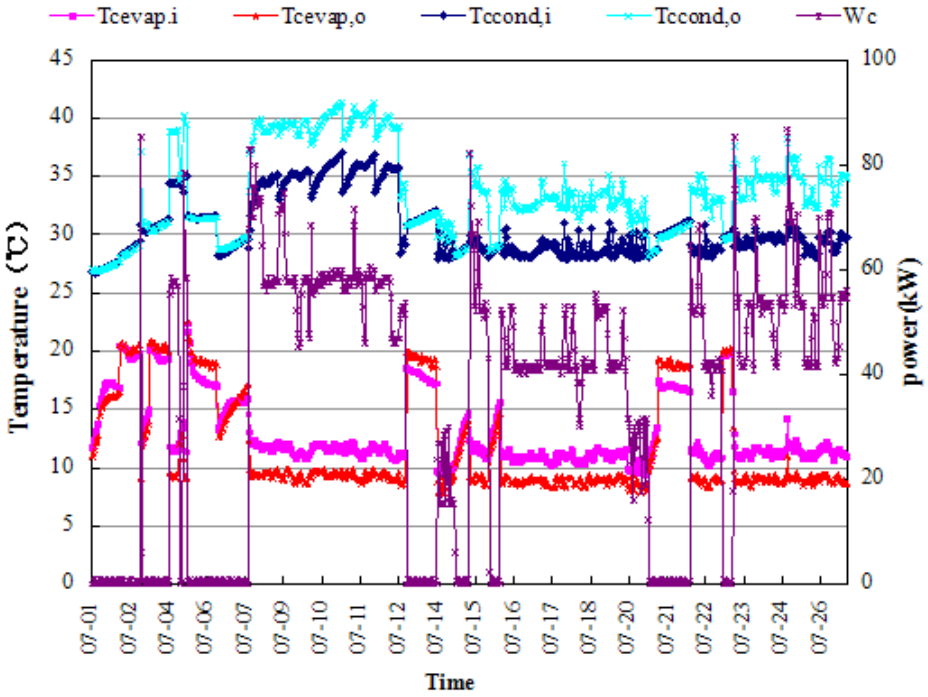

Fig.3. The variation of water temperature, power consumption of chilled water unit

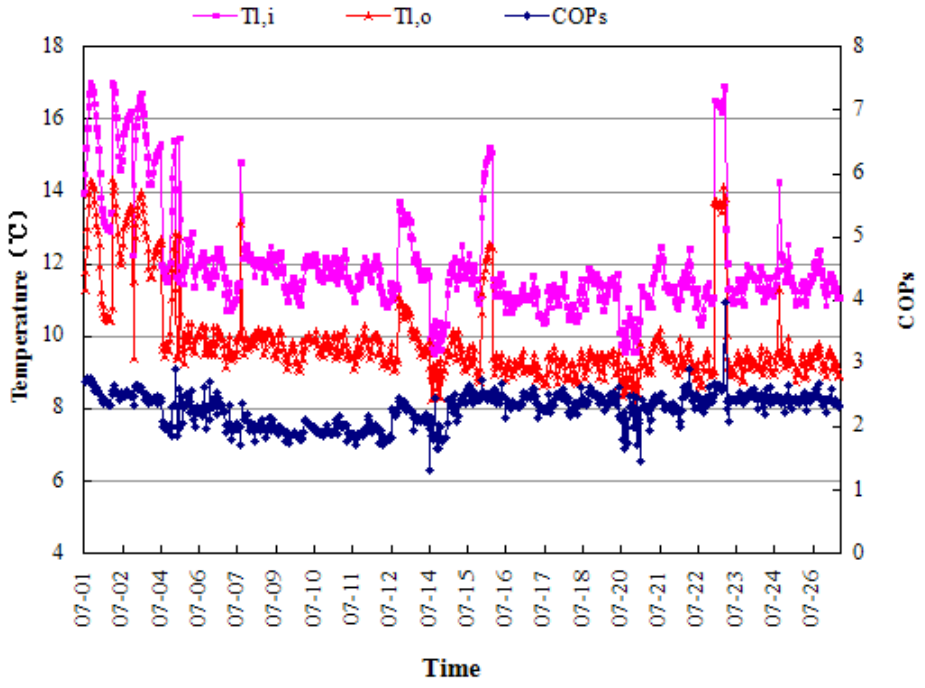

Fig.4. The variation of water temperature on the load side and the system COP_s

3. Artificial neural network (ANN) and adaptive neuro-fuzzy inference system (ANFIS)

3.1 Artificial neural network (ANN)

ANN is interconnected by lots of joins (or named as neurons) which are nonlinear information processing units with multiple inputs and single output. Every point stands for an activation function which can be defined in many ways such as threshold function, sigmoid function and hyperbolic tangent function [9].

ANN operates much as a “black box” model, requiring no detailed information about the system. On the other hand, they learn the relationship between the input and the output based on the training data [10]. There are numerous algorithms available for training neural network models. The most popular one is the back propagation algorithm, which has different variants. Standard back propagation is a gradient descent algorithm.

A typical BP artificial neural network structure is illustrated by Fig.4. It includes three layers: input layer, hidden layer and the output layer. The input layer receives the input signals by weights, and transfers the processed signal to the hidden layer; the hidden layer is inner processing layer which converses the information, it can be classified as single hidden layer and multiple hidden layer, the last hidden layer exports information to the output layer. After a further processing, a forward propagation learning process is completed. The output layer exports the information processing results, but if the actual output is not agree with the expected result, ANN will steps into the mean square error (MSE) back propagation stage. The cycle of information forward propagation and error back propagation is a adjustment process of each layer’ weights, it is also the learning process of ANN. The process won’t stop until the MSE decreases to an acceptable level or the training epochs are reached.

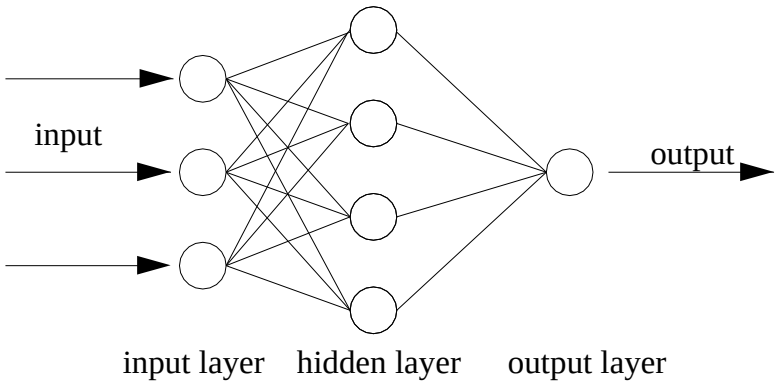

Fig.5. A typical BP artificial neural network structure

3.2 Adaptive neuro-fuzzy inference system (ANFIS)

The Adaptive neuro-fuzzy inference system (ANFIS) was came up with by Jang Roger, its function is similar with the first order Sugeno fuzzy inference system. ANFIS combined the self-learning ability of neural network and the advantage of fuzzy inference together, being able to approximating any linear or nonlinear system [33]. ANFIS is based on data sets rather than experience or intuitions, the membership function and the fuzzy rule are obtained by learning with the data sets. This is important for the complex system or the system whose properties are not realized fully by people [34].

The typical structure of ANFIS is illustrated by Fig.5 [35], the membership functions of one layer are same (set the output of the layer of i as $O_{l,i}$), x, y is the input of the system and f is the output.

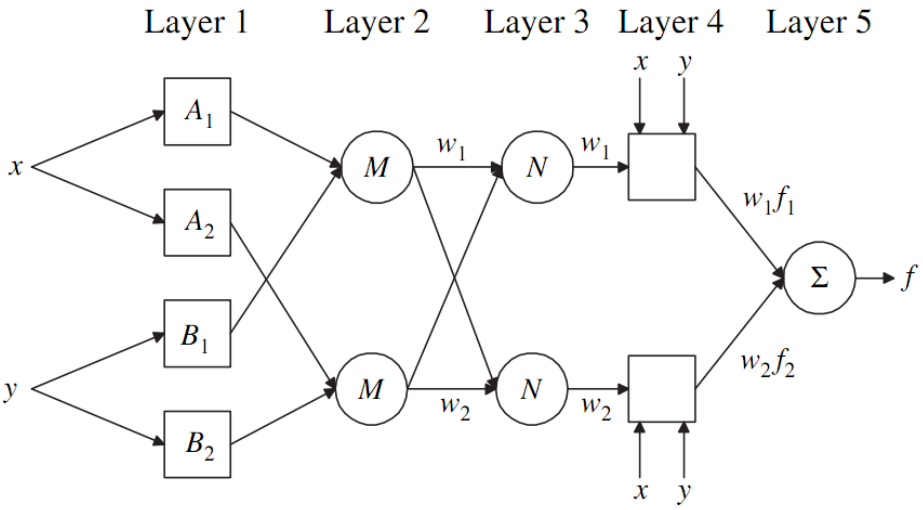

Fig.6. The structure of a typical ANFIS model

The first layer: the input signals are fuzzified by the nodes in this layer.

$$O_{1,i} = \mu_{Ai}(x), i = 1,2 \; O_{1,i} = \mu_{Bj-2}(y), i = 3,4 \tag{5}$$

Where A/B are fuzzy sets, $O_{l,i}$ is the membership function of the fuzzy sets, the default is bell-shape.

The second layer: the nodes in this layer is to calculate the fitness of each rules,

$$O_{2,i} = \omega = \mu_{Ai}(x)\mu_{Bi}(y), i = 1,2 \tag{6}$$

The third layer: normalize the fitness of each rules.

$$O_{3,i} = \overline{\omega} = \omega/(\omega_1 + \omega_2), i = 1,2 \tag{7}$$

The fourth layer: calculate the output of each rules

$$O_{4,i} = \overline{\omega} f_i = \overline{\omega}(p_i x + q_i y + r_i), i = 1,2 \tag{8}$$

The fifth layer: there is only one node in this layer which can calculate the final output of the system.

$$O_{5,i} = y = \sum_i \overline{\omega} f_i = \frac{\sum_i \overline{\omega} f_i}{\sum_i \omega}, i = 1,2 \tag{9}$$

A hybrid algorithm which combined the black propagation and the test squares method together is adopted to train ANFIS, it can help the system to model the data sets.

4. ANN and ANFIS models for case study

The ANN and ANFIS models for calculating the GSHP unit COP is illustrated in Fig.6. The ANN and ANFIS have the same parameters $T_{gevap,i}$, $T_{gevap,o}$, $T_{gcond,i}$ and $T_{gcond,o}$ in the put layer and the same parameters COP in the output layer. The ANN and ANFIS models for calculating the system COP_s is illustrated in Fig.7. The ANN and ANFIS have the same parameters $T_{gcond,i}$, $T_{gcond,o}$, $T_{ccond,i}$ and $T_{ccond,o}$ in the put layer and the same parameters COP_s in the output layer. $T_{ccond,i}$ and $T_{ccond,o}$ values are set as 0 when the running state of the chilled water unit is off which means these values make no difference to COP_s.

Both for the models for calculating the GSHP unit COP and the system COP, 424 data patterns from July 1st to July 16st selected from the total 729 data patterns were used for training the ANN model, the total data patterns included 1030 patterns from July 1st to July 28st were used for testing the trained ANN model.

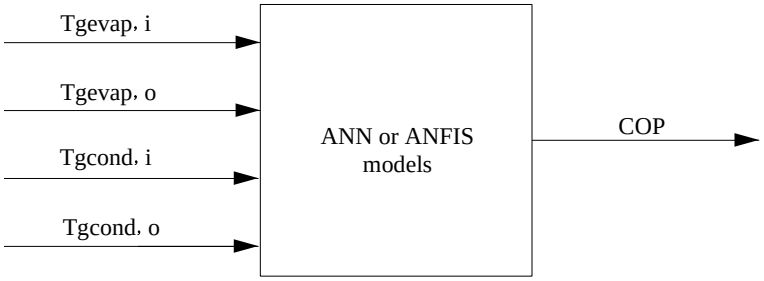

Fig.7. ANN and ANFIS models for calculating GSHP unit COP

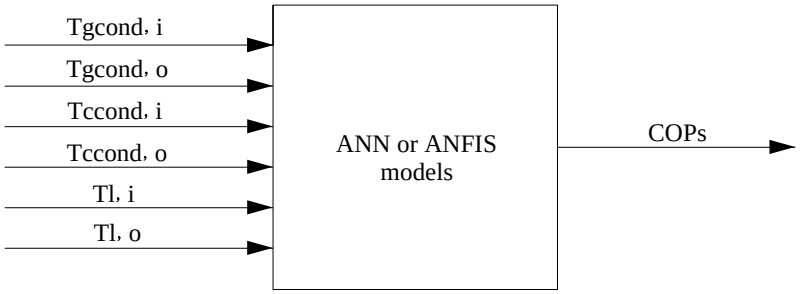

Fig.8. ANN and ANFIS models for calculating system COP_s

$$m = \sqrt{n+l} + \alpha \tag{9}$$

$$m = \sqrt{nl} \tag{10}$$

$$m = \frac{1}{2}(n+l) + \sqrt{t} \tag{11}$$

Where m is the number of neurons on hidden layer; n is the number of neurons on input layer; l is the number of neurons on output layer; α is a constant value between 0~10 and t is the number of training data patterns. For ANFIS model, three membership functions named Gaussmf are chosen, the training epochs is 600, and the MSE is 0, other parameters are default value. ANN and ANFIS models were programmed in the MATLAB 7.0 environment.

The main training program of ANN model is as following:

```
[Input,mintraininput,maxtraininput] = premnmx(traininput);    % Normalize the input data
net=newff(minmax(Input),[14,1],{'tansig','purelin'},'trainlm');    % Build an ANN
net.trainParam.epochs=5000;    % Set the training epochs as 5000
```

net.trainParam.goal=1E-06; % The training goal is 1E-07

[net,tr]=train(net,Input,t); % Train the net

save net % Save the net

The main testing program of ANN model is as following:

[Testinput] = tramnmx(testinput,mintraininput,maxtraininput); % Normalize the input data

load net % Load the trained net

output=sim(net,Testinput); % Get the output by the net

The main program of ANFIS model is as following:

fismat=genfis1(trndata,[numMFS1numMFS2numMFS3],char(mfType1,mfType2,mfType3),'constant'); % generate the initial ANFIS using mesh cutting method

[Fis, error, stepsize, chkFis, chkEr]=anfis(trnData,fisMat,trnOpt,disOpt,chkData); % train the model based on training data

anfis_cop=evalfis(chkdata1,chkFis); % input the testing data to the trained ANFIS and get the output we need

Some statistical methods, absolute error ε, relative error δ, root-mean squared (RMS), absolute fraction of variance (R^2) were adopted to validate the model, they were obtained by Eqs(12)-(15) respectively. The smaller of absolute error ε,root-mean squared (RMS)and relative error δ, the more accurate of the ANN model. Absolute fraction of variance (R^2) was in the range of (0~1), value of 1 denotes perfect model.

$$\varepsilon = x_{calculate,m} - x_{actual,m} \tag{12}$$

$$\delta = \frac{x_{calculate,m} - x_{actual,m}}{x_{actual,m}} \tag{13}$$

$$RMS = \sqrt{\frac{\sum_{m=1}^{n}(x_{calculate,m} - x_{actual,m})^2}{n}} \tag{14}$$

$$R^2 = 1 - \frac{\sum_{m=1}^{n}(x_{calculate,m} - x_{actual,m})^2}{\sum_{m=1}^{n}(x_{actual,m})^2} \tag{15}$$

Where $x_{calculate,m}$ is the value calculated byANN models; $x_{actual,m}$ is the actual value; n is the number of data patterns.

5. **Results and discussions**

Suitable ANN and ANFIS models were developed by trail and error. Figs. 8-9 are the plots of GSHP COP calculated by the ANN and ANFIS model vs. the corresponding values obtained from experiments respectively. Figs. 10-11 are the plots of system COP_s calculated by the ANN and ANFIS model vs. the corresponding values obtained from experiments respectively. And for the system COP_s the statistical values are showed in Table 2.

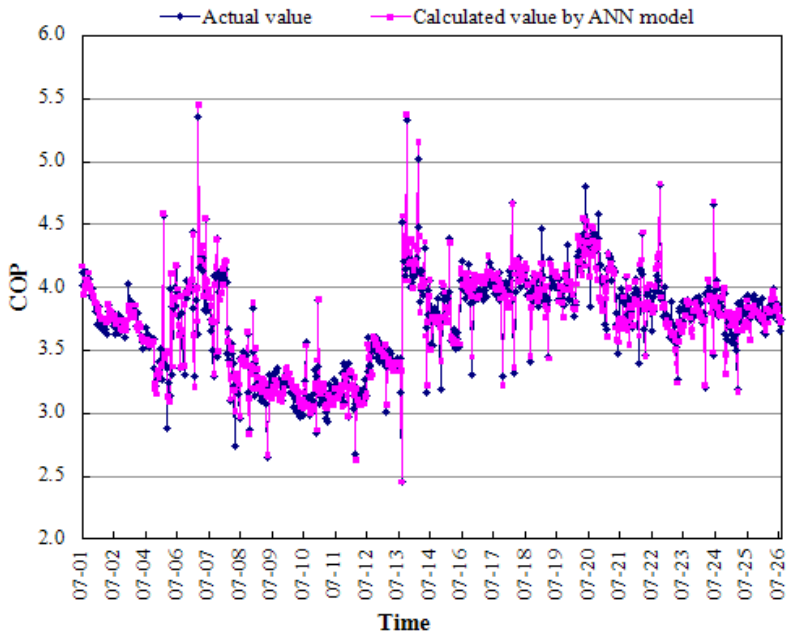

Fig.9. Comparison of actual and ANN calculated values of the GSHP COP

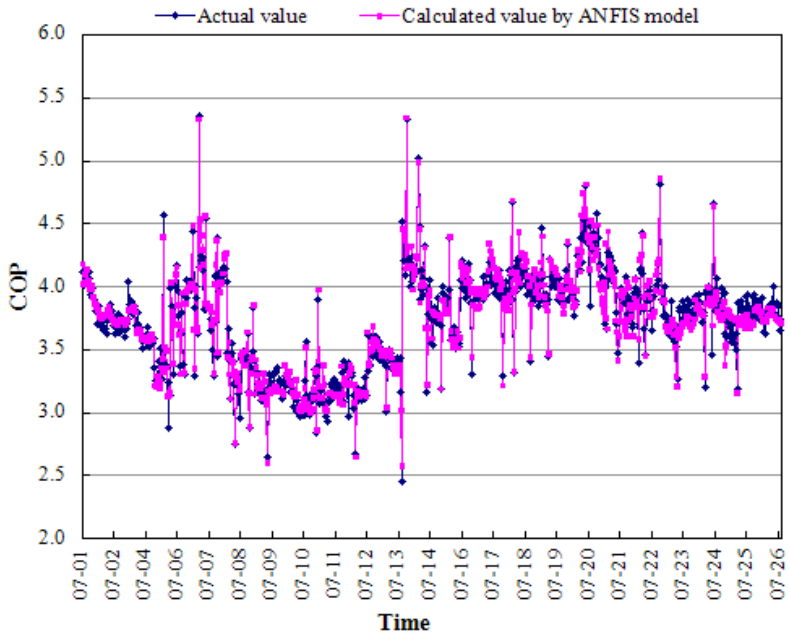

Fig.10. Comparison of actual and ANFIS calculated values of the GSHP COP

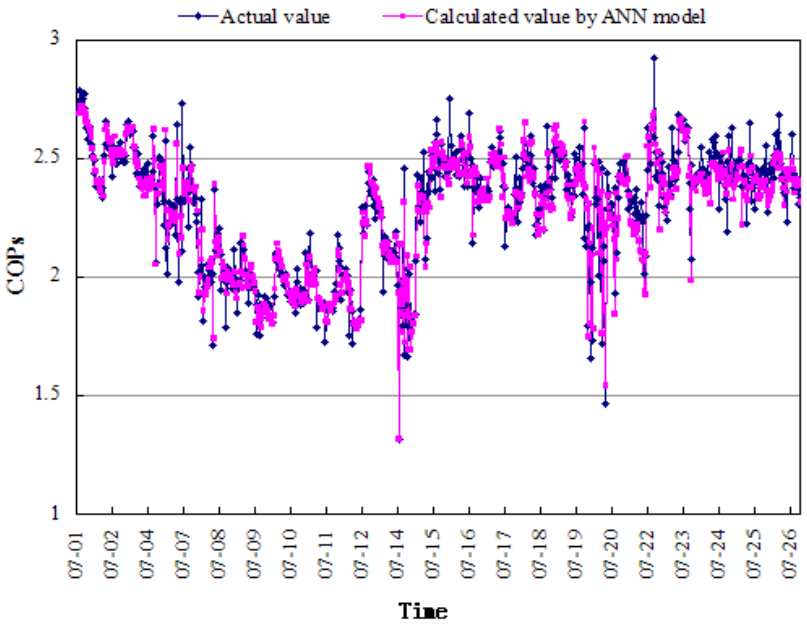

Fig.11. Comparison of actual and ANN calculated values of the system COP_s

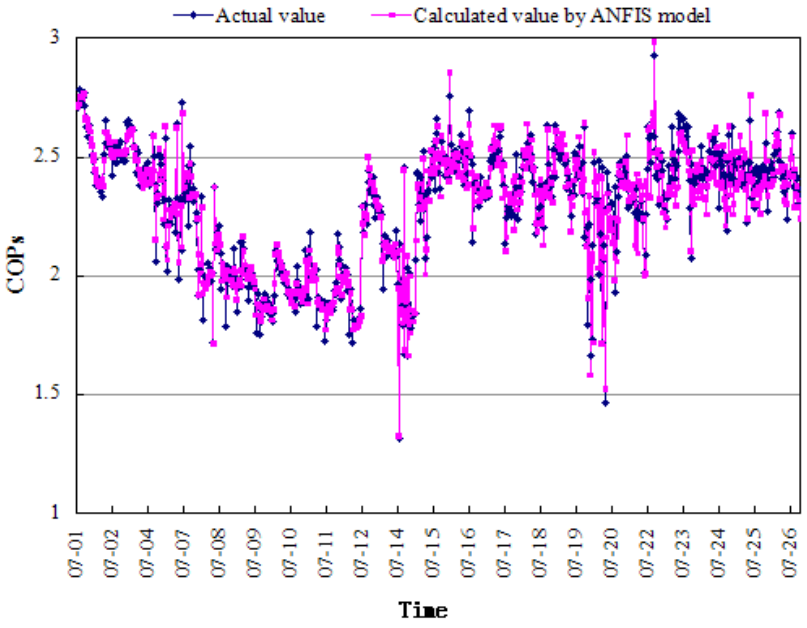

Fig.11. Comparison of actual and ANFIS calculated values of the system COP_s

Table 1

Comparison of ANN and ANFIS statistical values for calculated GSHP COP

	RMS	R^2	ε	δ
ANN	0.09943	0.99929	-0.29~0.26	-9%~7%
ANFIS	0.09601	0.99934	-0.28~0.32	-10%~9%

Table 1

Comparison of ANN and ANFIS statistical values for calculated system COP_s

	RMS	R2	ε	δ
ANN	0.06475	0.99920	-0.21~0.27	-9.8%~10%
ANFIS	0.05524	0.99942	-0.20~0.18	-9%~7.8%

Figs. 8-11 show that calculated values by ANN and ANFIS models agree well with the actual values. Once been trained, the models can calculate the GSHP COP and the system COP_s in high precision just based on fewer parameters. What's more, the models have high calculation accuracy not only for the trained data patterns but also for the untrained data patterns which shows they have an excellent capability of generalization.

For calculating the GSHP unit COP, the properties of the ANN and ANFIS models which are evaluated by statistical values are tabulated in Table 1. The relative error δ of ANN models are all within 10% and the relative error δ of 94.2% data patterns are within 5%. And for ANFIS models, the relative error δ of all the data patterns are within 10% too and of 92.% data patterns are within 5%. For calculating the system COP_s, the properties of the ANN and ANFIS models which are evaluated by statistical values are tabulated in Table 2. The relative error δ of all the data patterns are within 10% for both ANN model and ANFIS model. The relative error δ of 89.6% data patterns are within 5% for both ANN model and it is 94.9% for ANFIS model. The relative errors are all within the acceptable limits.

From Table 1 and 2 we can see that ANN and ANFIS models both have a good calculation accuracy. the relative error δ and absolute error ε of them are all very low. Whether for the heat pump COP or for the system COP_s, ANFIS model always have a higher accuracy than ANN models, the absolute error, the relative error and RMS are smaller, R^2 is closer to1, it proves that the ANFIS models is more appropriate to calculate the GSHP COP and the system COP_s based on fewer parameters.

6. Conclusion

In this thesis an ANN and an ANFIS models were built based on fewer parameters to calculate the important performance evaluation indexes: the GSHP COP and system COP of the GSHP system. To obtain the training and test data for the calculation model, a GSHP air conditioning system were monitored in a cooling season. One GSHP unit and a chilled water unit connect in parallel in the system. For the ANN and ANFIS models for calculating the GSHP COP, the parameters in the input layer are: the evaporator inlet and outlet water temperature of the GSHP unit and the condenser inlet and outlet water temperature of the GSHP unit. For the ANN and ANFIS models calculating the system COP_s, six parameters are in the input layer: the condenser inlet and

outlet water temperature of the GSHP unit, the the condenser inlet and outlet water temperature of the chilled water unit and the inlet and outlet water temperature on the load side of the system.

424 data patterns are used as training data and all the data patterns (729 data patterns) are used as test data. The trained models can calculate the performance indexes of the GSHP system. Some statistical methods, absolute error ε, relative error δ, root-mean squared (RMS), absolute fraction of variance (R^2) were adopted to validate the model. The results show that the ANN and ANFIS models are capable to calculate the GSHP unit COP and the system COP_s with a good accuracy based on fewer parameters and ANFIS model shows better performance.

Acknowledgments

The authors would like to acknowledge the supports from the National Natural Science Foundation of China (Grant NO. 51078160)

References

[1] N.R DIAO and Z.H FANG, "Ground coupled heat pump technology," Beijing: *Higher Education Press*.2006:4-6.

[2] Z.X GE and Z.Q SUN, "Neural network theory and MATLAB 2007 realization," Beijing: Industry Publishing House, 2007.

[3] H. Esen, M. Inalli, A. Sengur, and M. Esen, "Forecasting of a ground-coupled heat ump performance using neural networks with statistical data weighting pre-processing," *International Journal of Thermal Sciences*, vol. 47, pp. 431-441, 2008.

[4] H. M. Kamar, R. Ahmad, N. B. Kamsah, and A. F. Mohamad Mustafa, "Artificial neural networks for automotive air-conditioning systems performance prediction," *Applied Thermal Engineering*, vol. 50, pp. 63-70, 2013-01-10 2013.

[5] Ş. Şahin, "Performance analysis of single-stage refrigeration system with internal heat exchanger using neural network and neuro-fuzzy," *Renewable Energy*, vol. 36, pp. 2747-2752, 2011.

[6] C. Chang, J. Zhao and N. Zhu, "Energy saving effect prediction and post evaluation of air-conditioning system in public buildings," *Energy and Buildings*, vol. 43, pp. 3243-3249, 2011.

[7] J ZHAO, "Technological system on energy efficiency diagnosis and evaluation for large-scale public buildings,": Tianjin University,2010.

[8] Y.Y LI and Y.J WANG, "Artificial neural network (ANN) in HVAC area," *HVAC*. pp. 38-41, 2001.

[9] C.H DONG," MATLAB neural network and application," Beijing: National Defense Industry Press, 2005.

[10] S. A. Kalogirou, "Applications of artificial neural networks in energy systems," *Energy Conversion and Management*, vol. 40, pp. 1073-1087, 1999.

[11] J. S. R. Jang, "ANFIS: adaptive-network-based fuzzy inference system," *Systems, Man and Cybernetics, IEEE Transactions on*, vol. 23, pp. 665-685, 1993-01-01 1993.

[12] X.Y LIU and H.X PAN, "Realization of Self- adaptive Fuzzy- neural Control System Based on MATLAB," Mechanical Engineering & Automation pp. 162-164, 2010.

[13] Z.X ZHANG, C.Z SUN and (Japan) E.MIZIZUTANI, "Neural-fuzzy and soft computing," ZHANG P.A,GAO C.H. Xi'an: Xi'an Jiaotong University Press,2006,237-259.

Comfort demand leading the optimization of energy supply from the Smart Grid

Wim Zeiler, Tom Thomassen, Gert Boxem, Kennedy Aduda
TU Eindhoven Faculty of the Built Environment
Eindhoven, Netherlands
w.zeiler@bwk.tue.nl

Abstract
The Smart Grid is being developed to cope with fluctuations in energy generation from different energy sources. To better match energy demand and energy supply and to achieve improved overall efficiency, the process control of the energy infrastructure within buildings also needs to become smart. Therefore it is necessary to measure and develop new control strategies for the major energy consumers like Air Handlings Unit of the Heating Ventilation and Air Conditioning system with its ventilators. This process control of the energy demand on building level must be in the future in interaction with the energy supply by the Smart Grid as well as the outdoor environment (solar energy and outside temperature), but under strict conditions for a healthy and comfortable indoor environment. In the last year experiments were conducted in an office building to get insight into different process control strategies in Building Energy Management Systems that incorporate Smart Grid interaction and offers possibilities for energy reduction while maintaining the required comfort of occupants. Initial results are presented regarding control strategies which are flexible enough to cope with the dynamic demands from the user and at the same time allow the use of economic benefits of the Smart Grid.

Keywords; Smart grid, energy management, BEMS.

INTRODUCTION

In Europe the built environment accounts for nearly 40% of the total energy use (EIA 2011). Most of this energy (nearly 87% for non-residential) is used for building systems with the goal of providing comfort for the building occupants (Opstelten et al 2007). Due to unintended use and inadequate building management, 85% of buildings do not function properly (Elkhuizen and Rooijackers 2008). Energy use in the built environment can be reduced by improved building design and energy management during lifecycle without compromising the desired indoor comfort of the users. Energy management is necessary to reduce energy usage and optimize supply. This can be achieved by integrated management of energy flows in buildings (Kyung et al 2011(Georgievski et al 2011). It is important to look at the energy demand and the interaction with the energy grid, integrating the communications with the building systems in and around the building, while keeping occupants comfort primodal. Recent initiatives to upgrade the existing power grid to the so called 'Smart Grid' (SG) requires a transition in the distribution part of the grid: turning it from a passive system into an active system. A key characteristic of the smart grid is its multi-directional flow of power and information and hence transformation of the demand side management to demand side integration philosophy at low level voltage. The local generated energy can be in mismatch between demand and supply resulting in the desired increase of buffer capacity(Sapurto et al. 2012). Mostly in the case of heat, storage is less of a problem compared to electrical energy. In most cases the surplus in electrical generated energy is fed back to the grid. This development introduces a new challenge for the grid, namely, possible changing energy flow direction at lower grid levels due to the feed in of renewable generated electrical energy (Slootweg et al., 2011). This implies that building must also provide service to the electrical smart grid in as much as it is also serviced by the later.
Current grid management maintains balance by increasing or decreasing centralised power generation based on demand side behaviour or requirements. With the expected increase of renewable generated energy in the total generated energy mix, this introduces a stochastic behaviour, which necessitates for a change in the the management of the grid
Slootweg et al., 2011 statedthe increase in decentralised active loads such as, micro Combined Heat and Power (μCHP), Electrical-vehicles, heat pumps which can participate in the energy management and possibly react on grid requests or economic stimulations, compared to the passive loads connected to the grid can be a solution for future grid management. Active loads can request or in some cases even deliver energy to the grid and schedule their demand or even change their characteristics online.
In order to compensate active loads, there has to be an economic compensation. A classic example of economic stimulation is the double tariff structure, evoking households to shift their energy use to economic stimulated period which is the most convenient period for the grid. For now the more flexible tariff structures are still in experimental phase. The mix of connected active and passive loads will keep changing in future even as the mix of electricity

generators. The Smart Grid (SG) is required to be the solution to all mentioned possible challenges managing electrical energy production, distribution, buffering, and consumption matching supply and demand making use of the available system flexibilities (Slootweg et al. 2011). Grid management, control, voltage management, power quality, and the need to modify the system security will change due to all mentioned development. New policies and contracting with flexible tariff structures are possibilities which are being investigated.
The SG incorporates current physical electrical grid infrastructure integrated with Information and Communications Technology (ICT) in grid components, and a communication network to enable energy management. (Wang et al., 2011) The real 'Smartness' of the SG is integration of multiple functionalities to guarantee properties including; reliability, availability, stability, controllability, and security, and at the same time realise overall system optimisation. Functionalities boil down to energy management making use of the flexibilities of all grid elements connected. The purpose of energy management measures, should be to compensate surpluses and deficits in the network. Flexibility is the degree to which the pattern of consumption and generation can be influenced. In the systems view, this will lead to a better balanced and controlled network at all levels (Acevedo and Molinas 2012, Lo and Ansari 2011, Dave et al. 2011, Lopes et al. 2011).
In offices Building Management Systems (BMS), also known as Building Automation Systems (BAS), controls the HVAC systems to facilitate building operation. These BMS evolved over time with the addition of more and more systems, functionalities, and requirements. BMS with energy use reduction during life time as an extra goal, turned into Building Energy Management Systems (BEMS) (Choi et al. 2011) and (Han et al. 2011). The main goal of the BEMS is to fulfil the occupant comfort requirements while reducing energy consumption during building operations (Yang and Wang, 2011). The BEMS uses peak shaving and load shifting based on planning to reduce the energy consumption together with energy efficiency improvements of systems equipment and energy management strategies.

METHODOLOGY

To study the possibilities and restrictions using a Building Energy Management System(BEMS) for the information exchange between building and Smart Grid, a middle-out approach was chosen. This middle-out approach is from the interface towards the SG and towards the BEMS and focuses on the communication and interaction between the SG and the BEMS. This approach also deals with the actual comfort and energy demands of the user and optimization of the energy flows. In the process the user has the leading role by setting the desired inside climate conditions.

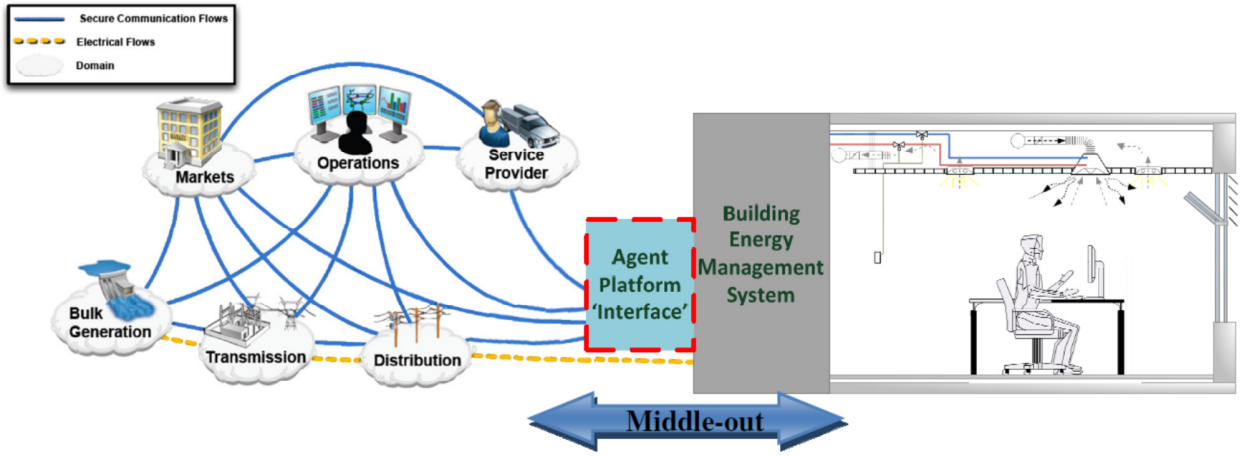

Figure 1: Middle-out approach from interface to building and Built Environment level.

The energy demand of buildings is related to the physics of the building, the environmental climate, and significantly to the specific control scenario for indoor environment and building operations. According to Robinson et al (2011) there has been no attemptto develop a general model predicting the probability of switching on or off the range of HVAC equipment, together with occupants' desired set point temperature, and how these choices depend on the range of key environmental stimuli. In addition, user's preferences are considered as a vital factor in deriving the appropriate control strategy (Yang and Wang 2011) .
The building systems control strategy rely on code defined occupant comfort ranges (Klein et al 2012) and operate according to fixed schedules and a constant occupancy. This is inefficient in their energy usage for maintaining

occupant comfort as they do not in-cooperate the effects of real occupant behaviour. Li et al (2012) identify a number of control strategies based on accurate building occupancy:

- Lower temperature demands in unoccupied areas. Zhang et al (2009) concluded that building energy reductions can be obtained when temperature was lower in winter period and higher in summer period;
- Maintaining lower ventilation rates in unoccupied areas; leading to less ventilation losses and building energy needed;
- Supplying airflow based on occupancy; two researches (Yang et al 2011; Sun et al., 2011) looked at dynamic airflows based on the CO_2 concentrations. Applying these strategies savings could be achieved of 15% to 56% found by Sun on the ventilation energy;
- Responding to dynamic heat loads on a timely manner; if a change of the occupancy is detected in real time, associated changes of internal heat loads can be calculated, HVAC systems can respond to these changes immediately, before the temperature varies to an extent that is detectable by thermostats.

For evaluating the effects of power management on thermal comfort and IAQ a case study building was used, a typical Dutch office building was selected for the experiments. Before starting the experiments, the building was analyzed and prepared for the experiments. This so called 'zero measurement' is used to identify aberrations in the building operation. The results of the test will also serve as reference for the experiments. After this it was experimented with different energy management scenarios to reduce building systems energy demand as service to the Smart Grid. An experiment to reduce the air-flow of the constant volume air handling unit system while staying within the comfort and IAQ boundary conditions are presented in this paper. The initial and reduced air-flow were measured together with the corresponding CO2 concentration and energy use with the goal to identify when and to what extent it was acceptable to reduce the air-flow.

The Case Study Office Building

The Office was built in 1992 and revised in 2009. It is a three story high building. Building characteristics:

- 3 floors;
- +/- 1400 m² floor space;
- +/- 48 fixed employees;
- 59 office desks;
- windows can be opened;
- solar shading devices;
- mainly shallow plan;
- office hours between: 7:00 and 18:00;
- working days: Monday – Friday.

Figure 2: Test case office building Kropman Breda.

The characteristics of the technical building equipment are:

- mechanical ventilation system;
- air handling unit of 15.000 m³/hour;
- heat recovery wheel (no recirculation of air);
- central cooling by three air supply group after coolers;
- central heating by air and two radiator groups;
- electrical steam humidifier.

The first floor was chosen for more detailed measurements because all the supply system groups were situated on the first floor (Figure), and the first floor was the most regularly occupied floor. Measurements used by the BMS to maintain a comfortable indoor environment were the outside temperature and the inside temperature of two rooms at the first floor. Positions of both measurements were indicated in the floor plan, see Fig. 3. In order to evaluate the indoor climate, additional measurements were done in the rooms on floor one. In each room the temperature, CO2

concentration, humidity and average airspeeds were measured during the project. The measurements were done in accordance to ISO 7726 (ISO, 1998) and the ASHRAE Performance Measurement Protocol (ASHRAE, 2010).

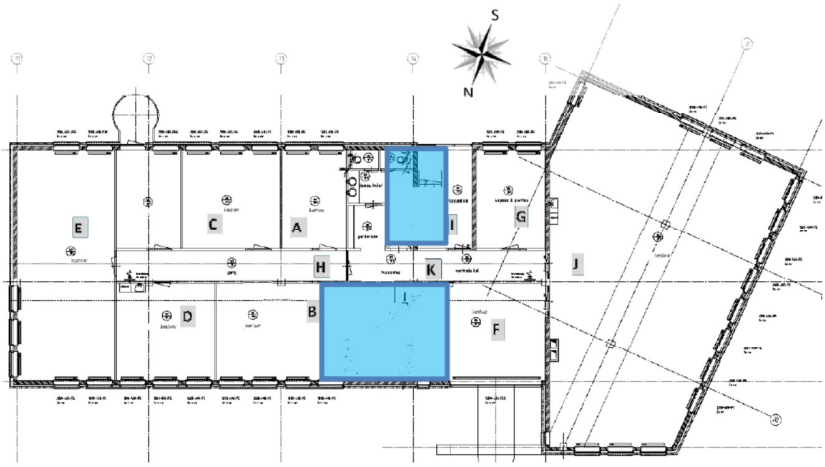

Figure 3: Floor plan first floor test case office building Kropman Breda

Room A has the external wall orientated on the south and is setup as a one person work
room. Room B has an external wall orientated on the north and is setup with multiple workplaces. During the measurement period a maximum of three people were present in the room while most of the measurement period not all of them worked simultaneous in the room due to holidays.

The office building is connected to a mid-voltage transformer stationIn the building the two main connections and main power systems connected were measured. Fig. 4 below illustrates major electricity load groups of the office building.

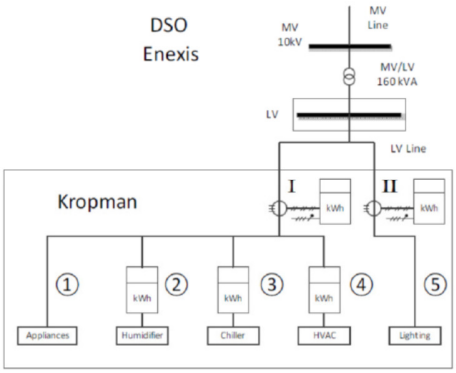

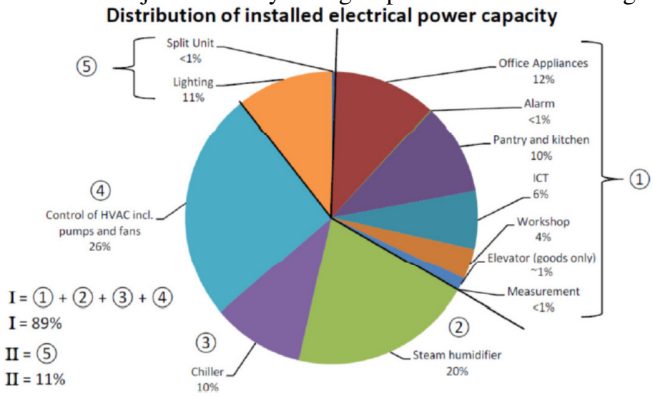

Figure 4: Abstract representation of the electrical connections from Mid Voltage grid to building and Figure 5. Distribution of installed electrical power capacity.

The distribution of installed electrical power capacities for both groups is presented in Fig. 5.. Notice the installed electrical power capacity for lighting is about 11% of the total. While the other power connection covers about 89% of the installed capacity. The HVAC control unit, controls the building systems by sending the control signals, supplies the electrical power to the fans and pumps, and facilitates the communication signals to the BAS and all connected components. In order to evaluate the characteristics of the energy use of the installed systems measurements were done:

- Main supply electrical energy measurements; main supply power group; main supply lighting group;
- Sub supply electrical energy measurements; electrical energy chiller; supply electrical energy humidifier; electrical energy systems control;
- Electrical energy use of lighting equipment; TL lighting of 7 rooms on the first floor; 2 down lighters of the two hallway on the first floor;
- Electrical energy use of appliances in 7 rooms; Personal Computers; laptops; laptop docking stations; monitors; small printers; phone chargers; water boiler; split unit;

RESULTS

Overall energy use

All the presented energy use profiles together form the total energy use profile as presented in Figure 6. Continuous main base load of the office building was approximately about 4 kWh/h represented in dark-blue (A Fig. 6). The maximum power use measured by the main connections I + II during the project was 36 kWh/h, represented in red (B Fig. 6). The main energy use profile during the day looks quite stable (C) while some profile of appliances can be clearly seen in the total profile. The early start scenarios are indicated in figure 6DThe Energy use profile of the Chiller isalso clearly visible (E) in Fig. 6.

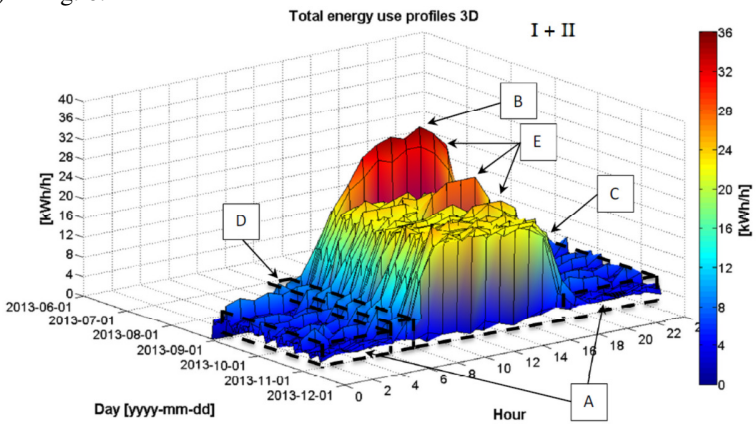

Figure 6:Total energy use profiles stacked by date.

Energy efficiency scenarios for the HVAC, lighting, and remaining have the biggest potential since the energy use of these groups are main components of the total consumption. Energy consumption by the chiller and humidifier are more dependent on the weather conditions and on the time of year:. Even with the chiller active (week 36), see Fig. 7, the lighting and remaining consist each of 30 % of the total energy consumption. Compared to the ratio of the installed capacities, see Fig. 5, where lighting only consists of 11% of the total installed capacity, the energy consumption of the lighting also has relative big share.

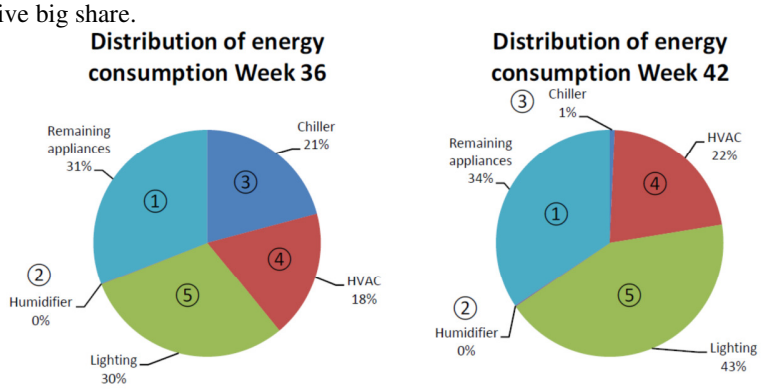

Figure 7:Total energy consumption for calendar week 36 and 42 divided by main appliances.

HVAC Air Handlings Unit

Fig. 8 shows two different energy profiles for the HVAC control unit, the left profile consists of Monday morning early start setting, and the right shows the profile with active night ventilation.
As can be seen from this figure, the maximum energy use by the system is 6 kWh and minimum is 0 kWh.
In the right figure, the energy use by night ventilation can clearly be seen due to the energy use from 0:00 hr. till 6:00 hr. The energy consumption due to night ventilation was maximum 5 kWh. This gives an insight in the amount of energy use by the fans compared to the other components powered by the HVAC control unit. In Fig. 8 block A represents the night ventilation. Block B represents the normal start-up profile and block C the normal day ventilation profile. The left figure shows an early start, block D, as the clock program lets the building systems start up earlier on Monday morning.

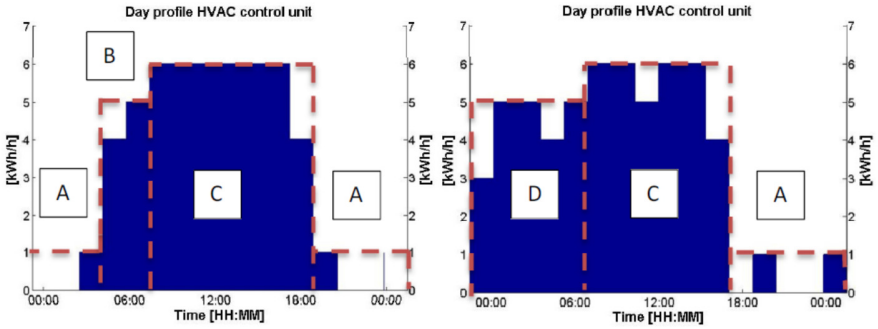

Figure 8: Energy use day profiles of the HVAC control unit, left early start (Monday), right active night ventilation.

Fig. 9 presents the energy profiles for each day in a 3D plot. Here the energy profile with night ventilation versus the normal day profile can be seen more clear. The energy use is given a colour where red presents the maximum use of 6kWh/h.

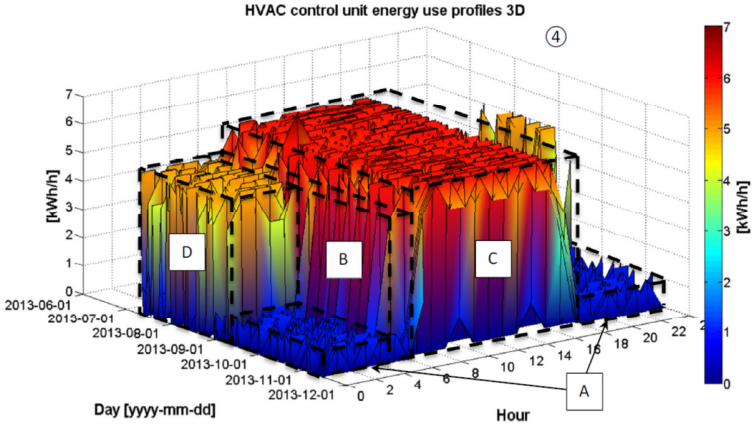

Figure 9: HVAC control unit energy use profiles stacked by date.

Experiment: Fan power reduction

The ventilation supply is divided into 3 groups respectively; north, south and the drawing room. The building is mechanically ventilated by a central AHU with a steam humidifier and heat recovery wheel. The air is supplied and extracted through the ceiling in the different rooms. The main task for the ventilation system is supplying fresh air for a healthy work environment; the humidity content during winter is set at 8.0 (g/kg), for a temperature of 21.5 (˚C) this results in a RH of 51%. The fresh air is controlled by valves and supplied- as well as extracted by fans, the heat is recovered by a heat recovery wheel. The operating components of the AHU requires real time data, so sensors are installed for the humidity, duct pressure and temperature.. The pressure in the intake duct is controlled by an RPM (rotations per minute) controller connected to the supply fan. This is PI-D-controlled, based on the desired and measured pressure in the supply duct.

Table 1: Control strategies supply- and exhaust fan

Event:	*Variable parameter:*
Supply fan	250 [Pa]
Exhaust fan	Control supply fan – 5% offset
Time interval adaptions fan speed	00:30 [mm:ss]
PI-D automatically controlled	20 – 100 [%]
Fan stops, belt breakage	10 [Pa]
Fan stops, dirty filter	280 [Pa]

An overview of the Air Handling Unit and its components is shown below. The biggest energy consumers during winter time were the humidifier, supply fan and exhaust fan. During summer the cooling machine is also a large energy consumer, but is not taken into account, because this study aims the AHU analysis during autumn/winter time when no significant cooling is needed. In this experiment we looked at the reduction of the air supply and exhaust.

The supply and exhaust fans have a maximum rated power of 5.5 and 4.0 (kW) respectively. The control is set according to the pressure at the supply duct, namely 250 (Pa), 1200 RPM. The fans consumes about 5 (kW) during this normal operation and The PI-D control value, is automatically set to ±0.80. Table 2 shows the settings of the experiment. Between these intervals there is at least 1 hour 'normal set point' and the timeframe is given in Table 3.

Table 2: Fan reduction experiment

Interval time:	*Supply and exhaust fan*
15 minutes	25% supply reduction (PI-D control value 0.60)
30 minutes	25% supply reduction (PI-D control value 0.60)
60 minutes	25% supply reduction (PI-D control value 0.60)

Table 3: Short time adaptions supply & exhaust fans

Interval time I	15 minutes
Return to normal setpoint	60 minutes
Interval time II	30 minutes
Return to normal setpoint	60 minutes
Interval time III	60minutes
Total experimental period:	3 hours and 45 minutes

The energy use of the fans was monitored to determine how much energy could be saved by reducing the fans speed by 25% while keeping the carbon dioxide concentration within the set comfort boundary conditions.

Results of the experiment

The PI-D control value in the BMS was maximized from unlimited to 0.60 to reach 25% with reductions at time intervals I, II and III. Before start of the experiment, the following settings were found from the AHU, BMS: PI-D automatically at 0.80 ~ 0.81; Supply fan 1210 RPM; 250 (Pa) at supply duct; Exhaust fan 1072 RPM

The control value of the fan was reduced to 0.60, for achieving 25% fan reduction. This resulted in the following settings: Supply fan 900 RPM; 142 (Pa) at supply duct; Exhaust fan 767 RPM. Carbon dioxide concentration and relative humidity are the most important climate parameters for analyzing the effect to the indoor environment during the experiment all are shown in Fig. 10 and Fig. 11.

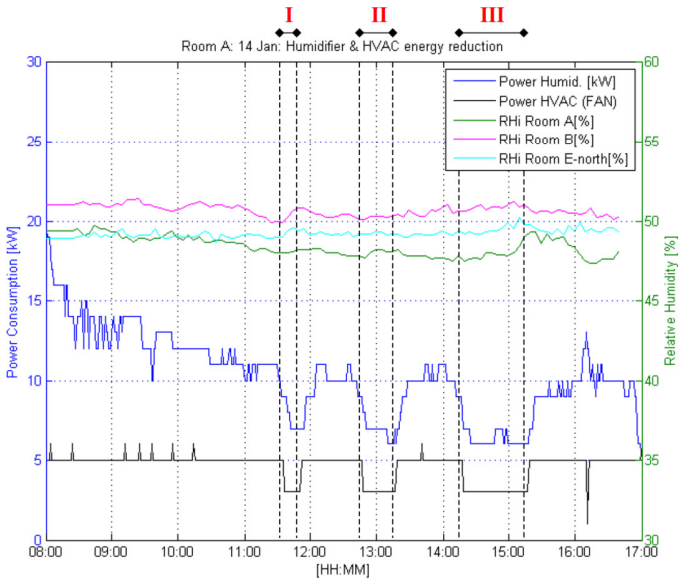

Figure 10: Energy consumption fans and humidifier during experiment II, interval times are black dashed

From Fig. 10 it can be concluded that a fan supply reduction of 25% also result in a decreased energy use. Another positive energy effect of this fan supply reduction is related to the humidifier power consumption. The energy consumption of the steam humidifier is also significantly reduced during interval time I, II and III, see Table 4.

Table 4: Power reduction during experiment II

	Power reduction fans	*Power reduction humidifier*	*Indoor RH*
Interval time I	± 2 kW	± 5 kW	Remains stable
Interval time II	± 2 kW	± 5 kW	Remains stable
Interval time III	± 2 kW	± 4 – 5 kW	Remains stable

The fans (RPM) almost immediately responded to the changed (PI-D) control value. Compared to a normal day, energy was saved during and slightly after the interval times because of the response time of the humidifier. The RH indoor remained stable at about 50 (%), compared to a day in December when the humidifier also did operate.
The CO2 concentration was recorded during the experiment and shown in Fig. 11.

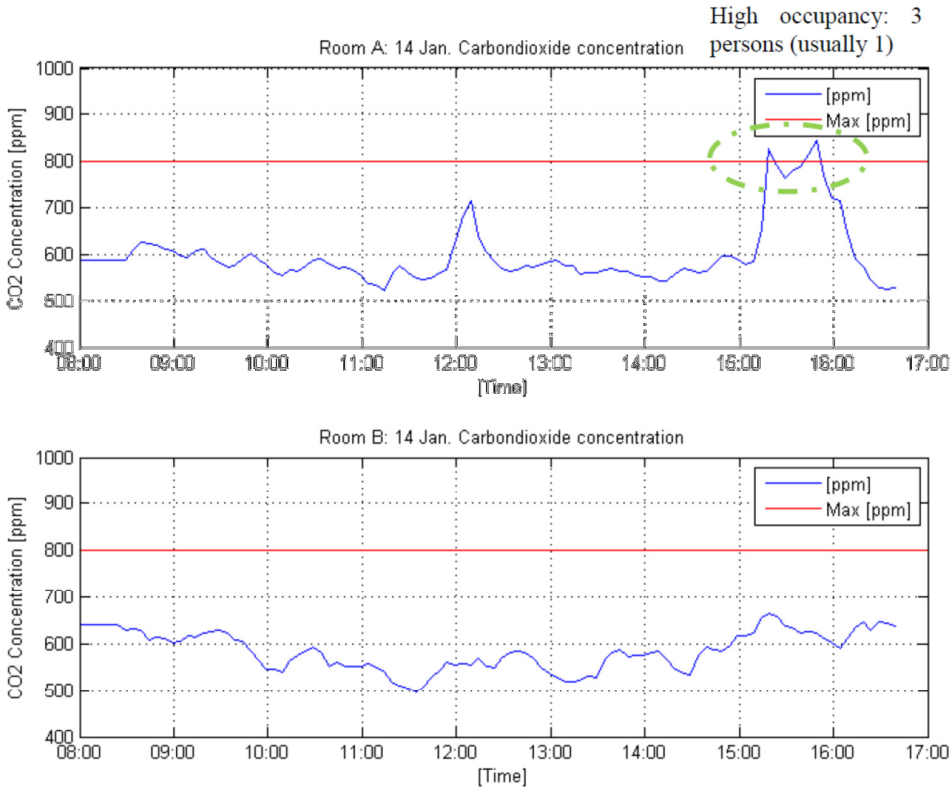

Figure 11: CO_2 concentration during experiment II for Room A & B

Interval time I (11:33 – 11.48)
During this first time interval, an extra energy reduction from the steam humidifier resulted in total saved energy during this interval of approximately 7 (kW). This value differs because of the high fluctuating energy demand of the steam humidifier. The absolute humidity instantly increased to 8.6 (g/kg) at the moment that the fans were reduced. This is explained by the fact that the flow rate was decreased, so the same steam input resulted in higher humidity levels in the supplied air. This event caused energy reduction for the steam humidifier, since less flow required less steam to fulfill the required vapor demand (or set point). During this interval, the occupancy in Room A was 1 person and in Room B 2 persons. Doors to the corridor were opened. The carbon dioxide concentration in Room A remained stable and in Room B it was slightly increased, but within set comfort boundaries.

Interval time II (12:45 – 13:15)
During this second time interval, approximately the same energy savings (as interval time I) occurred. At the time of the fan speed reduction, the measured absolute humidity instantly rose to 8.7 (g/kg).

In room A nobody was present and in room B at start also nobody was present and at the end of interval time II: 1 person was present. The CO2 concentration in room A decreased from 567 to 559 (ppm). In room B; the CO2 concentration decreased from 583 to 523 (ppm)

Interval time III (14:15 – 15:15);
During this interval about 6 – 7 (kW) power was reduced, at the time of reducing the fan speeds, measured absolute humidity instantly rises to 8.5 (g/kg). The CO2 in room A ranged between 557 to 657 (ppm). 5 minutes after this period (15:19h) a concentration of 828 (ppm) was measured. The CO_2 concentration did not exceed the set comfort limit of 800 (ppm) during experimental time (11:33h – 15:15h). The concentration did increase from the end of the experimental time interval III this was because the relatively small room A was occupied with 3 persons. These higher concentration was maintained for 40 minutes even when the fans were already on normal set point. This can be explained by the occupancy in this small room at the time. The CO_2 in room B rangedbetween545 – 656 (ppm), a small concentration reduction from the start and then an increase. The occupancy in this room started with one person and later on with a second person.

DISCUSSION AND CONCLUSIONS

The shift towards smart electrical grid cannot ignore connected buildings. This implies active participation of buildings in the grid. Energy management in the Micro Grid, the electrical infrastructure directly around buildings, depends highly on the energy management inside the buildings, called the Nano Grid. In this study, with respect to the Micro Grid within the Smart Grid, the network and electrical energy consuming systems in the building managed by the BEMS were called Nano Grid.

For an optimal SG from a system of systems point of view, the BEMS has to be coupled with the management platform of the grid (Dave et al., 2011). The control of loads in the building, may also be a resource to the grid using the flexibilities in service of the grid in Demand Side Management (DSM) scenarios as so called Demand Response (DR) or Load Control (LC). (Callaway and Hiskens 2011) However, these flexibilities remain largely undefined with respect to interactions with the power grid. Also, the development of the Smart Grid is still at an early stage and some parameters are yet to be fully defined with respect to interactions with NanoGrid.

With the development of a communication platform between the BEMS and Grid Energy Management System (GEMS) both systems get more interconnected and thus more dependent on each other. The present choices made in energy management have the capacity to, affect future choices. (Callaway and Hiskens 2011) This means goals and functionalities of both coupled energy management systems have the potential to effect each other.

For the built environment, now is the chance to prepare for the coming SG. New strategies of energy management, building management, and comfort management have to be developed to anticipate on the coming possible changes on Demand Side Management by Demand Response (DR) and Load Control (LC).

This study is a first step towards the evaluation of the possibilities for adapting the consumption patterns of an office building and the impact of energy management with grid interaction. Here the focus was on the air handlings unit and the amount of supply air. Air-flow reduction can be used as a service to the grid or energy efficiency measure, with a power of 2 kW. Beside the direct energy use reduction of the air handling unit fans the cooling demand reduces with 22%. Reduction of the airflow can be used almost during the entire year maintaining acceptable CO_2 concentrations.
In future research the effects of other interventions in relation to lighting and cooling will
be studied to get an overall insight of the possibilities of reducing the energy demand of the building as a service to the Smart Grid.

References

Acevedo,S. S., Molinas M., 2012, Identifying Unstable Region of Operation in a Micro-grid System.Energy Procedia 20: 237-246.

Callaway D. S., Hiskens I.A., 2011. Achieving Controllability of Electric Loads, Proceedings of the IEEE 99(1): 184-199

Choi C.-S., Han, J. Park W.-K., Jeong Y.-K., Lee I.-W., 2011, Proactive energy management system architecture interworking with Smart Grid, 2011 IEEE 15th International Symposium on Consumer Electronics (ISCE).

Dave S., Sooriyabandara M., Yearworth M., 2011, A Systems Approach to the Smart Grid. The First International Conference on Smart Grids, Green Communications and IT Energy-aware Technologies.
EIA, US E. I. A. , 2011, U.S. Energy Information Administration - Independent Statistics and Analysis, http://www.eia.doe.gov/
Elkhuizen, B. and E. Rooijakers, 2008, Visie op ontwikkeling Gebouwbeheersystemen, Verwarming en Ventilatie (mei 2008): 336-338
Georgievski I., Degeler V., Pagani G. A., Nguyen T. A., Lazovik A. and M. Aiello, 2011, Optimizing Offices for the Smart Grid, Technical Report.
Han J., Jeong Y., Lee I., 2011, Efficient Building Energy Management System Based on Ontology, Inference Rules, and Simulation, International Conference on Intelligent Building and Management.
Choon H., 2011, Building Energy Management System based on Smart Grid, Telecommunications Energy Conference (INTELEC), 2011 IEEE 33rd International.
Klein L., Kwak J., Kavulya G., Jazizadeh F., Becerik-Gerber B., Varakantham, P., Tambe M., 2012, Coordinating occupant behavior for building energy and comfort management using multi-agent systems. Automation in Construction 22: 525–532
KyungGyu P., Yoonkee K., SeonMi K., KwangHo K., WookHyun L. and P.
Li N., Calis G., Becerik-Gerber B., 2012, Measuring and monitoring occupancy with an RFID based system for demand-driven HVAC operations. Automation in Construction 24:89–99.
Lo C., Ansari N., 2011, The Progressive Smart Grid System from Both Power and Communications Aspects, Communications Surveys & Tutorials, IEEE PP(99): 1-23.
Lopes, A. J., Lezama R., Pineda R., 2011, Model Based Systems Engineering for Smart Grids as Systems of Systems, Procedia Computer Science 6(0): 441-450.
Opstelten I., Bakker E., Kester J., Borsboom W. and B. Elkhuizen, 2007, Bringing an energy neutral built environment in the Netherlands under control Petten, The Netherlands Energy research Centre of the Netherlands.
Robinson D., Wilke U., Haldi F., 2011, Multi agent simulation of occupants presence and behavior, Proceedings Building Simulation 2011, Sydney
Saputro N., Akkaya K., Uludag S., 2012, A survey of routing protocols for smart grid communications." Computer Networks 56(11): 2742-2771.
Slootweg J. v. d., Meijden M., Knigge J., Veldman E., 2011, Demystifying smart grids - Different concepts and the connection with smart metering. S.l.
Sun Z., Wang S.M.Z., 2011, In-situ implementation and validation of a CO2-based adaptive demand-controlled ventilation strategy in a multi-zone office building, Building and Environment 46(1): 124-133.
Wang W., Xu Y., Khanna M., 2011, A survey on the communication architectures in smart grid, Computer Networks 55(15): 3604-3629.
Yang R,., Wang L., 2011, Multi-objective optimization for decision-making of energy and comfort management in building automation and control, Sustainable Cities and Society 2(1): 1-7.
Zhang H., Hoyt T., Lee K.H., Arens E., Webster T., 2009, Energy savings from extended air temperature set points and reductions in room air mixing, Proceedings Environmental Ergonomics, Boston

Detecting and tracing building occupants to optimize process control

Wim Zeiler, Timilehin Labeodan, Gert Boxem, Rik Maaijen
TU Eindhoven Faculty of the Built Environment
Eindhoven, Netherlands
w.zeiler@bwk.tue.nl

ABSTRACT

.Occupant behaviour has been shown to have a large impact on the energy consumed in buildings than other thermal related process. For worthwhile energy savings, it is therefore crucial that occupant behaviour be included in the process control of building systems. For this set of control objective with the user central in the control of building systems, it is most important to detect the individual user on a specific workplace within a time span of minutes because the inertia of the building systems is in this order of his magnitude. The indoor occupancy detection system should be able to detect every individual in a spatial area and to be able to track and trace the person. Therefore an indoor occupancy detection and positioning system is being designed which, can communicate with a Building Energy Management System (BMS). The results of a first experiment are described in this paper.

Keywords; occupancy, HVAC control, user behavior, energy.

INRODUCTION

Energy consumption in commercial office buildings has been rapidly increasing in the last two decades, rising by about 70% between 1980 and 2005 in the US alone (IEA 2011). The energy consumption of the built environment is now around 40% of all energy used in the Netherlands. An intelligent electrical energy supply grid is being developed, i.e., the Smart Grid, to cope with fluctuations in energy generation from the different energy sources. Currently the focus of energy policy is towards diversification of energy supply (distributed energy resources (DER) and especially distributed generation (DG), and deployment of renewable energy (RES) within Smart Energy Systems (El Bakari et al. 2009). The possible interaction of decentralized renewable energy sources with the existing energy infrastructure of a building, the nanoGrid (Nordman 2009, Nordman 2011, Marnay et al. 2011), needs to be optimized. This leads to intensified intermittency of supply, resulting in challenging operational aspects. The objectives in uncertainty reduction in smart energy systems require novel system concepts in the control and management of Smart Energy Systems, which must include the essential connection to the user and its real behaviour.

To achieve improved overall energy efficiency it is necessary to better match energy demands and energy need in buildings. Therefore the process control of the energy infrastructure within the built environment, the so called micro grid, needs to become smart, intelligent and capable of adaptable behaviour in changing conditions. The sustainability demand leads to buildings which will use more and more renewable energy sources and will have energy storage capacity. Office buildings become a potential source of energy flexibility which can be offered to the grid as a Virtual Power Plant (VPP). In order to minimize uncertainty in the balance between energy supply and demand, it is necessary to develop realistic process control strategies based on real behaviour of user, installations, energy storage devices and grid interaction. Monitoring the needs and preferences of users is crucial to predict future states of the demand for the Smart Energy Systems (e.g. based on real human behaviour and energy needs). An automated adaptive process control is needed to optimize interaction between offices and Smart grid. Building Management Systems (BMS) could reduce the energy use within the micro grid by controlling the thermal indoor environment on the perceived comfort by the individual occupant in relation to the dynamic outside conditions like air temperature, solar radiation and wind. However the current BMS are limited in their ability to perform intelligently and show adaptive behaviour under changing circumstances. By the intended use of multi-agent

technology in combination with state-of-the-art Building Management Systems, new possibilities occur. It will enable real time interaction between outside environment and indoor conditions, process control based on the behaviour of occupants as well as a nanoGrid strategy which aims for optimal interaction with the Smart Grid. According to Robinson et al (2011) one of the greatest sources of uncertainty in building simulation and in the real behaviour of buildings are the individual differences in presence and behaviour of building occupants. From another study byParijs et al (2011), the authors suggested using a range of values between 0.5 to 0.9 for the parameter of turn-up in applications of uncertainty analysis when no building specific data on the occupancy are available. Together with the uncertainties relating to occupants t control of shading devices, windows, artificial lighting, thermal environment and the use of electrical appliances, these actions combined increases the level of uncertainty. . The uncertainty introduced by occupants behaviour is undeniable (Burak Gunay et al 2014). More knowledge and insight about the real occupants behaviour is necessary to better predict the heat/cold flows in buildings as well as the electrical power demand of lights, appliances and HVAC equipment (Robinson et al. 2011). The focus of the project is on occupancy on workplace/floor level, this to be able to optimize the energy interchange with Smart Grid energy supply on building level based on the actual energy demand derived from the real user behaviour.

METHODOLOGY

Building occupancy information is a crucial factor that should be considered in the control strategy of building operations for improved energy efficiency and occupant comfort. Building systems generally operate according to fixed schedules and to assumed occupied and unoccupied periods of the day as in EN 15232 (e.g. 8 AM to 7 PM). They do not consider when buildings are partly occupied which could be of influence as occupancy in buildings varies from day to day and from time to time (2-4).

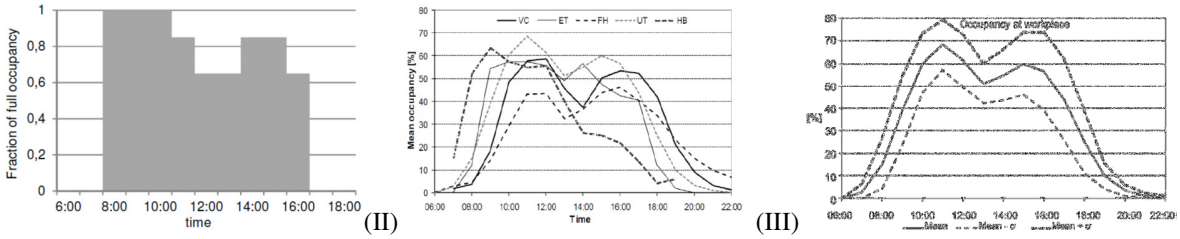

(I) (II) (III)

Figure 1 **(I)** Occupancy profile according to the standard EN 15232, modified from (EN 15232), **(II)** Mean occupancy level for a reference day. VC: International organization (Vienna); FH: University (Vienna); ET: Telecom. services (Eisenstadt); UT: Insurance (Vienna); HB: State government (Hartberg) (Mahdavi, 2008) **(III)** Mean occupancy level at workplace and standard deviation for an insurance office Vienna, for 14 months, 89 workplaces, modified from (Mahdavi, 2011)

To get a better understanding of the occupancy, Mahdavi extracted behavioural trends and patterns for groups of building occupants from long-term observational data from different buildings (Mahdavi et al., 2009). Figure 1 shows that there are considerable difference in the mean occupancy at workplaces for the different building types. Analysing further, from observations in an insurance office, see Fig. 1 (III) a standard deviation up to 15% is visible. Although these figures give a better representation of occupancy patterns in different office buildings. However, still a lot of information is missing, e.g.: Variation of occupancy from time to time; location of the people within the building and which individual is at what position in the building. To overcome the first two missing points, a more dynamic approach was presented by Wang et al (2005) which presents occupant presence by using so-called ‘’diversity profiles’’. The profiles depend on the type of building and sometimes even on the type of occupants. Wang et al., (2005) tried to understand, and predict the transient nature of occupancy during nominally occupied periods. Wang examined the statistical properties of occupancy in single person offices of a large office building in San Francisco. Fig. 2 shows the distribution of hourly occupied time as function of time of day.

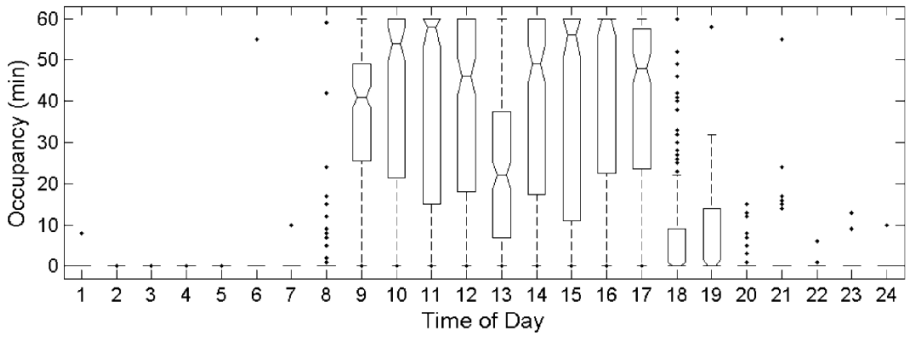

Figure 2 Distribution of hourly occupied time over 24-h of day for an office in San Francisco (Wang et al., 2005)

This figure indicates that from 8.00 to 17.00 h 75% of the workers are more than 25 minutes at their workplace hourly, except 12.00 to 13.00 h giving a more reliable vision on occupancy. Both the research of Wang (Wang et al., 2005) and Page (Page et al., 2008) looked at the probability of the vacancy interval. Fig. 3 and Fig. 4 show similarities, where the probability of short vacancy is the highest and lower for the longer vacancy intervals.

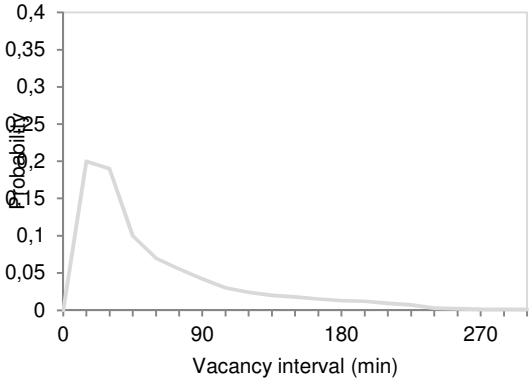

Figure 3 Probability distribution of the vacancy intervals for an office, modified from (Page et al., 2008)

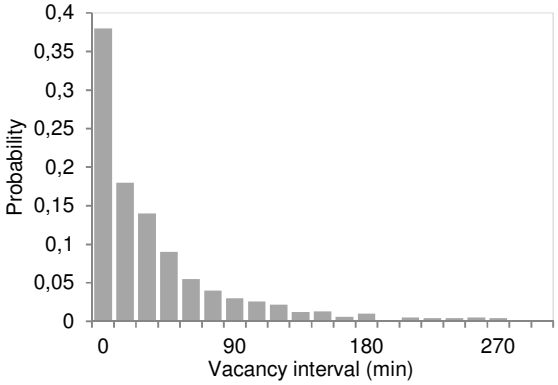

Figure 4 Probability distribution of the vacancy intervals for an office, modified from (Wang et al., 2005)

These probability functions can be used as input for building simulation models, and are better describe the deterministic occupancy behaviour of the individual building occupant. The weakness of probability profiles lies in the repetition of one or possibly two profiles and the fact that the resulting profile represents the behaviour of all the occupants of a building. "The latter simplification reduces the variety of patterns of occupancy particular to each person by replacing it with an averaged behaviour. The former simplification neglects the temporal variations, such as seasonal habits, differences in behaviour between weekdays (that appear in monitored data) and atypical behaviours (early departures from the zone, weeks of intense presence and of total absence, unpredicted presence on weekends in the case of office buildings—events that all appear in monitored data)" (Page et al., 2008).
Despite all effort, no current model is capable of describing the individual human position in buildings. This was also acknowledged by Mahdavi et al. (2009), who concluded that different researches tried to describe the human position and its actions by a model. From all the models he investigated it turned out that interactions with buildings' environmental systems are difficult or even impossible to predict at the level of an individual person. User presence is a complete stochastic and random process, where even the next state of presence cannot be described by the previous. For optimal building operation, real-time information about the building user is needed. Dynamic control of building services systems in relation to actual building occupancy profile presents an opportunity for more efficient use of energy for improvement of occupants comfort. However, human occupancy

information was not until recently considered in buildings energy performance analysis (Zeiler et al 2012). The use of real-time occupancy information has been shown by a number of studies (Khoury et al 2009, Dong et al 2010, Melfi et al 2011, Li et al 2012, Martani et al 2012, Erickson et al 2013), to have the potential to provide the worthwhile energy savings required to reduce the energy consumption of office buildings without compromising on occupant's thermal comfort needs.

EXPERIMENT WITH WSN AND RFID IN AN EXISTING BUILDING

Spartaru and Gauthier (2014) tested he performance of various technologies for monitoring people within buildings, systems which can help to asses potential energy reduction due to activity and occupancy and energy use. They found that each technology has intrinsic restrictions (Spartaru and Gauthier 2014). Based on our evaluation (Zeiler et al 2012) we applied RFID (Radio-frequency identification technology to incorporate human occupancy in demand driven HVAC control applications using a typical office building as a test-bed. (RFID) is the wireless non-contact use of radio-frequency electromagnetic fields to transfer data, for the purposes of automatically identifying and tracking The study focused on the use of RFID systems for a number of reasons: first, RFID systems are intrinsic devices commonly found in large office buildings in the form of identification cards and door/room access cards. Secondly, RFID technology can provide adequate accuracy; it is cost efficient; it does not require line of sight conditions and has the capability to incorporate additional functionalities such as building asset management (Li et al 2012).
Low-budget wireless sensor networks combined with portable nodes (RFIDs) are very promising technologies (Ruiz-Garcia et al 2009, Vishwakarma and Shukla 2013) and have the potential for real-time indoor localization for demand driven HVAC applications. Therefore static wireless sensor nodes were mounted on the floor and communicated with mobile nodes depicted in figure 5 (or in the future smart phones) carried by the occupant to determine the position of building occupants on workplace level. RFID system uses a number of active mobile tags worn by building users and multiple readers to triangulate the position of tags. The feasibility of this system in HVAC control in a large office building was explored by Li et al (2012) using battery powered RFID tags; mobile occupants were identified and tracked over a period of time. The collected data was used in calibrating an occupancy prediction model but the author showed it was possible to make use of the system for real-time localization for demand driven HVAC control.

Measurement set-up

A wireless sensor network (WSN) based on RFID technique was installed on the case study office floor of Royal Haskoning. Using the complete third floor of an office building with surface area of approximately 475m2, comprising two large open-plan office spaces and 6 cell offices, the possibility to incorporate RFID tags into the operation of the building were studied. The applied system RFID localization system has the following characteristics features:

- The static and mobile nodes are physically the same (Fig.5). The static nodes are programmed with a known location, and mounted on known spots of interest e.g. between the workplaces, nearby the printer, coffee machine and toilet;
- Mobile nodes are attached to occupants to denote occupants' locations, meanwhile the static nodes are deployed in the environment to provide references for location estimation with their own known locations;
- Based on signal strength from the surrounding static nodes, the mobile node takes over the location of the closest static node. The location is sent to the receiver which uploads the ID, time and location to the online cloud;
- This sensor network is a completely self-organizing WSN, meaning nodes need no configuration to form a network where nodes can freely enter and leave existing networks. Thereby the operation of the network never depends on particular topologies or on single nodes. The platform of the WSN is modular designed, meaning all other kind of different sensors and communication modules can be connected to the network.

The wireless static nodes as depicted in Fig. 5 for position tracking of the occupants were placed at locations on the floor with high occupant flow and use pattern, such as workspaces, printers and coffee machine location.
In total eighteen employees wore a mobile node the six weeks duration of the experiment. The employees were randomly chosen and represent almost 80% of the building occupants working on the case study floor. The measurements on the case study floor only took place for a period of six weeks in winter period. Firstly this means that the obtained results may only be accounted to this measurement period and secondly they are only valid for this case study floor.. After the measured period the employees were asked with what accuracy they think the node worked well. Different reasons for dysfunction are empty battery; forget to wear the node; node seemed not to work; etc. The accuracy of the nodes was weighted to the time the employee said to be present during the measured period. The average weighted accuracy of the measurements is 85% over the period of 6 weeks. The accuracy was that low because two occupants had a node that was not functioning properly all the time during the experiment. Therefor these results had to be skipped out, leading to useable data for sixteen employees.

Figure 5. Floor plan with the measured grid in the case study office (orange), formed by 30 static nodes, Floor occupancy hotspots as factor of the most occupied spot during the measured period.

RESULTS

The mean floor occupancy for a period of 3 weeks for the tracked participants as shown in Fig.6 is below 50%. The occupancy patterns varies for each day of week. Fig. 7 shows the occupancy level between 7AM and 7PM, with the highest floor occupancy on Tuesday which is much lower than the designed and the lowest on Thursday.

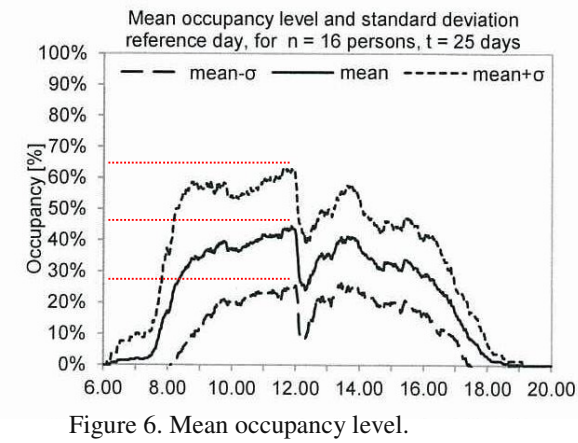

Figure 6. Mean occupancy level.

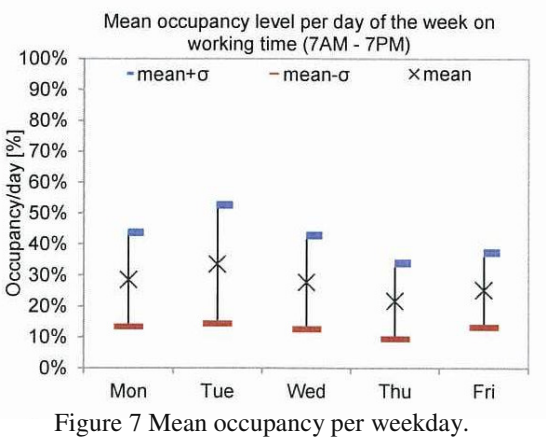

Figure 7 Mean occupancy per weekday.

Occupancy on workplace level

Since the interest is on the user, a closer look is made at the workplace level. Figure 8 shows the occupancy rate for four CAD workplaces in zone 22. Figure 9 shows the occupancy rate for four office workplaces in zone 20. A time step of 5 minutes is used.

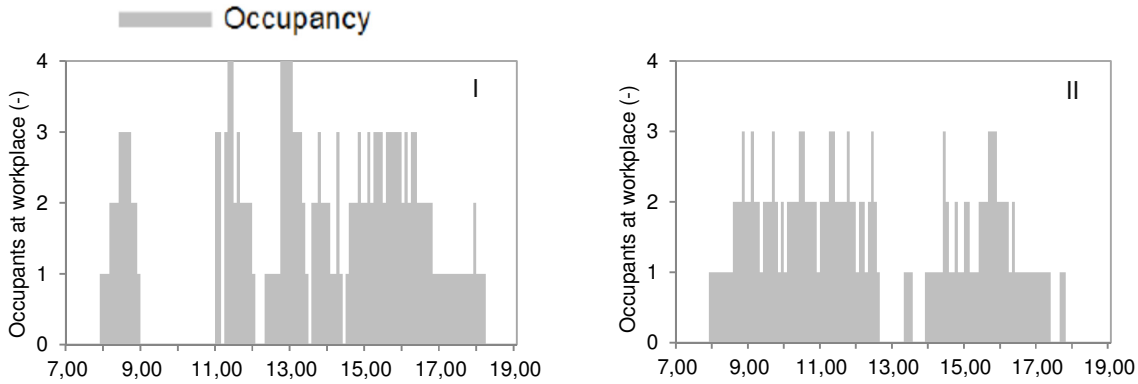

Figure 8 Occupancy of 4 CAD workplaces and electrical load, time step = 5 min, date I and II.

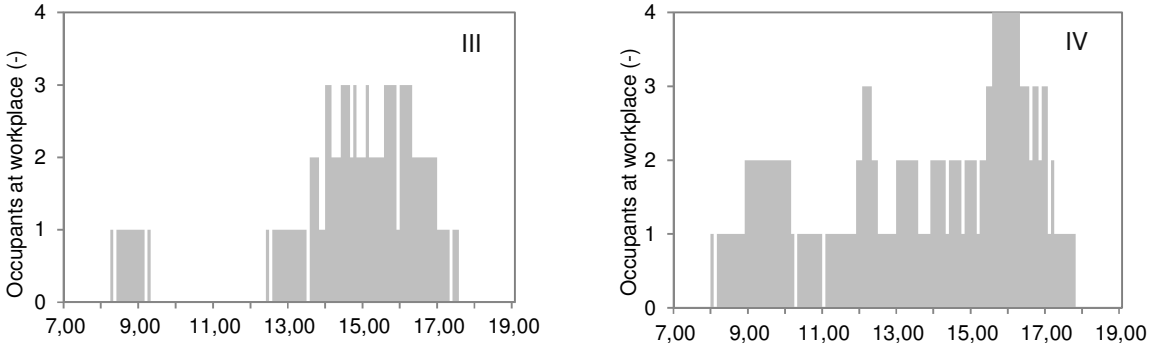

Figure 9 Occupancy of 4 office workplaces time step = 5 min, date III.and IV.

Modelling of the movement of occupants

Besides the level of occupancy we are also interested in the locations and movements of the occupants. The location of occupants can be represented within a timeline, see Fig. 10. Of more interest is to trace the movements of the occupants with the floor area, For a part of the floor, see Fig. 11 this was done. The movements of the occupant were drawn in the floor map to get a graphical representation of the movement. What is visible in Figure 12 and Figure 13 is that 13 of the 20 movements the user stays less than 10 minutes at his position. In these figures the lines

of one person moving one day inside the building already gives a complex view.

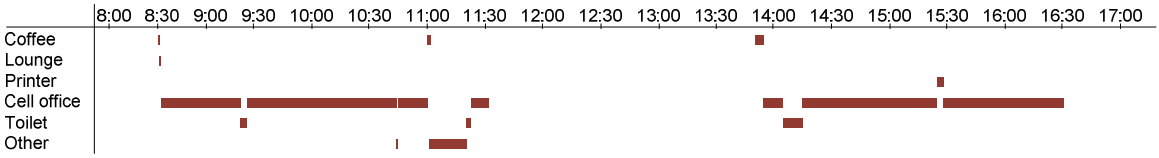

Figure 10 Timeline with the position for a reference day of an occupant

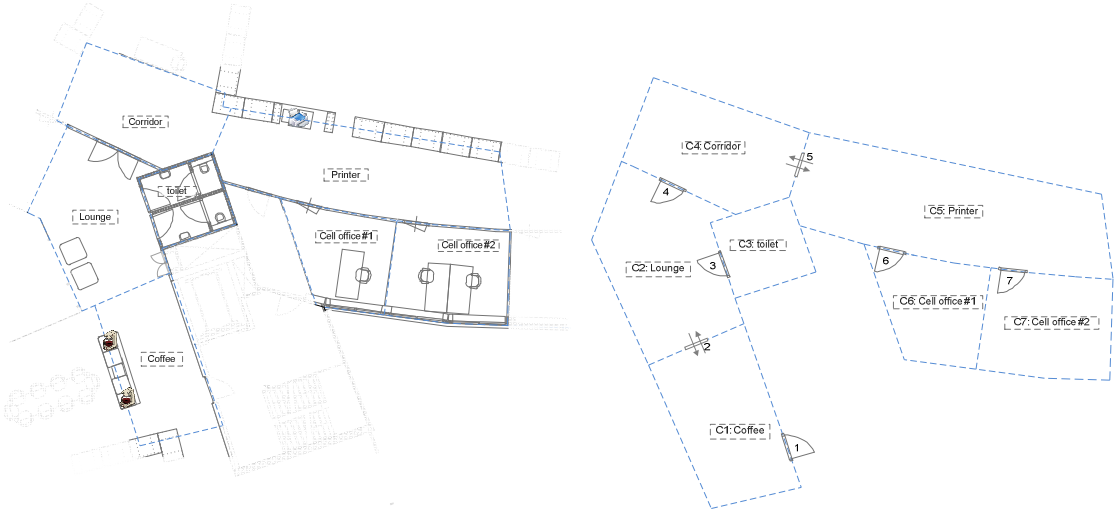

Figure 11 Part of the building model used for modeling, with the coffee machine, lounge, printer and toilet as special spots included in the model.

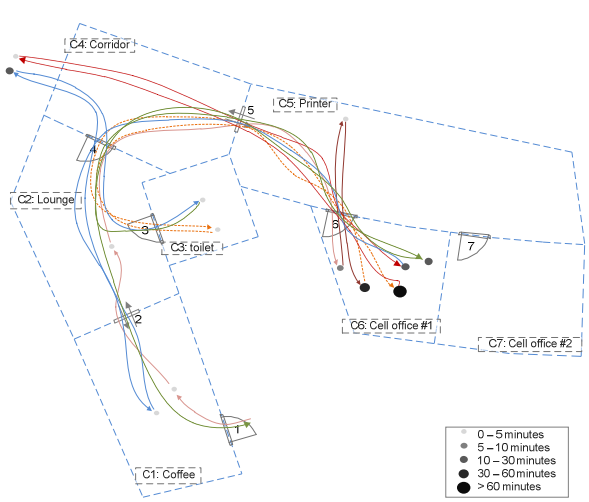

Figure 12 Movement over the floor before leaving the floor.

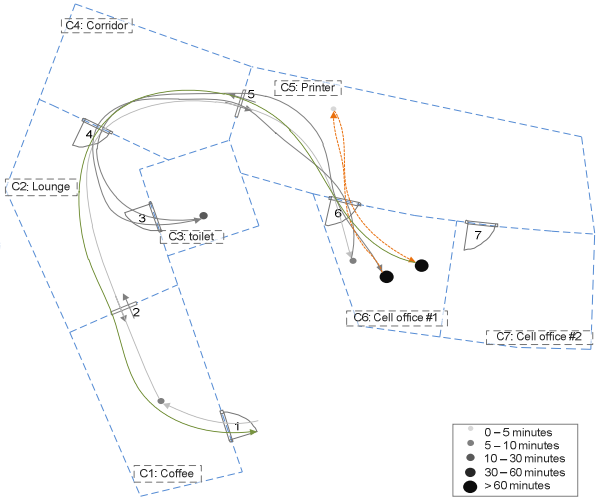

Figure 13 Movement on the floor in the afternoon

DISCUSSION AND CONCLUSIONS

The measurements on the case study floor only took place for a period of six weeks in winter period. Firstly this means that the obtained results may only be accounted to this measurement period and secondly they are only valid

for this case study floor. Mahdavi et al. (2009) already described that results from one building cannot be transposed without extensive calibration measures, considering differences in buildings use.

A number of implementation challenges were experienced during the study, besides the issue of privacy of the occupants, the most important being occupants adaption to the use of RFID technology. Occupants at some points forgot to make use of the tags, which equivocally affected the results obtained. The accuracy of the nodes was weighted to the time the employee said to be present during the measured period. The average weighted accuracy of the measurements is 85% over the period of 6 weeks. However, further experiments with the use of mobile phones and user identification cards equipped with localization capabilities are been planned for use in further studies. Benezeth et al (2011) proposed a vision-based system for occupancy detection based on video analysis, using a static camera. The total accuracy of counting the occupants found by Benezeth is 83%. So clearly our new approach is within the same level of accuracy.

Real-time measurement of actual building occupancy was shown through this experiment to represent a fraction of the standard occupancy profile. Despite the sparse and partial floor occupancy, the installed HVAC system remained operational at full capacity resulting in inefficient use of energy, so there is a potential for energy demand reduction.

Our experiment showed that it is possible to locate the user position, which in principle enables to apply energy to the spots where there is a demand of the building user based on his or her individual comfort. This does not mean that control devices, operable windows, and other adaptive user actions on room or workplace level are superfluous. As the study by Huizenga et al, (2006) and Hoes et al. (2009) already showed, the ability for a person to control his environment has a significant impact on occupant satisfaction. This asks for a system which combines (i) localizing the building occupant and automatic conditioning of his workplace, and (ii) the possibilities for adjustments of the users' environment. To apply the individual preferences on the workplace, the human should be included in the loop through controlling his individual comfort level to prevent discomfort and energy consuming behaviour of the occupant to restore his comfort level.

Having the data for occupancy it is still unclear how to present them in the best way to get the maximum insight of them. Especially using the data to track the individual persons is still a challenge which needs more research.

REFERENCES.

Benezeth, Y., Laurent, H., Emile, B., Rosenberger, C. (2011). Towards a sensor for detecting human presence and characterizing activity, Energy and Buildings 43: 305-314

Burak Gunay, H., O'Brien, W., Beausoleil-Morisson, I., Goldstein, R., Breslav, S., Khan, A., (2014) Coupling stochastic models to building performance simulations using the discrete event systems specification formalism, Journal of Building Performance Simulation 7(6): 457-478

Dong, B., Andrews, B., Lam, K., Hoynck, M., Zhang, R., Chiou, Y., & Benitez, D. (2010). An information technology enabled sustainability test-bed (ITEST) for occupancy detection through an environmental sensing network, Energy and Buildings, 42:1038-1046.

EIA (2011) Annual Energy Review 2010, Annual report, The World Business Council for Sustainable Development, October 2011.

El Bakari K.E, Myrzik, J.M.A., Kling, W.L. (2009) Prospects of a virtual power plant to control a cluster of distributed generation and renewable energy sources, Proceedings of the 44th International Universities Power Engineering Conference

Erickson, V., Achleitner, S., & Cerpa A. (2013). POEM: Power-efficient occupancy-based energy management system, Proceedings Information Processing in Sensor Networks, Philadelphia, USA

Hoes P., Hensen J., Loomans M., Vries B. de, Bourgeois D. (2009) User behavior in whole building simulation, Energy and Buildings 41: 295-302.

Huizinga, C., Abbaszadeh, S., Zagreus, L., Arens, E., (2006) Air quality and thermal comfort in office buildings: results of a large indoor environmental quality survey, Proceedings Healthy Buildings, Lisbon

Khoury, H., & Kamat, V. (2009). Evaluation of position tracking technologies for user localization in indoor construction environments, Automation in Construction 18: 444–457.

Labeodan, T., Maaijen, R., Zeiler, W. (2013) The Human Behaviour: a tracking system to follow the Human occupancy, Proceedings CISBAT, Lausanne.

Li, N., Calis, G., & Becerik-Gerber, B. (2012). Measuring and monitoring occupancy with an RFID based system for demand-driven HVAC operations. Automation in Construction 24:89–99.

Mahdavi, A., Mohammadi, A., Kabir, E., Lambeva, L. (2008) Occupants' operation of lighting and shading systems in office buildings; Journal of Building Performance Simulation 1(1): 57-65.

Mahdavi, A., (2009) Cogitative buildings: concepts, technologies, implementations, ITcon Special Issue Building Information Modeling Applications, Challenges and Future Directions 14: 692-704

Mahdavi, A. (2011) The human dimension of building performance simulation, Proceedings IBPSA Conference, Sydney

Marnay, C., Nordman, B., Lai, J. (2011) Future roles of Milli-, Micro-, and Nano-Grids, Proceedings CIGRÉ, Bologna, Italy

Martani, C., Lee, D., Robinson, P., Britter R.,& Ratti C. (2012). ENERNET: studying the dynamic relationship between building occupancy and energy consumption, Energy and Buildings 47: 584-591

Melfi, R., Rosenblum, B., Nordman, B., & Christensen, K. (2011). Measuring building occupancy using existing network infrastructure, Proceedings Green Computing Conference, Orlando, Florida, USA.

Nobe, T., Tanab,e S., Lee S., Tomioka, Y. (2002). Investigation of seat occupancy rate in office, Proceedings Roomvent, Copenhagen

Nordman, B. (2009) NanoGrids: Evolving our electricity systems from the bottom up, Darnell's Green Building Power Forum, Anaheim, USA

Nordman, B. (2011) Nanogrids, Power Distribution, and Building Networks, EEDN Seminar

Page, J., Robinson, D., Morel, N., & Scartezzini, J. (2008). A generalized stochastic model for the simulation of occupant presence', Energy and Buildings 40: 83- 98.

Parys, W., Saelens, D., Hens, H. (2011) Coupling of dynamic building simulation with stochastic modelling of occupant behavior in offices – a review-based integrated methodology, Journal of Building Simulation 4(4): 339-358

Robinson, D., Wilke, U., Haldi, F. (2011) Multi agent simulation of occupants presence and behavior, Proceedings Building Simulation 2011, Sydney

Ruiz-Garcia, L., Lunadei, L., Barreiro, P., Robla, J.I. (2009). A Review of Wireless Sensor Technologies and Applications in Agriculture and Food Industry: State of the Art and Current Trends, Sendors 2009(9): 4728-4750

Spataru, C., Gauthier, S.. (2014) How to monitor people 'smartly' to help reducing energy consumption in buildings?, Architectural Engineering and design management 10(1-2): 60-78

Struck, C., Roelofs, J.G.J., Schijndel, H. van, Hensen, J.L.M., Wijsman, A.J.T.M. (2009). A comparison of measured and estimated electric energy use and the impact of assumed occupancy pattern, Proceedings IBPSA-Switzerland

Vishwakarma, U.K., Shukla, R. N. (2013). WSN and RFID: Differences and Integration, International Journal of Advanced Research in Electronics and Communication Engineering 2(9): 778-780

Wang, D., Federspiel, C., Rubinstein, F.(2005) Modelling occupancy in single person offices,Energy and Buildings 37: 121-126

Zeiler, W., Boxem, G., Maaijen, R. (2012). Wireless sensor technology to optimize the occupant's dynamic demand pattern within the building, Proceedings ICEBO 2012,Manchester

Zeiler, W., Labeodan, T., Boxem, G., Maaijen, R. (2013) Towards building occupants positioning: track and trace for optimal process control, Proceedings ICEBO 2013, Montreal

The Exploration on the Energy Saving Potential of an Innovative Dual-temperature Air Conditioner and the Mechanism of the Theoretical Mixed Refrigeration Cycle

Zhao Lei, Zhao Xijin, Hu Andu

Professor, graduate student, graduate student

(School of Environ. & Muni. Engi., Xi'an University of Architecture and Technology,

Xi'an, Shaanxi, 710055, P.R.China)

Abstract A conventional room air conditioner can cause unpleasant draft sensations and to produce poor indoor air quality. A typical energy-saving radiant cooling air conditioning system makes use of chilled water for cooling. It may also incur energy losses due to secondary heat transfer existing in the whole process. To overcome these disadvantages, an innovative dual-temperature air conditioning system and its corresponding theoretical mixed refrigeration cycle are proposed. This consists of a separate air handling unit and a metal radiation panel as the dual-temperature evaporators, a compressor, a condenser, two thermal expansion valves and an ejector. Mass and energy conservation equations are established for the air handling process and the theoretical mixed refrigeration cycle is analyzed. The state properties in the thermal processes and system performance are determined and compared with those of the conventional air conditioner with fresh air. It is found that the coefficient of performance（COP）of the theoretical dual-temperature refrigeration cycle improves by 13.35% to 7.47.

Keywords dual-temperature air conditioner; mixed-refrigeration cycle; COP; ejector; metal radiation panel.

Zhao, Lei, Ph.D., Professor, Xi'an University of Architecture & Technology
leizhao0308@hotmail.com,+86-29-82202169
Research fields: Characteristics of HVAC and refrigeration systems, Innovative technologies to reduce building energy consumption.

In a room with a conventional air conditioner, the supplied air is not evenly distributed and there may be a draft sensation, which may cause "air-conditioning symptoms", such as headache, chest distress, dizziness, etc. [1] In comparison, the indoor air temperature distribution in rooms with radiant cooling is relatively even and the thermal comfort sensation can be improved. The energy consumption can be reduced to some extent as well. If the radiant cooling can be supplemented by a fresh air supplying system, it may even improve the indoor air quality [2, 3]. However, radiant cooling usually uses chilled water as the medium to supply cooling, that is, the chilled water flows through the pipes embedded on the panel which cools the surface of the panel by heat convection and conduction. Then the panel cools the indoor air and walls by heat convection and radiation to achieve the desired air-conditioning effect. It can reach thermal balance and meet the requirement of building cooling load. [4, 5] In general, low temperature water needs to be used to dehumidify the air to offset the indoor humidity generation. Thus, condensation on the panel surface may occur and the evaporation temperature of the refrigeration cycle is relatively low as well. Therefore, the COP of the refrigeration cycle remains relatively low. In addition, energy losses caused by secondary heat transfer leave more room for the whole system performance to be improved if they

can be avoided.

For the above reasons, an innovative dual-temperature air-conditioner and the corresponding theoretical refrigeration cycle were proposed，which can provide cooling as well as fresh air. The operational states at the design condition were determined and the performance of the theoretical refrigeration cycle was analyzed and compared with those of the conventional air conditioner with fresh air handling.

1. MECHANISM AND SYSTEM PATTERN OF THE INNOVATIVE DUAL-TEMPERATURE ROOM AIR CONDITIONER

The system schematic and the corresponding refrigeration cycle of an innovative air-conditioner are shown in Fig.1 (a) and (b). Refrigerant vapor at low temperature (state 1a) is sucked into the compressor and compressed to be superheated vapor (state 2) and then leaves the compressor at the condensation pressure. It is cooled and condensed to be the saturated refrigerant liquid (state 3) in the condenser and is discharged into the suction-line exchanger, where it exchanges heat with the refrigerant vapor leaving the ejector to become sub-cooled liquid (state 3a). The sub-cooled liquid at the condensation pressure flows through two thermal expansion valves throttled to be wet vapors at two different evaporation pressures (state 4 and 5). Then they enter the radiant panel and the air handling unit, respectively, and absorb heat to evaporate. The radiant panel acts as the high temperature evaporator of the dual-temperature air conditioner. On the top of the panel are embedded pipes of small diameter, in which the refrigerant flows and becomes a saturated vapor (state 6) through heat exchange with room air and walls by heat convection and heat radiation. The tube-fin heat exchanger in the air-handling unit (AHU) acts as the low temperature evaporator, in which the refrigerant evaporates to saturated vapor at low evaporation pressure (State 7) by absorbing heat from the fresh air supplied as required to provide good indoor air quality. The refrigerant vapor leaving the high temperature evaporator flows into the ejector and induces the refrigerant leaving the low temperature evaporator into the ejector. These two streams of refrigerant mix and diffuse to become state 1 and enter the suction-line heat exchanger, in which it exchanges heat with the refrigerant leaving the condenser. Then it becomes superheated vapor (state 1a) and returns to the compressor. Thus, the cycle is completed [6].

The evaporation temperature of the refrigerant in the low temperature evaporator is comparatively low and is used to dehumidify the fresh air, which offsets the latent cooling load. The amount of the air handled reduces, comparing with that in the conventional air conditioner. Thus, the size of the tube-fin heat exchanger can be reduced appropriately. The fresh air flows through a specifically designed nozzle, inducing indoor air to mix and reach a proper temperature, which is supplied to the occupied zone. The condensing water formed on the surface of the tube-fin heat exchanger can be easily collected and discharged to outdoor through a pipe [7]. The refrigerant flowing through the radiant panel evaporates at a comparatively high evaporation temperature, only meeting the sensible cooling load. Thus, condensation can be avoided from occurring on the panel. And the improved evaporation temperature helps to improve the COP of the refrigeration cycle. The chilled radiation may help to better the indoor thermal comfort as well.

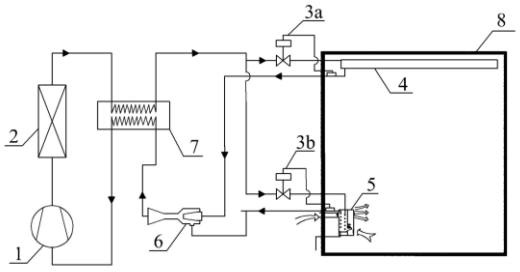

1.Compressor 2.Condenser 3a/3b.Thermal expansion valve

4.Metal radiant panel 5.Air-handling unit 6.Ejector

7.Suction-line heat exchanger 8. Room

(a)

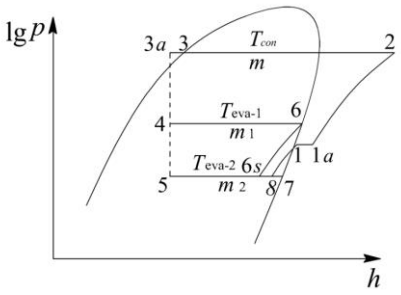

(b)

Fig.1 Schematic of the dual-temperature air conditioner and the corresponding theoretical refrigeration cycle

2 OPERATIONAL STATES AND PERFORMANCE ANALYSIS ON THE DUAL-TEMPERATURE AIR CONDITIONER

Mass and energy conservation equations were established for the theoretical refrigeration cycle and the air-handling process of the conventional and the dual-temperature air-conditioner in order to find the energy saving potential of the new system proposed. The operational states and performance were analyzed.

2.1 Determination on the Ratio of the Load Shared by Two Evaporators and the Supply Air Parameters

How the cooling load is shared by the radiant panel and the AHU in the dual-temperature air conditioner not only determines the indoor thermal comfort and the indoor air quality, but also determines the mass flow rates through the two evaporators, the cooling capacity and the COP of the whole system.[8–11]This is mainly decided by the sensible and latent cooling loads. An office of 40 m^2 in Xi'an was selected as an example. The design calculation was conducted for the dual-temperature air conditioning system to determine the ratio of cooling load shared by the radiant panel and AHU.

There is a west-facing exterior wall and two windows of size 2m×1.8m each facing westward. The adjacent rooms are all air-conditioned, and considered adiabatic Suppose that there are four persons, from whom the sensible and latent heat emissions are 60.5W/(h•p) and 73.3W/(h•p) , respectively, with the moisture emission rate of 109g/(h•p). The heat emission rate of the illumination and office equipment are 160W and 200W, respectively. The design air-conditioning outdoor dry-bulb and wet-bulb temperature are 35℃ and 25.8℃. The indoor design temperature and relative humidity are 26℃ and 50%. To achieve the desired indoor thermal comfort and to ensure satisfactory indoor air quality, the amount of the fresh air to be supplied is chosen to be 30m^3/（h•p）, that is, 120 m^3/h in total. This is 8.3 L/s-p or 4 cfm/p. There is a small air outlet installed in the office to ensure indoor pressure balance and mass conservation. The office design cooling load was calculated to be 5031W， using the method recommended by the local code and handbook[12,13].

The dual-temperature air conditioner makes use of the radiant panel and the air-handling unit as the evaporators. The structure of the AHU and the air handling process are schematically shown in 2(a) and 2(b). The outdoor fresh air is cooled and dehumidified in the AHU and induces the indoor air to mix and reach the feasible supply air state *SA2*. Then it is supplied into the office. That is, the fresh air supplied offsets the indoor moisture generation. Thus, the humidity ratio and the dew-point *SA1* of the supplied fresh air can be obtained by calculations using eq. (1)~(4).

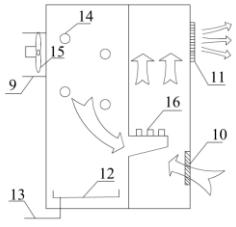

9. Outdoor air inlet 10.Return air inlet 11.Supply air outlet 12.Condensate drain plate 13.Condensate drain pipe 14. Coil of evaporator 15.Fan 16.Induction nozzle

(a)

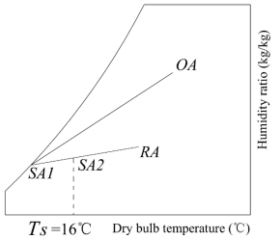

(b)

Fig.2 Structure of the induction type fan coil and the *h-d* diagram of the air handling process

$$\dot{V}_{OA}\times\rho\,(d_{RA}-d_{SA1})=\dot{D} \tag{1}$$

where $\dot{V}_{OA}$ denotes the volumetric flow rate of the outdoor fresh air, m^3/h; ρ denotes the air density, kg/m^3; d_{RA} represents the humidity ratio of the return air, kg/kg; d_{SA1} represents the humidity ratio of the air at apparatus dew point, kg/kg; $\dot{D}$ represents the indoor moisture generation rate, kg/h.

$$(\dot{V}_{OA}\rho+\dot{V}_{RA}\rho)\times d_{SA2}=\dot{V}_{OA}\rho\times d_{SA1}+\dot{V}_{RA}\rho\times d_{RA} \tag{2}$$

where $\dot{V}_{RA}$ represents the volumetric flow rate of the return air, m^3/h; d_{SA2} represents the humidity ratio of the supply air, kg/kg.

$$(\dot{V}_{OA}\rho+\dot{V}_{RA}\rho)\times h_{SA2}=\dot{V}_{OA}\rho\times h_{SA1}+\dot{V}_{RA}\rho\times h_{RA} \tag{3}$$

where h_{SA1} is the enthalpy of the air at apparatus dew point, kJ/kg; h_{SA2} is the enthalpy of the supply air, kJ/kg; h_{RA} is the enthalpy of the return air（kJ/kg）.

$$h_{SA2}=1.01t_{SA2}+0.001d_{SA2}(2501+1.86t_{SA2}) \tag{4}$$

where t_{SA2} is the supply air temperature,℃.

Taking the supply air temperature as 16℃, the parameters of each state can be obtained. Results are listed in Table 1. Since the amount of the fresh air is $120m^3/h$, the energy consumed in processing the fresh air to the state *SA1, the* apparatus dew point, can be calculated by: $\dot{Q}_2=\dot{V}_{OA}\rho(h_{OA}-h_{SA1})=2.031\text{kW}$. The other part of the cooling load, that is, $\dot{Q}_1=3\text{kW}$, will be handled by the radiant panel. For the office studied, the cooling capacity ratio of the chilled panel and the AHU should be 3:2 at the design condition.

To make the supply air temperature reach 16℃, some of the indoor air will be induced to mix with the fresh air after handling. The amount of the indoor air to be induced is calculated to be $\dot{V}_{RA}=75.31\,m^3/h$, and the relative humidity is 76.3%. All the state parameters experienced in the air handling processes are illustrated in Table 1.

Table 1 The air parameters of each state

	t/℃	t_{wet}/℃	φ/%	h/kJ/Kg	t_{dew}/℃	*d*/g/kg
OA	35	25.80	48.41	79.435	22.486	17.182
RA	26	18.64	50	53.012	14.796	10.495
SA1	9.68	9.68	100	28.587	9.68	7.467
SA2	16	13.50	76.3	38.009	11.503	8.635

2.2 Analysis on the Theoretical Refrigeration Cycle of the Dual-Temperature Air-Conditioner

In order to analyze an idealized refrigeration cycle, the following assumptions were taken: (1) the pressure loss along flow pipes, in the condenser and evaporators, etc. are neglected. (2) The refrigerant leaving the condenser and the evaporator are deemed as saturated liquid and saturated vapor, respectively. (3) The refrigerant is in quasi-equilibrium state and the processes occurring in the ejector are idealized neglecting various losses. The acceleration and the diffusion process in the ejector are deemed as isentropic, which can make use of the energy to its advantages. (4) The pressure of the refrigerant leaving the nozzle in the ejector drops to the low evaporation pressure and mixes with the refrigerant induced from the evaporator of low evaporation pressure at constant pressure. (5) The kinetic energies of the refrigerant entering the nozzle, leaving the evaporators and the ejector are neglected.

2.2.1 Determination on the refrigerant mass flow rates of the two evaporators

The refrigerant mass flow rates through the high and low temperature evaporators at their individual evaporation pressures are crucial parameters for the dual-temperature refrigeration cycle. As shown in Fig.1 (b), the refrigerant leaving the condenser flowing through the suction-line heat exchanger exchanges heat with the refrigerant from the ejector

and becomes sub-cooled, then it is divided into two parts. One part flows through the thermal expansion valve 3a, reaching the state 4 and enters the radiant panel, in which it evaporates by absorbing heat from the indoor air and surfaces through heat convection and heat radiation and reaches the state 6. The other part flows through the thermal expansion valve 3b, reaching the state 5, and enters the air-handling unit, in which it evaporates by absorbing the energy from the fresh air to reach the state 7.

Assume the condensing temperature to be 40℃, the high evaporating temperature to be 15℃ to avoid condensation from occurring on the radiant panel, and the low evaporating temperature to be 5℃ so that the fresh air can be dehumidified. Two streams of refrigerants mix in the ejector and flow into the suction-line heat exchanger absorbing heat from the refrigerant leaving the condenser to become superheated vapor. Assume the superheated temperature is 15℃. Taking R22 as the refrigerant, the state properties of state 3、3a、4、5、6 and 7 can be calculated by using the software REFROP8.0, as shown in Table 2. Since the energy the refrigerant absorbs in the two evaporators are 3.0kW and 2.031kW，the mass flow rates of the refrigerant flowing through them are 17.950 g/s and 12.399 g/s, respectively, in terms of $\dot{Q}_1 = \dot{m}_1(h_6 - h_4)$ and $\dot{Q}_2 = \dot{m}_2(h_7 - h_5)$.

2.2.2 Determination on the suction pressure of the theoretical refrigeration cycle

The evaporating pressures of the refrigerant in two evaporators are different. The refrigerant leaving the high temperature evaporator enters the ejector as the main stream accelerating through an isentropic process in the nozzle to reach state 6s. Then it induces the refrigerant leaving the low temperature evaporator into the ejector and mixes together to reach state 8. And then, it is diffused to reach state 1 in the diffuse section in the ejector. Leaving the ejector, it flows into the suction-line heat exchanger and is superheated to be state 1a, which is the suction state of the compressor. The states and velocity of the refrigerant flowing through the ejector are calculated as following.

Define the eject coefficient as the ratio of the mass flow rate of the induced fluid to that of the main stream fluid, that is $\mu = \dot{m}_2 / \dot{m}_1$. For the dual-temperature refrigeration cycle, the eject coefficient is the ratio of the mass flow rate of the refrigerant leaving the radiant panel to that of the refrigerant leaving the air-handling unit.

Based on the energy conservation principle, the refrigerant of mass flow rate $\dot{m}_1$ flows through the nozzle with its pressure decreased to the low evaporation pressure, and it is accelerated to the speed,

$$c_{6s} = \sqrt{2(h_6 - h_{6s})} \qquad (5)$$

Then it mixes with the induced refrigerant vapor of $\dot{m}_2$ leaving the low temperature evaporator at constant pressure. In terms of the momentum conservation equation, the speed of the mixed refrigerant reaches

$$c_{mix} = \frac{c_{6s} + \mu c_7}{1+\mu} \approx \frac{c_{6s}}{1+\mu} \approx \frac{\sqrt{2(h_6 - h_{6s})}}{1+\mu} \qquad (6)$$

Thus, the enthalpy of the refrigeration at this point becomes,

$$h_8 = \frac{(h_{6s} + \frac{1}{2}c_{6s}^2) + \mu h_7}{1+\mu} - \frac{c_{mix}^2}{2} \qquad (7)$$

The refrigerant is diffused in the ejector during an isentropic compression process, that is $s_8 = s_1$, reaching the inlet state of the suction-line heat exchanger. It can be expressed as,

$$h_1 = h_8 + \frac{c_{mix}^2}{2} = \frac{(h_{6s} + \frac{1}{2}c_{6s}^2) + \mu h_7}{1+\mu} = \frac{h_6 + \mu h_7}{1+\mu} \qquad (8)$$

In the suction-line heat exchanger, refrigerant vapor at suction pressure absorbs heat from the refrigerant liquid leaving the condenser to reach the state point

1a at 15℃. Then it enters the compressor and experiences an isentropic compression process to reach state point 2, that is, $s_1 = s_2$. The properties of the characteristic states in the refrigeration cycle are listed in Table 2

The suction vapor is superheated by 6.6 ℃. The compressor suction vapor pressure and discharge temperature are 0.64833MPa and 1.5336MPa, respectively. And the pressure ratio of the compression process is 2.365.

Table 2 Refrigerant properties of the characteristic states in the theoretical dual temperature refrigeration cycle

State Point	Pressure /MPa	Temp. /℃	Enthalpy /kJ/kg	Entropy kJ/（kg·k）
1	0.64833	9.4	408.81	1.7418
1a	0.64833	15	413.12	1.7569
2	1.5336	60.32	435.12	1.7569
3	1.5336	40	249.65	1.1665
3a	1.5336	36.75	245.33	1.1526
4	0.78931	15	245.33	1.1582
5	0.58411	5	245.33	1.1629
6	0.78931	15	410.16	1.7302
6s	0.58411	5	403.12	1.7302
7	0.58411	5	406.85	1.7436
8	0.58411	5	406.34	1.7418

2.2.3 Performance analysis on the theoretical dual-temperature refrigeration cycle

The theoretical energy consumption of the compressor can be calculated as

$$W = (\dot{m}_1 + \dot{m}_2)(h_2 - h_1) = 0.668 \text{ kW} \quad (9)$$

Since the cooling capacities at two evaporation temperatures are 2.031 kW and 3.0 kW, respectively, for the dual-temperature refrigeration cycle, the *COP* is, $COP = \frac{\dot{Q}_1 + \dot{Q}_2}{W}$, it may reach 7.54 ideally.

3 OPERATIONAL STATES AND PERFORMANCE ANALYSIS OF A SIMILAR CONVENTIONAL AIR-CONDITIONER

3.1 Determine the Air Supply State

The theoretical refrigeration cycle and air-handling process of the conventional air-conditioner with fresh air handling are illustrated in Fig.3 (a) and 3(b).

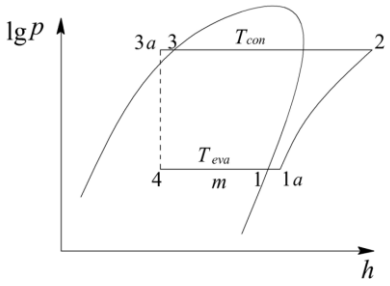

(a)

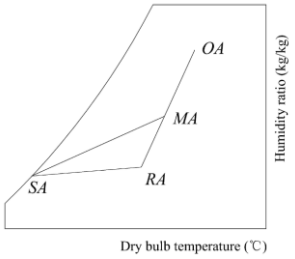

(b)

Fig.3 Theoretical refrigeration cycle of the conventional air conditioner with fresh air and the *h-d* diagram of the air handling process

The return air and fresh air mix and flow across the evaporator and reject heat to the refrigerant inside. The air is supplied into the room to offset the cooling load and humidity generation. In terms of the heat and humidity balance and the supply air is disposed to be saturated air, we can write

$$(\dot{V}_{OA} + \dot{V}_{RA}) \times \rho (d_{RA} - d_{SA}) = \dot{D} \quad (10)$$

$$(\dot{V}_{OA} h_{OA} + \dot{V}_{RA} h_{RA})\rho - (\dot{V}_{OA} + \dot{V}_{RA})\rho h_{SA} = \dot{Q} \quad (11)$$

where h_{OA} is the enthalpy of the outdoor fresh air, kJ/kg; h_{RA} is the enthalpy of the return air, kJ/kg; $\dot{Q}$ represents the heat load of the room, kW.

The supply air state can be determined, that is, $d_o = 10.129$g/kg, $h_0 = 39.982$kJ/k g, and the required

amount of the return air can also be obtained to be 872.7m^3/h. All the state properties in the air-handling process are listed in Table 3.

Table 3 State properties involved in air handling process of conventional air conditioner with fresh air

	t/℃	t_{wet} /℃	φ /%	h/ /kJ/kg	t_{dew} /℃	d /g/kg
OA	35	25.8	48.4	79.435	22.486	17.182
RA	26	18.64	50	53.012	14.796	10.495
SA	14.24	14.24	100	39.982	14.24	10.129

3.2 Analysis on Theoretical Refrigeration Cycle of Conventional Air-Conditioner

Taking the rated refrigeration condition of the conventional air-conditioner as an example, that is, supposing the condensing temperature to be 40℃, the evaporating temperature to be 5℃ and the superheated suction vapor temperature to be 15℃, the state properties of every state in the theoretical refrigeration cycle are determined, as listed in Table 4.

Table 4 Refrigerant states properties in the theoretical refrigeration cycle of a conventional air conditioner

State Point	Pressure /MPa	Temp. /℃	Enthalpy /kJ/kg	Entropy /kJ/(kg.K)
1	0.58411	5	406.85	1.7436
1a	0.58411	15	414.38	1.7702
2	1.5336	65.42	439.59	1.7702
3	1.5336	40	249.65	1.1665
3a	1.5336	35	243.04	1.1452
4	0.58411	5	243.04	1.1547

From $\dot{Q} = \dot{m}(h_1 - h_4)$, the required refrigerant mass flow rate can be calculated to be $\dot{m} = 30.71\text{g/s}$. The pressure ratio of the compress process is 2.626 and the COP of the theoretical refrigeration cycle is $COP = \frac{h_1 - h_4}{h_2 - h_1} \approx 6.50$.

4 COMPARISION OF THE PERFORMANCE OF THE TWO TYPES OF THE AIR-CONDITIONERS

The analysis stated above indicates that the flow rate of the air to be handled by the AHU in the dual temperature air-conditioner is just 120m^3/h, which can satisfy the fresh air requirement of 4 persons indoor. However, the flow rate of the air to be handled by the conventional air-conditioner is about 992m^3/h, which consists of 120 m^3/h fresh air and 872 m^3/h circulating air. Thus, the size of the air-handling unit and the required fan power can both be reduced significantly. In addition, the supply air temperature can reach 16℃ in the newly proposed air-conditioner, in which the proposed fresh air flows through a nozzle and induces the return air to form the supply air. Fresh air and return air mix firstly and are cooled to become the supply air, which is at the dew point, 14.2℃, to offset the indoor humid generation. This indicates the supply air flow rate is reduced apparently. Thus, the draft sensation and the noise can be reduced. Also the thermal comfort can be improved by radiant cooling, compared with that produced by the conventional room air conditioner.

In comparison with the theoretical refrigeration cycle of the conventional air-conditioner, the suction pressure of the theoretical refrigeration cycle of the dual-temperature air conditioner improves to 0.6483 MPa from 0.5481 MPa. The pressure ratio of the compression process reduces by 9.94%. As a result the power consumption decreases from 0.770kW to 0.677 kW, neglecting the fan power. The COP of the theoretical refrigeration cycle improves by 13.73% to be 7.43.

5 CONCLUSION

An innovative dual-temperature air-conditioner with air-handling unit and radiant panel as separate evaporators is proposed. The theoretical refrigeration cycle and its working mechanism are introduced. The operational states and system performance are determined and compared with those of a conventional air-conditioner with fresh air for a typical office cooling load. Results indicate the COP

of the new system may improve by 13.73% to reach 7.47 when the required amount of fresh air and indoor humid generation are not very large.

The structure of the radiant panel and the air-handling unit are being designed and needs further investigations, which will be published soon.

ACKNOWLEDGEMENT

This paper is sponsored by the key Shaanxi Provincial innovative team project （2012KTC-11） and Xi'an scientific research plan project (CX12176-⑤).

REFERENCES

[1] Wu Xiping.2000. The Volume of Outdoor Air, the Way of Air Distribution and Air Conditioning Diseases. Building Energy & Environment 4:67-68.

[2] Stanley A. Mumma.2001. Ceiling Panel Cooling Systems. ASHRA Journal (43):28-32.

[3] Xia Xueying, Zhang Xv, Cai Ning,et al. 2008. Technology Analysis and Experimental Research on Radiant Floor Cooling Combined with Dedicated 0ut-door Air System. Journal of Refrigeration 4:19~23.

[4] Yan Zhenhua, Huang Xiang, Xuan Yong mei.2008. Application Research on Air conditioning System of Radiative Cooling by Capillary Tube. Refrigeration 27(1): 65-68.

[5] Wang Zijie.2004. Low-temperature radiant heating and radiant cooling .Bei Jing: Machinery Industry Pre- ss.

[6] Liu Jinghui, Chen Jiangping, Chen Zhijiu.2006. COP Comparison of Refrigeration Cycles with Two-Stage Evaporating Temperatures. Journal of Applied Sciences 24(5): 538-542.

[7] Heating Class 22 of the Civil Engineering Department at Tsinghua University. Selection Calculation and System Design of Induced Air-conditioner [J]. Communication of Building Technology (HV&AC), 1976, (2): 1-14.

[8] Liu Shuanqiang, Liu Xiaohua, Jiang Yi. 2010. Dedicated outdoor air system in the THIC air conditioning system (1): calculation of space moisture load. HV&AC 40(1):80~84

[9] Liu Shuanqiang, Liu Xiaohua，Jiang Yi.2010. Dedicated outdoor air system in the THIC air conditioning system (2): Determination of Supply air parameters. HV&AC 40(12): 85~90.

[10] Zhao Rongyi , Fan Cunyang, Xue Dianhua,et al.2009. Air Conditioning. Bei Jing: China Building Industry Press.

[11] Yin Ping.2000. Research of large temperature difference in air conditioning (2): The design method of a large temperature difference air conditioning supply system. HV&AC, 30(5):63-66.

[12] Lu Yaoqing.2007. Practical Design Manual heating and air conditioning. Beijing: China Building Industry Press.

[13] 2012. Design code for heating ventilation and air conditioning of civil buildings, GB50736-2012